

***New Psychoactive Substances  
– New Analytical Challenges  
and Approaches***

A thesis submitted in partial fulfilment of the  
requirements of Manchester Metropolitan  
University for the degree of Doctor of  
Philosophy

Matthew Carl Hulme

Department of Natural Sciences  
Manchester Metropolitan University

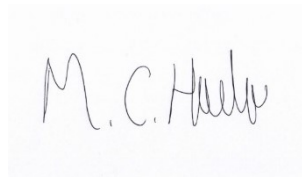
2018

## Author's declaration

*I declare that none of the work detailed herein has been submitted for any other award at Manchester Metropolitan University or any other Institution."*

*"I declare that, except where specifically indicated, all the work presented in this report is my own, and I am the sole author of all parts. I understand that any evidence of plagiarism and/or the use of unacknowledged third part data will be dealt with as a very serious matter."*

Signature

A handwritten signature in black ink on a light blue background. The signature reads "M. C. Hally" in a cursive, slightly slanted script.

Date: 20-December-2018

## **Acknowledgements**

Massive thanks to Dr. Oliver Sutcliffe for the opportunities to continue studying after undergraduate level. Thanks for the continued supervision and continued support and guidance in and outside of studies. Thanks also to Dr. Ryan Mewis for supervision and help with NMR work. Without the support of both completion of the three years of work would have been a struggle.

I would like to thank all PhD students within the Sutcliffe research group for all support they have provided. This also includes any MChem students who have worked within the group and provided support both inside and outside of studies within the 4 years. I would like to thank all research students on level 7 who have made the study time enjoyable especially with outside social activities including the football group. Main thanks to both Jack Marron and Nick Gilbert who have made the 4 years of study within the group very enjoyable.

Thanks also to Oxford Instruments for the continued support financially with funding for the PhD and access to instrumentation. Special mentions and thanks to Dr. David Williamson for initial contact and continued support and advice on your visits to Manchester.

Thanks to all technical staff at MMU on both level 6 and level 7. Special thanks to Lee Harman for initial training and continued technical support with use of the GC-MS instrumentation.

Finally, a big thank you to my family for continued support throughout all my years of study at Manchester Metropolitan University.

## Abstract

In recent years Novel Psychoactive Substances (NPS), including diphenidine and ephedrine, have emerged and an increase in the number of substances encountered each year has increased, even with the introduction of the Psychoactive Substances Act (2016).<sup>1</sup> More derivatives are also reported containing fluorine substituents due to the increased stability.<sup>2</sup> The appearance of novel fluorinated substances creates analytical challenges for their detection. This results in the need for the development of new rapid, selective and inexpensive analytical methods for both their separation and detection. Colour test reagents are commonly used for the presumptive testing of these emerging substances, however as the number of encountered compounds increases so does the number of false positives produced with these tests.<sup>3</sup> Gas Chromatography-Mass Spectroscopy (GC-MS) is also a commonly used method for the detection and separation of controlled substances, with methods reported previously for fluorinated cathinones.<sup>4</sup> However, it also reports on the tailing of peaks through thermal degradation, which makes separation of regioisomers difficult.

This thesis demonstrates the synthesis of a number of fluorinated and non-fluorinated diphenidine and ephedrine derivatives. Synthesis of fluorinated diphenidine analogues will also outline the ease of production of NPS along with the difficulties in their detection and separation. The use of presumptive colour testing shows the difficulty of distinguishing between regioisomers, as well as the increase to the number of false positives.

The development of GC-MS methods has aided with the separation and detection of diphenidine and ephedrine derivatives. A method has also been developed and validated for the identification of fluorinated cathinones and amphetamines with improved symmetry and a removal of any tailing/fronting. Runs for all separation and identification last 20 minutes or longer.



60 MHz NMR has the ability to perform  $^1\text{H}$  and  $^{19}\text{F}$  NMR experiments, while still providing matching spectrum patterns and splitting to higher-powered magnets. This is utilised for the detection of diphenidine, ephedrine, cathinone and amphetamine derivatives with the ability to distinguish between regioisomers. 2D NMR experiments can also allow for further identification of difluorinated ephedrine derivatives. This allows for the possibility of using 60 MHz NMR as a presumptive test for NPS. The use of  $^{19}\text{F}$  NMR experiments also provides an ability to perform quantitative analysis. Street samples can then be analysed both qualitatively and quantitatively, using 60 MHz NMR, with results confirmed by GC-MS. All  $^1\text{H}$  and  $^{19}\text{F}$  NMR experiments occur within 5 minutes meaning detection can occur rapidly which aids with forensic testing and shows that 60 MHz instrumentation can be utilised at locations such as festivals, airport security and police custody.

## Contents

Author's declaration	p 2
Abstract	p 4
List of Tables	p 10
List of figures	p 14
Abbreviations and Acronyms	p 24
1.0. Chapter 1 – Introduction	p 26
1.1. UK Misuse of Drugs Act (1971)	p 26
1.2. Psychoactive Substances Act (2016)	p 31
1.3. Amphetamines	p 35
1.4. Cathinones	p 38
1.4.1. Methcathinones	p 40
1.4.2. 4-Methylmethcathinones	p 41
1.4.3. 4-Fluoromethcathinone (flephedrone)	p 42
1.4.4. <i>ortho</i> -, <i>meta</i> - and <i>para</i> - trifluoromethylmethcathinones	p 45
1.5. PCP to MXE	p 47
1.6. Diphenidine and Methoxphenidine	p 50
1.7. Lefetamine and Ephedrine	p 52
1.8. Prolintane and fluorolintane	p 54
1.9. Presumptive Testing	p 56
1.10. Gas Chromatography – Mass Spectroscopy	p 59
1.11. Nuclear Magnetic Resonance (NMR) Spectroscopy	p 63
1.11.1. Fluorine ( <sup>19</sup> F) NMR	p 65
1.11.2. 60 MHz NMR screening	p 66
1.12. Aims and Objectives	p 67
2.0. Chapter 2 – Experimental methods	p 70
2.1. Synthetic Methods	p 71
2.1.1. Synthesis of the diphenidine derivatives and analogues	p 71
2.2. Presumptive tests reagents	p 81
2.3. Thin Layer Chromatography	p 83

2.4. Gas Chromatography–Mass Spectroscopy (GC-MS)	p 84
2.4.1. GC-MS of diphenidine derivatives	p 84
2.4.2. GC-MS of cathinones, amphetamines, halogenated diphenidine derivatives, ephedrine and diphenidine analogues	p 84
2.4.3. Oven temperature programmes	p 85
2.4.3.1. Initial Screening method 1	p 85
2.4.3.2. Initial Screening method 2	p 85
2.4.3.3. Developed cathinone and amphetamine method	p 85
2.4.3.4. Developed diphenidine derivatives method	p 86
2.4.3.5. Developed halogenated diphenidines method	p 86
2.4.3.6. Developed diphenidines analogues method	p 87
2.4.3.7. Developed polyfluorinated ephedridines method	p 87
2.4.4. Standards and test solution preparation	p 88
2.4.4.1. Reference standard preparation	p 88
2.4.4.2. Fluorinated cathinone, amphetamine and diphenidine calibration standards	p 88
2.4.4.3. Diphenidine derivatives calibration standards	p 88
2.4.4.4. Halogenated diphenidine calibration standards	p 89
2.4.4.5. Diphenidine analogues calibration standards	p 89
2.4.5. Street sample preparation	p 89
2.4.5.1. Fluoroamphetamine street samples	p 89
2.4.5.2. Diphenidine street sample analysis	p 89
2.4.5.3. Halogenated diphenidine street samples	p 90
2.5. NMR spectroscopy	p 91
2.5.1. Quantitative <sup>19</sup> F NMR on 60 MHz instrument	p 92
2.5.2. Street sample preparation	p 92
2.5.3. 60 MHz 2-dimensional NMR experiments	p 92
3.0. Fluorinated cathinones and amphetamines	p 94
3.1. Overview	p 94
3.2. Synthesis	p 95
3.3. Presumptive Testing	p 106
3.4. Gas Chromatography-Mass Spectroscopy	p 110

3.5. 60 MHz NMR presumptive testing	p 122
3.6. GC-MS and 60 MHz NMR quantitative analysis	p 127
3.7. Street sample analysis	p 131
3.8. Conclusions	p 138
4.0. Chapter 4 – Separation and identification of diphenidine derivatives using GC-MS analysis results	p 140
4.1. Overview	p 140
4.2. Synthesis	p 141
4.3. Presumptive Testing	p 157
4.4. Thin Layer Chromatography	p 161
4.5. Gas Chromatography-Mass Spectrometry	p 163
4.6. Forensic Application	p 172
4.7. Conclusions and future work	p 175
5.0. Chapter 5 – Halogenated diphenidine derivatives	p 177
5.1. Overview	p 177
5.2. Synthesis of halogenated diphenidine derivatives	p 178
5.3. Presumptive Testing	p 190
5.4. Thin Layer Chromatography (TLC)	p 193
5.5. Gas Chromatography-Mass Spectroscopy	p 194
5.6. 60 MHz NMR presumptive testing	p 203
5.7. Forensic Application	p 211
5.8. Conclusions	p 220
6.0. Chapter 6 – Fluorinated diphenidine analogues	p 222
6.1. Overview	p 222
6.2. Synthesis	p 223
6.3. Presumptive Testing	p 240
6.4. Thin Layer Chromatography	p 245
6.5. Gas Chromatography-Mass Spectroscopy	p 247
6.6. 60 MHz NMR presumptive testing	p 261
6.7. Quantitative 60 MHz NMR analysis	p 273

6.8. Conclusions	p 275
7.0. Chapter 7 – Separation and identification of polyfluorinated Ephedrine regioisomers	p 277
7.1. Overview	p 277
7.2. Synthesis	p 278
7.3. Presumptive Testing	p 284
7.4. Thin Layer Chromatography	p 287
7.5. Gas Chromatography-Mass Spectroscopy	p 288
7.6. 60 MHz NMR screening	p 293
7.7. 60 MHz NMR <i>J</i> -resolved experiments	p 299
7.8. <sup>19</sup> F TOCSY NMR	p 307
7.9. Conclusions	p 311
8.0. Final conclusions and future work	p 312
9.0. References	p 317

## List of tables

**Table 1:** Classifications of controlled substances and examples of drugs in each class

**Table 2:** Table showing maximum punishments for possession and supply of controlled substances

**Table 3:** Drug schedules and an explanation of what constitutes each schedule

**Table 4:** Commonly used presumptive test reagents along with compound classes tested and common colour changes

**Table 5:** Advantages and disadvantages of using 60 MHz compared to GC-MS

**Table 6:** List of diphenidine derivatives and analogues synthesised including abbreviations, compound numbers, yields, melting points,  $R_f$  values (DCM:MeOH, 9:1) and aldehydes and amines used in synthesis

**Table 7:** Oven temperature programme for the initial screening of diphenidine and ephenidine derivatives

**Table 8:** Oven temperature programme for the initial screening of monofluorinated cathinones, amphetamines and diphenidine analogues

**Table 9:** Developed oven temperature programme for the separation of fluorinated cathinone and amphetamine regioisomers

**Table 10:** Developed oven temperature programme for the separation of thirteen diphenidine derivatives

**Table 11:** Oven temperature programme for the separation of the halogenated diphenidines

**Table 12:** SIM ions used for all of the diphenidine analogue regioisomers

**Table 13:** Developed oven temperature programme for the diphenidine analogues

**Table 14:** Developed oven temperature programme for the attempted separation of the polyfluorinated ephenidine isomers

**Table 15:** Calibration standard preparation for  $^{19}\text{F}$  NMR quantitative analysis

**Table 16:**  $^{19}\text{F}$  NMR chemical shift values for all fluorinated amphetamine and cathinone regioisomers

**Table 17:** Colour changes reported for fluoroamphetamine (**4a–4c**), fluoromethcathinone (**8a–8c**) and trifluoromethylmethcathinone (**9a–9c**) regioisomers using a range of presumptive test reagents

**Table 18:** GC retention times for the monofluorinated amphetamine (**4a–4c**) and cathinone (**8a–8c**) regioisomers and trifluoromethylmethcathinone (**9a–9c**) regioisomers, including relative retention times (RRt) relative to eicosane (**E**, Rt = 7.281 mins)

**Table 19:** GC retention times for the monofluorinated amphetamine (**4a–4c**) and cathinone (**8a–8c**) regioisomers and trifluoromethylmethcathinone (**9a–9c**) regioisomers, including relative retention times (RRt) relative to eicosane (**E**, Rt = 30.850 mins) using the developed GC oven temperature programme

**Table 20:** Validation values for the FMC (**8a–8c**) and TFMMC (**9a–9c**) regioisomers including LOD, LOQ and %RSD for all calibration standards

**Table 21:** <sup>19</sup>F NMR chemical shift values for all fluorinated amphetamine and cathinone derivatives run on a 60 MHz instrument

**Table 22:** LOD and LOQ values for the three FA (**4a–4c**) regioisomers from the calibration series produced on the 60 MHz NMR instrument

**Table 23:** Quantification results for active component, 4-FA, in the two street samples from GC-MS analysis

**Table 24:** Quantification results for active component, 4-FA, in the two street samples from 60 MHz NMR analysis

**Table 25:** <sup>19</sup>F NMR chemical shifts for the three trifluoromethoxyphenidine regioisomers (**13e – 13g**) run in DMSO

**Table 26:** Colour changes observed with presumptive test reagents for 13 diphenidine derivatives (**13a–13m**) immediately after addition and after 5 minutes of addition

**Table 27:** Thin Layer Chromatography data for diphenidine (**13a**) and its substituted derivatives (**13b–13m**)

**Table 28:** Summary of GC-MS validation data for the quantification of diphenidine (**13a**) and its substituted derivatives (**13b–13m**). NB. Rt (eicosane) = 21.55 min. See Figure 75 for representative chromatogram.

**Table 29:** Percentage yields for the halogenated regioisomers (**20a–20l**)

**Table 30:** <sup>19</sup>F NMR chemical shift values for the fluphenidine regioisomer (FP, **20a–20c**)

**Table 31:** Colour changes observed with presumptive test reagents for the 12 halogenated diphenidine derivatives (**20a–20l**) immediately after addition and after 5 minutes of addition

**Table 32:** Thin Layer Chromatography data for the halogenated diphenidine regioisomers (**20a–20l**)

**Table 33:** GC retention times for the 12 halogenated diphenidine derivatives (**20a–20l**) including relative retention time (RRt) relative to diphenidine (**15a**, Rt = 15.262 mins) with eicosane (**E**) added as an internal standard (Rt = 14.464, RRt = 0.95)

**Table 34:** GC-MS validation figures for the halogenated diphenidine derivatives (**20a-20l**) and the three added adulterants: benzocaine (**B**); paracetamol (**P**) and caffeine (**C**). Key: x Relative Retention time with respect to eicosane (E, Rt = 14.464 min)

**Table 35:** Table containing  $^{19}\text{F}$  NMR chemical shift data for the fluphenidine regioisomers (**20a–20c**)

**Table 36:** Table showing concentrations and percentage weights of active ingredients in both SS-H1 and SS-H2 of caffeine and 2-CP

**Table 37:** Percentage yields of all fluorinated diphenidine analogues showing all names, abbreviations and different amines used in synthesis

**Table 38:** Reported colour changes for a range of presumptive test reagents on multiple fluorinated diphenidine analogues

**Table 39:** Rf values for all the monofluorinated diphenidine analogues

**Table 40:** GC retention times for the diphenidine analogues, including relative retention time (RRt) relative to eicosane (**E**, Rt = 7.281 mins)

**Table 41:** GC retention times for the diphenidine analogues on the developed GC method, including relative retention time (RRt) relative to eicosane (**E**, Rt = 7.281 mins)

**Table 42:** GC-MS validation figures for the monofluorinated diphenidine analogues and the three added adulterants: benzocaine (**B**); paracetamol (**P**) and caffeine (**C**). Key: x Relative Retention time with respect to eicosane (**E**, Rt = 31.58 min)

**Table 43:** Table containing  $^{19}\text{F}$  NMR chemical shift data for all monofluorinated diphenidine analogues



**Table 44:** Integrated area values for the calibration solutions from  $^{19}\text{F}$  NMR experiments on a 60 MHz instrument

**Table 45:** Chemical shift values for a number of polyfluorinated ephenidine regioisomers. TFA used as an internal standard ( $\delta$  ppm = -76.55

**Table 46:** Colour changes observed with presumptive test reagents for the DFEP (**15d-15i**) regioisomers, TriFEP (**15j**), TeFEP (**15k**) and PFEP (**15l**) compounds immediately after addition and after 5 minutes of addition

**Table 47:** Thin Layer Chromatography data for the nine polyfluorinated ephenidine regioisomers (**15d-15l**)

**Table 48:** GC-MS retention times for the polyfluorinated ephenidine regioisomers along with relative retention times compared to eicosane

**Table 49:**  $^{19}\text{F}$  chemical shift data for the polyfluorinated ephenidine regioisomers (15d – 15l) using 60 MHz NMR instrument

**Table 50:** Instrumental comparison between the 60 MHz and the GC-MS

## List of figures

**Figure 1:** Chemical structures of cocaine (1), morphine (2), amphetamine (3a) and methamphetamine (3b)

**Figure 2:** Chemical structure of 3,4-methylenedioxymethamphetamine (MDMA), 3c

**Figure 3:** Image showing the countries that reported the presence of NPS in 2017, to the UNODC and the number of NPS reported.

**Figure 4:** Image showing the classification of NPS reported to the EU early warning system.<sup>23</sup>

**Figure 5:** Chemical structure of phenethylamine (3d)

**Figure 6:** Chemical structure of regioisomeric fluoroamphetamine (4)

**Figure 7:** Chemical structure of cathinone (5)

**Figure 8:** Chemical structure of methcathinone (6)

**Figure 9:** Chemical structures of the methylmethcathinone regioisomers (7a – 7c)

**Figure 10:** Chemical structures of fluoromethcathinone regioisomers (FMC, 8a–8c)

**Figure 11:** Chemical structures of the trifluoromethylmethcathinone regioisomers (TFMMC, 9a – 9c)

**Figure 12:** Chemical structure of phencyclidine (PCP, 10)

**Figure 13:** Chemical structure of ketamine (11)

**Figure 14:** Chemical structure of methoxetamine (MXE, 12)

**Figure 15:** Chemical structures of diphenidine (13a) and the methoxphenidine regioisomers (MXP, 13b – 13d)

**Figure 16:** Chemical structure of lefetamine (14)

**Figure 17:** Chemical structure of ephenidine (15)

**Figure 18:** Chemical structure of prolintane (16)

**Figure 19:** Chemical structures of pyrovalerone (17) and methylenedioxyvalerone (18)

**Figure 20:** Chemical structure of fluorolintane regioisomers (19)

**Figure 21:** Common presumptive colour testing kit used by law enforcement officers

**Figure 22:** Image of a GC-MS instrument

**Figure 23:** GC-MS chromatographs for the 3- (a) and 4- (b) fluoroamphetamine regioisomers

**Figure 24:** Mass spectrum for the fluoroamphetamine regioisomers.

**Figure 25:** GC-MS chromatographs for the 2' and 3'-fluoromethcathinone regioisomers

**Figure 26:** GC-MS chromatograph of the 2' (1), 3' (2) and 4'-trifluoromethylmethcathinone (3) regioisomers

**Figure 27:** General structure of diphenidine and all its derivatives and analogues

**Figure 28:** Reaction scheme for the synthesis of FA isomers (**4a–4c**)

**Figure 29:** Reaction scheme for the synthesis of FMC isomers (**8a–8c**)

**Figure 30:** Reaction scheme for the synthesis of TFMMC isomers (**9a – 9c**)

**Figure 31:** General 400 MHz <sup>1</sup>H NMR spectrum for the 4-fluoroamphetamine hydrochloride (4-FA, **4a**) run in DMSO-d<sub>6</sub> (δ ppm = 2.50)

**Figure 32:** Stacked 400 MHz aliphatic region of the three fluoroamphetamine (FA, **4a – 4c**) hydrochloride regioisomers run in DMSO-d<sub>6</sub> (δ ppm = 2.50)

**Figure 33:** Stacked 400 MHz aromatic region of the three fluoroamphetamine (FA, **4a – 4c**) hydrochloride regioisomers run in DMSO-d<sub>6</sub> (δ ppm = 2.50)

**Figure 34:** General 400 MHz <sup>1</sup>H NMR spectrum for 4-fluoromethcathinone (4-FMC, **8c**) run in DMSO-d<sub>6</sub> (δ ppm = 2.50)

**Figure 35:** Stacked 400 MHz aromatic region of the three fluoromethcathinone (FMC, **8a – 8c**) hydrochloride regioisomers run in DMSO-d<sub>6</sub> (δ ppm = 2.50)

**Figure 36:** Stacked 400 MHz aromatic region of the three trifluoromethylmethcathinone (FMC, **9a – 9c**) hydrochloride regioisomers run in DMSO-d<sub>6</sub> (δ ppm = 2.50)

**Figure 37:** <sup>19</sup>F NMR spectrum for a mixture of FMC (**8a–8c**) and TFMMC (**9a–9c**) regioisomers with TFA added as an internal reference (δ ppm = -76.55)

**Figure 38:** Reaction scheme for the reaction between methcathinone and the Marquis reagent

**Figure 39:** Reaction scheme for the reaction between methcathinone (**6**) and the Zimmerman reagent

**Figure 40:** Superimposed GC chromatographs of the three fluoroamphetamine (**4a–4c**) regioisomers

**Figure 41:** Superimposed GC chromatographs for the fluoromethcathinone (FMC, **8a–8c**) and trifluoromethylmethcathinone (TFMMC, **9a–9c**) regioisomers

**Figure 42:** MS fragmentation for the fluoroamphetamine (FA, **4a–4c**) regioisomers

**Figure 43:** MS fragmentation for the fluoromethcathinone (FMC, **8a–8c**) regioisomers

**Figure 44:** MS fragmentation pattern for the trifluoromethylmethcathinone (TFMMC, **9a–9c**) regioisomers

**Figure 45:** Mass spectra for the fluoroamphetamine (**4a–4c**) and fluoromethcathinone (**8a–8c**)

**Figure 46:** Mass spectrum for the trifluoromethylmethcathinone (**9a–9c**) regioisomers

**Figure 47:**  $^1\text{H}$  NMR spectra for the fluoroamphetamine regioisomers (FA, **4a–4c**), run on a 60 MHz instrument in DMSO- $\text{d}_6$  ( $\delta$  ppm = 2.50)

**Figure 48:**  $^1\text{H}$  NMR spectra for the fluoromethcathinone regioisomers (FMC, **8a–8c**), run on a 60 MHz instrument in DMSO- $\text{d}_6$  ( $\delta$  ppm = 2.50)

**Figure 49:**  $^1\text{H}$  NMR spectra for the trifluoromethylmethcathinone regioisomers (TFMMC, **9a–9c**), run on a 60 MHz instrument in DMSO- $\text{d}_6$  ( $\delta$  ppm = 2.50)

**Figure 50:** Stacked  $^{19}\text{F}$  NMR spectra for the trifluoromethylmethcathinone regioisomers

**Figure 51:** Stacked  $^{19}\text{F}$  NMR spectra for all fluoroamphetamine (FA, **4a–4c**) and fluoromethcathinone (FMC, **8a–8c**) regioisomers

**Figure 52:** Calibration series performed using GC-MS on all three fluoroamphetamine (FA, **4a–4c**) regioisomers

**Figure 53:** Calibration graphs for the FA regioisomers using  $^{19}\text{F}$  NMR experiments on a 60 MHz NMR

**Figure 54:** Image of the seized street sample (SS1)

**Figure 55:**  $^1\text{H}$  NMR spectra for the street sample run in DMSO- $\text{d}_6$  ( $\delta$  ppm = 2.50)

**Figure 56:**  $^{19}\text{F}$  NMR spectrum for the street samples with TFA added as an internal reference ( $\delta$  ppm = -76.55)

**Figure 57:** GC-MS chromatographs for the two street samples run with eicosane added as an internal standard ( $R_t$  = 30.85 mins)

**Figure 58:** Mass spectrum produced for the two street samples

**Figure 59:** Reaction scheme for the synthesis of the diphenidine derivatives

**Figure 60:** Chemical structures for diphenidine (**13a**), the three methoxyphenidine (MXP, **13b–13d**) and trifluoromethoxyphenidine (TFMXP, **13e–13f**) regioisomers along with the 2,3,4-trimethoxyphenidine (mescphenidine, **13h**) derivative

**Figure 61:** Chemical structures for the methylenedioxyphenidine (MDDP, **13i–13j**), naphthenidine (NPD, **13k–13l**) and the IAS-013 (**13m**) derivatives

**Figure 62:** Stacked <sup>1</sup>H NMR aromatic region for the two-naphthenidine regioisomers (NP, **13k** (top) – **13l** (bottom))

**Figure 63:** <sup>1</sup>H NMR (400 MHz, CD<sub>2</sub>Cl<sub>2</sub>) spectrum of diphenidine hydrochloride (**13a**)

**Figure 64:** Stacked <sup>1</sup>H NMR for the aliphatic region of diphenidine (**13a**), 2-MXP (**13b**), 3-MXP (**13c**) and 4-MXP (**13d**)

**Figure 65:** Stacked <sup>1</sup>H NMR for the aromatic region of diphenidine (**13a**), 2-MXP (**13b**), 3-MXP (**13c**) and 4-MXP (**13d**)

**Figure 66:** Stacked <sup>1</sup>H NMR for the aliphatic region of diphenidine (**13a**), 2-TFMXP (**13e**), 3-TFMXP (**13f**) and 4-TFMXP (**13g**)

**Figure 67:** Stacked <sup>1</sup>H NMR for the aromatic region of diphenidine (**13a**), 2-TFMXP (**13e**), 3-TFMXP (**13f**) and 4-TFMXP (**13g**)

**Figure 68:** Stacked <sup>1</sup>H NMR for the aliphatic region of diphenidine (**13a**), 2,3-MDDP (**13i**), 3,4-MDDP (**13j**) and mescphenidine (**13h**)

**Figure 69:** : Stacked <sup>1</sup>H NMR for the aromatic region of diphenidine (**13a**), 2,3-MDDP (**13i**), 3,4-MDDP (**13j**) and mescphenidine (**13h**)

**Figure 70:** Stacked <sup>1</sup>H NMR for the aliphatic region of diphenidine (**13a**), 1-NPD (**13k**), 2-NPD (**13l**) and IAS-013 (**13m**)

**Figure 71:** Stacked <sup>1</sup>H NMR for the aromatic region of diphenidine (**13a**), 1-NPD (**13k**), 2-NPD (**13l**) and IAS-013 (**13m**)

**Figure 72:** Proposed scheme for the colour change in the Scott's reagent

**Figure 73:** Proposed reaction scheme for the Marquis reagent with diphenidine

**Figure 74:** Reaction scheme for the positive colour change in the Mandelin reagent

**Figure 75:** GC-MS chromatogram demonstrating the separation of the thirteen diphenidine derivatives (**13a–13m**) along with the relevant adulterants: benzocaine (**B**); caffeine (**C**) and procaine (**P**), with eicosane (**E**) added as an internal standard.

**Figure 76:** structure of the benzyl cation

**Figure 77:** GC-MS fragmentation for diphenidine (**13a**) base peak

**Figure 78:** GC-MS fragmentation of the MXP (**13b–13d**) and TFMXP (**13e–13g**) regioisomers

**Figure 79:** GC-MS fragmentation of the MDDP (**13i–13j**) and NP (**13k–13l**) regioisomers

**Figure 80:** GC-MS fragmentation pattern for TMXP (**13h**)

**Figure 81:** GC-MS fragmentation pattern for IAS-013 (**13m**)

**Figure 82:** EI-MS spectra of (a) diphenidine (**13a**) and its substituted derivatives (b) 2-methoxyphenidine (2-MXP, **13b**); (c) 3-methoxyphenidine (3-MXP, **13c**); (d) 4-methoxyphenidine (4-MXP, **13d**); (e) 2-trifluoromethoxyphenidine (2-TFMXP, **13e**); (f) 3-trifluoromethoxyphenidine (3-TFMXP, **13f**) and (g) 4-trifluoromethoxyphenidine (4-TFMXP, **13g**).

**Figure 83:** EI-MS spectra of (a) mescphenidine (3,4,5-TMXP, **13h**); (b) 2,3-(methylenedioxy)diphenidine (2,3-MDDP, **13i**); (c) 3,4-(methylenedioxy)diphenidine (3,4-MDDP, **13j**); (d) 1-naphthenidine (1-NPD, **13k**); (e) 2-naphthenidine (2-NPD, **13l**); (f) IAS-013 (**13m**).

**Figure 84:** GC-MS analysis of the two street samples SS-1 and SS-2

**Figure 85:** <sup>1</sup>H NMR analysis of SS-1 (a) and SS-2 (b) run in CD<sub>2</sub>Cl<sub>2</sub> (10 mg mL<sup>-1</sup>)

**Figure 86:** Quantitative GC-MS analysis containing both GC chromatographs and mass spectra data of SS-1 (a and b) and SS-2 (c and d) (0.1 mg mL<sup>-1</sup> in methanol containing 0.1 mg mL<sup>-1</sup> eicosane, **E**)

**Figure 87:** Reaction scheme for the synthesis of the halogenated diphenidine derivatives (**20a-20l**)

**Figure 88:** Stacked <sup>1</sup>H-NMR spectra of diphenidine (**13a**) run in DMSO-d<sub>6</sub> (δ ppm = 2.50) and CDCl<sub>3</sub> (δ ppm = 7.26)

**Figure 89:** <sup>1</sup>H-NMR spectra of diphenidine (**13a**) run in DMSO-d<sub>6</sub> (δ ppm = 2.50)

**Figure 90:** Stacked  $^1\text{H}$ -NMR spectra for the fluphenidine regioisomers (**20a–20c**) run in  $\text{DMSO-d}_6$  ( $\delta$  ppm = 2.50)

**Figure 91:** Stacked  $^1\text{H}$  NMR spectra showcasing the aromatic region of the fluphenidine regioisomers (**20d–20f**)

**Figure 92:** Stacked  $^1\text{H}$  NMR spectra showcasing the aromatic region of the 2'-positional isomers of the halogenated diphenidines

**Figure 93:** Stacked  $^1\text{H}$  NMR spectra showcasing the aromatic region of the 3'-positional isomers of halogenated diphenidines

**Figure 94:** Stacked  $^1\text{H}$  NMR spectra showcasing the aromatic region of the 4'-positional isomers of halogenated diphenidines

**Figure 95:** Base peak fragmentation for all the halogenated diphenidine regioisomers

**Figure 96:** GC spectra for the mixture of 2'-positional halogenated diphenidine compounds with the inclusion of common adulterants: benzocaine (**B**); paracetamol (**P**); caffeine (**C**) and the internal standard eicosane (**E**)

**Figure 97:** GC spectra for the mixture of 3'-positional halogenated diphenidine compounds with the inclusion of common adulterants: benzocaine (**B**); paracetamol (**P**); caffeine (**C**) and the internal standard eicosane (**E**)

**Figure 98:** GC spectra for the mixture of 4'-positional halogenated diphenidine compounds with the inclusion of common adulterants: benzocaine (**B**); paracetamol (**P**); caffeine (**C**) and the internal standard eicosane (**E**)

**Figure 99:** Mass spectra for all fluphenidine regioisomers (**20a–20c**)

**Figure 100:** Mass spectra for all chlophenidine regioisomers (**20d–20f**)

**Figure 101:** Mass spectra for all brophenidine regioisomers (**20g–20i**)

**Figure 102:** Mass spectra for all iodophenidine regioisomers (**20j–20l**)

**Figure 103:** Mass spectrum for benzocaine (**B**)

**Figure 104:** Mass spectrum for paracetamol (**P**)

**Figure 105:** Mass spectrum for caffeine (**C**)

**Figure 106:** 60 MHz  $^1\text{H}$  NMR spectra for the 2'-positional halogenated derivatives acquired in  $\text{DMSO-d}_6$  ( $\delta$  ppm = 2.50)

**Figure 107:**  $^1\text{H}$  NMR spectra showing the aromatic region only of the fluphenidine regioisomers (**20a–20c**) acquired on a 60 MHz instrument

**Figure 108:**  $^1\text{H}$  NMR spectra showing the aromatic region only of the chlophenidine regioisomers (**20d–20f**) acquired on a 60 MHz instrument

**Figure 109:**  $^1\text{H}$  NMR spectra showing the aromatic region only for the brophenidine regioisomers (**20g–20i**) acquired on a 60 MHz instrument

**Figure 110:**  $^1\text{H}$  NMR spectra showing the aromatic region only for the iodophenidine regioisomers (**20j–20l**) acquired on a 60 MHz instrument

**Figure 111:** Stacked  $^{19}\text{F}$  NMR spectra for the fluphenidine regioisomers run in DMSO with the inclusion of trifluoroacetic acid (TFA,  $\delta$  ppm = -76.55)

**Figure 112:**  $^1\text{H}$  NMR spectra run in DMSO ( $\delta$  ppm = 2.50), measured on a 60 MHz instrument for the two street samples (SS-H1 and SS-H2)

**Figure 113:** Full  $^1\text{H}$  NMR spectrum for the 2-CP standard (**20d**), performed on a 60 MHz instrument in DMSO- $d_6$  ( $\delta$  ppm = 2.50)

**Figure 114:** GC-MS chromatograph for SS-H1 with the inclusion of internal reference eicosane (**E**,  $R_t$  = 14.464 min)

**Figure 115:** GC-MS chromatograph for SS-H2 with the inclusion of internal reference eicosane (**E**,  $R_t$  = 14.464 min)

**Figure 116:** Mass spectra for the sample peak produced in both SS-H1 and SS-H2

**Figure 117:** Mass spectrum produced for the adulterant peak of SS-H2

**Figure 118:** Stacked  $^1\text{H}$ -NMR spectra comparison for SS-H1, SS-H2 and 2-CP run in DMSO ( $\delta$  ppm = 2.50) acquired using a 400 MHz instrument

**Figure 119:** Reaction scheme for the synthesis of the fluorinated diphenidine analogues

**Figure 120:** Chemical structures for all fluorinated diphenidine analogues synthesised

**Figure 121:** 400 MHz  $^1\text{H}$  NMR spectrum for 2-fluoroephenidine (2-FEP, **15a**) run in DMSO- $d_6$  ( $\delta$  ppm = 2.50)

**Figure 122:** Stacked 400 MHz  $^1\text{H}$  NMR aromatic region for the fluoroephenidine regioisomers (FEP, **15a – 15c**)

**Figure 123:** 400 MHz  $^1\text{H}$  NMR spectrum for 2-fluorolintane (2-FL, **19a**) run in DMSO- $d_6$  ( $\delta$  ppm = 2.50)

**Figure 124:** Stacked 400 MHz  $^1\text{H}$  NMR aromatic region for the fluorolintane regioisomers (FL, **19a – 19c**)

**Figure 125:** 400 MHz  $^1\text{H}$  NMR spectrum for 2-fluoromephenidine (2-FMP, **21a**) run in DMSO- $d_6$  ( $\delta$  ppm = 2.50)



**Figure 126:** Stacked 400 MHz <sup>1</sup>H NMR aromatic region for the fluoromephenidine regioisomers (FMP, **21a** – **21c**)

**Figure 127:** 400 MHz <sup>1</sup>H NMR spectrum for 2-fluorodimephenidine (2-FDMP, **22a**) run in DMSO-d<sub>6</sub> (δ ppm = 2.50)

**Figure 128:** Stacked 400 MHz <sup>1</sup>H NMR aromatic region for the fluorodimephenidine regioisomers (FDMP, **22a** – **22c**)

**Figure 129:** 400 MHz <sup>1</sup>H NMR spectrum for 2-fluorodiephenidine (2-FDEP, **23a**) run in DMSO-d<sub>6</sub> (δ ppm = 2.50)

**Figure 130:** Stacked 400 MHz <sup>1</sup>H NMR aromatic region for the fluorodiephenidine regioisomers (FDEP, **23a** – **23c**)

**Figure 131:** 400 MHz <sup>1</sup>H NMR spectrum for 2-fluorotrifluoroephenidine (2-FTFEP, **24a**) run in DMSO-d<sub>6</sub> (δ ppm = 2.50)

**Figure 132:** Stacked 400 MHz <sup>1</sup>H NMR aromatic region for the fluorotrifluoroephenidine regioisomers (FTFEP, **24a** – **24c**)

**Figure 133:** GC-MS chromatograph for the 2' positional isomers of the monofluorinated diphenidine analogues including internal standard eicosane (**E**) and common adulterants: benzocaine (**B**); paracetamol (**P**) and caffeine (**C**), run in a full scan mode.

**Figure 134:** GC-MS chromatograph for the 3' positional isomers of the monofluorinated diphenidine analogues including internal standard eicosane (**E**) and common adulterants: benzocaine (**B**); paracetamol (**P**) and caffeine (**C**), run in a full scan mode.

**Figure 135:** GC-MS chromatograph for the 4' positional isomers of the monofluorinated diphenidine analogues including internal standard eicosane (**E**) and common adulterants: benzocaine (**B**); paracetamol (**P**) and caffeine (**C**), run in a full scan mode.

**Figure 136:** Mass spectrum for the fluoroephenidine (FEP) regioisomers (**15a**–**15c**)

**Figure 137:** Mass spectrum for the fluorolintane (FL) regioisomers (**19a**–**19c**)

**Figure 138:** Mass spectrum for the fluphenidine (FP) regioisomers (**20a**–**20c**)

**Figure 139:** Mass spectrum for the fluoromephenidine (FMP) regioisomers (**21a**–**21c**)

**Figure 140:** Mass spectrum for the fluorodimephenidine (FDMP) regioisomers (**22a**–**22c**)

**Figure 141:** Mass spectrum for the fluorodiephenidine (FDEP) regioisomers (23a–23c)

**Figure 142:** Mass spectrum for the fluorotrifluoroephenidine (FTFEP) regioisomers

**Figure 143:** Stacked 60 MHz  $^1\text{H}$  NMR spectra showcasing the aliphatic regions for the monofluorinated diphenidine analogues run in DMSO- $d_6$  ( $\delta$  ppm = 2.50)

**Figure 144:** Stacked 60 MHz  $^1\text{H}$  NMR spectra showcasing the aromatic region for the fluoroephenidine regioisomers (4-FEP, 15a–15c)

**Figure 145:** Stacked 60 MHz  $^1\text{H}$  NMR spectra showcasing the aromatic region for the fluorolintane regioisomers (FL, 19a–19c)

**Figure 146:** Stacked 60 MHz  $^1\text{H}$  NMR spectra showcasing the aromatic region for the fluphenidine regioisomers (FP, 20a–20c)

**Figure 147:** Stacked 60 MHz  $^1\text{H}$  NMR spectra showcasing the aromatic region for the fluoromephenidine regioisomers (FMP, 21a–21c)

**Figure 148:** Stacked 60 MHz  $^1\text{H}$  NMR spectra showcasing the aromatic region for the fluorodimephenidine regioisomers (FDMP, 22a–22c)

**Figure 149:** Stacked 60 MHz  $^1\text{H}$  NMR spectra showcasing the aromatic region for the fluorodiephenidine regioisomers (FDEP, 23a–23c)

**Figure 150:** Stacked 60 MHz  $^1\text{H}$  NMR spectra showcasing the aromatic region for the fluorotrifluoroephenidine regioisomers (FTFEP, 24a–24c)

**Figure 151:** Stacked 60 MHz  $^{19}\text{F}$  NMR spectra for the fluorotrifluoroephenidine regioisomers (FTFEP, 24a–24c)

**Figure 152:** Calibration graph for the 4-FEP isomer using  $^{19}\text{F}$  NMR spectroscopy on a 60 MHz instrument

**Figure 153:** Reaction scheme for the synthesis of the polyfluorinated ephenidine compounds (15d – 15l)

**Figure 154:**  $^1\text{H}$  NMR spectrum (400 MHz) of the 2,3-difluoroephenidine (2,3-DFEP, 15d) isomer run in DMSO- $d_6$  ( $\delta$  ppm = 2.50)

**Figure 155:** Stacked  $^1\text{H}$  NMR spectra for the DFEP regioisomer aromatic regions run in DMSO- $d_6$  ( $\delta$  ppm = 2.50) acquired using a 400 MHz instrument

**Figure 165:** GC-MS chromatographs for all nine polyfluorinated ephenidines (15d–15l)

**Figure 166:** Mass spectrometry fragmentation pattern for polyfluorinated ephenidine regioisomers

**Figure 167:** EI-MS spectra for all the DFEP regioisomers (**15d–15i**)

**Figure 168:** EI-MS spectra for the TriFEP, TeFEP and PFEP compounds

**Figure 169:**  $^1\text{H}$  NMR comparison using 400 MHz and 60 MHz instruments for the 2,3-DFEP (**15d**) and 2,6-DFEP (**15g**) isomers

**Figure 170:** Stacked  $^1\text{H}$  NMR spectra for all DFEP regioisomers (**15d–15i**) focusing on the aromatic region

**Figure 171:** Stacked  $^{19}\text{F}$  NMR spectra for all DFEP isomers (**15d–15i**)

**Figure 172:** Stacked  $^{19}\text{F}$  NMR spectra for the tri (bottom), tetra (middle) and pentafluoroephenidine (top) regioisomers (**15j–15k**) using 60 MHz NMR

**Figure 173:**  $^{19}\text{F}$  NMR *J*-resolved spectra for the 2,3-difluoroephenidine (**15d**) sample

**Figure 174:**  $^{19}\text{F}$  NMR *J*-resolved spectra for the 2,4-difluoroephenidine (**15e**) sample

**Figure 175:**  $^{19}\text{F}$  NMR *J*-resolved spectra for the 2,5-difluoroephenidine (**15f**) sample

**Figure 176:**  $^{19}\text{F}$  NMR *J*-resolved spectra for the 2,6-difluoroephenidine (**15g**) sample

**Figure 177:**  $^{19}\text{F}$  NMR *J*-resolved spectra for the 3,4-difluoroephenidine (**15h**) sample

**Figure 178:**  $^{19}\text{F}$  NMR *J*-resolved spectra for the 3,5-difluoroephenidine (**15i**) sample

**Figure 179:**  $^{19}\text{F}$  NMR TOCSY spectra of a mixture of six DFEP (**15d–15i**) regioisomers

**Figure 180:** Truncated  $^{19}\text{F}$  NMR TOCSY spectrum shown in figure 190 to highlight the coupling interactions

## Abbreviations and Acronyms

ACMD	Advisory Council on the Misuse of Drugs
ADD	Attention Deficit Disorder
ADHD	Attention Deficit Hyperactivity Disorder
BP	Brophenidine
COSY	Correlation Spectroscopy
CP	Chlophenidine
DAT	Dopamine transporter
DEA	Drug Enforcement Administration
DFEP	Difluoroephedrine
ELISA	Enzyme-linked immunosorbent assay
EMCDDA	European Monitoring Centre for Drugs and Drug Addiction
EWA	Early Warning Advisory
FA	Fluoroamphetamine
FDEP	Fluorodiephenidine
FDMP	Fluorodimephenidine
FEP	Fluoroephedrine
FL	Fluorolintane
FMC	Fluoromethcathinone
FMP	Fluoromephedrine
FP	Fluphenidine
FTFEP	Fluorotrifluoroephedrine
GBL	Gamma-butyrolactone
GC-MS	Gas Chromatography - Mass Spectroscopy
GHB	Gamma-hydroxybutyrate
GMP	Greater Manchester Police
HPLC	High Performance - Liquid Chromatography
IP	Iodophenidine
LC	Liquid Chromatography
LC-MS-MS	Liquid Chromatography - Tandem Mass Spectroscopy
LOD	Limits Of Detection
LOQ	Limit Of Quantification
MCAT	Methcathinone
MDDP	Methylenedioxydiphenidine
MDMA	Methylenedioxymethamphetamine
MDPV	Methylenedioxypropylone
mg	Milligrams
MHz	Megahertz
MIP	Molecularly Imprinted Polymers
mL	Millilitres
MMC	Methylmethcathinone

MoDA	Misuse of Drugs Act
MS	Mass Spectroscopy
MXE	Methoxetamine
MXP	Methoxphenidine
NET	Norepinephrine transporter
NMDA	N-methyl-D-aspartate
NMR	Nuclear Magnetic Resonance
NPD	Naphthenidine
NPS	New Psychoactive Substances
PCP	Phencyclidine
PFEP	Pentafluoroephenidine
qNMR	Quantitative Nuclear Magnetic Resonance
R <sub>f</sub>	Retention factor
RR <sub>t</sub>	Relative Retention time
RSD	Relative Standard Deviation
R <sub>t</sub>	Retention time
SERT	Serotonin transporter
SIM	Single Ion Monitoring
SPE	Solid Phase Extraction
SS	Street Sample
TeFEP	Tetrafluoroephenidine
TFA	Trifluoroacetic acid
TFMMC	Trifluoromethylmethcathinones
TFMXP	Trifluoromethoxphenidine
TLC	Thin Layer Chromotography
TMS	Tetramethylsilane
TOCSY	Total Correlation Spectroscopy
TriFEP	Trifluoroephenidine
UHPLC	Ultra-High Pressure Liquid Chromotography
UNODC	United Nations On Drugs and Crime
VMAT2	Vesicle monoamine transporter 2

# 1. Chapter 1 – Introduction

## 1.1. UK Misuse of Drugs Act (1971)

In the United Kingdom, the main control of drugs and illegal substances is the Misuse of Drugs Act (1971), which makes new laws with respect to dangerous or otherwise harmful drugs and related matters.<sup>5</sup> Prior to the Misuse of Drugs Act (1971), substances had been controlled through separate acts and new substances were added upon discovery and realisation of the potential for harm. Opium was regulated through the Pharmacy Act of 1868, while cocaine (Figure 1, **1**) and morphine (Figure 1, **2**), isolated from opium plants, were restricted later through the Poisons and Pharmacy Act 1908.<sup>6</sup> The Drugs (Prevention of Misuse) Act 1964 was produced to control amphetamine (Figure 1, **3a**) and its derivatives, including substances such as methamphetamine (Figure 1, **3b**), which had grown in popularity over previous years due to the stimulating and hallucinogenic properties that they exhibit upon consumption.

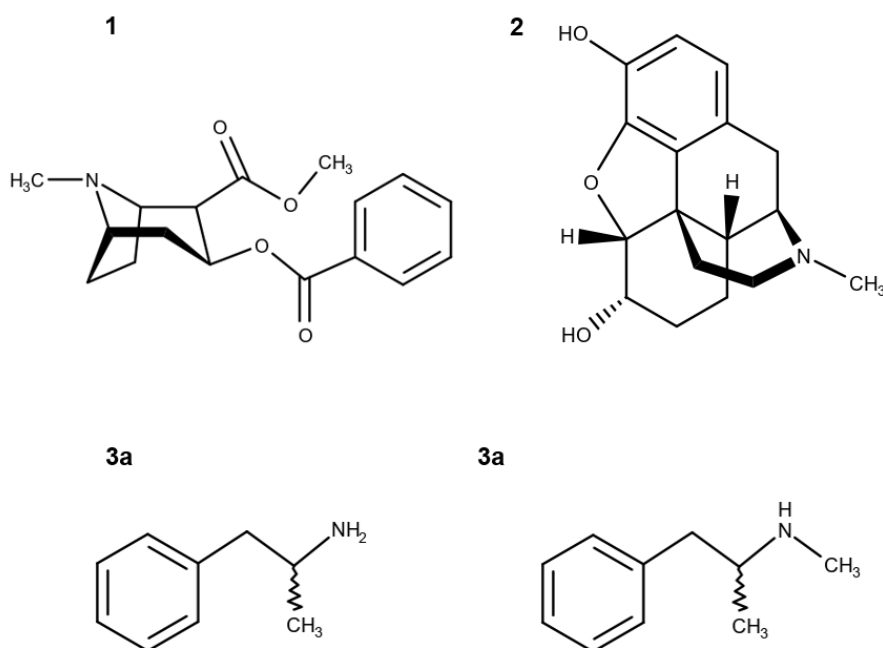


**Figure 1:** Chemical structures of cocaine (**1**), morphine (**2**), amphetamine (**3a**) and methamphetamine (**3b**)

The United Kingdom government then produced the Medicines Act (1968) in order to control the production and supply of medicines aimed for human use.<sup>7</sup> This act controls whether a drug can be purchased generally over the counter, through a pharmacist or through proscribed prescriptions. Punishments for possession of harmful drugs obtained for reasons other than medicinal use cannot be enforced through the Medicines Act and this led to the creation of the Misuse of Drugs Act (1971).

The Misuse of Drugs Regulations (2001) were produced in order to allow the lawful production and possession of controlled substances for legitimate circumstances. This regulation covers the administration, possession, destruction and disposal of these substances.<sup>8</sup> The Misuse of Drugs Act (1971) was amended in 2005 to review the classification system of controlled substances and amendments were made to schedule 1. Changes were also made to policing powers relating to drugs and sentencing punishments.<sup>9</sup>

It is the duty of the Advisory Council on the Misuse of Drugs (ACMD), founded in 1971, to keep under review the situation in the UK regarding drugs that are, or appear to be, misused or where misuse appears capable of having harmful effects sufficient to constitute a social problem.

Controlled drugs can be placed into three different classes (A, B or C) depending on how dangerously the advisory council views them to society. The Misuse of Drugs Act (1971) also defines the penalties associated with a series of offences including unlawfully supplying, producing or possessing controlled substances. Examples of controlled drugs and their classes can be seen in Table 1.

**Table 1:** Classifications of controlled substances and examples of drugs in each class

<b>Class</b>	<b>Examples of controlled substances within class</b>
<b>A</b>	cocaine, methadone, methamphetamine, MDMA and heroin
<b>B</b>	mephedrone, methylone, MDPV, ketamine and cannabis
<b>C</b>	anabolic steroids, GBL, GHB and khat

The advisory council is constantly reviewing the list of controlled drugs with methamphetamine reclassified from a class B substance to a class A drug in January 2007. Ketamine was added as a class C drug in 2006 before being reclassified to a class B substance as recently as 2014.<sup>10</sup>

Substances are also controlled by the controlled substances act, which is part of the Comprehensive Drug Abuse Prevention and Control Act (1970). The Drug Enforcement Administration (DEA) divided substances into schedules based on potential for abuse and addictiveness, as well as whether or not the substance has any legitimate medicinal uses.<sup>5</sup> Substances deemed to have the highest potential for abuse or potential for severe psychological and physical dependence are listed under schedule 1. Drugs on schedule 1 have no current accepted medicinal use. Schedule 5 substances are deemed to have the least potential for abuse.

There are some crossovers between class A substances and schedule 1 substances with compounds such as heroin and MDMA appearing on both lists. There are also differences with substances such as cocaine and methadone appearing as class A drug but being placed into schedule 2.

Currently, punishments are scaled based on a substances classification; however, processes by which harm is determined can be unclear. New



systems are being suggested for assessing the potential harm of controlled substances based on physical harm, social harm and dependence.<sup>11</sup>

Identification of samples is important for prosecution in order to make sure the correct punishment is enforced. The maximum sentences for supplying and possessing controlled substances can be seen in Table 2. In 2001 the regulations were revised to take into account the circumstances where it is lawful to possess, or produce and supply substances that have medicinal or therapeutic values. These substances were divided into five schedules (Table 3) with freedom to possess and supply being restricted by the assignment of a controlled drug to a schedule.

**Table 2:** Table showing maximum punishments for possession and supply of controlled substances <sup>12</sup>

<b>Drug Class</b>	<b>Possession</b>	<b>Supply and intent to supply</b>
<b>A</b>	7 years imprisonment and unlimited fine	Life imprisonment and unlimited fine
<b>B</b>	5 years imprisonment and unlimited fine	14 years imprisonment and unlimited fine
<b>C</b>	2 years imprisonment and unlimited fine	14 years imprisonment and unlimited fine

**Table 3:** Drug schedules and an explanation of what constitutes each schedule <sup>13</sup>

Drug Schedule	Schedule explanation
1	Includes drugs not used medicinally including hallucinogenic drugs (such as LSD), ecstasy type substances, raw opium and cannabis. A home office license is required for their production, possession and supply.
2	Includes opiates (such as heroin, morphine and methadone hydrochloride), major stimulants, cocaine, ketamine and cannabis-based products for medicinal uses. Schedule 2 controlled drugs are subject to the full controlled drug requirements
3	Includes the barbiturates which are subject to the special prescription requirements. Safe custody requirements do apply although records in registers do not need to be kept.
4	Schedule 4 is split into two parts. Part 1 includes drugs that are subject to minimal control, such as benzodiazepines and non-benzodiazepine hypnotics. Part II includes androgenic and anabolic steroids. Controlled drug prescription requirements do not apply and schedule 4 controlled drugs are not subject to safe custody requirements.
5	Includes preparations of certain controlled drugs, such as codeine, pholcodine or morphine, which due to their low strength, are exempt from virtually all controlled drug requirements other than retention of invoices for two years.

## 1.2. Psychoactive Substances Act (2016)

New Psychoactive Substances (NPS), which have recently been controlled by the Psychoactive Substances Act (2016),<sup>1</sup> have continued to feature prominently on the recreational drug scene. Synthetic recreational drugs have reportedly been produced since the 1920s with prevalence coming more recently through “head shops” and the rise of online markets.<sup>14</sup> In 2006, the European Monitoring Centre for Drugs and Drug Addiction (EMCDDA) began to monitor the number of new compounds reported annually, with the amount of substances reported rising sharply from 5 – 45 within 4 years.<sup>15</sup> It is reported that by 2006 clandestine labs and manufacturers of NPS had begun searching through failed pharmaceuticals or “designer medicines” which could be altered in order to produce new substances undetected by analytical techniques.<sup>16</sup> The control of popular psychoactive substances such as amphetamine (Figure 1, **3a**) and 3,4-methylenedioxymethamphetamine (MDMA, Figure 2, **3c**) led to a need for legal alternatives to be produced.

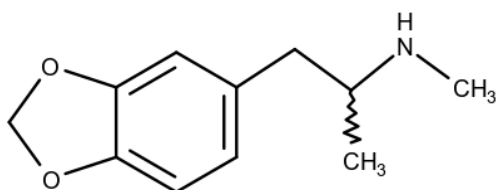


**Figure 2:** Chemical structure of 3,4-methylenedioxymethamphetamine (MDMA), **3c**

Prior to the introduction of the Psychoactive Substances Act (2016), NPS had grown in popularity due to their capability of avoiding control, as they are not scheduled under the Misuse of Drugs Act (1971), and their ability to mimic psychotropic effects of illicit substances. Although “designer drugs” had been observed in the late 1970s and early 1980s, production and marketing of these substances had dramatically increased in the 21st century and is still prevalent in the present day.<sup>17</sup>

Post mortem and criminal casework studies have been carried out involving NPS with 203 cases reported between 2010 and 2012 with 120 NPS observed in 2012 alone. From these reports effects and toxicities of the NPS could be

seen and reported for future encounters with the substances.<sup>18</sup> In 2014, 101 substances were reported to EU Early Warning System.<sup>19</sup> Constant analysis of NPS has been on going prior to the introduction of the New Psychoactive Substances Act (2016), showing limitations of current techniques, such as liquid chromatography, and toxicology information with the introduction of new compounds.<sup>20</sup> NPS have also been encountered alongside controlled substances under the Misuse of Drugs Act (1971).<sup>21</sup>

Popularity of NPS has also increased due to the ease of accessibility. NPS were originally sold in 'head shops' and these substances had been encountered, in colourful packaging, labelled as 'plant food', 'bath salts' or 'not fit for human consumption'.<sup>22</sup> More than 600 substances had been reported to the United Nations on Drugs and Crime Early Warning Advisory (UNODC EWA) council by the end of 2016 with the number increasing to just under 800, from 110 territories, by the end of 2017 (Figure 3).<sup>23</sup>

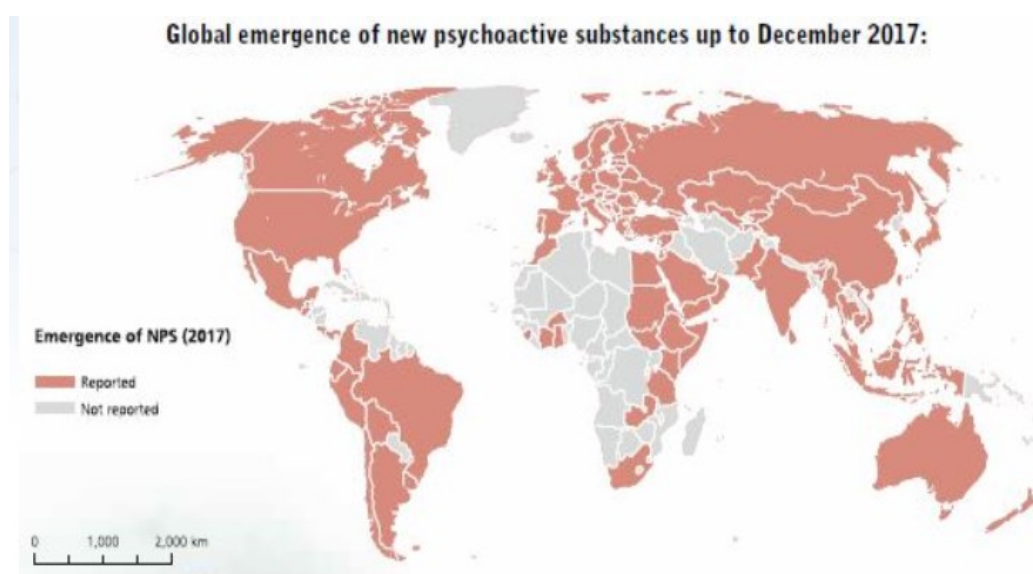


**Figure 3:** Image showing the countries that reported the presence of NPS in 2017, to the UNODC and the number of NPS reported.<sup>23</sup>

This shows the lack of impact the Psychoactive Substances Act (2016) had on the production and distribution of NPS with more substances still being reported after the act was established. One reason for the continued increase in the number of NPS in circulation is through the emergence of the Dark Web

(hidden websites that require encryption or specific software to uncover).<sup>24</sup> There is a danger to the online marketing of these samples as there is a lack of knowledge and intelligence surrounding the compounds and information based on dosage and side effects may be limited. This can lead to NPS becoming more dangerous than substances controlled by the misuse of drugs act and more work is needed for harm reduction and detection.<sup>25</sup>

Synthesis of many NPS occurs through legitimate medical research or as a result of clandestine adaptation and derivatisation of drugs previously controlled. Although synthesis of these substances can, at times, be complicated, it can be carried out in clandestine labs with basic chemistry knowledge. Literature has been published showing the synthesis of multiple NPS reference standards used for testing.<sup>26</sup> It is the slight alteration of chemical structures that allows substances to avoid initial detection and allows production of samples, which can then be supplied and offered without repercussions.

The introduction of the Psychoactive Substances Act (2016) also causes analytical challenges for prosecution, due to the differences in sentencing compared to the Misuse of Drugs Act (1971), making it essential to be able to identify and distinguish substances. NPS can cause significant and life threatening side effects, especially when a dosage is taken to match the effects of controlled substances, and this means health-care providers must be familiar with these novel psychoactive substances. There is also a clear importance to developing rapid and mobile techniques, that can be used by all involved with medical toxicology and providing primary care, to recognize and report these materials as soon as they are encountered.<sup>27, 28</sup>

Many of the NPS that are encountered or seized in criminal cases can be classified as synthetic cathinones (e.g. mephedrone and MDPV),<sup>29</sup> piperazines (e.g. N-benzylpiperazine) and pyrrolidines (e.g. prolintane),<sup>30</sup> benzodiazepines,<sup>31, 32</sup> piperidines (e.g. diphenidine),<sup>33, 34</sup> aminoindanes (e.g. MDAI) or phenethylamines (e.g. NBOMe derivatives) (Figure 4).<sup>35, 36</sup>

Synthetic cannabinoid receptor agonists are a class of psychoactive substances that have also been encountered more frequently in the past few years and have shown prevalence in prisons.<sup>37</sup> These principle classes of substances are discussed in the subsequent sections.

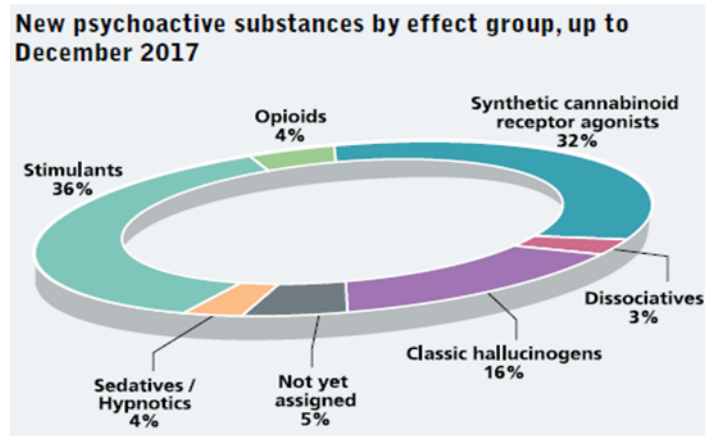


**Figure 4:** Image showing the classification of NPS reported to the EU early warning system.<sup>23</sup>

### 1.3. Amphetamines

Amphetamine (Figure 1, **3a**) is a substance that belongs to the phenethylamine (Figure 5, **3d**) class of psychoactive drugs. Amphetamines are controlled substances and are scheduled as a class B drug under the Misuse of Drugs Act (1971).<sup>5</sup> Many controlled substances, including the class methamphetamine (Figure 1, **3b**) and 3,4-methylenedioxymethamphetamine (MDMA) (Figure 2, **3c**), are derived from the amphetamine structure and are described as “substituted amphetamines”. Along with cocaine, amphetamines are one of the most commonly used illicit substances and this prevalence along with abuse of methamphetamine has led to a dramatic increase in the number of emergency department visits for amphetamine intoxication.<sup>38, 39</sup>

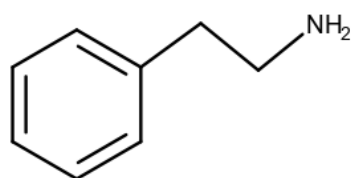


**Figure 5:** Chemical structure of phenethylamine (**3d**)

Amphetamines are abused due to the stimulating and physiological effects they generate. MDMA, also known for its entactogenic effects inducing a pleasant and relaxed feeling of happiness that results in consumers becoming addicted to the substance.<sup>40</sup> Methamphetamine also provides stimulating effects as well as sympathomimetic effects through interaction with the sympathetic nervous system receptors.<sup>41</sup> Reports have shown that the biological effects observed when comparing amphetamine and methamphetamine do not differ significantly in the stratum, however dopamine release is increased in the prefrontal cortex to a greater extent through amphetamine use as opposed to methamphetamine.<sup>42</sup> Amphetamines also increase the levels of norepinephrine in a corresponding manner to the release of dopamine.<sup>43</sup> Reports by Shoblock *et al.* suggest there is no difference in the addictive nature or psychostimulant potency between amphetamine and methamphetamine.<sup>44</sup>

Amphetamines were initially used as a treatment for narcolepsy, however research has shown therapeutic uses for the treatment of disorders such as Attention Deficit Disorder (ADD) and Attention Deficit Hyperactivity Disorder (ADHD) as well as uses in cases of obesity and depression.<sup>45</sup>

The enzyme-linked immunosorbent assay (ELISA) based test has become a screening test developed for analysis of amphetamines in a forensics laboratory environment. It is a biochemical technique that will allow detection of an analyte through the use of antibodies. An enzyme will link to this antibody and a detectable signal is emitted usually in the form of a colour change. Testing has been carried out using ELISA tests on a number of matrixes including blood plasma, oral fluids, sweat and hair samples for the detection of amphetamines.<sup>46, 47</sup> ELISA testing relies on the production of antibodies, for the enzyme binding to occur, which means the drug must have previously been encountered. This becomes a problem when novel designer drugs are first observed as a slight alteration in structure will mean specific immunoassay kits will no longer recognise target compounds. This has been reported with designer drugs of amphetamine and methamphetamine, where amphetamine specific ELISA tests have been unable to produce a positive result for any of the amphetamine designer drugs at concentrations representative of forensic samples.<sup>48</sup>

As well as ELISA testing, liquid chromatography (LC) and ultra-high pressure liquid chromatography (UHPLC) have been utilised for the detection of amphetamine both qualitatively and quantitatively.<sup>49, 50</sup> Tandem mass spectroscopy has also been attached to the chromatography analysis in order to provide further identification information.

In recent years the mono-fluorinated substituted derivatives, fluoroamphetamine (Figure 6, FA, **4**) have been discovered in forensic cases and on the recreational drug's market, mainly around Europe, incorrectly marketed as amphetamine and MDMA.<sup>51, 52</sup> 4'-fluoroamphetamine (4-FA) has



been reportedly detected in both urine and serum using validated GC-MS methods.<sup>53, 54</sup>

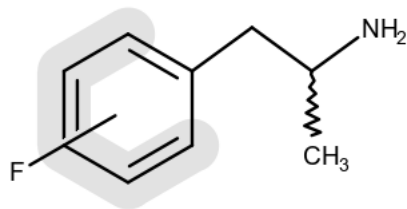


**Figure 6:** Chemical structure of regioisomeric fluoroamphetamine (**4**)

## 1.4. Cathinones

As listed in the Misuse of Drugs Act (1971), cathinone derivatives are currently controlled as class B substances. Cathinone (Figure 7, **5**) is an alkaloid present in the khat bush leaves and was discovered twenty-five years ago. Inhabitants of East Africa and Southern Arabia chewed khat due to the stimulating properties that consumers experienced. After testing and analysis, it was soon discovered that the pharmaceutical profile of cathinone closely resembled that of amphetamine.<sup>55</sup>

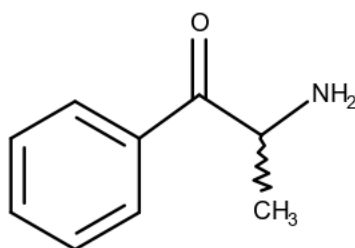


**Figure 7:** Chemical structure of cathinone (**5**)

Cathinones are phenylisopropylamine compounds, with a carbonyl at the benzylic position of the molecule.<sup>4</sup> Prior to the Psychoactive Substances Act (2016), cathinone (**5**) and synthetic cathinone derivatives had been encountered as pure substances but also as the active ingredients (or in combination with other psychoactive substances) in street samples such as “bath salts”.<sup>56, 57</sup>

Cathinone is a hydrophobic (lipophilic) molecule meaning it can cross cell membranes easily and block the uptake of neurotransmitters or increase their secretion. (Hugins, 2014) Similar to amphetamines, cathinones act on dopamine, serotonin and epinephrine transporters, increasing their levels and identified biological targets for cathinones include acetylcholine, serotonin, dopamine, norepinephrine, histamine and sigma-1 receptors, voltage-gated sodium and calcium ion channels, plasma membrane transporters for serotonin, norepinephrine and dopamine (SERT, NET and DAT respectively) and the vesicle monoamine transporter 2 (VMAT2).<sup>4</sup>

The khat plant was used to help with depression due to the stimulating effects that it provides. Khat was also used to help with obesity as the substance has a tendency to suppress the appetite. Effects that were also reported including a feeling of calm during the periods where khat was chewed, feelings of elation and an increase in alertness. However, migraines, insomnia, feelings of anxiety and aggression, paranoia, high blood pressures and heart problems have all been reported as side effects that occur after constant usage of khat plants.<sup>58</sup>

Cathinone and its derivatives are not detectable using the ELISA-based amphetamine test, showing the desperate need for an alternative rapid screening test.<sup>59</sup> Detection of cathinone has been reported for urine and plasma from khat users using techniques such as GC-MS and high performance - liquid chromatography (HPLC).<sup>60, 61</sup>

### 1.4.1. Methcathinone

Methcathinone (Figure 8, **6**), also known as ephedrone or MCAT, is a substituted cathinone and an illicit drug scheduled as a class B drug under the Misuse of Drugs Act (1971). Methcathinone is a monoamine alkaloid and the stimulating properties that methcathinone provide means that it is abused as a recreational drug.

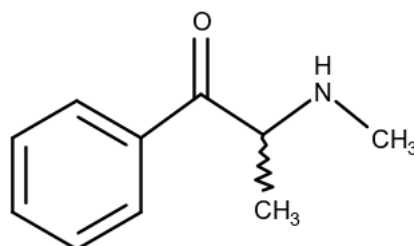


**Figure 8:** Chemical structure of methcathinone (**6**)

Reports have suggested that users complain of the need for increased dosages, when using synthetic cathinones, such as methcathinone, and a frequent need to reuse in order to prolong effects. Studies also show that there is a threefold increase in activity in certain areas of the brain, compared to  $\beta$ -keto-amphetamines, when being used for its stimulating effects. This shows the potential danger of overdosing that surrounds the use of cathinones and the threat to health that these substances pose. It has been reported that methcathinone has an addictive nature with symptoms of withdrawal being experienced after prolonged usage or administration of high dosages.<sup>62, 63</sup>

Detection of methcathinone has been reported utilizing a variety of chromatographic methods such as GC-MS and LC/MS-MS. This has included methcathinone samples that have been discovered alongside phenalkylamines as well as cathinone in both urine specimens and human blood plasma. This has shown that methcathinone can be detected using these techniques, however, it has also been reported that when using GC-MS to detect methcathinone a second peak is observed and characterized as 2,3-enamine, produced through thermal oxidation during heating in the column. This is similar to the thermal degradation seen with the fluoroamphetamines.

This shows that difficulties do arise when testing cathinones through this instrumentation and alternative methods may be needed to detect these samples especially when purity testing or testing of mixtures is required.<sup>64-66</sup>

#### 1.4.2. 4'-Methylmethcathinone

4-Methylmethcathinone (4-MMC) is a stimulant drug similar in structure to ephedrone and is another synthetic derivative of cathinone. 4-Methylmethcathinone (Figure 9, **7c**, 4-MMC) is also known as mephedrone, however the regioisomers of 4-methylmethcathinone, 2-methylmethcathinone and 3-methylmethcathinone (Figure 9, **7a** and **7b** respectively) have also been observed and reported in the literature.<sup>67</sup>

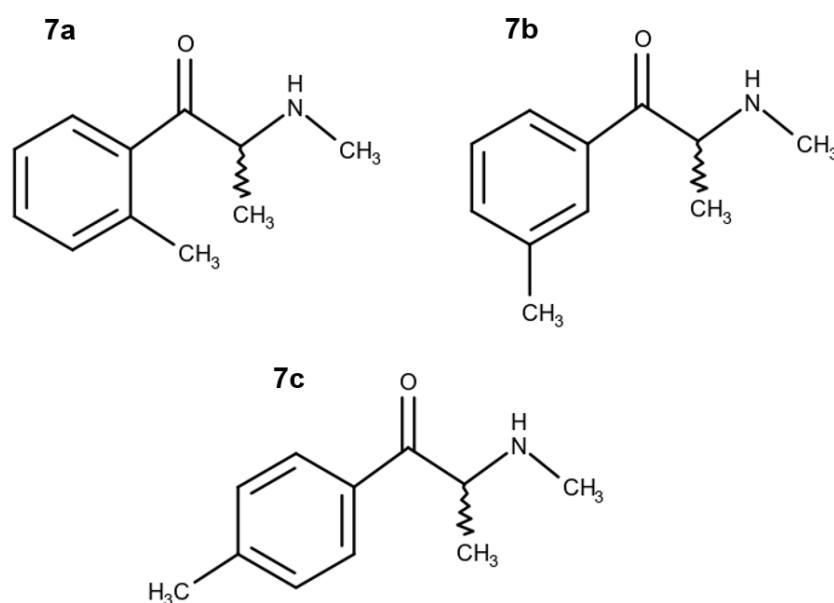


**Figure 9:** Chemical structures of the methylmethcathinone regioisomers (**7a – 7c**)

Investigations show that users complain of the need for high doses (200 mg of 4-methylmethcathinone taken orally) and a frequent need to reuse as the effects only last around 2-4 hours. Some users also reported to taking as much as two grams in a 4 hour period to prolong the psychoactive effects of the drug.<sup>68</sup> This is an important fact as if a greater amount of 4-MMC is needed in order to match the effects of other recreational drugs then there is an increased risk that overdoses will occur, leading to emergency cases where

people's health is at severe risk. 4-methylmethcathinone targets similar receptors to those reported for cathinone and ephedrone.<sup>69</sup>

Analysis for the detection of mephedrone has been reported via GC-MS methods along with quantitative analysis using LC-MS. This has been applied to hair samples where a positive test has shown the presence of mephedrone. There are also reports of quantitative and qualitative analysis of mephedrone being performed on blood samples taken from fatalities linked to the drug. NMR analysis is also available for the structural elucidation of the mephedrone isomers and can be used as reference spectra.<sup>70-73</sup>

#### 1.4.3. 4'-Fluoromethcathinone (flephedrone)

4'-Fluoromethcathinone (4-FMC), also known as flephedrone, is a new psychoactive substance that was discovered in samples that were previously sold as "plant feeders" from head shops and internet retailers. The samples were observed as capsules as well as white powders and the majority of samples seized were either 4'-fluoromethcathinone (Figure 10, **8c**, 4-FMC) or 3-fluoromethcathinone (Figure 10, **8b**, 3-FMC). The position of the fluorine on the benzyl ring was determined using reference samples synthesized and purchased from suppliers.<sup>68</sup>

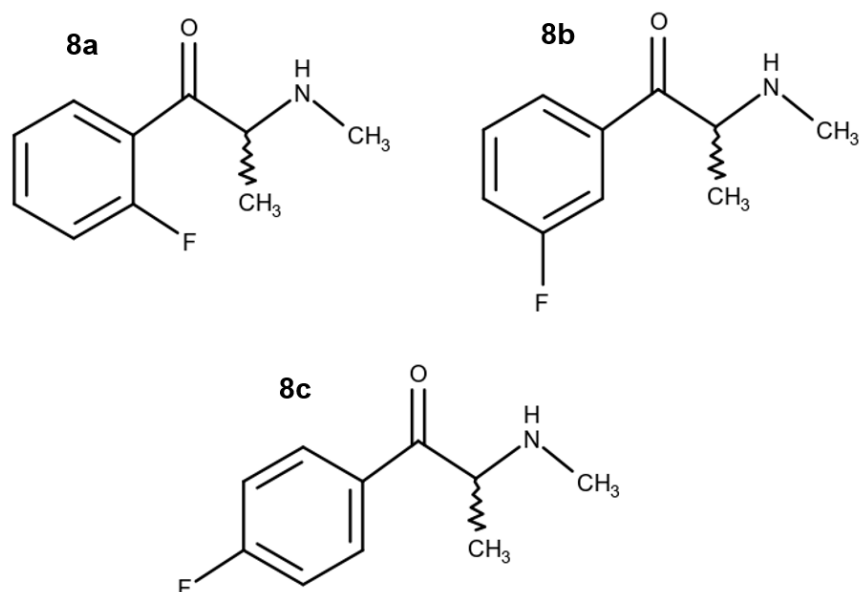


**Figure 10:** Chemical structures of fluoromethcathinone regioisomers (FMC, **8a–8c**)

Fluoromethcathinone regioisomers are reported to induce the release of dopamine in a similar manner to both methcathinone and methylmethcathinone.<sup>68, 74</sup>

Detection and analysis of flephedrone and the regioisomers including 2-fluoromethcathinone (Figure 10, **8a**, 2-FMC) has been reported previously although it has not been as extensively covered when compared to methcathinone and its methyl derivatives. Detection of the 4-FMC isomer has been applied using both GC-MS and high resolution LC-MS. This analysis has been performed on urine and liver microsomes as well as on street samples where FMC may be cut with adulterants such as benzocaine or caffeine. 4-FMC has also been detected in hospital cases where it has been taken along with other psychoactive substances.<sup>68, 75, 76</sup>

Again as with other amphetamines and cathinones the fluorine derivatives show thermal degradation in the injection heating with GC-MS analysis. Reports have shown difficulties in attempts to separate the 3- and 4-FMC isomers when run using matching methods showing a need for new methods to be developed or new techniques to be introduced.<sup>77</sup> Baseline separation has been achieved for all three regioisomers, using GC-MS, however this was

done through heptafluorobutyrylation derivatisation which can be time consuming as sample preparation.<sup>78</sup> It has also been shown through characterisation of the 3- and 4- isomers that the <sup>19</sup>F NMR provides differing chemical shifts and can be used to distinguish between isomers, however this has not been done on mixtures or for all three isomers.<sup>68</sup>

Fluorine is commonly used in pharmaceuticals to increase polarity in compounds, which also effects receptor binding and biological activity.<sup>2</sup> Fluorine is one of the most electronegative elements and has a higher bond energy with carbon when compared to the hydrogen-carbon bond. This means the carbon-fluorine bond is stronger and more stable, meaning it is less sensitive to metabolic degradation and metabolic rates are slowed. Adding fluorine to compounds can also increase their lipophilicity, which is the ability to dissolve in fats. This is due to the fluorine-carbon bond being more hydrophobic than the carbon-hydrogen bond. This usually results in increased cell membrane penetration and increased drug bioavailability.<sup>79, 80</sup> The most common general anaesthetic agents now contain fluorine as they have been shown to be safer longer lasting.<sup>81</sup>



#### 1.4.4. Ortho-, meta- and para- trifluoromethylmethcathinone

Trifluoromethylmethcathinones (TFMMC) are trifluoromethyl (CF<sub>3</sub>) analogues of methcathinone where the substituent may reside at the 2-, 3- and 4- position of the aromatic ring (Figure 11, **9a**, **9b** and **9c** respectively).

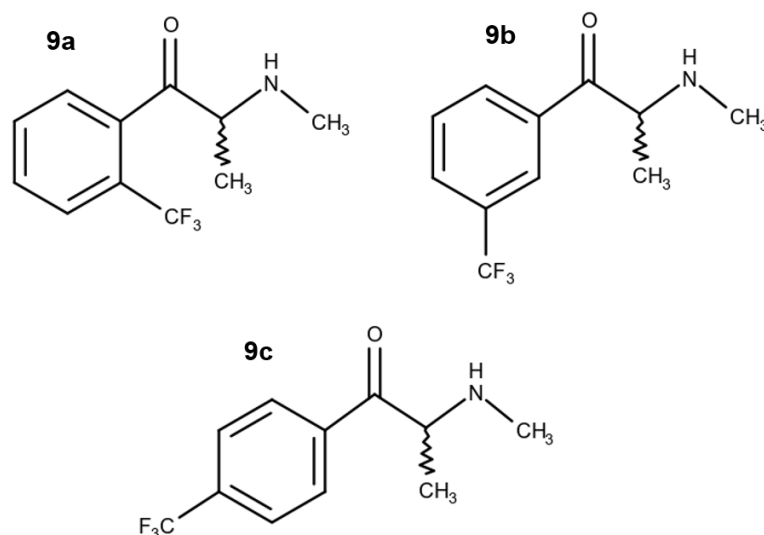


**Figure 11:** Chemical structures of the trifluoromethylmethcathinone regioisomers (TFMMC, **9a – 9c**)

The report by Cozzi *et al.* also shows that 3-trifluoromethylmethcathinone and 4-trifluoromethylmethcathinone were both 10-fold more potent than methcathinone as uptake inhibitors and releasing agents at the serotonin transporter, but 2-trifluoromethylmethcathinone was both a weak uptake inhibitor and releaser. This is an important fact due to the different isomers having different effects biologically. It is important medically, as well as forensically, to be able to separate them in order to determine what substances have been sold or taken for health concerns. At the norepinephrine and dopamine transporters (NET and DAT) all trifluoromethylmethcathinone isomers were less potent than methcathinone as uptake inhibitors and releasers. The research highlights that in medical and psychiatric conditions trifluoromethylmethcathinones may have therapeutic values and uses. The decrease in DAT activity also shows that there is a lower likelihood of abuse and dependence of the drug compared to methcathinone.<sup>4</sup>

Literature has shown separation of the three TFMMC regioisomers using GC-MS analysis, however degradation has been shown in a similar manner to the FMC isomers, which would make quantification analysis difficult. No validation or quantification analysis has been performed using GC-MS. Again in a similar manner to the FMC isomers  $^{19}\text{F}$ -NMR analysis has shown distinguishable chemical shifts, although no mixtures or calibrations for quantification have been performed.<sup>82</sup> 4-TFMMC has also been analysed using a developed LC-MS method, along with its metabolites.<sup>83</sup>

## 1.5. PCP to MXE

Multiple substances, now controlled by the Misuse of Drugs Act (1971), existed prior to the production of diphenidine (**13a**, figure 15) and these were introduced in order to replace the previous substance that had been controlled. Phencyclidine (Figure 12, **10**, PCP) was first discovered and synthesized in 1956 and was marketed as an anaesthetic pharmaceutical drug, however it soon became popular on the illicit drugs market and through street vendors.<sup>84</sup> PCP, also referred to as angel dust, is a member of the arylcyclohexylamine class and became popular due to its hallucinogenic and dissociative properties. Other side effects with PCP usage include euphoria and a loss of ego boundaries, however, negative side effects also include paranoia, withdrawal symptoms and suicidal thoughts. It has been reported that the effects observed through PCP abuse are due to the substance selectively interacting with a specific (PCP receptor) binding site that is linked closely to the *N*-methyl-D-aspartate (NMDA) receptor.<sup>85</sup>

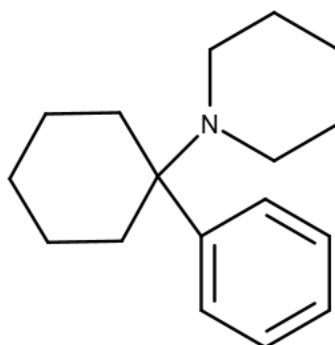


**Figure 12:** Chemical structure of phencyclidine (PCP, **10**)

Ketamine (Figure 13, **11**) is a NMDA antagonist and was first developed as a surgical anaesthetic to replace PCP due to quicker recovery times and less severe side effects experienced. Similar to PCP, ketamine also displays dissociative properties and can also be used to treat chronic pain utilizing its potential to provide pain relief, sedation and memory loss. Ketamine interacts with NMDA receptors in a similar manner to PCP and inhibits its actions, which gives it its sedative qualities.<sup>86-88</sup>

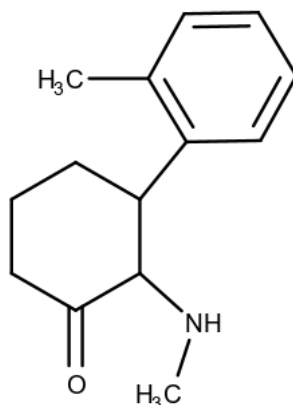


**Figure 13:** Chemical structure of ketamine (11)

Within a few years of medical use, an increase of illicit use was observed for ketamine. It quickly became labelled as a class C drug in 2006 and in 2013 it was reclassified to a class B drug, based on the advisory council's advice on the potential harm that the substance can cause. Many users noted severe hallucinatory effects known as a "K-hole" and long-term users were reported to suffer irreversible damage to the body such as renal failure. Other side effects included abnormal heart rates leading to either extreme high or low blood pressure, anorexia and vomiting.<sup>89-91</sup>

Methoxetamine (Figure 14, **12**, MXE) is an analogue of ketamine and grew in popularity as a legal alternative, which still provided the same dissociative effects to consumers due to the similarities in chemical structure. MXE is believed to be abused due to the prolonged and enhanced effects exhibited prior to consumption. Like ketamine and PCP, MXE is an NMDA antagonist, which will provide sedation and anaesthetic effects as well as analgesia and amnesia. MXE is also a dopamine reuptake inhibitor.<sup>92, 93</sup> Methoxetamine became commercially available in 2010 with negative side effects such as severe nausea, vomiting, diarrhoea, paranoia, and anxiety linked to consumption of MXE.<sup>94, 95</sup>

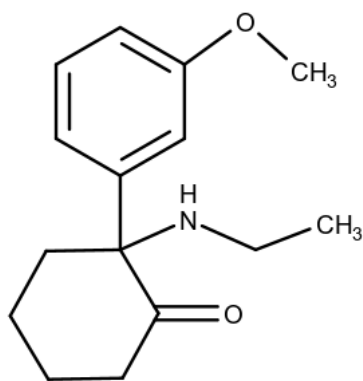


**Figure 14:** Chemical structure of methoxetamine (MXE, 12)

## 1.6. Diphenidine and methoxphenidine

Diphenidines, one of the most recent classes to emerge prior to the NPS act, has been sold on the illicit drugs market and via online vendors. Diphenidine (Figure 15, **13a**) acts as an NMDA antagonist and its 2-methoxy substituted derivative methoxphenidine (Figure 15, **13b**, 2-MXP) was marketed in 2013 as a replacement for the recently controlled compound methoxetamine (MXE).<sup>96</sup>

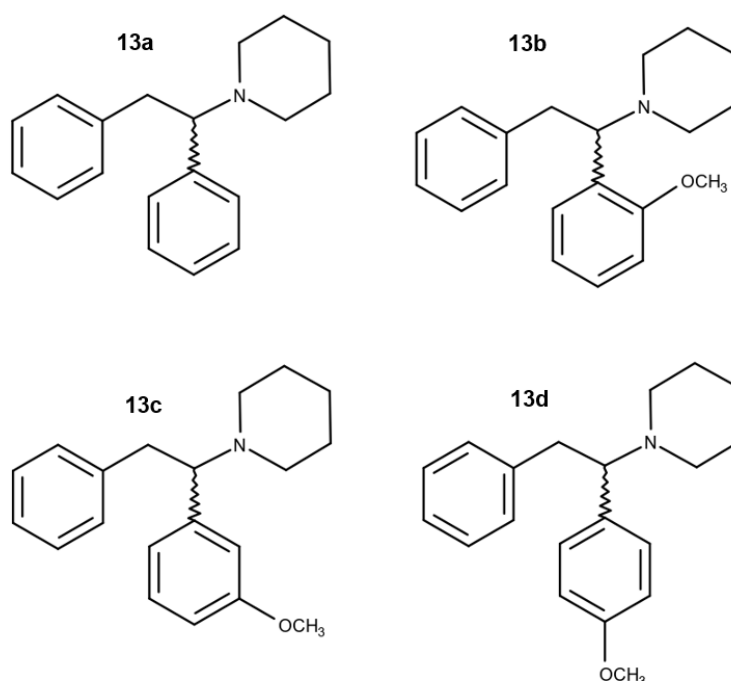


**Figure 15:** Chemical structures of diphenidine (**13a**) and the methoxphenidine regioisomers (MXP, **13b – 13d**)

Diphenidine and MXP were both sold as designer drugs for their dissociative properties and the effects of anaesthesia and euphoria that they provide, in a similar manner to PCP, ketamine and MXE. Both diphenidine and MXP are controlled by the New Psychoactive Substances Act (2016), however, new diphenidine derivatives are constantly being produced, including the regioisomers of 2-MXP, 3-methoxphenidine (Figure 15, **13c**, 3-MXP) and 4-methoxphenidine (Figure 15, **13d**, 4-MXP). These samples create new challenges to prosecute correctly, and also analytically, as a lack of reference material and data on these substances is available.

Diphenidine and MXP have been involved with a number of intoxications and fatalities both as individual components and also when used in combination with one another.<sup>97, 98</sup> Diphenidine and MXP have also been encountered in mixtures along with other psychoactive drugs such as synthetic cannabinoids like AB-CHMINACA, 5F-AMB and 5F-AB-PINACA.<sup>99</sup> Characterization of diphenidine has been performed on a full range of analytical techniques such as <sup>1</sup>H NMR, <sup>13</sup>C NMR, HR-ESI-MS, ESI-MS-MS, GC-(EI/CI)-MS and ATR-IR.<sup>96</sup> Detection of diphenidine has been carried out on a number of samples including blood, tissue, gastric fluid and hair.<sup>100, 101</sup>

McLaughlin *et al.* reported the full characterization of the MXP regioisomers using the same analytical techniques in 2016.<sup>102</sup> The increasing prevalence and detection of both diphenidine and methoxphenidine shows the need for rapid tests to be developed due to the lack of reference standards and data available especially for newly emerging substances. A validated UHPLC method for the separation of the three MXP isomers has also been reported.<sup>103</sup> The regioisomers of MXP have also been detected and quantified using molecularly imprinted polymers (MIPs).<sup>104</sup>

## 1.7. Lefetamine and ephedidine

Lefetamine (**Error! Reference source not found.**Figure 16, **14**) a class B substance, related to the 1,2-diphenylethylamine class of compounds, that was first synthesised and reported in 1945 and has been reported to have effects similar to substances such as codeine and other opiates.<sup>105</sup> Although initial abuse of lefetamine was observed in Japan during the 1950s, it was then introduced in Italy in the 1980s for its use in pain relief in surgery before quickly becoming a substance of abuse.<sup>106</sup> It was shown to be a weaker opiate agonist than most opiates such as morphine and abuse of the substance tended to lead to many users experiencing severe withdrawal symptoms.<sup>107, 108</sup> In 2008, lefetamine and a couple of designer drugs based on lefetamine have been encountered in Germany and possibly shows the re-emergence of this class of compounds as a drug of abuse again.<sup>109</sup>

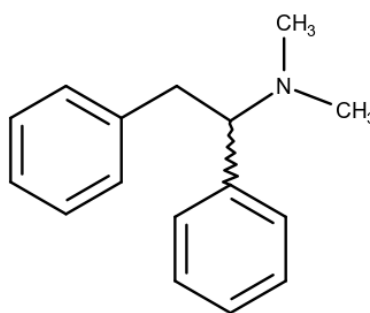


**Figure 16:** Chemical structure of lefetamine (**14**)

Lefetamine and its metabolites have been identified in rat urine as well as human liver, showing the potential for detection in human urine. Both GC-MS and liquid chromatography-high resolution-tandem mass spectrometry (LC-HR-MS/MS) were utilised in order to detect lefetamine in these matrixes.<sup>110</sup>

Ephedidine (Figure 17, **15**) is a recent substance to emerge on the NPS drugs market with its presence being reported in 2017, but there is little literature published on its toxicological effects and methods of identification. Ephedidine was also first marketed as a replacement for PCP, MXE and ketamine for its use as a dissociative anaesthetic. It is a structural isomer of lefetamine with the dimethyl side chain replaced with an ethyl chain. In a similar way to



diphenidine, ephenidine acts as an NMDA receptor antagonist and has been reported in a few intoxications in France.<sup>34, 111, 112</sup>

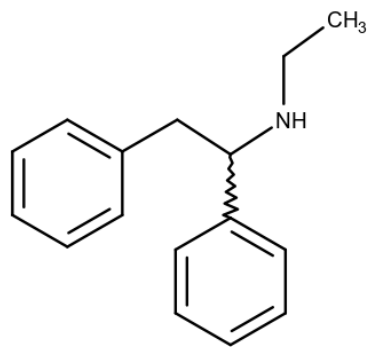


**Figure 17:** Chemical structure of ephenidine (15)

## 1.8. Prolintane and fluorolintane

Prolintane (Figure 18, **16**) was first synthesised and reported around the same time as lefetamine, however it has been used as a substance of abuse since it was first marketed in Europe as an anti-fatigue agent.<sup>113</sup>

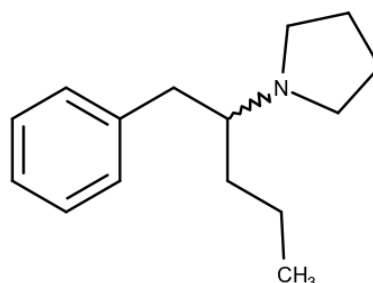


**Figure 18:** Chemical structure of prolintane (**16**)

Similar in structure to the synthetic cathinones pyrovalerone (Figure 19, **17**) and methylenedioxyvalerone (Figure 19, **18**), it was abused for its stimulating properties similar to that of amphetamine. Hallucinations, psychosis, and deaths have been reported after overdosing on prolintane. Metabolic studies have been carried out in both rats and rabbits and GC-MS has been utilised as a method of analysis.<sup>114-116</sup>

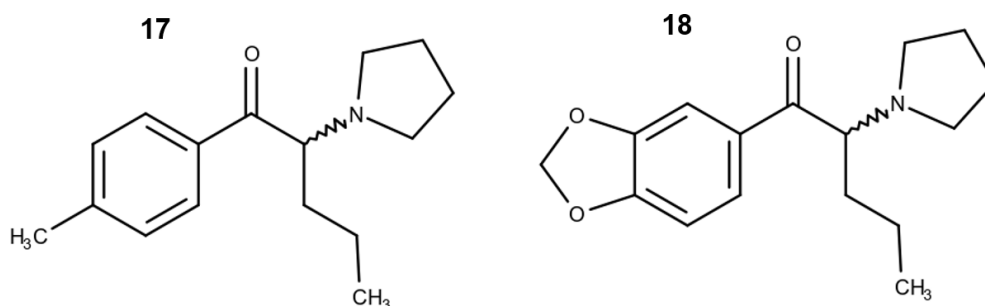


**Figure 19:** Chemical structures of pyrovalerone (**17**) and methylenedioxyvalerone (**18**)

Fluorolintane (Figure 20, **19**) has also been synthesised in a manner similar to diphenidine, ephenidine and lefetamine and is also an NMDA receptor antagonist with dissociative properties.<sup>117</sup> The main structural difference from diphenidine to fluorolintane derives from the alteration of the piperidine ring to a pyrrolidine ring. There is no current literature related to the toxicology of fluorolintane or its detection, however no reports of overdosing related to this substance have been published.

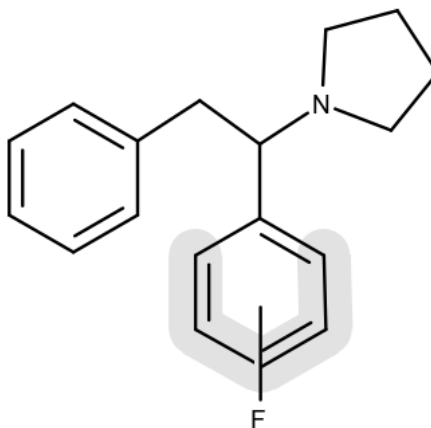


**Figure 20:** Chemical structure of fluorolintane regioisomers (**19**)

## 1.9. Presumptive Testing

In forensic testing, presumptive tests are vital as a rapid response to the presence of possible controlled substances and can act as an important harm reduction tool. The main form of presumptive testing used by police forces and forensic laboratories comes in the form of colour test reagents (Figure 21). The United Nations on Drugs and Crime (UNODC) has guidelines based on the production of test reagents and the positive reactions of commonly encountered controlled substances and NPS.<sup>118</sup> Colour tests are preferred due to their inexpensive nature and ability to provide a fast and simple result, without any analytical instrumentation. However, presumptive colour tests can only identify the possible presence of a specific class being present and not which specific substance is present. A problem also arises with the introduction of multiple new substances as this increases the number of false positives that can be associated with a specific testing reagent.<sup>3</sup>

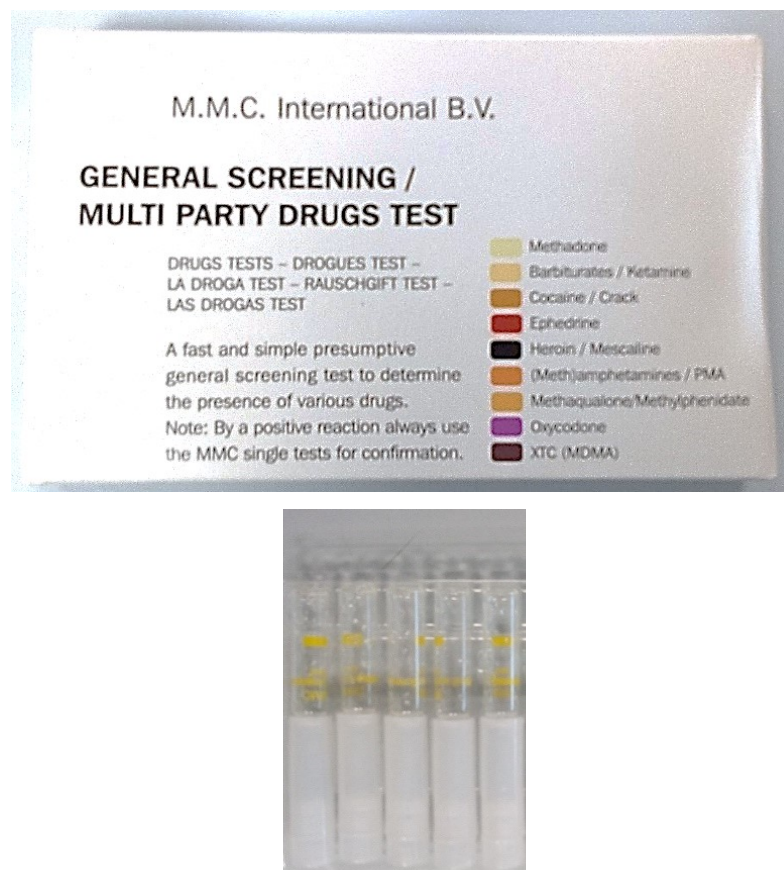


**Figure 21:** Common presumptive colour testing kit used by law enforcement officers

Multiple reports have been published based on the presumptive testing of specific classes of controlled substances especially classes such as amphetamines, piperazines and opiates as well as substances such as cocaine and ketamine.<sup>119-122</sup> The advisory council on the misuse of drugs has previously reported on the prevalence of cathinones on online markets and the need to increase knowledge of cathinones in relation to their reaction to screening tests.<sup>70, 123</sup> There is also a lack of literature on the presumptive testing of diphenidine and its analogues.

In order to determine the specific substance that is present in a sample confirmatory testing would be needed. These techniques are usually more expensive and require more expertise to perform.

No reported colour testing has been reported on the fluoroamphetamine regioisomers meaning further experimental work is needed to expand on this. Cathinones such as the trifluoromethylmethcathinones (TFMMC) have been analysed using the Zimmerman reagent and produce a purple colour when tested.<sup>70</sup> No presumptive reagent testing has been performed on any of the diphenidine derivatives meaning this testing needs to be performed and reported.

Colour tests for specific classes are reported and shows the ability of forensic presumptive tests to quickly identify classes based on colour changes. These reports also show the difficulties of these reagents to identify differing regioisomers, due to the lack of distinctive differences in colour and very similar  $\lambda_{\max}$  values following UV spectral analysis. Commonly used reagents and the changes observed by commonly encountered controlled substances can be seen in Table 4.<sup>124, 125</sup>

**Table 4:** Commonly used presumptive colour test reagents along with compound classes tested and common colour changes.

Test reagent	Common drugs tested	Reported colour changes
Marquis reagent	Opiates	Violet or reddish/Purple
	Amphetamine	Red/Brown
	MDMA	Purple/Black
	Methoxetamine	Pink
Nitric acid reagent	Heroin	Yellow
	Morphine	Red
Scotts reagent	Cocaine	Blue
	Diphenidines	Blue
Mandelin Reagent	Acetaminophen	Green
	Cocaine	Deep yellow
	Methamphetamine	Dark Green
Liebermann Reagent	Cocaine	Yellow
	Methcathinone	Bright Yellow
	4-fluoroamphetamine	Orange
Zimmerman Reagent	Methcathinone	Purple
	Diazepam	Red/Purple
Froehde Reagent	Cathinone	No reaction
	Amphetamine	Red
	MDMA	Black
	4-fluoromethcathinone	No reaction

## 1.10. Gas Chromatography–Mass Spectroscopy

In order to definitively detect whether a specific substance is present, rather than just a possible class, further testing to presumptive tests are commonly required. These techniques are usually more expensive and require more in depth expertise to perform, however they can provide results for use evidentially, with more repeatability and less room for false positives and methodical errors. In a similar way to presumptive testing, the constantly changing face of NPS requires the development of new confirmatory testing methods that are both quick and accurate.

Gas chromatography–mass spectrometry (GC-MS, Figure 22) is the most common technique used as a confirmative test for the detection of controlled drug substances and NPS. This is due to the ability of gas chromatography to separate volatile substances with good resolution and of mass spectrometry to provide detailed structural information through fragmentation patterns.



**Figure 22:** Image of a GC-MS instrument

Sample preparation is usually straightforward with samples analysed as organic solutions after any extraction or derivatisation necessary. The sample solution is then injected and vaporised before being carried though a chromatographic column by a carrier gas, allowing for separation of samples to occur through interaction with the stationary phase. An electron beam is

produced which allows for electron ionisation of the sample and this produces a molecular ion. Due to the large amount of energy involved, the molecular ion will usually fragment further into smaller ions, detected by the mass spectrometer, which will provide a pattern that is characteristic of the substance in question. Multiple controlled substances and NPS have been detected using GC-MS, including opiates, cathinones, amphetamines and piperazines with multiple methods being developed for their detection in multiple matrixes including bodily fluids.<sup>70, 126-128</sup>

The fluoroamphetamines have previously been analysed using GC-MS analysis with all three of the regioisomers analysed but not reportedly separated, with retention times overlapping especially between the 3' (figure 23, **a**) and 4' (figure 23, **b**) positional isomers. It is also reported that thermal degradation occurs during analysis of the fluoroamphetamine regioisomers, with tailing occurring in the chromatographs of all samples. Acetylation of the compounds was shown to help increase the separation between regioisomers.<sup>129</sup> GC-MS also has a difficulty in separating these regioisomers as reports have shown that all three regioisomers produce the same mass spectra (figure 24).

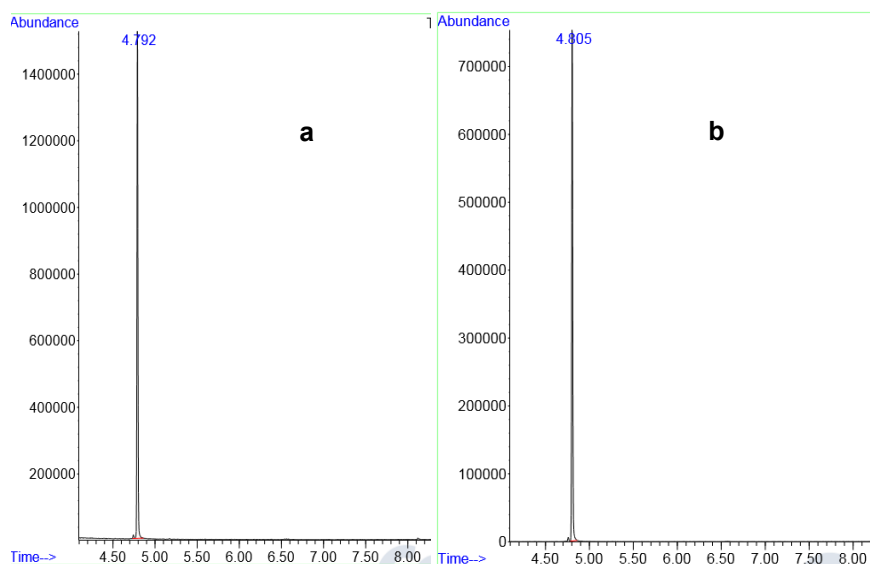


**Figure 23:** GC-MS chromatographs for the 3- (**a**) and 4- (**b**) fluoroamphetamine regioisomers



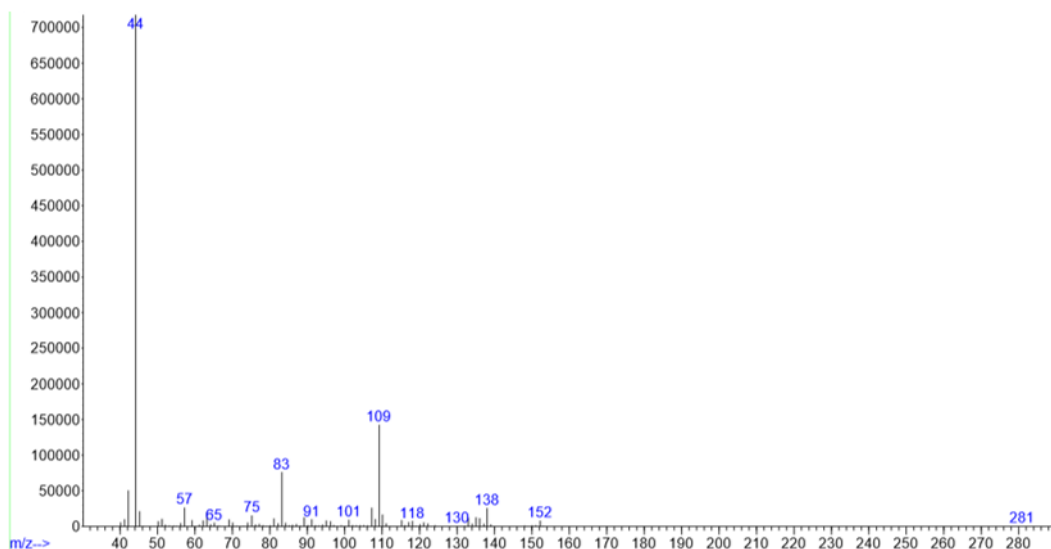


**Figure 24:** Mass spectrum for the fluoroamphetamine regioisomers.

GC-MS analysis of the three fluoromethcathinone regioisomers again highlights the problem this technique has with separating regioisomers as the 2' and 3' regioisomers cannot be separated and thermal degradation is again shown through the tailing of peaks in the chromatographs, especially in the 2' isomer (figure 25).<sup>68</sup>

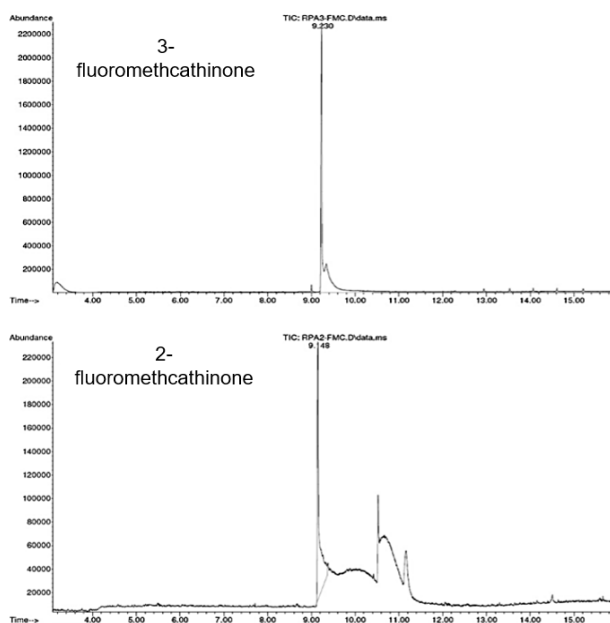


**Figure 25:** GC-MS chromatographs for the 2' and 3'-fluoromethcathinone regioisomers<sup>68</sup>

The GC-MS analysis of the three trifluoromethylmethcathinone regioisomers has been reported and shows that the three isomers can be distinguished even though they are not baseline separated (figure 26). In a similar manner to the fluoromethcathinone regioisomers the trifluoromethylmethcathinone regioisomers show thermal degradation with the tailing of peaks.<sup>82</sup>

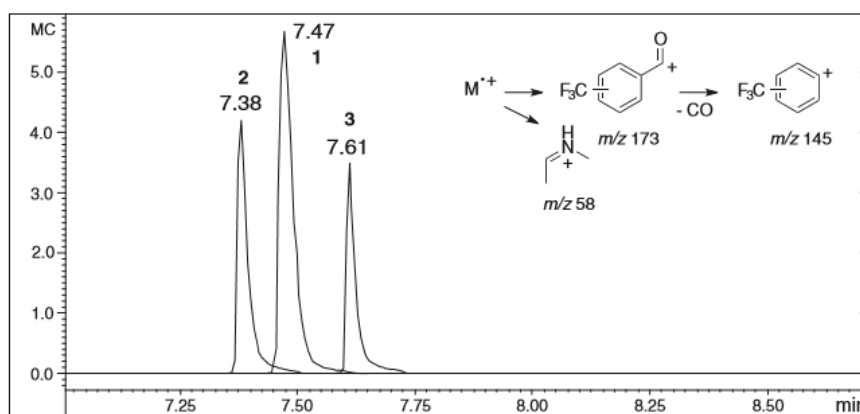


**Figure 26:** GC-MS chromatograph of the 2' (1), 3' (2) and 4'-trifluoromethylmethcathinone (3) regioisomers<sup>82</sup>

Reports regarding GC-MS analysis of controlled substances, especially those which are fluorinated, show difficulty in identification and separation of regioisomers. Reports of tailing due to thermal degradation makes baseline separation difficult and regioisomers produce matching mass spectra when using this technique. Due to these reasons the use of NMR as a technique for identification becomes more important.

## 1.11. Nuclear Magnetic Resonance (NMR) spectroscopy

Nuclear magnetic resonance (NMR) spectroscopy is a technique used to provide complete structural analysis of chemical structures and allows both quantitative and qualitative analysis of complex mixtures.<sup>130</sup> NMR spectroscopy takes advantage of the magnetic properties and spin properties that all the nuclei possess. In the synthesis of organic molecules and psychoactive substances isotopes with spin  $\frac{1}{2}$  become the main focus. These isotopes include  $^1\text{H}$ ,  $^{13}\text{C}$  and  $^{19}\text{F}$  which can all be used to fully characterize reference and seized samples. For spin  $\frac{1}{2}$  nuclei two spin states will exist when an external magnetic field ( $B_0$ ) is present; one spin in line with the magnetic field ( $+\frac{1}{2}$ ) and one spin opposed to the field ( $-\frac{1}{2}$ ). Both will be parallel to the magnetic field, (z-plane), however the two spins will possess a difference in energy that will increase as the strength of the magnetic field increases. If a radio frequency (RF) pulse is applied, with enough energy, the nuclei will be forced out of alignment, such that they have a component in the transverse plane. The nuclei can now be thought as being in a high energy state - they will relax back once the RF pulse is turned off. Energy is released as the nuclei relax and this is observed and measured as a Free Induction Decay (FID).<sup>131, 132</sup>

$^1\text{H}$  NMR can yield a number of key information points regarding hydrogen atoms that are present in sample molecules. Using  $^1\text{H}$  NMR the number of protons in a structure can be determined based on the number of signals observed in the spectra. Each equivalent hydrogen will produce a separate peak, so if two hydrogens are present in the same chemical environment they will produce just one signal. A ratio of equivalent protons can be determined by integrating the sample peaks to show relative intensities. This will show how many protons exist within the same chemical environment. Chemical shift values will provide information on the magnetic field effects of nearby nuclei on the proton nucleus and can give information on the atoms bonded to the hydrogen or the functional groups in which the hydrogen atom exists. Finally, the number of protons that neighbor a specific proton can be determined based on the splitting pattern of the sample signals.<sup>133</sup>

Internal standards, such as tetramethylsilane (TMS) can be added to samples allowing comparison of spectra to other samples identified or to literature data provided for reference samples. Research and literature also shows the typical chemical shift values that are observed when common laboratory solvents are present in a sample when dissolved in deuterated solvents.<sup>134</sup> Research has shown that  $^1\text{H}$  NMR has been used to analyze a number of psychoactive substances including cathinones and compared to reference standards.<sup>135, 136</sup> Quantitative NMR (qNMR) has also been performed on a variety of drug samples in order to extensively analyze samples.<sup>130</sup>

This means that more than just the structural characterization can be obtained and levels of impurities present can be evaluated and composition of mixtures can be determined. Research for samples containing synthetic cannabinoids that have been encountered individually and in herbal blends has shown the ability to determine percentages of samples in mixtures.<sup>137</sup> There are some difficulties when using  $^1\text{H}$  as the nucleus to run qNMR especially when testing mixtures as the spectrum can become convoluted and difficult to distinguish due to multiple sample signals. Fluorine NMR ( $^{19}\text{F}$  NMR) can be utilised for fluorinated samples to perform quantitative and qualitative NMR due to the simplistic nature of the spectrum produced.

NMR can be carried out using a 60 MHz magnet, which allows a smaller instrument to be used. This lower magnetic field results in lower resolution of spectra although splitting patterns are not lost completely compared to higher magnetic fields. 60 MHz NMR has advantages over other confirmatory tests such as GC-MS due to the ease of sample preparation, cost of instrumentation, the possibility of it being field deployable and the need of less expertise for data analysis. The simplicity of  $^{19}\text{F}$  NMR spectra means less interpretation is needed and therefore less expertise is needed in determining samples present. The instrument being field deployable allows the possibility of the technique to be used at locations such as police custody suits, airport terminal security and music festivals. Sample run times are also significantly quicker for both  $^1\text{H}$  and  $^{19}\text{F}$  experiments compared to GC-MS runs. GC-MS

still produces lower limits of detection and quantification compared to NMR and is more reproducible with lower standard deviations produced when multiple runs of the same sample are performed. In the case of fluorinated amphetamines and cathinones it has been shown that degradation occurs, when GC-MS is run meaning tailing occurs and identification of compounds becomes harder based on retention times. This is why 60 MHz analysis should be performed on all fluorinated amphetamine and cathinone derivatives.

### 1.11.1. Fluorine ( $^{19}\text{F}$ ) NMR

In a similar manner to the proton nucleus, the fluorine nucleus has a nuclear spin of  $\frac{1}{2}$  so the technique is similar to that of  $^1\text{H}$  NMR.  $^{19}\text{F}$  NMR enables the determination of the number of fluorine atoms present in a molecule. Signals for  $^{19}\text{F}$  NMR may split if an uncoupled experiment is run due to coupling occurring to other  $\frac{1}{2}$  spin nuclei such as other fluorine atoms and hydrogen atoms. The  $^{19}\text{F}$  isotope has a 100% natural abundance and will be highly responsive to NMR techniques due its high magnetogyric ratio.  $^{19}\text{F}$  NMR produces a much larger chemical shift range in comparison to  $^1\text{H}$  NMR and this means that molecules that possess more than one fluorine atom may usually have peaks that are well separated and spectra that is easier to interpret.

The simplicity of  $^{19}\text{F}$  NMR spectra will allow not only qualitative analysis and comparison between samples in mixtures and reference standards but also quantitative analysis in a simpler manner when internal references are added. Due to the lower number of sample peaks likely in mixtures quantitative analysis becomes easier to perform using  $^{19}\text{F}$  NMR. Fluorotrichloromethane ( $\text{CFCl}_3$ ) and trifluoroacetic acid ( $\text{CF}_3\text{COOH}$ ) are two of the more commonly used internal reference standards and can be chosen depending on the chemical shift ranges of the samples in question.

The coupling that fluorine experiences between other  $\frac{1}{2}$  spin nuclei allows further two dimensional fluorine experiments to be performed in order to fully elucidate and explain the coupling interactions present in a molecule.

### 1.11.2. 60 MHz NMR screening

NMR is more capable of identifying a possible compound based on every compound having a specific  $^1\text{H}$  NMR spectrum. This gives it an advantage over GC-MS when trying to screen drug samples for potential controlled substances. When using a 60 MHz instrument over a higher-powered instrument, such as a 400 MHz spectrometer, slight details may decrease such as clear coupling constants, however spectra for differing compounds will still be unique. This means that when an unknown sample is encountered the NMR spectra can be compared to a known reference and the sample can be identified. 60 MHz NMR also has other advantages and disadvantages compared to GC-MS which can be seen in Table 5.

**Table 5:** Advantages and disadvantages of using 60 MHz NMR compared to GC-MS

<b>Advantages</b>	<b>Disadvantages</b>
<ul style="list-style-type: none"><li>• A 60 MHz instrument has a simpler interface and doesn't require special expertise to operate<ul style="list-style-type: none"><li>• Cheaper instrument</li></ul></li><li>• Cost per sample – GC-MS forensic analysis can cost between £120-£200 per sample whereas NMR analysis is performed for the cost of consumables (around £50 for 10 DMSO solvent ampules and NMR tubes from Sigma Aldrich)</li><li>• Quicker analysis times. 5 minute runs for both <math>^1\text{H}</math> and <math>^{19}\text{F}</math> experiments compared to runs &gt; 10 mins for GC-MS analysis.<ul style="list-style-type: none"><li>• Field deployable</li></ul></li></ul>	<ul style="list-style-type: none"><li>• NMR not currently utilised in forensic laboratories and 60 MHz NMR is not currently used for evidence gathering</li><li>• Higher LOD for NMR meaning more sample is needed to test using NMR</li><li>• Difficulty with mixture analysis as signals for different compounds will coalesce</li></ul>

## 1.12. Aims and Objectives

Since the introduction of the Misuse of Drugs Act, illicit drug suppliers and clandestine labs have been looking at ways to avoid detection and alter structures of controlled substances. One way this is achieved is to add fluorine into the molecule and research into drug development has shown this to have effects regarding enhancement of biological activity and increased chemical and metabolic stability.<sup>2</sup> It is of vital importance both forensically and from a criminological point of view that substances can be identified in a rapid and accurate manner. This is due to differences in sentencing between substances belonging to the New Psychoactive Substances Act (2016) and those that belong to the Misuse of Drugs Act (1971). The changing face of new psychoactive substances, with the alteration of structures and the changing drugs market from “head shops” to the “dark web” has provided an even greater analytical challenge for the detection of NPS. The main aim of this report will be to show the ease of structure alteration in NPS and develop analytical methods that will aid with the detection of these compounds. A 60 MHz instrument will be used in order to perform a rapid screening method, where runs will ideally last between 5-10 minutes. This system can then be used by people with limited scientific backgrounds or training due to the ease of sample preparation and processing. This system could then be utilised within airport, police custody, festival and other public event environments as a “field deployable” system, where quick analysis is necessary for prosecution, safety and healthcare purposes. Both qualitative and quantitative analysis will be performed and can be compared to GC-MS analysis, which is currently the main analytical method used within Forensic Science testing. The method can also be compared to colour testing as a presumptive testing method, as colour tests have been previously performed by law enforcement to show the possibility of NPS being present. However, this report will show that with the increase in novel psychoactive substances there is also an increase in the number of false positives to already controlled drugs, under the Misuse of Drugs Act 1971, with which the colour tests are intended. Colour testing will also be used in order to see whether positional isomers can be distinguished based on colour change.

Initially, chapter three will show testing on trifluoromethylmethcathinone and fluoromethcathinone regioisomers (**8a-8c**, **9a-9c**) as well as the three fluoroamphetamine regioisomers (**4a-4c**). Full characterization will be performed in order to compare with previous literature data that has been reported for these compounds. A GC-MS method will be developed in order to try and achieve possible separation of these nine compounds for identification. <sup>19</sup>F NMR experiments will be run, on a 60 MHz instrument, to show the possibility of using this technique as an initial presumptive testing experiment. This experiment will provide a simplified spectrum, with only 1-2 peaks, which is easier to interpret by non-scientifically trained personal. Quantitative analysis will be performed using this technique to then show that concentration of samples can be determined with the same precision to GC-MS in a quicker run. GC-MS is currently used in forensic environments for evidence collection and therefore if the 60 MHz instrument can perform to the same standard then there is a possibility it can be used for this purpose in forensic laboratories. Street samples will then be analysed in order to show the ability of both methods to identify active components and provide quantitative analysis.

Chapter four will show the synthesis of thirteen diphenidine derivatives including diphenidine (**13a**) and the three methoxphenidine regioisomers (**13b-13d**). Full characterisation will be performed and a GC-MS method will be developed and validated with two samples bought from online vendors tested to show the ability of GC-MS to separate and identify this class of compounds. This chapter will show how altering structures slightly can alter analytical data produced in order to try to avoid detection from previously encountered drugs. It will also help to identify drugs that may emerge in future.

Chapter five will look into the synthesis of halogenated (fluoro-, bromo-, chloro- and iodo-) diphenidine derivatives. Addition of different halogenated substituents will effect bioavailability as lipophilicity will increase as the halogenated substituent is changed from fluorine to iodine. This will mean that the iodine compounds will have a higher affinity for the lipid phase and an increased, however it will also have a negative effect on oral adsorption. <sup>138</sup>



Full characterisation will be performed, and analysis will be performed using both GC-MS and NMR in order to show whether differences can be seen when different halogen substituents are used and when regioisomers of the same halogen are observed.

In chapter six, a range of substances will be synthesised, based on the synthesis of diphenidine, where the amine used will be altered in order to achieve slightly differing side chains and rings on the final compound produced. Chapter seven will show the ease of synthesis of slightly altered chemical structures of an original compound backbone. Monofluorinated compounds will be produced in each case and these compounds will be separated using GC-MS instrumentation.  $^{19}\text{F}$  NMR and  $^1\text{H}$  NMR on a 60 MHz instrument will also be tested as a possible replacement for current presumptive tests. This chapter will show that even though the colour tests will not be able to distinguish regioisomers by colour the 60 MHz instrument will produce unique proton and fluorine spectrum that can identify an individual compound from 24 structurally similar compounds.

Chapter seven will show the synthesis of six difluoroephenidine regioisomers as well as trifluoro-, tetrafluoro- and pentafluoroephenidine compounds. These nine compounds will be fully characterised and GC-MS and  $^{19}\text{F}$  NMR experiments will be utilised in order to show potential separation of these compounds. Further to this, a number of 2D NMR experiments will be performed on a 60 MHz NMR spectrometer in order to further distinguish between the six difluorinated isomers. This will show that as well as presumptive testing on the 60 MHz NMR, further longer experiments can be performed that will further confirm the presence of specific drugs.

## 2. Chapter 2 – Experimental methods

All reagents and chemicals were purchased from Sigma Aldrich (Gillingham, UK) or Fluorochem Limited (Hadfield, UK) and used without further purification. Solvents were purchased from Sigma Aldrich and Fisher Scientific (Loughborough, UK).  $^1\text{H}$ ,  $^{13}\text{C}$  and  $^{19}\text{F}$  NMR for characterisation was acquired on a JEOL (JEOL, Tokyo, Japan) NMR spectrometer operating at a proton resonance frequency of 400 MHz. All NMR data has been discussed in the relevant results sections (Chapter 3 - Chapter 7). Presumptive  $^1\text{H}$  and  $^{19}\text{F}$  NMR analysis was performed on a Pulsar (Oxford Instruments, Abingdon, UK) NMR spectrometer operating at a resonance frequency of 60 MHz. Trifluoroacetic acid was added (0.1 % v/v), as an internal reference, to samples requiring analysis using a  $^{19}\text{F}$  experiment. Infrared spectra were obtained in the range 4000 – 400  $\text{cm}^{-1}$  using a Thermo Scientific Nicolet iS10ATR-FTIR instrument (Thermo Scientific, Rochester, USA). All IR spectra have been included in the supplementary information. All test street samples were provided by Greater Manchester Police (GMP) personnel, in accordance with the legislation and under the approved Memorandum of Understanding operating between the **MAN**chester **DR**ug **A**nalysis and **K**nowledge **E**xchange (MANDRAKE) and GMP. All controlled substances and restricted materials were synthesised, stored, used and destroyed in accordance with Home Office regulations and the Misuse of Drugs Act (1971).<sup>5</sup>

The fluoroamphetamine (FA, **4a** – **4c**), fluoromethcathinone (FMC, **8a** – **8c**) and trifluoromethylmethcathinone (TFMMC, **9a** – **9c**) regioisomers were synthesised previously at Manchester Metropolitan University (MMU) and Strathclyde University under home office license.<sup>70, 83, 139</sup> Diphenidine (**13a**) and twelve of its derivatives (**13b** – **13m**) were also synthesised prior to the project at Manchester Metropolitan University.

## 2.1. Synthetic Methods

### 2.1.1. Synthesis of the diphenidine derivatives and analogues

Twelve halogenated diphenidine derivatives, 18 diphenidine analogues and 9 polyfluorinated ephenidine derivatives were synthesised as part of the project using different aldehydes and amines. Compound names and abbreviations along with the aldehyde and amine used can be seen in Table 6.

**Table 6:** List of diphenidine derivatives and analogues synthesised including abbreviations and compound numbers along with the aldehyde and amine used in synthesis

Compound no.	Compound name	Abbreviation	Aldehyde used (X)	Amine used (NHR)
15a	2-fluoroephenidine	2-FEP	2-fluorobenzaldehyde	ethylamine
15b	3-fluoroephenidine	3-FEP	3-fluorobenzaldehyde	ethylamine
15c	4-fluoroephenidine	4-FEP	4-fluorobenzaldehyde	ethylamine
15d	2,3-difluoroephenidine	2,3-DFEP	2,3-difluorobenzaldehyde	ethylamine
15e	2,4-difluoroephenidine	2,4-DFEP	2,4-difluorobenzaldehyde	ethylamine
15f	2,5-difluoroephenidine	2,5-DFEP	2,5-difluorobenzaldehyde	ethylamine
15g	2,6-difluoroephenidine	2,6-DFEP	2,6-difluorobenzaldehyde	ethylamine
15h	3,4-difluoroephenidine	3,4-DFEP	3,4-difluorobenzaldehyde	ethylamine
15i	3,5-difluoroephenidine	3,5-DFEP	3,5-difluorobenzaldehyde	ethylamine
15j	2,3,4-trifluoroephenidine	TriFEP	2,3,4-trifluorobenzaldehyde	ethylamine
15k	2,3,4,5-tetrafluoroephenidine	TeFEP	2,3,4,5-tetrafluorobenzaldehyde	ethylamine
15l	2,3,4,5,6-pentafluoroephenidine	PFEP	2,3,4,5,6-pentafluorobenzaldehyde	ethylamine
19a	2-fluorolintane	2-FL	2-fluorobenzaldehyde	pyrrolidine
19b	3-fluorolintane	3-FL	3-fluorobenzaldehyde	pyrrolidine
19c	4-fluorolintane	4-FL	4-fluorobenzaldehyde	pyrrolidine
20a	2-fluphenidine	2-FP	2-fluorobenzaldehyde	piperidine
20b	3-fluphenidine	3-FP	3-fluorobenzaldehyde	piperidine
20c	4-fluphenidine	4-FP	4-fluorobenzaldehyde	piperidine
20d	2-chlophenidine	2-CP	2-chlorobenzaldehyde	piperidine
20e	3-chlophenidine	3-CP	3-chlorobenzaldehyde	piperidine
20f	4-chlophenidine	4-CP	4-chlorobenzaldehyde	piperidine
20g	2-brophenidine	2-BP	2-bromobenzaldehyde	piperidine
20h	3-brophenidine	3-BP	3-bromobenzaldehyde	piperidine
20i	4-brophenidine	4-BP	4-bromobenzaldehyde	piperidine
20j	2-iodophenidine	2-IP	2-iodobenzaldehyde	piperidine
20k	3-iodophenidine	3-IP	3-iodobenzaldehyde	piperidine
20l	4-iodophenidine	4-IP	4-iodobenzaldehyde	piperidine
21a	2-fluoromephenidine	2-FMP	2-fluorobenzaldehyde	methylamine
21b	3-fluoromephenidine	3-FMP	3-fluorobenzaldehyde	methylamine
21c	4-fluoromephenidine	4-FMP	4-fluorobenzaldehyde	methylamine
22a	2-fluorodimephenidine	2-FDMP	2-fluorobenzaldehyde	dimethylamine
22b	3-fluorodimephenidine	3-FDMP	3-fluorobenzaldehyde	dimethylamine
22c	4-fluorodimephenidine	4-FDMP	4-fluorobenzaldehyde	dimethylamine
23a	2-fluorodiephenidine	2-FDEP	2-fluorobenzaldehyde	diethylamine
23b	3-fluorodiephenidine	3-FDEP	3-fluorobenzaldehyde	diethylamine
23c	4-fluorodiephenidine	4-FDEP	4-fluorobenzaldehyde	diethylamine
24a	2-fluorotrifluoroephenidine	2-FTFEP	2-fluorobenzaldehyde	trifluoroethylamine
24b	3-fluorotrifluoroephenidine	3-FTFEP	3-fluorobenzaldehyde	trifluoroethylamine
24c	4-fluorotrifluoroephenidine	4-FTFEP	4-fluorobenzaldehyde	trifluoroethylamine

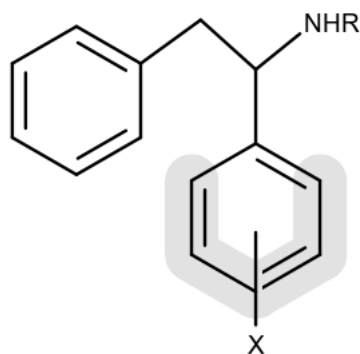


**Figure 27:** General structure of diphenidine and all its derivatives and analogues

Synthesis of all diphenidine derivatives and analogues were synthesised using an adaptation of the published method from Le Gall *et al.*<sup>140</sup> (figure 26). The following modifications were applied to the published method: To a dried round bottomed flask (250 mL) containing zinc dust (2.0 g, 30 mmol) suspended in acetonitrile (40 mL), was added benzyl bromide (0.4 mL) and trifluoroacetic acid (0.2 mL). The resulting solution was stirred for 5 minutes and then benzyl bromide (3.0 mL, 25 mmol), the required amine (0.99 mL, 10 mmol) followed by the pre-requisite benzaldehyde (11 mmol), were introduced to the mixture, and the solution was stirred at room temperature for an additional 1 h. The resulting solution was poured into a saturated aqueous NH<sub>4</sub>Cl solution (150 mL) and extracted with dichloromethane (2 × 100 mL). The combined organic layers were dried (MgSO<sub>4</sub>) and concentrated *in vacuo* to give a crude yellowish oil. The oil was then dissolved in diethyl ether (150 mL) and concentrated sulphuric acid (0.75 mL) was added dropwise, to the vigorously stirred solution. After five minutes, the precipitated ammonium salt was filtered, washed with diethyl ether (2 × 50 mL) and air dried for 5-10 minutes. The ammonium salt was re-dissolved in aqueous sodium hydroxide (5% w/v, 150 mL) and then extracted with dichloromethane (2 × 100 mL). The combined organic fractions were again dried (MgSO<sub>4</sub>) and concentrated *in vacuo* to give a yellow oil. The oil was dissolved in diethyl ether (200 mL), treated with hydrogen chloride (4M in dioxane, 3.0 mL, 12 mmol) and left to stand for 5 minutes. The crystallized products were filtered and washed sequentially with the minimum amount of ice-cold acetone and if necessary an ice-cold mixture

of ethyl acetate-diethyl ether (1:5) to afford the corresponding hydrochloride salts as colourless to off-white powders.

2-Fluoroephenidine (2-FEP, **15a**) afforded 2.24 g (64%) of a white powder. MP 189 °C. <sup>1</sup>H NMR (400 MHz, DMSO-*d*<sub>6</sub> δ ppm = 2.50) δ 1.27 (t, 3H, J = 8.12 Hz, NHCH<sub>2</sub>CH<sub>3</sub>), 2.75 – 2.81 (m, 1H, NHCH<sub>2</sub>CH<sub>3</sub>), 2.85 – 2.95 (m, 1H, NHCH<sub>2</sub>CH<sub>3</sub>), 3.18 – 3.24 (m, 1H, NHCHCH<sub>2</sub>), 3.78 (dd, 1H, J = 13.1, 5.2 Hz, NHCHCH<sub>2</sub>), 4.78 – 4.88 (m, 1H, NHCHCH<sub>2</sub>), 6.98-7.08 (m, 2H, Ar-H), 7.12 – 7.21 (m, 4H, Ar-H), 7.30 – 7.42 (m, 2H, Ar-H), 7.98 – 8.08 (m, 1H, Ar-H), 9.47 – 9.80 (br s., 1H, NH), 10.05 – 10.28 (br s., 1H, NH); <sup>13</sup>C NMR (400 MHz, DMSO-*d*<sub>6</sub>) δ 11.95, 39.25, 41.41, 55.80, 116.41, 122.64, 126.02, 127.74, 129.25, 129.99, 130.52, 132.09, 136.60, 161.32 (d, C-F, J = 246.30); <sup>19</sup>F NMR (400 MHz, DMSO-*d*<sub>6</sub>) δ -118.77; IR: 2950 cm<sup>-1</sup> (C-H), 1240 cm<sup>-1</sup> (C-F), 1550 cm<sup>-1</sup> (N-H), 1450 cm<sup>-1</sup> (C=C benzene). TLC R<sub>f</sub>: 0.56

3-Fluoroephenidine (3-FEP, **15b**) afforded 2.10 g (60%) of a white powder. MP 174 °C. <sup>1</sup>H NMR (400 MHz, DMSO-*d*<sub>6</sub> δ ppm = 2.50) δ 1.22 (t, 3H, J = 7.3 Hz, NHCH<sub>2</sub>CH<sub>3</sub>), 2.62 – 2.66 (m, 1H, NHCH<sub>2</sub>CH<sub>3</sub>), 2.83 (m, 1H, NHCH<sub>2</sub>CH<sub>3</sub>), 3.16 - 3.19 (m, 1H, NHCHCH<sub>2</sub>), 3.64 (dd, 1H, J = 13.3 3.7 Hz, NHCHCH<sub>2</sub>), 4.51 – 4.57 (m, 1H, NHCHCH<sub>2</sub>), 6.88 (s, 2H, Ar-H), 6.98 (m, 1H, Ar-H), 7.00 – 7.10 (m, 4H, Ar-H), 7.20 (dd, 1H, J = 13.7 8.2 Hz, Ar-H), 7.25 (d, 1H, J = 9.6 Hz, Ar-H), 9.73 (br s., 1H, NH), 10.14 (br s., 1H, NH); <sup>13</sup>C NMR (400 MHz, DMSO-*d*<sub>6</sub>) δ 11.96, 39.86, 41.25, 62.60, 116.51 (d, J = 23.0 Hz), 116.77 (d, J = 21.1 Hz), 126.13, 127.56, 129.26, 130. 11, 131.65, 136.80, 138.51, 162.98 (d, C-F, J = 245.4 Hz); <sup>19</sup>F NMR (400 MHz, DMSO-*d*<sub>6</sub>) δ -111.43; IR: 1300 cm<sup>-1</sup> (C-F), 1460 cm<sup>-1</sup> (benzene C=C), 1550 cm<sup>-1</sup> (N-H stretch), 2950 cm<sup>-1</sup> (C-H), 3080 cm<sup>-1</sup> (C-H benzene); TLC R<sub>f</sub>: 0.61

4-Fluoroephenidine (4-FEP, **15c**) afforded 1.79 g (51%) of a white powder. MP 177 °C. <sup>1</sup>H NMR (400 MHz, DMSO-*d*<sub>6</sub> δ ppm = 2.50) δ 1.22 (t, 3H, J = 7.3 Hz, NHCH<sub>2</sub>CH<sub>3</sub>), 2.61 (m, 1H, NHCH<sub>2</sub>CH<sub>3</sub>), 2.81 (m, 1H, NHCH<sub>2</sub>CH<sub>3</sub>), 3.16 (dd, 1H, J = 13.1, 11.7 Hz, NHCHCH<sub>2</sub>), 3.63 (dd, 1H, J = 13.3, 4.1 Hz, NHCHCH<sub>2</sub>), 4.51 (m, 1H, NHCHCH<sub>2</sub>), 7.42 (m, 2H, Ar-H), 7.54 (m, 1H, Ar-H), 7.60 (dd, 2H, J = 8.20, 1.63 Hz, Ar-H), 7.62 (m, 2H, Ar-H), 7.97 (dd, 2H, J = 8.75, 5.5 Hz,

Ar-H), 9.66 (br s., 1H, NH), 10.08 (br s., 1H, Ar-H);  $^{13}\text{C}$  NMR (400 MHz,  $\text{DMSO-}d_6$ )  $\delta$  11.95, 39.95, 41.16, 62.41, 116.50 (d,  $J = 21.1$  Hz), 127.56, 129.25, 130.12, 131.94, 132.04, 136.97, 163.1 (d, C-F,  $J = 246.3$ );  $^{19}\text{F}$  NMR (400 MHz,  $\text{DMSO-}d_6$ )  $\delta$  -112.20; IR:  $1300\text{ cm}^{-1}$  (C-F),  $1460\text{ cm}^{-1}$  (benzene C=C),  $1550\text{ cm}^{-1}$  (N-H stretch),  $2950\text{ cm}^{-1}$  (C-H),  $3080\text{ cm}^{-1}$  (C-H benzene); TLC R<sub>f</sub>: 0.58

2,3-Difluoroephenidine (2,3-DFEP, **15d**) afforded 1.82 g (52%) of an off-white powder. MP  $202\text{ }^\circ\text{C}$ .  $^1\text{H}$  NMR (400 MHz,  $\text{DMSO-}d_6$ )  $\delta$  ppm = 2.50)  $\delta$  1.25 (t, 3H,  $J = 7.5$  Hz,  $\text{NHCH}_2\text{CH}_3$ ), 2.78 (m, 1H,  $\text{NHCH}_2\text{CH}_3$ ), 2.92 (m, 1H,  $\text{NHCH}_2\text{CH}_3$ ), 3.18 (m, 1H,  $\text{NHCHCH}_2$ ), 3.68 (dd, 1H,  $J = 13.1, 5.5$  Hz,  $\text{NHCHCH}_2$ ), 4.79 (m, 1H,  $\text{NHCHCH}_2$ ), 7.02 (d, 2H,  $J = 8.8$  Hz, Ar-H), 7.18 (m, 3H, Ar-H), 7.38 – 7.50 (m, 2H, Ar-H), 7.82 (dd, 1H,  $J = 13.1, 7.8$  Hz, Ar-H), 9.70 (br s., 1H, NH), 10.17 (br s., 1H, NH);  $^{19}\text{F}$  NMR (400 MHz,  $\text{DMSO-}d_6$ )  $\delta$  -140.18, -144.23; IR:  $1280\text{ cm}^{-1}$  (C-F),  $1480.6\text{ cm}^{-1}$  (benzene C=C),  $2706\text{ cm}^{-1}$  (C-H),  $2973\text{ cm}^{-1}$  (C-H benzene); TLC R<sub>f</sub>: 0.87

2,4-Difluoroephenidine (2,4-DFEP, **15e**) afforded 1.80 g (51%) of a white powder. MP  $195\text{ }^\circ\text{C}$ .  $^1\text{H}$  NMR (400 MHz,  $\text{DMSO-}d_6$ )  $\delta$  ppm = 2.50)  $\delta$  1.20 (t, 3H,  $J = 7.2$  Hz,  $\text{NHCH}_2\text{CH}_3$ ), 2.78 (m, 1H,  $\text{NHCH}_2\text{CH}_3$ ), 2.93 (m, 1H,  $\text{NHCH}_2\text{CH}_3$ ), 3.18 (m, 1H,  $\text{NHCHCH}_2$ ), 3.65 (dd, 1H,  $J = 12.8, 4.1$  Hz,  $\text{NHCHCH}_2$ ), 4.79 (m, 1H,  $\text{NHCHCH}_2$ ), 6.95 (m, 3H, Ar-H), 7.11 – 7.25 (m, 4H, Ar-H), 8.05 (m, 1H, Ar-H);  $^{19}\text{F}$  NMR (400 MHz,  $\text{DMSO-}d_6$ )  $\delta$  -110.70, -114.48; IR:  $1281\text{ cm}^{-1}$  (C-F),  $1489\text{ cm}^{-1}$  (benzene C=C),  $2706\text{ cm}^{-1}$  (C-H),  $2956\text{ cm}^{-1}$  (C-H benzene); TLC R<sub>f</sub>: 0.75

2,5-Difluoroephenidine (2,5-DFEP, **15f**) afforded 2.00 g (57%) of a white powder. MP  $211\text{ }^\circ\text{C}$ .  $^1\text{H}$  NMR (400 MHz,  $\text{DMSO-}d_6$ )  $\delta$  ppm = 2.50)  $\delta$  1.20 (t, 3H,  $J = 7.5$  Hz,  $\text{NHCH}_2\text{CH}_3$ ), 2.78 (m, 1H,  $\text{NHCH}_2\text{CH}_3$ ), 2.93 (m, 1H,  $\text{NHCH}_2\text{CH}_3$ ), 3.18 (m, 1H,  $\text{NHCHCH}_2$ ), 3.65 (m, 1H,  $\text{NHCHCH}_2$ ), 4.79 (m, 1H,  $\text{NHCHCH}_2$ ), 7.00 – 7.38 (m, 7H, Ar-H), 7.91 (dd, 1H,  $J = 11.2, 4.8$  Hz, Ar-H), 9.62 (br s., 1H, NH), 10.08 (br s., 1H, NH);  $^{19}\text{F}$  NMR (400 MHz,  $\text{DMSO-}d_6$ )  $\delta$  -118.58, -124.18; IR:  $1190\text{ cm}^{-1}$  (C-F),  $1496\text{ cm}^{-1}$  (benzene C=C),  $2710\text{ cm}^{-1}$  (C-H),  $2974\text{ cm}^{-1}$  (C-H benzene); TLC R<sub>f</sub>: 0.80

2,6-Difluoroephenidine (2,6-DFEP, **15g**) afforded 2.24 g (64%) of a white powder. MP 205 °C. <sup>1</sup>H NMR (400 MHz, DMSO-*d*<sub>6</sub> δ ppm = 2.50) δ 1.28 (t, 3H, J = 7.0 Hz, NHCH<sub>2</sub>CH<sub>3</sub>), 2.95 (m, 2H, NHCH<sub>2</sub>CH<sub>3</sub>), 3.18 (m, 1H, NHCHCH<sub>2</sub>), 3.65 (dd, 1H, J = 12.8, 4.8 Hz, NHCHCH<sub>2</sub>), 4.75 (m, 1H, NHCHCH<sub>2</sub>), 7.02 – 7.20 (m, 7H, Ar-H), 7.50 (dd, 1H, J = 11.2, 4.2 Hz, Ar-H), 9.18 (br s., 1H, NH), 10.26 (br s., 1H, NH); <sup>19</sup>F NMR (400 MHz, DMSO-*d*<sub>6</sub>) δ -113.68; IR: 1202 cm<sup>-1</sup> (C-F), 1475 cm<sup>-1</sup> (benzene C=C), 2670 cm<sup>-1</sup> (C-H), 2944 cm<sup>-1</sup> (C-H benzene); TLC R<sub>f</sub>: 0.83

3,4-Difluoroephenidine (3,4-DFEP, **15h**) afforded 1.89 g (54%) of a white powder. MP 188 °C. <sup>1</sup>H NMR (400 MHz, DMSO-*d*<sub>6</sub> δ ppm = 2.50) δ 1.20 (t, 3H, J = 7.5 Hz, NHCH<sub>2</sub>CH<sub>3</sub>), 2.78 (m, 1H, NHCH<sub>2</sub>CH<sub>3</sub>), 2.93 (m, 1H, NHCH<sub>2</sub>CH<sub>3</sub>), 3.18 (m, 1H, NHCHCH<sub>2</sub>), 3.65 (m, 1H, NHCHCH<sub>2</sub>), 4.79 (m, 1H, NHCHCH<sub>2</sub>), 7.05 (m, 2H, Ar-H), 7.12 – 7.30 (m, 4H, Ar-H), 7.42 (dd, 1H, J = 12.8, 5.2 Hz, Ar-H), 7.72 (d, 1H, J = 8.4 Hz, Ar-H), 9.68 (br s., 1H, NH), 9.95 (br s., 1H, NH); <sup>19</sup>F NMR (400 MHz, DMSO-*d*<sub>6</sub>) δ -139.56, -139.70; IR: 1282 cm<sup>-1</sup> (C-F), 1520 cm<sup>-1</sup> (benzene C=C), 2709 cm<sup>-1</sup> (C-H), 2971 cm<sup>-1</sup> (C-H benzene); TLC R<sub>f</sub>: 0.84

3,5-Difluoroephenidine (3,5-DFEP, **15i**) afforded 1.82 g (52%) of an off-white powder. MP 194 °C. <sup>1</sup>H NMR (400 MHz, DMSO-*d*<sub>6</sub> δ ppm = 2.50) δ 1.25 (t, 3H, J = 7.5 Hz, NHCH<sub>2</sub>CH<sub>3</sub>), 2.65 (m, 1H, NHCH<sub>2</sub>CH<sub>3</sub>), 2.86 (m, 1H, NHCH<sub>2</sub>CH<sub>3</sub>), 3.18 (m, 1H, NHCHCH<sub>2</sub>), 3.61 (m, 1H, NHCHCH<sub>2</sub>), 4.60 (m, 1H, NHCHCH<sub>2</sub>), 7.02 (m, 3H, Ar-H), 7.14 – 7.38 (m, 5H, Ar-H) 9.70 (br s., 1H, NH), 10.06 (br s., 1H, NH); <sup>19</sup>F NMR (400 MHz, DMSO-*d*<sub>6</sub>) δ -110.62; IR: 1322 cm<sup>-1</sup> (C-F), 1467 cm<sup>-1</sup> (benzene C=C), 2799 cm<sup>-1</sup> (C-H), 2969 cm<sup>-1</sup> (C-H benzene); TLC R<sub>f</sub>: 0.80

Trifluoroephenidine (TriFEP, **15j**) afforded 2.03 g (58%) of a white powder. MP 199 °C. <sup>1</sup>H NMR (400 MHz, DMSO-*d*<sub>6</sub> δ ppm = 2.50) δ 1.25 (t, 3H, J = 7.0 Hz, NHCH<sub>2</sub>CH<sub>3</sub>), 2.80 (m, 1H, NHCH<sub>2</sub>CH<sub>3</sub>), 2.91 (m, 1H, NHCH<sub>2</sub>CH<sub>3</sub>), 3.22 (m, 1H, NHCHCH<sub>2</sub>), 3.72 (m, 1H, NHCHCH<sub>2</sub>), 4.75 (m, 1H, NHCHCH<sub>2</sub>), 7.01 (m, 2H, Ar-H), 7.19 (m, 3H, Ar-H), 7.50 (t, 1H, J = 9.2 Hz, Ar-H), 7.96 (dd, 1H, J = 12.8, 3.8 Hz, Ar-H), 9.90 (br s., 1H, NH), 10.32 (br s., 1H, NH); <sup>19</sup>F NMR (400

MHz, DMSO-*d*<sub>6</sub>) δ -163.00, -138.89, -135.30; IR: 1282cm<sup>-1</sup> (C-F), 1500 cm<sup>-1</sup> (benzene C=C), 2698 cm<sup>-1</sup> (C-H), 2968 cm<sup>-1</sup> (C-H benzene); TLC R<sub>f</sub>: 0.72

Tetrafluoroephenidine (TeFEP, **15k**) afforded 1.86 g (53%) of a white powder. MP 205 °C; <sup>1</sup>H NMR (400 MHz, DMSO-*d*<sub>6</sub> δ ppm = 2.50) δ 1.25 (t, 3H, J = 7.0 Hz, NHCH<sub>2</sub>CH<sub>3</sub>), 2.82 (m, 1H, NHCH<sub>2</sub>CH<sub>3</sub>), 2.95 (m, 1H, NHCH<sub>2</sub>CH<sub>3</sub>), 3.20 (m, 1H, NHCHCH<sub>2</sub>), 3.68 (m, 1H, NHCHCH<sub>2</sub>), 4.81 (m, 1H, NHCHCH<sub>2</sub>), 7.08 (m, 2H, Ar-H), 7.24 (m, 3H, Ar-H), 8.22 (m, 1H, Ar-H), 9.89 – 10.30 (br s., 2H, NH); <sup>19</sup>F NMR (400 MHz, DMSO-*d*<sub>6</sub>) δ -157.68, -156.32, -142.77, -139.52; IR: 1280cm<sup>-1</sup> (C-F), 1475 cm<sup>-1</sup> (benzene C=C), 2748 cm<sup>-1</sup> (C-H), 2914 cm<sup>-1</sup> (C-H benzene); TLC R<sub>f</sub>: 0.74

Pentafluoroephenidine (PFEP, **15l**) afforded 1.92 g (55%) of a white powder. MP 189 °C; <sup>1</sup>H NMR (400 MHz, DMSO-*d*<sub>6</sub> δ ppm = 2.50) δ 1.28 (t, 3H, J = 7.8 Hz, NHCH<sub>2</sub>CH<sub>3</sub>), 3.03 (m, 1H, NHCH<sub>2</sub>CH<sub>3</sub>), 3.18 (m, 1H, NHCH<sub>2</sub>CH<sub>3</sub>), 3.40 (m, 1H, NHCHCH<sub>2</sub>), 3.71 (m, 1H, NHCHCH<sub>2</sub>), 4.80 (m, 1H, NHCHCH<sub>2</sub>), 7.15 – 7.28 (m, 5H, Ar-H), 9.67 (br s., 1H, NH), 10.50 (br s., 1H, NH); <sup>19</sup>F NMR (400 MHz, DMSO-*d*<sub>6</sub>) δ -163.30, -153.79, -140.90; IR: 1288 cm<sup>-1</sup> (C-F), 1475 cm<sup>-1</sup> (benzene C=C), 2752 cm<sup>-1</sup> (C-H), 2914 cm<sup>-1</sup> (C-H benzene); TLC R<sub>f</sub>: 0.70

2-Fluphenidine (2-FP, **20a**) afforded 1.40 g (40%) of a white powder. MP 194 °C; <sup>1</sup>H NMR (400 MHz, DMSO-*d*<sub>6</sub> δ ppm = 2.50) δ 1.32 (m, 1H, PPR-H), 1.68, (m, 1H, PPR-H), 1.70 – 1.82 (m, 3H, PPR-H), 2.05 (m, 1H, PPR-H), 3.48 (m, 1H, PPR-H), 3.51 (m, 1H, NHCHCH<sub>2</sub>), 3.70 (m, 1H, PPR-H), 3.88 (dd, 1H, J = 13.2, 3.8 Hz, NHCHCH<sub>2</sub>), 4.89 (dd, 1H, J = 12.8, 4.1 Hz, NHCHCH<sub>2</sub>), 7.00 – 7.18 (m, 6H, Ar-H), 7.28 – 7.40 (m, 2H, Ar-H), 8.00 (m, 1H, Ar-H), 11.45 (s, 1H, NH); <sup>13</sup>C NMR (400 MHz, DMSO-*d*<sub>6</sub> δ ppm = 39.51) δ 21.45, 21.68, 35.50, 48.22, 51.80, 116.45, 116.81, 125.95, 127.50, 129.82, 130.04, 132.15, 132.60, 136.22, 161.80 (d, J = 221.5 Hz); <sup>19</sup>F NMR (400 MHz, DMSO-*d*<sub>6</sub>) δ -115.71; IR: 2985 cm<sup>-1</sup> (C-H), 1250 cm<sup>-1</sup> (C-F), 1560 cm<sup>-1</sup> (C=C benzene); TLC R<sub>f</sub>: 0.65

3-Fluphenidine (3-FP, **20b**) afforded 1.15 g (35%) of a white powder. MP 224 °C; <sup>1</sup>H NMR (400 MHz, DMSO-*d*<sub>6</sub> δ ppm = 2.50) δ 1.28 (m, 1H, PPR-H), 1.68 – 2.10 (m, 5H, PPR-H), 2.60 – 2.70 (m, 2H, PPR-H), 3.41 (m, 1H, PPR-H),



3.50 (t, 1H, J = 8.4 Hz, NHCHCH<sub>2</sub>), 3.70 – 3.89 (m, 2H, PPR-H, NHCHCH<sub>2</sub>), 4.71 (dd, 1H, J = 12.8, 3.8 Hz, NHCHCH<sub>2</sub>), 7.00 – 7.30 (m, 6H, Ar-H), 7.38 – 7.48 (m, 2H, Ar-H), 7.54 (d, 1H, J = 7.2 Hz, Ar-H), 11.45 (s, 1H, NH); <sup>13</sup>C NMR (400 MHz, DMSO-*d*<sub>6</sub> δ ppm = 39.51) δ 22.05, 22.88, 35.41, 49.00, 52.40, 69.62, 116.80, 117.00, 117.77, 117.99, 127.03, 127.49, 128.79, 129.60, 134.99, 136.87, 162.44 (d, J = 205.5 Hz); <sup>19</sup>F NMR (400 MHz, DMSO-*d*<sub>6</sub>) δ -110.96; IR: 2980 cm<sup>-1</sup> (C-H), 1305 cm<sup>-1</sup> (C-F), 1570 cm<sup>-1</sup> (C=C benzene); TLC R<sub>f</sub>: 0.61

4-Fluphenidine (4-FP, **20c**) afforded 1.54 g (44%) of a white powder. MP 183 – 184 °C; <sup>1</sup>H NMR (400 MHz, DMSO-*d*<sub>6</sub> δ ppm = 2.50) δ 1.23 (m, 1H, PPR-H), 1.61 (m, 1H, PPR-H), 1.72 (m, 2H, PPR-H), 1.80 – 2.01 (m, 2H, PPR-H), 2.52 (m, 2H, PPR-H), 3.35 (m, 1H, PPR-H), 3.45 (m, 1H, NHCHCH<sub>2</sub>), 3.73 (m, 1H, PPR-H), 3.76 (d, 1H, J = 7.8 Hz, NHCHCH<sub>2</sub>), 4.65 (dd, 1H, J = 12.2, 3.8 Hz, NHCHCH<sub>2</sub>), 6.98 – 7.20 (m, 7H, Ar-H), 7.59 (d, 2H, J = 7.2 Hz, Ar-H), 11.29 (s, 1H, NH); <sup>13</sup>C NMR (400 MHz, DMSO-*d*<sub>6</sub> δ ppm = 39.51) δ 22.06, 22.87, 35.51, 48.68, 52.27, 69.48, 115.93, 116.14, 126.98, 128.05, 128.77, 129.61, 133.38, 133.46, 137.03, 162.50 (d, J = 220 Hz); <sup>19</sup>F NMR (400 MHz, DMSO-*d*<sub>6</sub>) δ -110.78; IR: 2980 cm<sup>-1</sup> (C-H), 1305 cm<sup>-1</sup> (C-F), 1570 cm<sup>-1</sup> (C=C benzene); TLC R<sub>f</sub>: 0.62

2-Chlophenidine (2-CP, **20d**) afforded 1.51 g (43%) of a white powder. MP 199 °C; <sup>1</sup>H NMR (400 MHz, DMSO-*d*<sub>6</sub> δ ppm = 2.50) δ 1.38 (m, 1H, PPR-H), 1.62 – 1.90 (m, 4H, PPR-H), 2.09 (m, 1H, PPR-H), 3.15 (m, 1H, PPR-H), 3.24 (m, 1H, PPR-H), 3.27 (m, 1H, PPR-H), 3.43 (m, 1H, NHCHCH<sub>2</sub>), 3.46 (m, 1H, PPR-H), 3.88 (m, 1H, NHCHCH<sub>2</sub>), 5.00 (dd, 1H, J = 12.8 3.8 Hz, NHCHCH<sub>2</sub>), 7.00 (m, 2H, Ar-H), 7.12 (m, 3H, Ar-H), 7.36 (d, 2H, J = 7.8 Hz, Ar-H), 7.49 (m, 1H, Ar-H), 8.27 (d, 1H, J = 7.5 Hz, Ar-H), 11.67 (br s., 1H, NH); <sup>13</sup>C NMR (400 MHz, DMSO-*d*<sub>6</sub> δ ppm = 39.51) δ 21.87, 23.00, 35.85, 49.55, 52.48, 66.20, 127.12, 127.97, 128.05, 129.86, 130.45, 130.94, 131.84, 131.99, 135.65, 136.20; IR: 2950 cm<sup>-1</sup> (C-H), 1570 cm<sup>-1</sup> (C=C benzene), 689 cm<sup>-1</sup> (C-Cl); TLC R<sub>f</sub>: 0.71

3-Chlophenidine (3-CP, **20e**) afforded 1.89 g (54%) of a white powder. MP 172 °C; <sup>1</sup>H NMR (400 MHz, DMSO-*d*<sub>6</sub> δ ppm = 2.50) δ 1.29 (m, 1H, PPR-H), 1.65 (m, 1H, PPR-H), 1.70 – 2.10 (m, 4H, PPR-H), 2.61 (m, 2H, PPR-H), 3.40 (m, 1H, PPR-H), 3.52 (m, 1H, NHCHCH<sub>2</sub>), 3.75 – 3.85 (m, 2H, PPR-H, NHCHCH<sub>2</sub>), 4.71 (d, 1H, J = 8.2 Hz, NHCHCH<sub>2</sub>), 7.00 - 7.20 (m, 4H, Ar-H), 7.42 (m, 2H, Ar-H), 7.60 (dd, 1H, J = 8.2, 3.3 Hz, Ar-H), 7.70 (s, 2H, Ar-H), 11.36 (s, 1H, NH); <sup>13</sup>C NMR (400 MHz, DMSO-*d*<sub>6</sub> δ ppm = 39.51) δ 22.01, 22.89, 35.26, 49.01, 52.36, 69.51, 127.04, 128.83, 129.60, 129.99, 130.10, 130.93, 133.79, 134.61, 136.82; IR: 2900 cm<sup>-1</sup> (C-H), 1565 cm<sup>-1</sup> (C=C benzene), 699 cm<sup>-1</sup> (C-Cl); TLC R<sub>f</sub>: 0.73

4-Chlophenidine (4-CP, **20f**) afforded 1.72 g (49%) of a white powder. MP 170 °C; <sup>1</sup>H NMR (400 MHz, DMSO-*d*<sub>6</sub> δ ppm = 2.50) δ 1.26 (m, 1H, PPR-H), 1.64 (m, 1H, PPR-H), 1.70 – 2.05 (m, 4H, PPR-H), 2.50 - 2.60 (m, 2H, PPR-H), 3.39 (m, 1H, PPR-H), 3.48 (m, 1H, NHCHCH<sub>2</sub>), 3.71 (m, 1H, PPR-H), 3.80 (dd, 1H, J = 12.8, 3.6 Hz, NHCHCH<sub>2</sub>), 7.00 – 7.20 (m, 5H, Ar-H), 7.43 (d, 2H, J = 8.8 Hz, Ar-H), 7.60 (d, 2H, J = 7.4 Hz, Ar-H), 11.42 (s, 1H, NH); <sup>13</sup>C NMR (400 MHz, DMSO-*d*<sub>6</sub> δ ppm = 39.51) δ 21.52, 22.37, 34.83, 48.23, 51.81, 68.93, 126.50, 128.31, 128.95, 129.11, 130.86, 132.55, 134.19, 136.42; IR: 2865 cm<sup>-1</sup> (C-H), 1540 cm<sup>-1</sup> (C=C benzene), 710 cm<sup>-1</sup> (C-Cl); TLC R<sub>f</sub>: 0.73

2-Brophenidine (2-BP, **20g**) afforded 1.65 g (47%) of a white powder. MP 185 °C; <sup>1</sup>H NMR (400 MHz, DMSO-*d*<sub>6</sub> δ ppm = 2.50) δ 1.40 (m, 1H, PPR-H), 1.70 – 1.90 (m, 4H, PPR-H), 2.04 (m, 1H, PPR-H), 2.68 (m, 1H, PPR-H), 2.76 (m, 1H, PPR-H), 3.26 (m, 1H, PPR-H), 3.44 (m, 1H, NHCHCH<sub>2</sub>), 3.88 (m, 2H, PPR-H, NHCHCH<sub>2</sub>), 4.95 (m, 1H, NHCHCH<sub>2</sub>), 7.00 (d, 2H, J = 7.5 Hz, Ar-H), 7.12 (m, 3H, Ar-H), 7.28 (dd, 1H, J = 9.2, 3.1 Hz, Ar-H), 7.54 (m, 2H, Ar-H), 8.25 (d, 1H, J = 9.2 Hz, Ar-H), 11.55 (s, 1H, NH); <sup>13</sup>C NMR (400 MHz, DMSO-*d*<sub>6</sub> δ ppm = 39.51) δ 21.31, 22.37, 22.49, 36.01, 49.45, 51.88, 68.50, 126.43, 126.66, 128.13, 128.50, 129.19, 130.96, 131.20, 132.56, 133.13, 135.58; IR: 2870 cm<sup>-1</sup> (C-H), 1540 cm<sup>-1</sup> (C=C benzene), 550 cm<sup>-1</sup> (C-Br); TLC R<sub>f</sub>: 0.80

3-Brophenidine (3-BP, **20h**) afforded 1.72 g (49%) of a white powder. MP 200 °C; <sup>1</sup>H NMR (400 MHz, DMSO-*d*<sub>6</sub> δ ppm = 2.50) δ 1.64 (m, 1H, PPR-H), 1.60

– 2.15 (m, 5H, PPR-H), 2.50 – 2.68 (m, 2H, PPR-H), 3.38 – 3.55 (m, 2H, PPR-H, NHCHCH<sub>2</sub>), 3.70 – 3.87 (m, 2H, PPR-H, NHCHCH<sub>2</sub>), 4.69 (d, 1H, J = 9.8 Hz, NHCHCH<sub>2</sub>), 7.00 - 7.20 (m, 4H, Ar-H), 7.33 (d, 2H, J = 7.2 Hz, Ar-H), 7.57 (d, 1H, J = 7.2 Hz, Ar-H), 7.65 (d, 1H, J = 7.0 Hz, Ar-H), 7.83 (s, 1H, Ar-H), 11.62 (s, 1H, NH); <sup>13</sup>C NMR (400 MHz, DMSO-*d*<sub>6</sub> δ ppm = 39.51) δ 21.51, 22.29, 34.77, 48.45, 51.85, 68.98, 121.85, 126.49, 128.28, 129.06, 129.89, 130.63, 132.33, 133.31, 134.39, 136.34; IR: 2900 cm<sup>-1</sup> (C-H), 1520 cm<sup>-1</sup> (C=C benzene), 570 cm<sup>-1</sup> (C-Br); TLC R<sub>f</sub>: 0.77

4-Brophenidine (4-BP, **20i**) afforded 2.14 g (61%) of a white powder. MP 198 – 200 °C; <sup>1</sup>H NMR (400 MHz, DMSO-*d*<sub>6</sub> δ ppm = 2.50) δ 1.23 (m, 1H, PPR-H), 1.58 – 2.05 (m, 5H, PPR-H), 2.50 – 2.60 (m, 2H, PPR-H), 3.35 (m, 1H, PPR-H), 3.45 (m, 1H, NHCHCH<sub>2</sub>), 3.70 (m, 1H, PPR-H), 3.80 (m, 1H, NHCHCH<sub>2</sub>), 4.64 (dd, J = 12.4, 3.8 Hz, NHCHCH<sub>2</sub>), 6.95 – 7.18 (m, 6H, Ar-H), 7.45 – 7.55 (m, 3H, Ar-H), 11.43 (s, 1H, NH); <sup>13</sup>C NMR (400 MHz, DMSO-*d*<sub>6</sub> δ ppm = 39.51) δ 21.89, 22.45, 35.80, 48.31, 53.88, 70.06, 123.87, 127.60, 129.83, 130.05, 132.14, 132.88, 133.74, 137.68; IR: 2865 cm<sup>-1</sup> (C-H), 1600 cm<sup>-1</sup> (C=C benzene), 560 cm<sup>-1</sup> (C-Br); TLC R<sub>f</sub>: 0.79

2-Iodophenidine (2-IP, **20j**) afforded 0.91 g (26%) of a white powder. MP 230 °C; <sup>1</sup>H NMR (400 MHz, DMSO-*d*<sub>6</sub> δ ppm = 2.50) δ 1.37 (m, 1H, PPR-H), 1.70 – 1.82 (m, 4H, PPR-H), 2.04 (m, 1H, PPR-H), 2.60 – 2.90 (m, 2H, PPR-H), 3.16 (m, 1H, PPR-H), 3.32 (m, 1H, NHCHCH<sub>2</sub>), 3.75 – 3.85 (m, 2H, PPR-H, NHCHCH<sub>2</sub>), 4.74 (m, 1H, NHCHCH<sub>2</sub>), 6.94 (d, 1H, J = 9.2 Hz, Ar-H), 7.08 (m, 3H, Ar-H), 7.50 (d, 1H, J = 11.2 Hz, Ar-H), 7.73 (dd, 2H, J = 13.2, 4.8 Hz, Ar-H), 8.13 (d, 2H, J = 9.2 Hz, Ar-H), 11.46 (br s., 1H, NH); <sup>13</sup>C NMR (400 MHz, DMSO-*d*<sub>6</sub> δ ppm = 39.51) δ 21.89, 23.10, 37.52, 50.72, 53.27, 74.21, 105.86, 127.59, 128.33, 129.92, 130.15, 130.97, 132.01, 136.18, 140.83; IR: 2940 cm<sup>-1</sup> (C-H), 1550 cm<sup>-1</sup> (C=C benzene); TLC R<sub>f</sub>: 0.83

3-Iodophenidine (3-IP, **20k**) afforded 1.89 g (54%) of an off-white powder. MP 249 °C; <sup>1</sup>H NMR (400 MHz, DMSO-*d*<sub>6</sub> δ ppm = 2.50) δ 1.22 (m, 1H, PPR-H), 1.52 – 2.00 (m, 5H, PPR-H), 2.50 – 2.70 (m, 2H, PPR-H), 3.30 – 3.50 (m, 2H, PPR-H, NHCHCH<sub>2</sub>), 3.62 – 3.80 (m, 2H, PPR-H, NHCHCH<sub>2</sub>), 4.59 (m, 1H,

NHCHCH<sub>2</sub>), 6.95 – 7.20 (m, 6H, Ar-H), 7.59 – 7.70 (m, 2H, Ar-H), 7.92 (s, 1H, Ar-H), 11.31 (br s., 1H, NH); <sup>13</sup>C NMR (400 MHz, DMSO-*d*<sub>6</sub> δ ppm = 39.51) δ 20.96, 22.89, 35.47, 48.91, 52.16, 69.58, 95.80, 127.48, 129.84, 130.28, 131.63, 131.90, 135.78, 137.05, 138.92, 139.70; IR: 2865 cm<sup>-1</sup> (C-H), 1620 cm<sup>-1</sup> (C=C benzene); TLC R<sub>f</sub>: 0.80

4-Iodophenidine (4-IP, **20I**) afforded 2.10 g (60%) of a white powder. MP 255 °C; <sup>1</sup>H NMR (400 MHz, DMSO-*d*<sub>6</sub> δ ppm = 2.50) δ 1.29 (m, 1H, PPR-H), 1.65 – 2.10 (m, 5H, PPR-H), 2.50 – 2.61 (m, 2H, PPR-H), 3.40 – 3.52 (m, 2H, PPR-H, NHCHCH<sub>2</sub>), 3.70 – 3.85 (m, 2H, PPR-H, NHCHCH<sub>2</sub>), 4.65 (dd, 1H, J = 12.8, 3.8 Hz, NHCHCH<sub>2</sub>), 7.00 – 7.15 (m, 5H, Ar-H), 7.38 (d, 2H, J = 8.2 Hz, Ar-H), 7.73 (d, 2H, J = 9.4 Hz, Ar-H), 11.43 (s, 1H, NH); <sup>13</sup>C NMR (400 MHz, DMSO-*d*<sub>6</sub> δ ppm = 39.51) δ 21.50, 22.58, 36.70, 51.00, 57.62, 71.58, 98.14, 126.77, 128.51, 131.30, 131.96, 132.86, 134.22, 136.78, 137.45, 139.43; IR: 2930 cm<sup>-1</sup> (C-H), 1600 cm<sup>-1</sup> (C=C benzene); TLC R<sub>f</sub>: 0.84

2-Fluoromphenidine (2-FMP, **21a**) afforded 2.10 g (60%) of a white powder. MP 155 °C; <sup>1</sup>H NMR (400 MHz, DMSO-*d*<sub>6</sub> δ ppm = 2.50) δ 2.45 (t, 3H, J = 7.6 Hz, CH<sub>3</sub>) 3.18 (m, 1H, NHCHCH<sub>2</sub>), 3.65 (dd, 1H, J = 7.2, 3.2 Hz, NHCHCH<sub>2</sub>), 4.72 (m, 1H, NHCHCH<sub>2</sub>), 7.00 – 7.20 (m, 4H, Ar-H), 7.28 – 7.45 (m, 3H, Ar-H), 7.90 (t, 2H, 5.4 Hz, Ar-H), 9.68 (br s., 1H, NH), 10.16 (br s., 1H, NH); <sup>13</sup>C NMR (400 MHz, DMSO-*d*<sub>6</sub> δ ppm = 39.51) δ 31.15, 38.57, 57.78, 116.60, 122.23, 123.79, 124.17, 125.69, 125.81, 128.92, 129.15, 129.76, 131.91, 136.08, 161.84 (d, J = 206.5 Hz); <sup>19</sup>F NMR (400 MHz, DMSO-*d*<sub>6</sub>) δ -118.24; R<sub>f</sub> 0.58

3-Fluoromphenidine (3-FMP, **21b**) afforded 1.68 g (48%) of a white powder. MP 162 °C; <sup>1</sup>H NMR (400 MHz, DMSO-*d*<sub>6</sub> δ ppm = 2.50) δ 2.29 (s, 3H, CH<sub>3</sub>), 3.18 (m, 1H, NHCHCH<sub>2</sub>), 3.55 (m, 1H, NHCHCH<sub>2</sub>), 4.60 (m, 1H, NHCHCH<sub>2</sub>), 7.05 (m, 3H, Ar-H), 7.18 – 7.25 (m, 4H, Ar-H), 7.62 (m, 2H, Ar-H), 9.65 (br s., 2H, NH); <sup>13</sup>C NMR (400 MHz, DMSO-*d*<sub>6</sub> δ ppm = 39.51) δ 31.40, 36.87, 60.21, 115.89, 122.20, 123.52, 124.35, 124.81, 125.73, 127.60, 129.06, 1209.76, 131.89, 134.56, 160.54 (d, J = 221.0 Hz); <sup>19</sup>F NMR (400 MHz, DMSO-*d*<sub>6</sub>) δ -111.26; R<sub>f</sub> 0.50

4-Fluoromephenidine (4-FMP, **21c**) afforded 1.99 g (57%) of a white powder. MP 178 °C; <sup>1</sup>H NMR (400 MHz, DMSO-*d*<sub>6</sub> δ ppm = 2.50) δ 2.41 (s, 3H, CH<sub>3</sub>), 3.18 (m, 1H, NHCHCH<sub>2</sub>), 3.60 (m, 1H, NHCHCH<sub>2</sub>), 4.51 (dd, 1H, J = 7.2, 3.8 Hz, NHCHCH<sub>2</sub>), 7.02 (d, 2H, J = 7.2 Hz, Ar-H), 7.10 – 7.25 (m, 5H, Ar-H), 7.55 (m, 2H, Ar-H); <sup>13</sup>C NMR (400 MHz, DMSO-*d*<sub>6</sub> δ ppm = 39.51) δ 31.58, 39.26, 63.18, 116.78, 127.13, 128.96, 130.07, 131.82, 136.91, 162.80 (d, J = 225 Hz); <sup>19</sup>F NMR (400 MHz, DMSO-*d*<sub>6</sub>) δ -111.94; R<sub>f</sub> 0.52

2-Fluorodimephenidine (2-FDMP, **22a**) afforded 1.54 g (44%) of a white powder. MP 183 °C; <sup>1</sup>H NMR (400 MHz, DMSO-*d*<sub>6</sub> δ ppm = 2.50) δ 2.68 (d, 3H, J = 7.2 Hz, CH<sub>3</sub>), 2.88 (d, 3H, J = 7.2 Hz, CH<sub>3</sub>), 3.48 (m, 1H, NHCHCH<sub>2</sub>), 3.71 (m, 1H, NHCHCH<sub>2</sub>), 4.98 (dd, 1H, J = 7.2, 3.4 Hz, NHCHCH<sub>2</sub>), 7.00 – 7.22 (m, 4H, Ar-H), 7.29 (m, 2H, Ar-H), 7.40 (m, 1H, Ar-H), 8.04 (m, 2H, Ar-H), 11.49 (br s., 1H, NH); <sup>13</sup>C NMR (400 MHz, DMSO-*d*<sub>6</sub> δ ppm = 39.51) δ 35.38, 41.92, 42.14, 63.04, 116.18, 116.41, 119.52, 125.42, 127.22, 128.83, 129.51, 131.40, 136.26, 161.40 (d, J = 202.5 Hz); <sup>19</sup>F NMR (400 MHz, DMSO-*d*<sub>6</sub>) δ -115.80; R<sub>f</sub> 0.63

3-Fluorodimephenidine (3-FDMP, **22b**) afforded 1.61 g (46%) of a white powder. MP 188 °C; <sup>1</sup>H NMR (400 MHz, DMSO-*d*<sub>6</sub> δ ppm = 2.50) δ 2.56 (d, 3H, J = 7.2 Hz, CH<sub>3</sub>), 2.78 (d, 3H, J = 6.8 Hz, CH<sub>3</sub>), 3.40 (m, 1H, NHCHCH<sub>2</sub>), 3.69 (m, 1H, NHCHCH<sub>2</sub>), 4.73 (m, 1H, NHCHCH<sub>2</sub>), 7.00 – 7.20 (m, 6H, Ar-H), 7.30 – 7.40 (m, 2H, Ar-H), 7.46 (d, 1H, J = 5.8 Hz, Ar-H), 11.61 (br s., 1H, NH); <sup>13</sup>C NMR (400 MHz, DMSO-*d*<sub>6</sub> δ ppm = 39.51) δ 35.63, 41.82, 69.40, 116.83, 117.40, 117.62, 127.18, 128.83, 129.59, 131.19, 134.88, 136.59, 162.57 (d, J = 214 Hz); <sup>19</sup>F NMR (400 MHz, DMSO-*d*<sub>6</sub>) δ -110.71; R<sub>f</sub> 0.64

4-fluorodimephenidine (4-FDMP, **22c**) afforded 1.44 g (41%) of a white powder. MP 197 °C; <sup>1</sup>H NMR (400 MHz, DMSO-*d*<sub>6</sub> δ ppm = 2.50) δ 2.46 (s, 3H, CH<sub>3</sub>), 2.72 (s, 3H, CH<sub>3</sub>), 3.39 (m, 1H, NHCHCH<sub>2</sub>), 3.65 (m, 1H, NHCHCH<sub>2</sub>), 4.70 (dd, J = 7.8, 3.2 Hz, NHCHCH<sub>2</sub>), 7.00 – 7.20 (m, 7H, Ar-H), 7.62 (m, 2H, Ar-H), 11.58 (br s., 1H, NH); <sup>13</sup>C NMR (400 MHz, DMSO-*d*<sub>6</sub> δ ppm = 39.51) δ 35.70, 41.69, 69.19, 116.18, 127.03, 128.81, 129.61, 133.07,

136.70, 162.88 (d, J = 210.5 Hz);  $^{19}\text{F}$  NMR (400 MHz, DMSO- $d_6$ )  $\delta$  -110.64;  $R_f$  0.61

2-Fluorodiephenidine (2-FDEP, **23a**) afforded 1.89 g (54%) of a white powder. MP 181 °C;  $^1\text{H}$  NMR (400 MHz, DMSO- $d_6$   $\delta$  ppm = 2.50)  $\delta$  1.17 (t, 3H, J = 7.2 Hz,  $\text{CH}_2\text{CH}_3$ ), 1.38 (t, 3H, J = 7.2 Hz,  $\text{CH}_2\text{CH}_3$ ), 2.79 (m, 2H,  $\text{CH}_2\text{CH}_3$ ), 3.23 (m, 2H,  $\text{CH}_2\text{CH}_3$ ), 3.41 (m, 1H,  $\text{NHCHCH}_2$ ), 3.80 (m, 1H,  $\text{NHCHCH}_2$ ), 4.85 (m, 1H,  $\text{NHCHCH}_2$ ), 6.95 – 7.15 (m, 4H, Ar-H), 7.30 – 7.42 (m, 3H, Ar-H), 8.15 (t, 2H, J = 7.8 Hz, Ar-H), 11.48 (br s., 1H, NH);  $^{13}\text{C}$  NMR (400 MHz, DMSO- $d_6$   $\delta$  ppm = 39.51)  $\delta$  8.50, 35.50, 43.77, 44.97, 59.43, 115.54, 120.02, 125.06, 128.25, 129.05, 130.84, 131.76, 135.75, 160.61 (d, J = 220 Hz);  $^{19}\text{F}$  NMR (400 MHz, DMSO- $d_6$ )  $\delta$  -117.89;  $R_f$  0.59

3-Fluorodiephenidine (3-FDEP, **23b**) afforded 1.92 g (55%) of a white powder. MP 177 °C;  $^1\text{H}$  NMR (400 MHz, DMSO- $d_6$   $\delta$  ppm = 2.50)  $\delta$  1.15 (t, 3H, J = 9.2 Hz,  $\text{CH}_2\text{CH}_3$ ), 1.33 (t, 3H, J = 8.5 Hz,  $\text{CH}_2\text{CH}_3$ ), 2.74 (m, 1H,  $\text{CH}_2\text{CH}_3$ ), 2.85 (m, 1H,  $\text{CH}_2\text{CH}_3$ ), 3.40 (m, 1H,  $\text{NHCHCH}_2$ ), 3.74 (m, 1H,  $\text{NHCHCH}_2$ ), 4.65 (m, 1H,  $\text{NHCHCH}_2$ ), 7.00 – 7.20 (m, 5H, Ar-H), 7.30 – 7.40 (m, 3H, Ar-H), 7.65 (d, 1H, J = 7.2 Hz, Ar-H), 11.45 (br s., 1H, NH);  $^{13}\text{C}$  NMR (400 MHz, DMSO- $d_6$   $\delta$  ppm = 39.51)  $\delta$  9.23, 36.38, 45.11, 66.89, 116.59, 117.26, 127.01, 128.73, 129.70, 131.07, 136.67, 162.44 (d, J = 210.5 Hz);  $^{19}\text{F}$  NMR (400 MHz, DMSO- $d_6$ )  $\delta$  -111.03;  $R_f$  0.61

4-Fluorodiephenidine (4-FDEP, **23c**) afforded 2.38 g (68%) of a white powder. MP 177 °C;  $^1\text{H}$  NMR (400 MHz, DMSO- $d_6$   $\delta$  ppm = 2.50)  $\delta$  1.18 (t, 3H, J = 7.8 Hz,  $\text{CH}_2\text{CH}_3$ ), 1.36 (t, 3H, J = 7.2 Hz,  $\text{CH}_2\text{CH}_3$ ), 2.73 (m, 2H,  $\text{CH}_2\text{CH}_3$ ), 3.16 (m, 2H,  $\text{CH}_2\text{CH}_3$ ), 3.41 (m, 1H,  $\text{NHCHCH}_2$ ), 3.78 (m, 1H,  $\text{NHCHCH}_2$ ), 4.66 (m, 1H,  $\text{NHCHCH}_2$ ), 7.00 – 7.25 (m, 7H, Ar-H), 7.70 (d, 2H, J = 7.4 Hz, Ar-H), 11.40 (br s., 1H, NH);  $^{13}\text{C}$  NMR (400 MHz, DMSO- $d_6$   $\delta$  ppm = 39.51)  $\delta$  9.40, 36.44, 44.79, 45.13, 66.75, 115.92, 129.96, 128.71, 129.70, 132.91, 132.99, 136.84, 162.89 (d, J = 218.5 Hz);  $^{19}\text{F}$  NMR (400 MHz, DMSO- $d_6$ )  $\delta$  -111.29;  $R_f$  0.64

2-Fluorotrifluoroephenidine (2-FTFEP, **24a**) afforded 1.44 g (41%) of a white powder. MP 204 °C; <sup>1</sup>H NMR (400 MHz, DMSO-*d*<sub>6</sub> δ ppm = 2.50) δ 3.15 (m, 1H, CH<sub>2</sub>CF<sub>3</sub>), 3.50 – 4.00 (m, 3H, CH<sub>2</sub>CF<sub>3</sub>, NHCHCH<sub>2</sub>), 4.71 (m, 1H, NHCHCH<sub>2</sub>), 7.00 – 7.50 (m, 8H, Ar-H), 7.91 (d, 1H, J = 7.8 Hz, Ar-H), 9.17 (br s., 2H, NH); <sup>13</sup>C NMR (400 MHz, DMSO-*d*<sub>6</sub> δ ppm = 39.51) δ 46.50, 57.21, 116.24, 123.79, 126.92, 129.12, 129.57, 131.65, 137.59, 161.75 (d, J = 221.5 Hz); <sup>19</sup>F NMR (400 MHz, DMSO-*d*<sub>6</sub>) δ –66.20, -117.81; R<sub>f</sub>0.55

3-Fluorotrifluoroephenidine (3-FTFEP, **24b**) afforded 1.29 g (37%) of a white powder. MP 211 °C; <sup>1</sup>H NMR (400 MHz, DMSO-*d*<sub>6</sub> δ ppm = 2.50) δ 3.15 (m, 1H, CH<sub>2</sub>CF<sub>3</sub>), 3.40 – 4.00 (m, 3H, CH<sub>2</sub>CF<sub>3</sub>, NHCHCH<sub>2</sub>), 4.49 (m, 1H, NHCHCH<sub>2</sub>), 7.05 (m, 2H, Ar-H), 7.15 – 7.25 (m, 4H, Ar-H), 7.38 (m, 3H, Ar-H), 9.15 (br s., 2H, NH); <sup>13</sup>C NMR (400 MHz, DMSO-*d*<sub>6</sub> δ ppm = 39.51) δ 48.25, 56.17, 115.91, 122.47, 124.93, 128.19, 129.54, 129.91, 130.82, 131.53, 134.63, 161.69 (d, J = 217 Hz); <sup>19</sup>F NMR (400 MHz, DMSO-*d*<sub>6</sub>) δ –66.20, -110.54; R<sub>f</sub>0.48

4-Fluorotrifluoroephenidine (4-FTFEP, **24c**) afforded 1.57 g (45%) of a white powder. MP 206 °C; <sup>1</sup>H NMR (400 MHz, DMSO-*d*<sub>6</sub> δ ppm = 2.50) δ 3.12 (m, 1H, CH<sub>2</sub>CF<sub>3</sub>), 3.40 – 4.00 (m, 3H, CH<sub>2</sub>CF<sub>3</sub>, NHCHCH<sub>2</sub>), 4.52 (m, 1H, NHCHCH<sub>2</sub>), 7.00 (m, 3H, Ar-H), 7.10 – 7.25 (m, 4H, Ar-H), 7.50 (d, 2H, J = 7.4 Hz, Ar-H), 9.08 (br s., 1H, NH); <sup>13</sup>C NMR (400 MHz, DMSO-*d*<sub>6</sub> δ ppm = 39.51) δ 45.89, 64.11, 116.33, 127.89, 128.54, 129.18, 131.89, 136.91, 162.15 (d, J = 208.8 Hz); <sup>19</sup>F NMR (400 MHz, DMSO-*d*<sub>6</sub>) δ –66.20, -110.79; R<sub>f</sub>0.50

## 2.2. Presumptive Test Reagents

Presumptive tests reagents were prepared according to the United Nations recommended guidelines.<sup>118</sup> The following standard presumptive tests applied in this study: (i) Marquis; (ii) Mandelin; (iii) Simon's; (iv) Robadope's; (v) Scott's; (vi) Zimmerman test(s). Sample solutions were prepared at  $10 \text{ mg mL}^{-1}$  by dissolving the reference standards in distilled water. Negative control samples (distilled water) were used in all tests in order to indicate clearly when a positive result occurred.

**Marquis Test:** 1% formaldehyde (37% aqueous solution) in concentrated sulphuric acid (10 mL). 5 drops of test sample in distilled water ( $10 \text{ mg mL}^{-1}$ ) was placed into a dimple well of a white spotting tile and 5 drops of the test reagent added. The Marquis test was used on all synthesised samples to presumptively identify alkaloids. Any immediate colour change or other noticeable effect occurring was noted and observations were made again after a 5 minute period.

**Mandelin Test:** 1% ammonium metavanadate in concentrated sulphuric acid (10 mL). 5 drops of test sample in distilled water ( $10 \text{ mg mL}^{-1}$ ) was placed into a dimple well of a white spotting tile and 5 drops of the test reagent added. The Mandelin test was used on all synthesised samples to presumptively identify alkaloids. Any immediate colour change or other noticeable effect occurring was noted and observations were made again after a 5 minute period.

**Simon's Test: Reagent 1:** 2% aqueous sodium carbonate solution (10 mL); **Reagent 2:** 1% aqueous sodium nitroprusside solution (10mL); **Reagent 3:** 50% methanolic acetaldehyde solution (10 mL). 5 drops of test sample in distilled water ( $10 \text{ mg mL}^{-1}$ ) was placed into a dimple well of a white spotting tile and 5 drops of the test reagent added. The Simon's test was used on all synthesised samples to presumptively identify alkaloids and any secondary amines. Any immediate colour change or other noticeable effect occurring was noted and observations were made again after a 5 minute period.



**Robadope's Test:** **Reagent 1:** 2% aqueous sodium carbonate solution (10 mL); **Reagent 2:** 1% aqueous sodium nitroprusside solution (10 mL); **Reagent 3:** 50% methanolic acetone solution (10 mL). 5 drops of test sample in distilled water ( $10 \text{ mg mL}^{-1}$ ) was placed into a dimple well of a white spotting tile and 5 drops of the test reagent added. The Robadope's test was used on all synthesised samples to presumptively identify alkaloids and primary amines. Any immediate colour change or other noticeable effect occurring was noted and observations were made again after a 5 minute period.

**Scott's Test:** 1% cobalt thiocyanate in a 50% aqueous glycerine solution (10 mL). 5 drops of test sample in distilled water ( $10 \text{ mg mL}^{-1}$ ) was placed into a dimple well of a white spotting tile and 5 drops of the test reagent added. The Scott's test was used on all synthesised samples to presumptively identify cocaine and other tertiary amines. Any immediate colour change or other noticeable effect occurring was noted and observations were made again after a 5 minute period.

**Zimmerman Test:** **Reagent 1:** 1% solution of 1,3-dinitrobenzene in methanol (10 mL); **Reagent 2:** 15% aqueous potassium hydroxide solution (10 mL). 5 drops of test sample in distilled water ( $10 \text{ mg mL}^{-1}$ ) was placed into a dimple well of a white spotting tile and 5 drops of the test reagent added. The Zimmerman test was used on all synthesised samples to presumptively identify cathinones. Any immediate colour change or other noticeable effect occurring was noted and observations were made again after a 5 minute period.

### 2.3. Thin Layer Chromatography

Thin layer chromatography (TLC) was carried out on aluminium-backed SiO<sub>2</sub> plates (Merck, Germany) and spots were visualised using ultra-violet light (254 nm). The mobile phase used was dichloromethane: methanol (9:1 v/v) containing 0.8% ammonia (7 N in methanol). The developed plate was viewed under UV light (254 nm) and any spots noted. The plate was sprayed with modified Dragendorff-Ludy-Tenger reagent the blood-red spots marked with a pencil and the Retention Factor ( $R_f$ ) calculated for each analyte.<sup>102</sup> For all diphenidine and ephenidine derivatives, including the halogenated samples, Relative Retention Factors ( $RR_f$ ) were calculated with respect to diphenidine (**13a**). Six repetitive tests of all compounds were conducted and negative control samples were used in all tests.

## 2.4. Gas Chromatography – Mass Spectroscopy (GC-MS)

### 2.4.1. GC-MS of diphenidine derivatives

An Agilent 6850 GC connected to a MS5973 mass selective detector (Agilent Technologies, Wokingham, UK) was used to perform GC-MS analysis on the thirteen diphenidine derivatives (**10a–10m**, Chapter 4). The mass spectrometer was operated in the electron ionisation mode at 70 eV. Separation was achieved with a capillary column (HP5 MS, 30 m  $\times$  0.25 mm i.d. 0.25  $\mu$ m), using a non-polar (5%-phenyl)-methylpolysiloxane stationary phase, with helium as the carrier gas at a constant flow rate of 1.0 mL min<sup>-1</sup>. Manual injections were performed with the GC injection temperature set to 280°C and the mass selective detector split temperature set to 300°C. The split ratio was set to 100:1, while the MS source and quadrupole temperatures were set at 230°C and 150°C respectively. Mass spectra were obtained in full scan mode (50–550 amu). All samples (qualitative analysis) were prepared as 1 mg mL<sup>-1</sup> solutions in methanol. Eicosane was added to each sample (1 mg mL<sup>-1</sup>) and a 2  $\mu$ L injection volume was used. Three commonly encountered adulterants benzocaine, caffeine and procaine were added into the mixture.

### 2.4.2. GC-MS of cathinones, amphetamines, halogenated diphenidine derivatives, ephenidines and diphenidine analogues

GC-MS analysis of all fluorinated cathinone and amphetamine regioisomers (chapter 3), halogenated diphenidines (chapter 5), diphenidine analogues (chapter 6) and the fluorinated ephenidine regioisomers (chapter 7), was performed on a 7890 B GC system connected to a 5977B mass spectrometer (Agilent Technologies, Wokingham, UK). Similar to the diphenidine analysis, an electron ionisation mode at 70 eV was used with a HP5 MS capillary column (30 m  $\times$  0.25 mm i.d. 0.25  $\mu$ m), using a non-polar (5%-phenyl)-methylpolysiloxane stationary phase and helium as the carrier gas at a flow rate of 1 mL min<sup>-1</sup>. The split ratio was set to 50:1 with the MS source and quadrupole temperatures set at 230°C and 150°C respectively. All samples were again prepared as 1 mg mL<sup>-1</sup> solutions in methanol for initial qualitative analysis with eicosane added as an internal standard at 1 mg mL<sup>-1</sup>, before

being diluted 1 in 10 to create a 100 µg mL<sup>-1</sup> sample and eicosane solution for analysis. 1 µL of sample was injected using an Agilent Technologies 7693 Autosampler (Agilent Technologies, Wokingham, UK).

### 2.4.3. Oven Temperature Programmes

#### 2.4.3.1. Initial screening method 1

All thirteen of the diphenidine derivatives (**13a–13m**) along with the halogenated derivatives (**20a–20l**) and the polyfluorinated ephenidine regioisomers (**15d–15l**) were run on an initial screening method. The oven temperature programme can be seen in Table 7.

**Table 7:** Oven temperature programme for the initial screening of diphenidine and ephenidine derivatives

Time (min)	Temperature (°C)	Rate (°C min <sup>-1</sup> )	Hold Time (min)
0	60-300	10	2

#### 2.4.3.2. Initial screening method 2

All the fluorinated cathinone and amphetamine derivatives along with the monofluorinated diphenidine analogues were run on a different initial screening run to determine whether samples could be initially separated. This oven temperature programme can be seen in Table 8.

**Table 8:** Oven temperature programme for the initial screening of monofluorinated cathinones, amphetamines and diphenidine analogues

Time (min)	Temperature (°C)	Rate (°C min <sup>-1</sup> )	Hold Time (min)
0	50-290	30	15

#### 2.4.3.3. Developed cathinone and amphetamine method

A new oven temperature programme was developed to help further separate the regioisomers of fluoroamphetamine (FA, **4a–4c**), fluoromethcathinone

(FMC, **8a–8c**) and trifluoromethylmethcathinone (TFMMC, **9a-9c**) isomers. Table 9 shows the developed oven temperature programme.

**Table 9:** Developed oven temperature programme for the separation of fluorinated cathinone and amphetamine regioisomers

Time (min)	Temperature (°C)	Rate (°C min <sup>-1</sup> )	Hold Time (min)
0	50-290	30	15

#### 2.4.3.4. Developed diphenidine derivatives method

A new oven temperature programme was developed for the separation of a range of diphenidine derivatives (**13a–13m**). The oven temperature programme can be seen in Table 10.

**Table 10:** Developed oven temperature programme for the separation of thirteen diphenidine derivatives

Time (min)	Temperature (°C)	Rate (°C min <sup>-1</sup> )	Hold Time (min)
0	60 – 170	10	13
24	170 – 200	20	12
37.5	200 – 260	10	0
43.5	260 – 280	20	1

#### 2.4.3.5. Developed halogenated diphenidines method

An oven programme was developed for all twelve halogenated diphenidine derivatives (**20a-20l**) in order to achieve separation. The temperature programme can be seen in Table 11. The oven temperature used produced an overall run time of 33 minutes.

**Table 11:** Oven temperature programme for the separation of the halogenated diphenidines

Time (min)	Temperature (°C)	Rate (°C min <sup>-1</sup> )	Hold Time (min)
0	80-210	10	0
13	210-240	2	0
28	240-280	20	3

#### 2.4.3.6. Developed diphenidine analogues method

A developed method was created for the separation of the diphenidine analogues. A single ion monitoring (SIM) detection mode was also used for the identification of classes of compounds with the SIM ions chosen shown in Table 12 and the developed oven temperature programme shown in Table 12.

**Table 12:** SIM ions used for all of the diphenidine analogue regioisomers

Compound	Abbreviation (No.)	SIM ion used
fluoroephenidine	FEP (15a–15c)	152.1
fluorolintane	FL (19a–19c)	178.1
fluphenidine	FP (20a–20c)	192.1
fluoromephenidine	FMP (21a–21c)	138.1
fluorodimephenidine	FDMP (22a–22c)	152.1
fluorodiephenidine	FDEP (23a–23c)	180.1
fluorotrifluoroephenidine	FTFEP (24a–24c)	206.1

**Table 13:** Developed oven temperature programme for the diphenidine analogues

Time (min)	Temperature (°C)	Rate (°C min <sup>-1</sup> )	Hold Time (min)
0	90 - 160	5	0
14	160 - 180	1	0
34	180 - 290	30	2

#### 2.4.3.7. Developed polyfluorinated ephenidines method

A developed oven temperature programme was made for the attempted separation of the polyfluorinated ephenidines (15d–15l). The temperature programme can be seen in Table 14.

**Table 14:** Developed oven temperature programme for the attempted separation of the polyfluorinated ephenidine isomers

Time (min)	Temperature (°C)	Rate (°C min <sup>-1</sup> )	Hold Time (min)
0	170-220	2	0
25	220-240	10	0
27	240-300	30	2

## 2.4.4. Standards and test solution preparation

### 2.4.4.1. Reference standard preparation

All reference samples were prepared as  $100 \mu\text{g mL}^{-1}$  solutions for initial GC-MS screening analysis. 4–5 mg of the reference materials were taken and dissolved in the matching volume of a  $1 \text{ mg mL}^{-1}$  eicosane in methanol solution in order to create a  $1 \text{ mg mL}^{-1}$  sample and eicosane solution. This was then diluted by a factor of ten in methanol to create the final  $100 \mu\text{g mL}^{-1}$  sample and eicosane solution. Eicosane was added as an internal reference.

### 2.4.4.2. Fluorinated cathinone, amphetamine and diphenidine analogues calibration standards

Five calibration standards were prepared for the fluorinated cathinone, amphetamine and diphenidine analogue isomers. Calibration solutions were prepared in the range of  $100\text{--}500 \mu\text{g mL}^{-1}$  with each solution containing  $100 \mu\text{g mL}^{-1}$  eicosane as an internal standard. Each calibration standard was run 6 times. Two percentage recovery samples were prepared at 80%, 100% and 120% of a target concentration of  $300 \mu\text{g mL}^{-1}$  and injected twice.

### 2.4.4.3. Diphenidine derivatives calibration standards

10.0 mg of analytes (**10a–10m**), benzocaine, caffeine and procaine were weighed into a 20.0 mL clear glass volumetric flask and diluted to volume with methanol to give a solution containing all components at  $500 \mu\text{g mL}^{-1}$ . This solution was then further diluted with methanol and 1 mL of eicosane ( $1.0 \text{ mg mL}^{-1}$  in methanol) added (in each case) to give calibration standards containing  $25.0 \mu\text{g mL}^{-1}$ ,  $50.0 \mu\text{g mL}^{-1}$ ,  $100.0 \mu\text{g mL}^{-1}$ ,  $200.0 \mu\text{g mL}^{-1}$  and  $250.0 \mu\text{g mL}^{-1}$  of each analyte and the internal standard at  $100 \mu\text{g mL}^{-1}$ . Two percentage recovery samples were prepared at 80%, 100% and 120% of a target concentration of  $100 \mu\text{g mL}^{-1}$  and injected twice.

#### 2.4.4.4. Halogenated diphenidine calibration standards

Five calibration standards were prepared for the halogenated diphenidine derivatives in the range 100–300  $\mu\text{g mL}^{-1}$ . All solutions contained 100  $\mu\text{g mL}^{-1}$  eicosane as an internal standard. An original stock solution was made at 1  $\text{mg mL}^{-1}$  before dilution and all solutions were repeated six times. Two percentage recovery samples were prepared at 80%, 100% and 120% of a target concentration of 200  $\mu\text{g mL}^{-1}$  and injected twice.

#### 2.4.4.5. Diphenidine analogues calibration standards

Five calibration standards were prepared for the diphenidine analogues in the range 100–500  $\mu\text{g mL}^{-1}$ . All solutions contained 100  $\mu\text{g mL}^{-1}$  eicosane as an internal standard. An original stock solution was made at 1  $\text{mg mL}^{-1}$  before dilution and all solutions were repeated six times. Two percentage recovery samples were prepared at 80%, 100% and 120% of a target concentration of 300  $\mu\text{g mL}^{-1}$  and injected twice.

### 2.4.5. Street sample preparation

#### 2.4.5.1. Fluoroamphetamine street samples

Two street samples were obtained from Greater Manchester Police (GMP). GC-MS solutions were initially made at a concentration of 100  $\mu\text{g mL}^{-1}$  for qualitative analysis. A solution was then prepared at a concentration of 300  $\mu\text{g mL}^{-1}$  containing 100  $\mu\text{g mL}^{-1}$  eicosane in order to fall in the middle of the calibration series. Both test samples were injected in duplicate.

#### 2.4.5.2. Diphenidine street sample analysis

The street samples of diphenidine (1.0 g) and methoxphenidine (1.0 g) were obtained as off-white crystalline powders, from “Buy Research Chemicals UK” (<http://www.brc-chemicals.com>) and used without further purification. The individual samples were homogenized and arbitrarily labelled, SS-1 and SS-2, prior to analysis. 10.0 mg of the test substance was weighed into a 50.0 mL



clear glass volumetric flask and diluted to volume with methanol. This solution was then further diluted (1:2, 10 mL) with methanol to give a test solution containing  $100.0 \mu\text{g mL}^{-1}$  of the sample. The test samples were injected in duplicate.

10.0 mg of the street sample was weighed (in triplicate) accurately into a 50.0 mL clear glass volumetric flask and diluted to volume with methanol for qualitative analysis. This solution was then further diluted (1:2, 10 mL) with methanol and 1.0 mL of eicosane ( $1.0 \text{ mg mL}^{-1}$  in methanol) added (in each case) to give a test solution containing  $100.0 \mu\text{g mL}^{-1}$  of the sample and the internal standard at  $100.0 \mu\text{g mL}^{-1}$ . The test samples were injected in duplicate.

#### 2.4.5.3. Halogenated diphenidine street samples

Two street samples were obtained from GMP presumed to contain a halogenated diphenidine derivative. The samples were prepared at a concentration of  $100 \mu\text{g mL}^{-1}$  for initial qualitative screening. Solutions of  $200 \mu\text{g mL}^{-1}$  were then prepared for quantitative analysis, of both street samples, in order to fit with the calibration series.  $100 \mu\text{g mL}^{-1}$  eicosane was also added to both solutions to fit with the calibration standards. Both test samples were injected in duplicate.

## 2.5. NMR spectroscopy

Deuterated water ( $D_2O$ ) and deuterated dimethyl sulfoxide (DMSO) were used as the solvent of choice for the fluorinated cathinone and amphetamine isomers, while deuterated dichloromethane (DCM) and DMSO were used for the diphenidine derivatives and analogues. All deuterated solvents were purchased from Sigma-Aldrich.  $^1H$  NMR analysis was performed at 21.2 °C with 8 scans and a relaxation delay of 5 seconds. The offset value was set at 7.5 ppm scanning a range of 15 ppm in order to observe the amine proton in the diphenidine samples. Where  $D_2O$  is used with the cathinone and amphetamine isomers, no amine proton will be observed due to the exchanging of this proton with deuterium ions.  $^{13}C$  NMR experiments were also run at 21.2 °C using 2048 scans and a relaxation delay of 1 second.  $^{19}F$  NMR, run at 21.2 °C, was obtained over 8 scans with an offset value of 0 ppm and chemical shift range of 400 ppm. A 3 second relaxation delay was applied to all samples.

For all  $^{19}F$  NMR and  $^1H$  NMR compound screening, a 60 MHz Pulsar NMR spectrometer (Oxford Instruments, Oxfordshire, UK), performing 32 scans with a filter file of 8000 Hz and a relaxation delay of 5 seconds for a  $^1H$  NMR experiment.  $^{19}F$  NMR experiments were run using 16 scans and a 3 second relaxation delay with a filter file of 5000 Hz.

All samples were made up with 20 mg of the hydrochloride salt dissolved in 600  $\mu L$  of solvent ( $33.3 \text{ mg mL}^{-1}$ ) for  $^1H$  NMR experiments and 10 mg of sample in 600  $\mu L$  of solvent ( $16.7 \text{ mg mL}^{-1}$ ) for  $^{19}F$  NMR experiments for both 400 MHz and 60 MHz analysis. Trifluoroacetic acid (TFA,  $\delta = -76.55 \text{ ppm}$ ) was added, as an internal standard, for the  $^{19}F$  NMR analysis, on both the 400 MHz and 60 MHz spectrometers, at 0.03% v/v.

### 2.5.1. Quantitative $^{19}\text{F}$ NMR on 60 MHz instrument

In order to show the potential of using a 60 MHz NMR instrument, to perform quantitative analysis, a calibration series was performed with a couple of fluorinated examples from different classes. A stock solution was made by taking 75 mg of sample and dissolving into a 5 mL volumetric flask containing  $\text{D}_2\text{O}$  for the cathinone and amphetamine isomers and  $\text{DMSO-d}_6$  for the diphenidine and ephenidine isomers ( $15 \text{ mg mL}^{-1}$ ). A blank stock solution of  $\text{D}_2\text{O}$  or  $\text{DMSO-d}_6$  was also made (5 mL).  $0.5 \mu\text{L}$  of TFA (0.01% v/v) was added to both the sample stock solution and the blank solvent stock solution. Specific amounts of the sample stock solution were used and mixed with the blank solvent stock solution, to a total volume of  $600 \mu\text{L}$ , in order to create samples ranging in concentration from  $15 \text{ mg mL}^{-1}$  to  $5 \text{ mg mL}^{-1}$ . The volumes used in order to create the calibration standards can be seen in Table 15.

**Table 15:** Calibration standard preparation for  $^{19}\text{F}$  NMR quantitative analysis

Sample stock volume used ( $\mu\text{L}$ )	Blank $\text{D}_2\text{O}$ stock volume used ( $\mu\text{L}$ )	Concentration ( $\text{mg mL}^{-1}$ )
600	0	15
480	120	12
400	200	10
320	280	8
200	400	5

### 2.5.2. Street sample preparation

The two FA street samples were prepared at a concentration of  $15 \text{ mg mL}^{-1}$  using a matching method to the preparation of the  $15 \text{ mg mL}^{-1}$  calibration solution. 0.1% v/v TFA was used as an internal standard in order to for integrated areas to be calculated.

### 2.5.3. 60 MHz 2-dimensional NMR experiments

$^{19}\text{F}$  NMR *J*-resolved and  $^{19}\text{F}$ -TOCSY (Total Correlation Spectroscopy) experiments were performed for the difluoroephenidine regioisomers using the 60 MHz Pulsar spectrometer. All samples were prepared as  $33.3 \text{ mg mL}^{-1}$

solutions by dissolving 20 mg of DFEP samples in 600  $\mu\text{L}$  of  $\text{DMSO-d}_6$ . 0.03% v/v TFA was also added to the sample.

For the  $^{19}\text{F}$  *J*-resolved experiment a 1250  $\text{cm}^{-1}$  filter file was used with a relaxation delay of 3 seconds. An 8.4  $\mu\text{s}$   $90^\circ$  pulse length and a 16.8  $\mu\text{s}$   $180^\circ$  pulse length was used with 128 and 2048 points collected for the F1 and F2 axis respectively. 32 scans were performed for the *J*-resolved experiment, while 8 scans were performed for the  $^{19}\text{F}$  TOCSY experiment. Offset frequencies were set in order for the spectra to be set at the midpoint of all fluorine chemical shift values representative of the compounds involved. A 5000 Hz filter file was used for the TOCSY experiment with a 2-second relaxation delay and an 8.4  $\mu\text{s}$   $90^\circ$  pulse length. Along the F1 and F2 axis, 128 and 1024 points were collected respectively.

## 3. Chapter 3 – Fluorinated cathinones and amphetamines

### 3.1. Overview

Fluorinated amphetamine and cathinone derivatives have been encountered previously, with literature reported on the characterisation and attempted separation of these compounds.<sup>53, 82</sup> Problems were seen with regards to full separation in the case of the fluoroamphetamines and tailing of peaks due to thermal degradation.<sup>4</sup>

Based on this the synthetic fluoroamphetamine (**4a–4c**), fluoromethcathinone (**8a–8c**) and trifluoromethylmethcathinone (**9a–9c**) will be prepared and fully characterised (using a range of techniques) in order to confirm their structure with the published literature. A GC-MS method will be developed to separate all nine of the fluorinated compounds as well as produce mass spectroscopy data to use as reference spectra. 60 MHz NMR will be used in order to show the potential for its use as a replacement presumptive test with comparisons made to spectra produced on a 400 MHz instrument and differences between regioisomers reported.

Qualitative analysis of the regioisomers will be obtained by utilising a developed GC-MS method and acquiring <sup>19</sup>F NMR spectra on a 1.4 T NMR spectrometer. Calibration graphs will be created which will aid the determination of the amounts of amphetamine and cathinones present in potential street samples.

### 3.2. Synthesis

The three fluoroamphetamine regioisomers (FA, **4a–4c**, figure 28) were all prepared as hydrochloride salts at Manchester Metropolitan University, under Home Office license using the methods reported by Rosner *et al*<sup>139</sup> with purities shown to be >95%, by both GC-MS and NMR. The compounds were prepared in the following yields: 37% (2-FA, **4a**); 45% (3-FA, **4b**) and 41% (4-FA, **4c**).

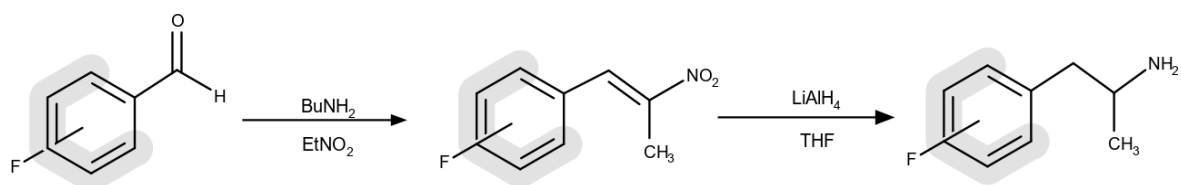


**Figure 28:** Reaction scheme for the synthesis of FA isomers (**4a–4c**)

The three fluoromethcathinone (FMC, **8a–8c**, figure 29) isomers were prepared similarly, using the synthesis method reported by Archer *et al*.<sup>68</sup> All reference samples were shown to have purities >95% with the following yields from the prerequisite 2-, 3- or 4-fluoropropiophenone: 57% (2-FMC, **8a**); 49% (3-FMC, **8b**); 61% (4-FMC, **8c**) respectively.

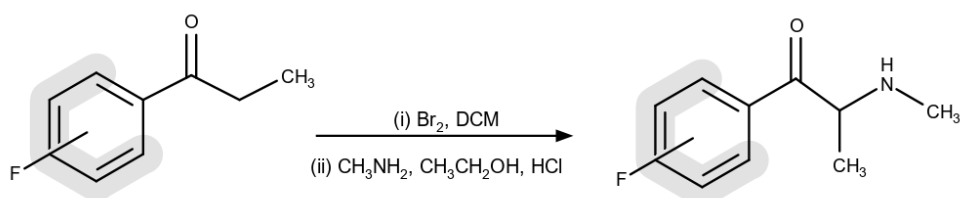


**Figure 29:** Reaction scheme for the synthesis of FMC isomers (**8a–8c**)

Trifluoromethylmethcathinone hydrochlorides (TFMMC, **9a–9c**, figure 30) were prepared at the University of Strathclyde under home office license, using previously reported methods from Khreit *et al*.<sup>83</sup> The hydrochloride salts were recrystallized from acetone to give reference materials with purities >95% with the following yields from the prerequisite 2-, 3- or 4-trifluoromethylpropiophenone: 69% (2-TFMMC, **9a**); 23% (3-TFMMC, **9b**) and 62% (4-TFMMC, **9c**).

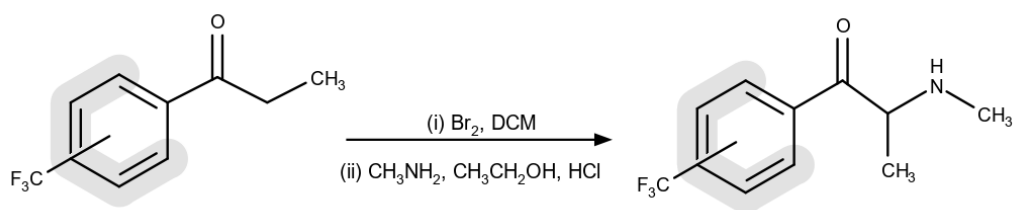


**Figure 30:** Reaction scheme for the synthesis of TFMMC isomers (**9a – 9c**)

All samples tested were colourless to off-white powders with full structural characterisation carried out through <sup>1</sup>H NMR (Figure 31 - Figure 36), <sup>19</sup>F NMR (Table 166) <sup>13</sup>C NMR (supplementary data: Figure 14 - Figure 19), and FTIR (supplementary data: Figure 63 - Figure 68). Purities of all samples was measured through GC-MS and 400 MHz NMR analysis. The hydrochloride salts were determined to be soluble (10 mg mL<sup>-1</sup>) in deionised water, methanol, dichloromethane and dimethyl sulfoxide.

The three fluoroamphetamine regioisomers (**4a–4c**) show very similar <sup>1</sup>H NMR spectra with slight differences in the aliphatic peak shifts and the only main differences occurring in the aromatic regions. This occurs due to the location of the fluorine substituent of the benzene ring and the changes in symmetry affecting the chemical shifts of the proton environments. In all three cases the peak representing the CH<sub>3</sub> group can be seen at a chemical shift of 1.13 ppm. This shows coupling to the chiral centre proton at 3.38 ppm, in all three cases, in the corresponding <sup>1</sup>H-<sup>1</sup>H COSY NMR spectra. This coalesces with the water peak at 3.33 ppm in the <sup>1</sup>H NMR spectra so cannot be properly observed. In DMSO, the two different proton environments of the CH<sub>2</sub> group adjacent to the chiral centre manifest as two separate peaks. These are observed at 2.69 and 3.03 ppm. The amine protons are seen at 8.28 ppm representing three protons due to it being the hydrochloride salt of a primary amine. The aromatic region for the *para*-substituted fluoroamphetamine shows symmetry with only two peaks representing the four protons at chemical shifts of 7.17 and 7.30 ppm, with roofing effects observed. The aromatic regions for the *ortho*- and *meta*-substituted isomers do not show the matching symmetry to the 4' isomer. All aromatic regions show slight differences based on splitting patterns through the coupling to adjacent protons.

The fluoromethcathinone regioisomers (**8a–8c**) is similar to the fluoroamphetamine structure, however there are differences in the aliphatic region of the  $^1\text{H}$  spectra. The  $\text{CH}_3$  group adjacent to the chiral centre is seen at 1.46 ppm and shows coupling to the chiral centre proton in the  $^1\text{H}$ - $^1\text{H}$  COSY NMR. This is similar to the FA regioisomers with the chiral centre proton peak seen at 5.22 for the 3' and 4' isomers. The peak for the chiral proton in the 2' isomer is shifted upfield, compared to the 3' and 4' isomers, to 4.89 ppm. The peak representing the  $\text{CH}_3$  adjacent to the amine is seen at 2.59 ppm and shows coupling to the amine proton at 9.55 ppm. In the 4' isomer the amine peak is one peak representing the two amine protons, while the 3' and 2' isomers are split into 2 peaks representing two protons. The aromatic region peaks are seen between 7.2–8.5 ppm with the 4' isomer again showing symmetry.

The trifluoromethylmethcathinone (TFMMC, **9a–9c**) isomers show similar aliphatic regions to the FMC isomers. The two  $\text{CH}_3$  groups are seen at 1.46 and 2.59 ppm, which is similar to the FMC isomers. The chiral proton for the 3' and 4' isomers can be seen at 5.25 ppm. This is again similar to the FMC isomers with the 2' isomer shifted upfield in a similar manner. The aromatic regions between the three isomers show slight differences in order to distinguish between the three. The matching aromatic regions of both the FMC and TFMMC using  $^1\text{H}$  NMR spectroscopy can make it difficult to identify specific compounds.

In order to help identify these compounds,  $^{19}\text{F}$  NMR spectroscopy was employed. The table of chemical shifts can be seen in Table 16, with an exemplar spectrum containing a mixture of the FMC and TFMMC shown in Figure 37. Trifluoroacetic acid ( $\delta$  ppm = -76.55) was added in order to accurately measure the chemical shifts of each sample peak. From the results it is shown that the  $^{19}\text{F}$  nucleus in each compound has a distinctive chemical shift value that can be used for identification purposes.



**Table 16:**  $^{19}\text{F}$  NMR chemical shift values for all fluorinated amphetamine and cathinone regioisomers reference to TFA ( $\delta$  ppm = -76.55)

<b>Compound no.</b>	<b>Compound</b>	<b><math>^{19}\text{F}</math> chemical shift (<math>\delta</math> ppm)</b>
<b>4a</b>	2-fluoroamphetamine	-115.40
<b>4b</b>	3-fluoroamphetamine	-112.97
<b>4c</b>	4-fluoroamphetamine	-117.28
<b>8a</b>	2-fluoromethcathinone	-110.61
<b>8b</b>	3-fluoromethcathinone	-112.72
<b>8c</b>	4-fluoromethcathinone	-103.02
<b>9a</b>	2-trifluoromethylmethcathinone	-58.89
<b>9b</b>	3-trifluoromethylmethcathinone	-63.70
<b>9c</b>	4-trifluoromethylmethcathinone	-64.18

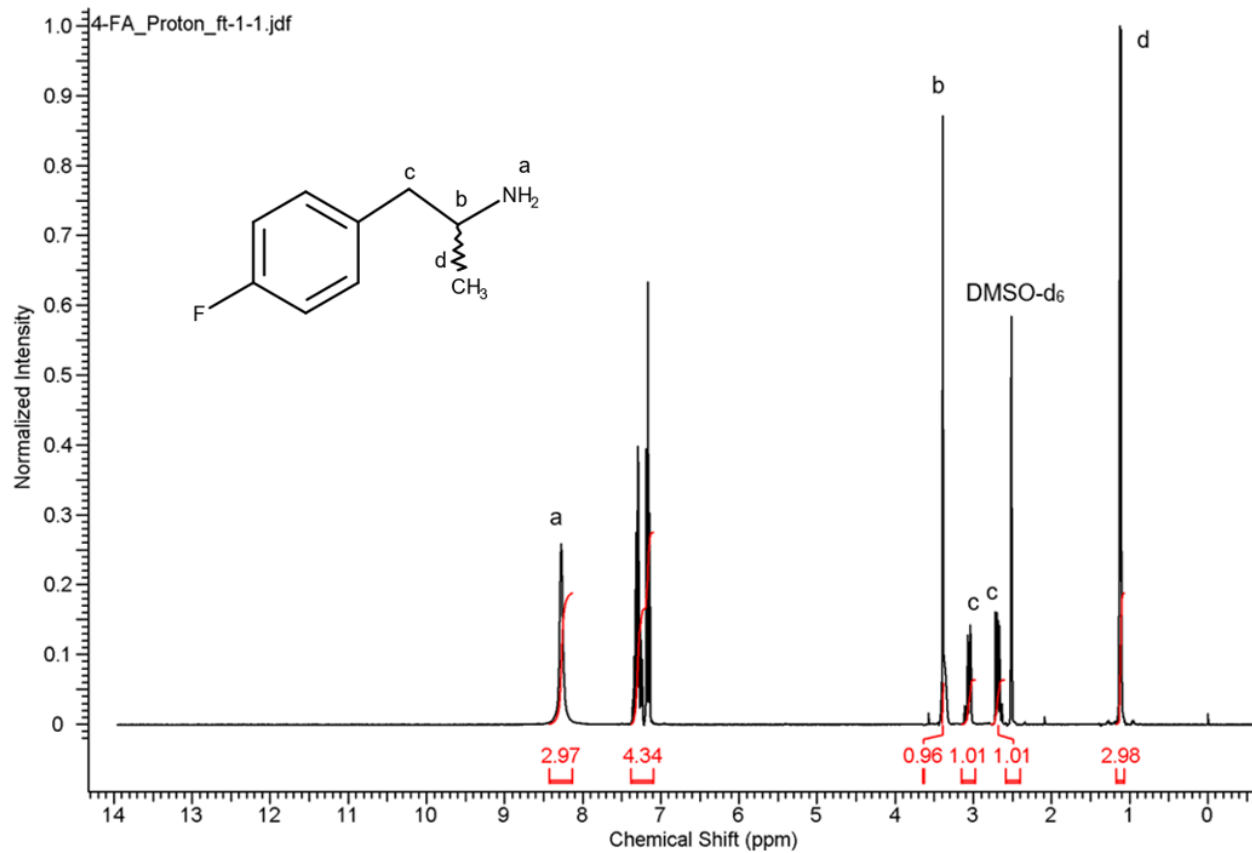


**Figure 31:** General 400 MHz <sup>1</sup>H NMR spectrum for the 4-fluoroamphetamine hydrochloride (4-FA, **4a**) run in DMSO-d<sub>6</sub> (δ ppm = 2.50)

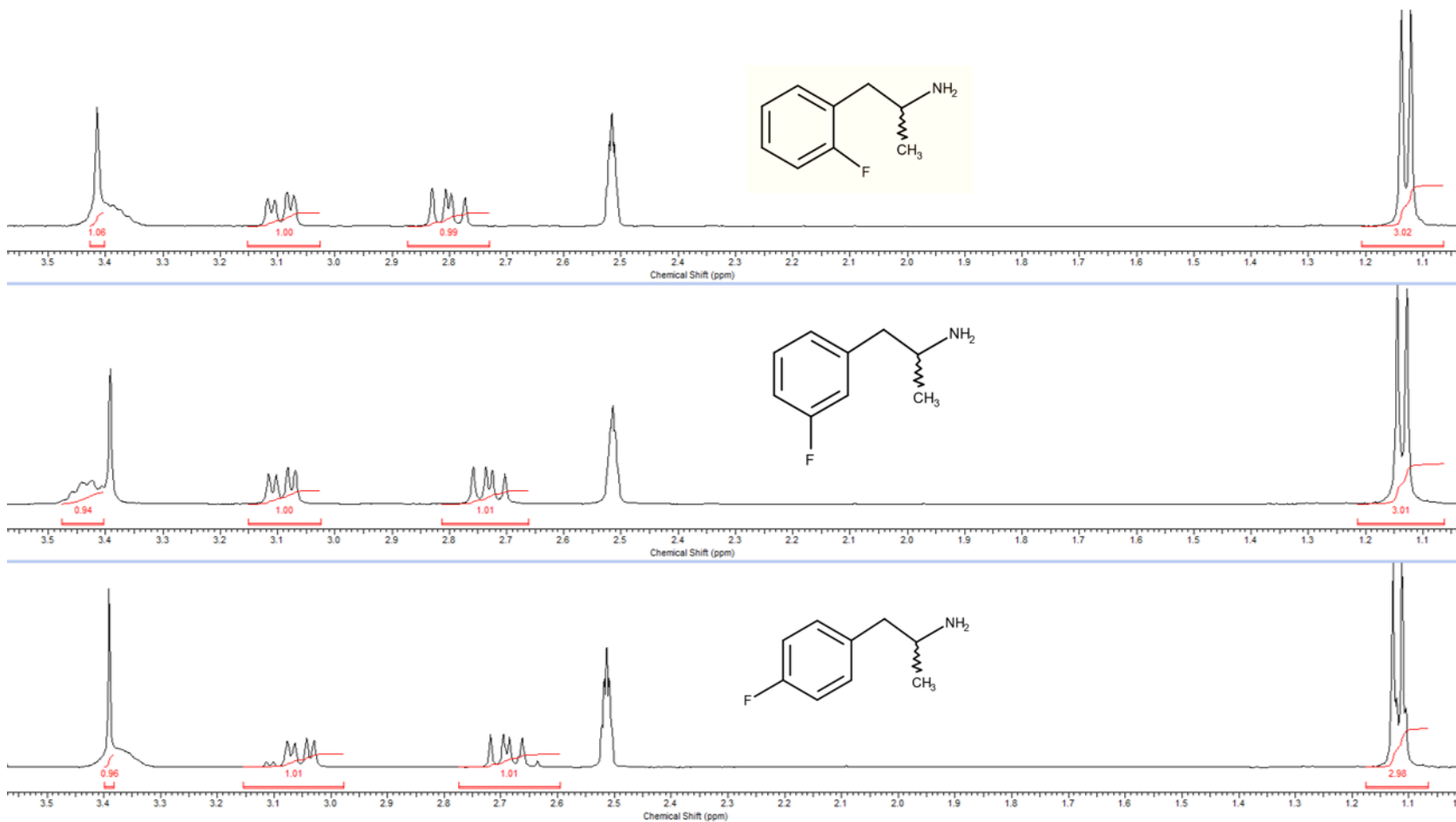


**Figure 32:** Stacked 400 MHz aliphatic region of the three fluoroamphetamine (FA, **4a** – **4c**) hydrochloride regioisomers run in DMSO-d<sub>6</sub> ( $\delta$  ppm = 2.50)

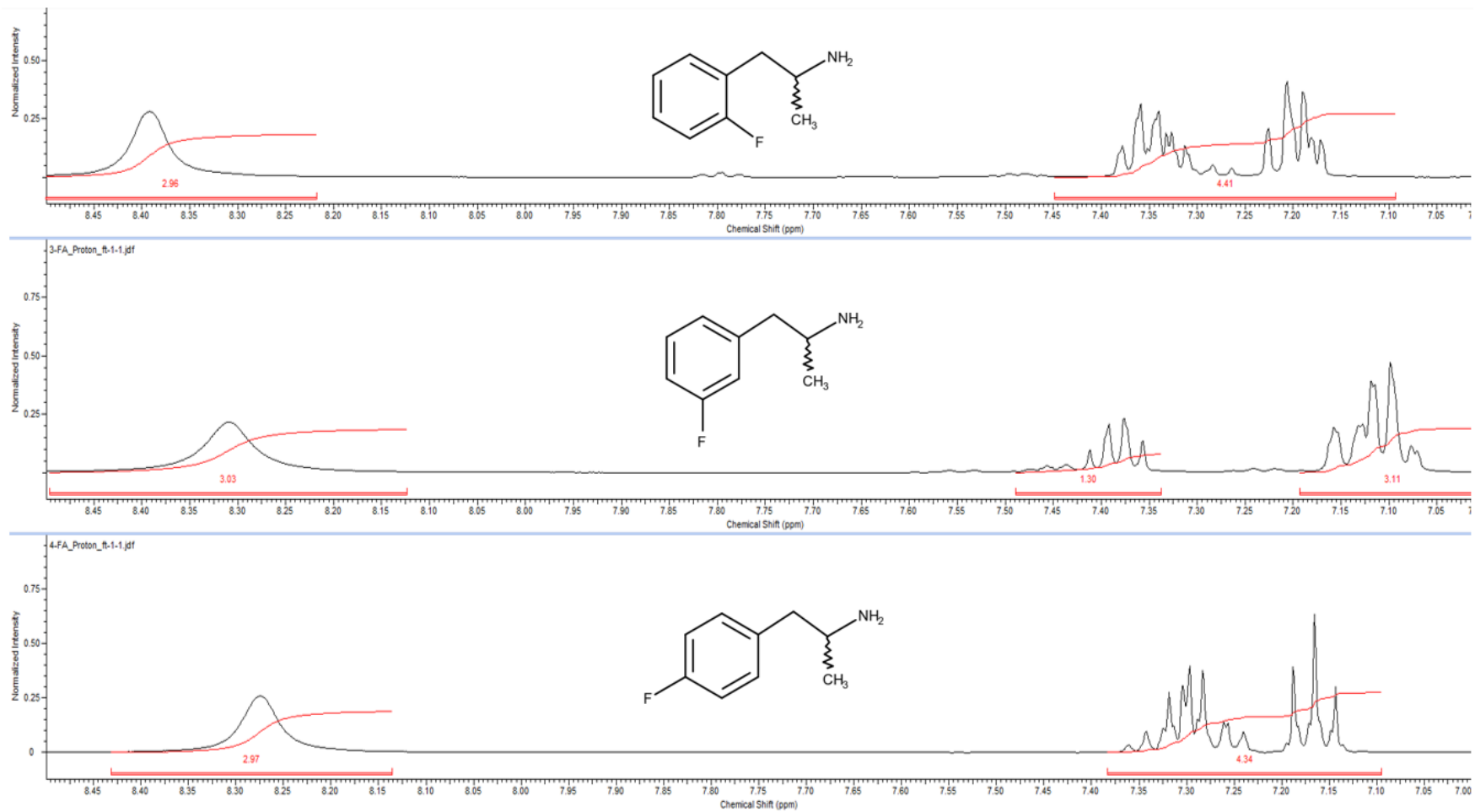


**Figure 33:** Stacked 400 MHz aromatic region of the three fluoroamphetamine (FA, **4a** – **4c**) hydrochloride regioisomers run in DMSO-d<sub>6</sub> ( $\delta$  ppm = 2.50)

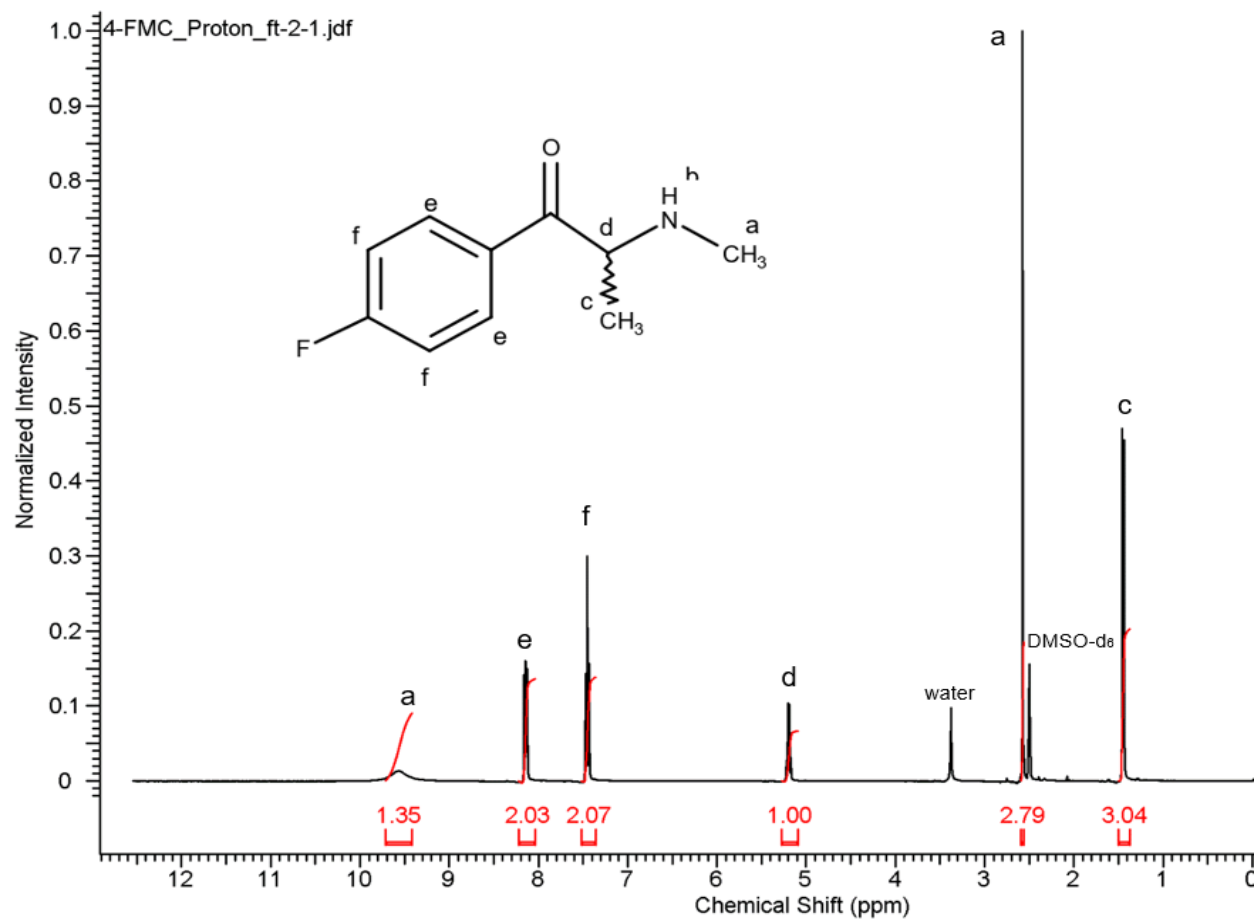


**Figure 34:** General 400 MHz  $^1\text{H}$  NMR spectrum for 4-fluoromethcathinone (4-FMC, **8c**) run in DMSO- $d_6$  ( $\delta$  ppm = 2.50)

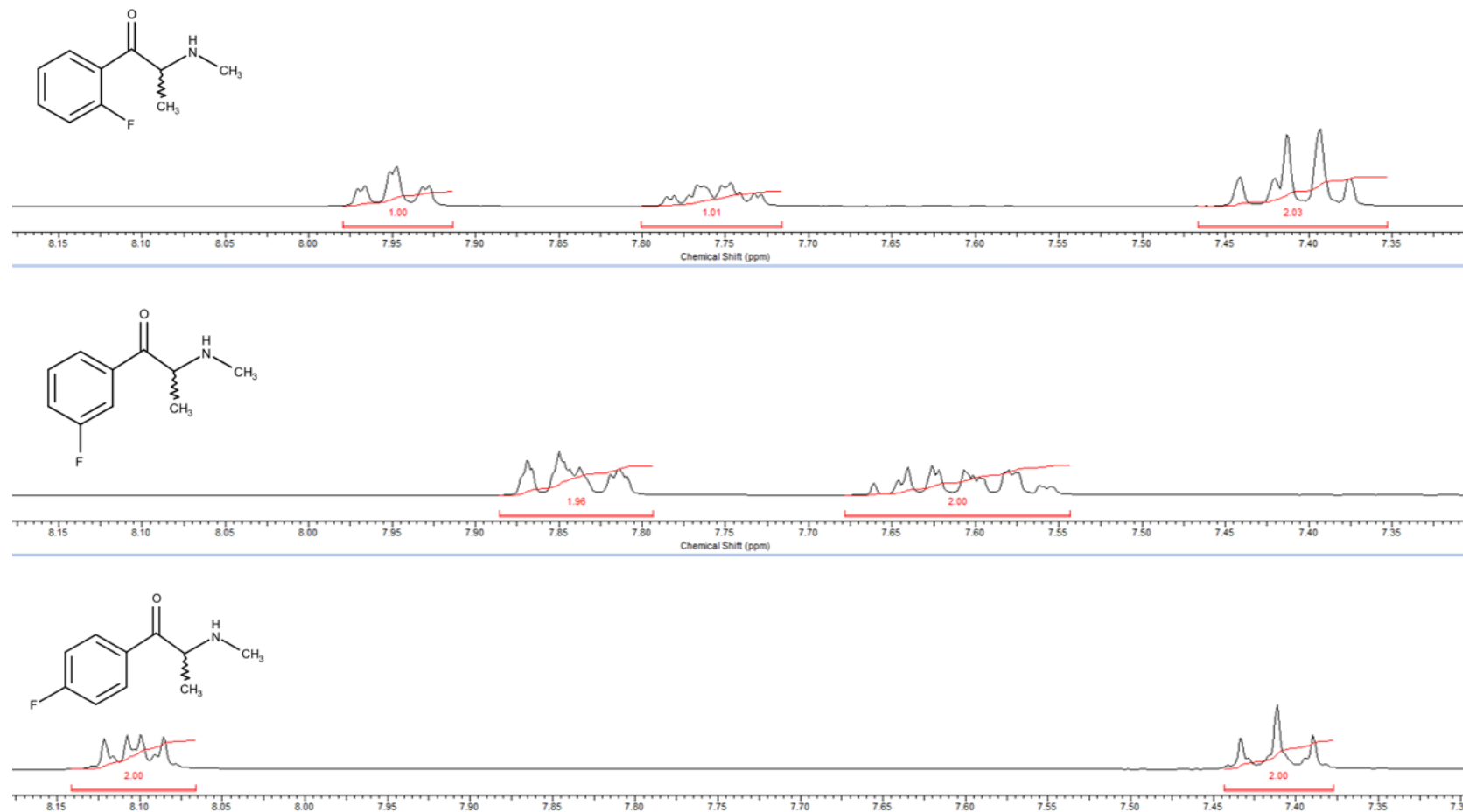


**Figure 35:** Stacked 400 MHz aromatic region of the three fluoromethcathinone (FMC, **8a** – **8c**) hydrochloride regioisomers run in DMSO- $d_6$  ( $\delta$  ppm = 2.50)

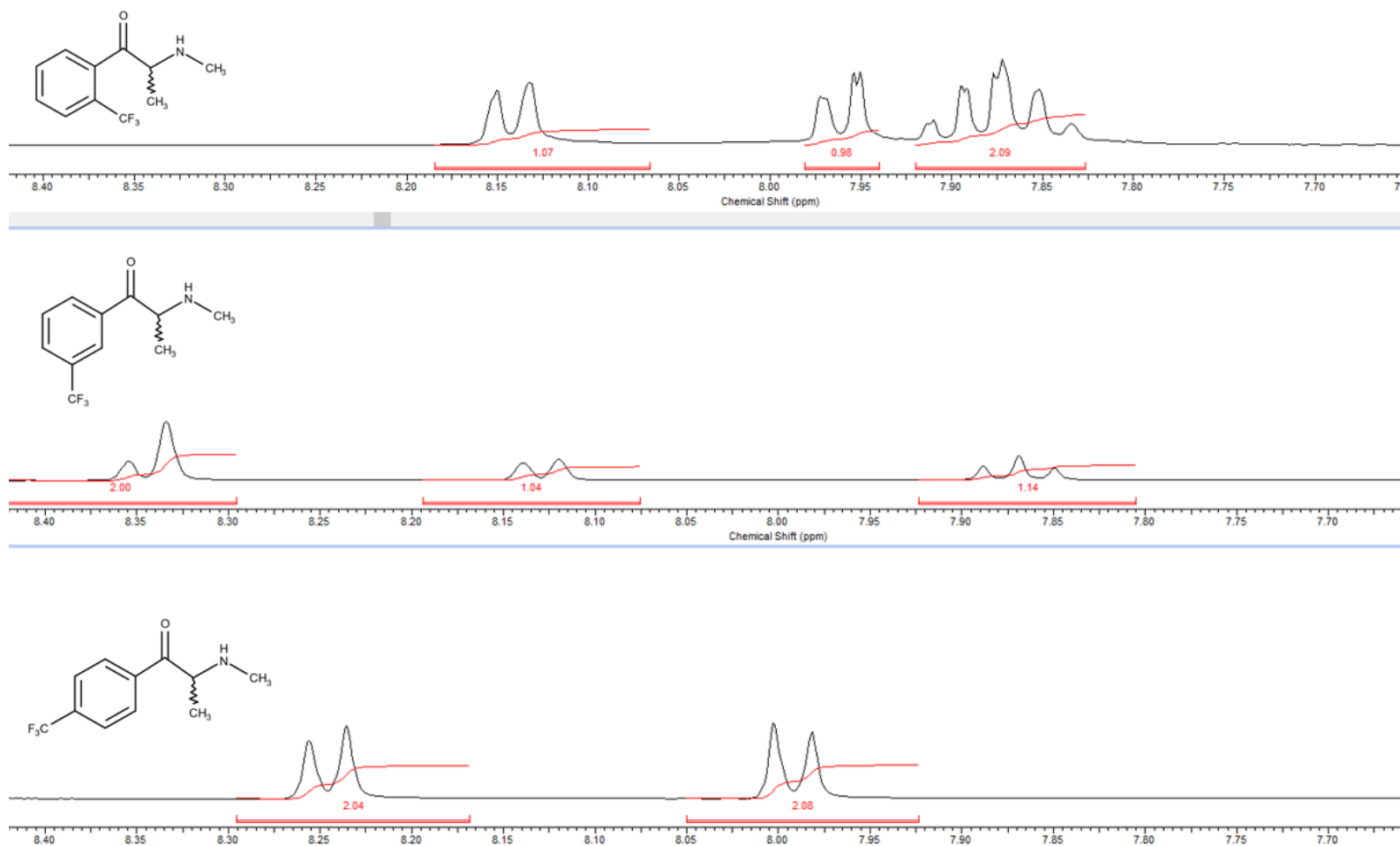


**Figure 36:** Stacked 400 MHz aromatic region of the three trifluoromethylmethcathinone (FMC, **9a** – **9c**) hydrochloride regioisomers run in DMSO-d<sub>6</sub> ( $\delta$  ppm = 2.50)

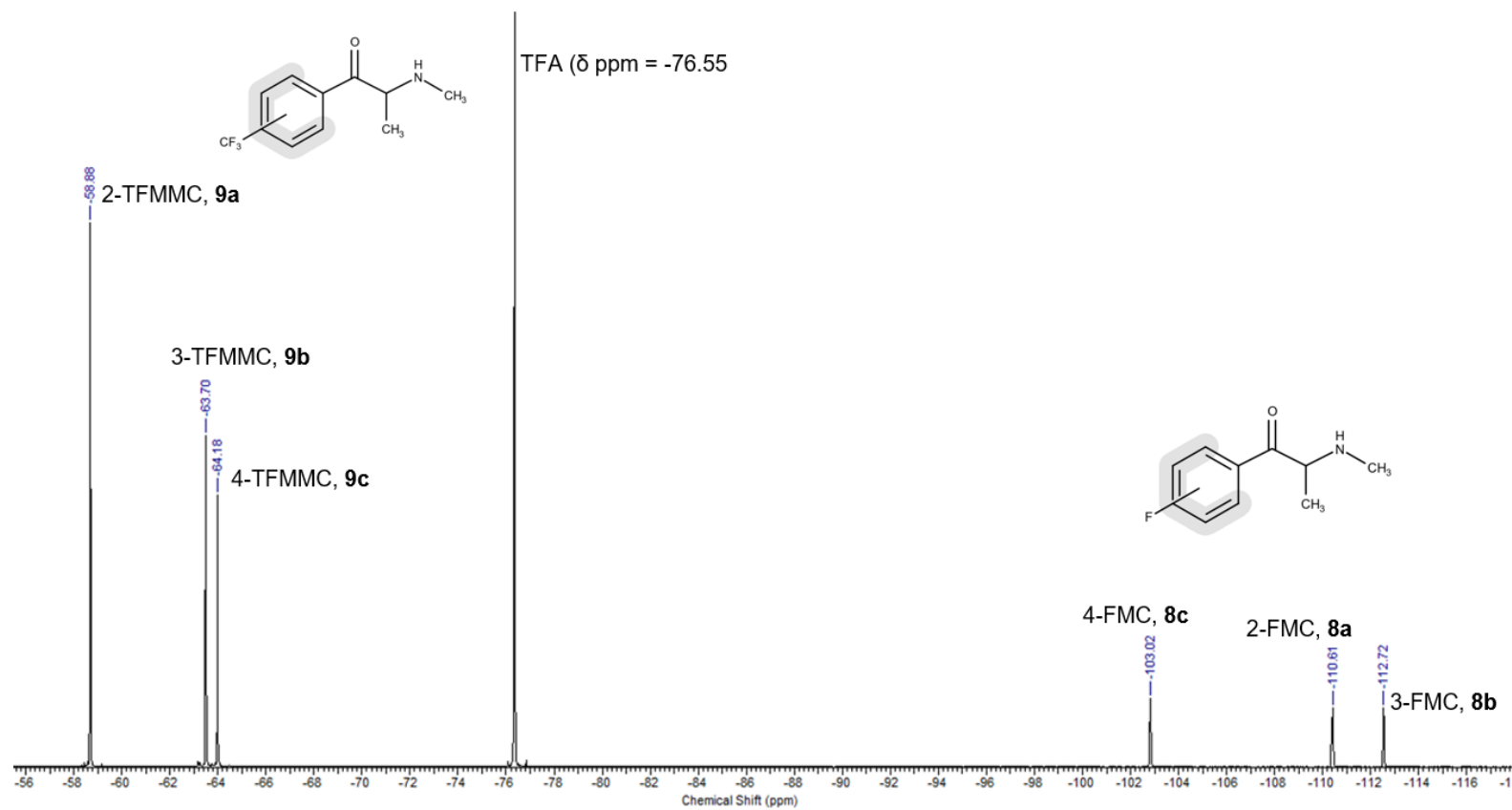


**Figure 37:**  $^{19}\text{F}$  NMR spectrum for a mixture of FMC (**8a–8c**) and TFMMC (**9a–9c**) regioisomers with TFA added as an internal reference ( $\delta$  ppm = -76.55)



### 3.3. Presumptive Testing

Presumptive testing was carried out on all of the fluoroamphetamine (**4a–4c**), fluoromethcathinone (**8a–8c**) and trifluoromethylmethcathinone (**9a–9c**) regioisomers using the United Nations recommended guidelines.<sup>118</sup> A range of tests were used to fully detail possible colour changes including (i) Marquis; (ii) Mandelin; (iii) Simon's; (iv) Robadope's; (v) Scott's and (vi) Zimmerman test reagents. A solution of each reference standard (10 mg mL<sup>-1</sup>) was prepared in deionised water and a couple of drops placed into a dimple well of a white spotting tile. The required presumptive test reagent (1-2 drops) was then added and any colour change upon initial addition of the reagents were noted and observations were made again after a five minute time period (Table 17). Blank solutions of deionised water were used in order to show the natural colour of the test reagents prior to being added to sample solution.

All monofluorinated cathinone and amphetamine regioisomers produce a positive reaction when tested against the Marquis reagent. It is expected that the colour change occurs due to the reaction of compound molecules with sulfuric acid with the same mechanism that has been reported for MDMA (Figure 38).<sup>3, 141</sup>

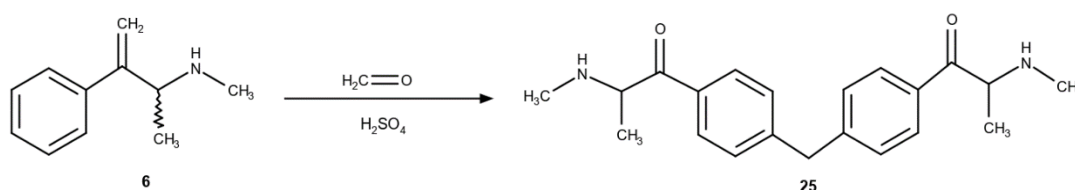


**Figure 38:** Reaction scheme for the reaction between methcathinone and the Marquis reagent

No positive reaction was seen for either the fluorinated amphetamines or cathinones when tested against the Mandelin and Scott's reagents.

It has been reported that altering the Simon's reagent by changing the acetaldehyde with acetone, to produce the Robadope's reagent, can help with the initial detection of primary amines.<sup>142</sup> This is different to the Simon's reagent that is used to detect secondary amines. The use of these two

reagents can help to distinguish between the monofluorinated amphetamine and methcathinones. All the fluoromethcathinone (**8a–8c**) and trifluoromethylmethcathinone (**9a–9c**) regioisomers produce green/brown colours with Simon's reagent, however the difference in colours is not significant enough to be able to identify unknown samples. The fluoroamphetamine (**4a–4c**) regioisomers do not react with Simon's reagent, but give a brown colour with Robadope's reagent, with no differences in colour between each positional isomer.

The Zimmerman reaction relies on the presence of an activated methylene group, which under alkaline conditions, reacts with 1,3-dinitrobenzene to give an intensely coloured Meisenheimer complex (Figure 39).<sup>143</sup> This is the reason the six cathinone samples produce a positive result with the Zimmerman test, however it cannot be used to distinguish between the different regioisomers within a class. The fluoroamphetamine regioisomers do not produce a positive reaction with the Zimmerman reagent due to the loss of the carbonyl.

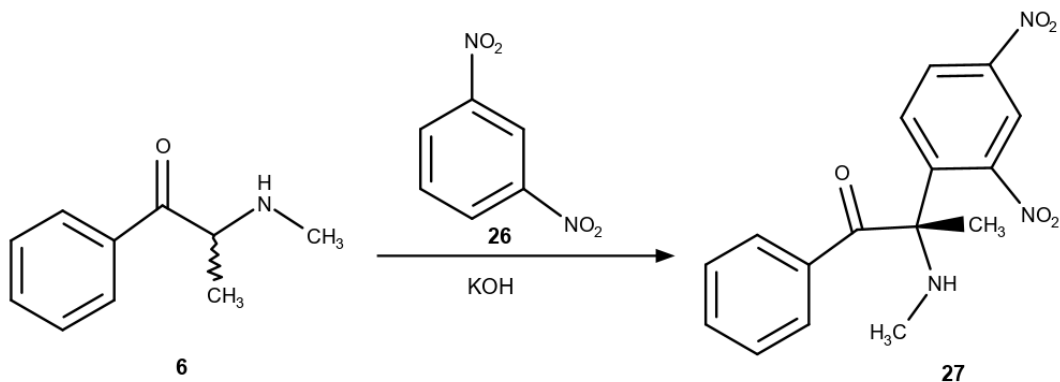


**Figure 39:** Reaction scheme for the reaction between methcathinone (**6**) and the Zimmerman reagent

From the colour changes it is observed that the Marquis reagent cannot discriminate between any of the nine compounds. The Zimmerman reagent can be used as a selective test for the presence of the cathinone regioisomers with the Simon's reagent providing a clearer indication that the substances are methcathinones (secondary amines). The combination of the Zimmerman and Simon's reagent allow discrimination between the three fluoromethcathinone

(FMC) regioisomers, however the discrimination between the three trifluoromethylmethcathinone (TFMMC) regioisomers is less clear. The Robadope reagent provides a more selective test for the fluoroamphetamine (FA) regioisomers, however it does not provide any discrimination between the three compounds.

**Table 17:** Colour changes reported for fluoroamphetamine (**4a–4c**), fluoromethcathinone (**8a–8c**) and trifluoromethylmethcathinone (**9a–9c**) regioisomers using a range of presumptive test reagents

	Marquis		Mandelin		Simon's		Robadope		Scott's		Zimmerman	
	Colour change	Colour after 5 minutes	Colour change	Colour after 5 minutes	Colour change	Colour after 5 minutes	Colour change	Colour after 5 minutes	Colour change	Colour change after 5 minutes	Colour change	Colour change after 5 minutes
<b>4a</b>	orange	colourless	-	-	-	-	Brown	brown	-	-	-	-
<b>4b</b>	orange	colourless	-	-	-	-	Brown	brown	-	-	-	-
<b>4c</b>	orange	colourless	-	-	-	-	Brown	brown	-	-	-	-
<b>8a</b>	orange/yellow	colourless	-	--	green	green	-	-	-	-	light red	light red
<b>8b</b>	yellow	colourless	-	-	pale brown	pale brown	-	-	-	-	purple	purple
<b>8c</b>	yellow/orange	colourless	-	-	grey	grey	-	-	-	-	purple	purple
<b>9a</b>	yellow	colourless	-	-	green	green	-	-	-	-	red	red
<b>9b</b>	orange	colourless	-	-	pale brown	pale brown	-	-	-	-	light purple	light purple
<b>9c</b>	orange	colourless	-	-	pale brown	pale brown	-	-	-	-	light purple	light purple

### 3.4. Gas chromatography – mass spectroscopy

All amphetamine and cathinones were analysed using gas chromatography–mass spectroscopy (GC-MS). Samples were prepared with a simple solvation in methanol ( $1 \text{ mg mL}^{-1}$ ) and dilution ( $100 \text{ } \mu\text{g mL}^{-1}$ ) with no derivatisation required. All samples were run individually before being run as mixtures in order to determine retention times and elution orders. A table of retention times for all compounds can be seen in Table 18, along with relative retention times in relation to the internal standard eicosane (**E**)

From the initial screening method it was seen that all the fluoroamphetamine regioisomers eluted rapidly ( $< 4 \text{ mins}$ ) and were only just seen after the mass spectrometer solvent delay. There is no clear separation in the retention times as indicated in the Relative retention times ( $RR_t$ ). The FMC and TFMMC regioisomers also elute very quickly on the screening run with elution times between 4.6 and 4.8 mins. The small gap between elution times for the FMC and TFMMC isomers shows that there is no clear separation between the six compounds. A new method was developed in order to try to separate all isomers based on retention times. This was done by slowing the rate initially from  $30^\circ\text{C min}^{-1}$  to  $10^\circ\text{C min}^{-1}$  before slowing the ramp down further to  $2^\circ\text{C min}^{-1}$  to begin to separate the FMC and TFMMC isomers. The table showing retention times and relative retention times to eicosane, for the developed method, can be seen in Table 19.

From the developed method retention times it is seen that the compounds begin to show greater separation than previously reported. The retention times increase compared to the screening method and this helps to ensure that peaks are not lost, in the solvent delay, as the methanol is pushed through the column by the helium carrier gas. The fluoroamphetamine regioisomers begin to separate compared to the initial screen where coelution between the 3' and 4' positional isomers was an issue. The superimposed spectra of all three fluoroamphetamine isomers can be seen in Figure 40 and shows that peaks can be distinguished, although baseline separation has not been achieved.

The superimposed spectra of both the FMC and TFMMC isomers can be seen in Figure 41. This image shows that all six of the fluorinated cathinone compounds can be distinguished based on retention times. The elution order can be determined based on the developed method with the order being as follows: 3-TFMMC → 2-FMC → 4-TFMMC → 3-FMC → 4-FMC → 2-TFMMC. The 3-TFMMC and 2-FMC peaks are not fully baseline resolved, however all other compounds are fully baseline separated. This shows that using the developed method unknown street samples that contain either fluorinated amphetamines or cathinones can be identified. The  $RR_t$  recorded suggest that there may not be any baseline separation, however the values only appear close to 2.d.p due to the significantly higher retention time of the eicosane (30.85 minutes compared to 7.28 minutes).

The developed method was validated individually for a mixture of the fluoromethcathinone isomers and then the trifluoromethylmethcathinone isomers. All correlation coefficients are above an acceptable level ( $>0.99$ ) for the FMC and TFMMC compounds, with limits of detection (LOD) and limits of quantification (LOQ) values shown in Table 20. LOD values range between  $8.0 - 16.0 \mu\text{g mL}^{-1}$  and LOQ values ranging from  $24.0 - 45.0 \mu\text{g mL}^{-1}$ . All relative standard deviation percentages fall below an acceptable 5% and can also be seen in Table 20. The retention times have been listed to 2.d.p as a difference in 0.01 minutes will begin to see peaks start to separate from one another even though the relative retention time ( $RR_t$ ) appears to have the same value.

**Table 18:** GC retention times for the monofluorinated amphetamine (**4a–4c**) and cathinone (**8a–8c**) regioisomers and trifluoromethylmethcathinone (**9a–9c**) regioisomers, including relative retention times (RR<sub>t</sub>) relative to eicosane (**E**, R<sub>t</sub> = 7.281 mins)

Compound no.	Compound Abbreviation	Compound retention time (R <sub>t</sub> / mins)	Relative Retention time (RR <sub>t</sub> )
<b>4a</b>	2-FA	3.80	0.52
<b>4b</b>	3-FA	3.84	0.53
<b>4c</b>	4-FA	3.85	0.53
<b>8a</b>	2-FMC	4.67	0.64
<b>8b</b>	3-FMC	4.71	0.65
<b>8c</b>	4-FMC	4.73	0.65
<b>9a</b>	2-TFMMC	4.76	0.65
<b>9b</b>	3-TFMMC	4.61	0.63
<b>9c</b>	4-TFMMC	4.65	0.64

**Table 19:** GC retention times for the monofluorinated amphetamine (**4a–4c**) and cathinone (**8a–8c**) regioisomers and trifluoromethylmethcathinone (**9a–9c**) regioisomers, including relative retention times (RR<sub>i</sub>) relative to eicosane (**E**, R<sub>t</sub> = 30.850 mins) using the developed GC oven temperature programme

<b>Compound no.</b>	<b>Compound Abbreviation</b>	<b>Compound retention time (R<sub>t</sub> / mins)</b>	<b>Relative Retention time (RR<sub>i</sub>)</b>
<b>4a</b>	2-FA	5.25	0.17
<b>4b</b>	3-FA	5.39	0.17
<b>4c</b>	4-FA	5.43	0.18
<b>8a</b>	2-FMC	10.12	0.33
<b>8b</b>	3-FMC	10.48	0.34
<b>8c</b>	4-FMC	10.68	0.35
<b>9a</b>	2-TFMMC	11.07	0.36
<b>9b</b>	3-TFMMC	10.06	0.33
<b>9c</b>	4-TFMMC	10.33	0.33



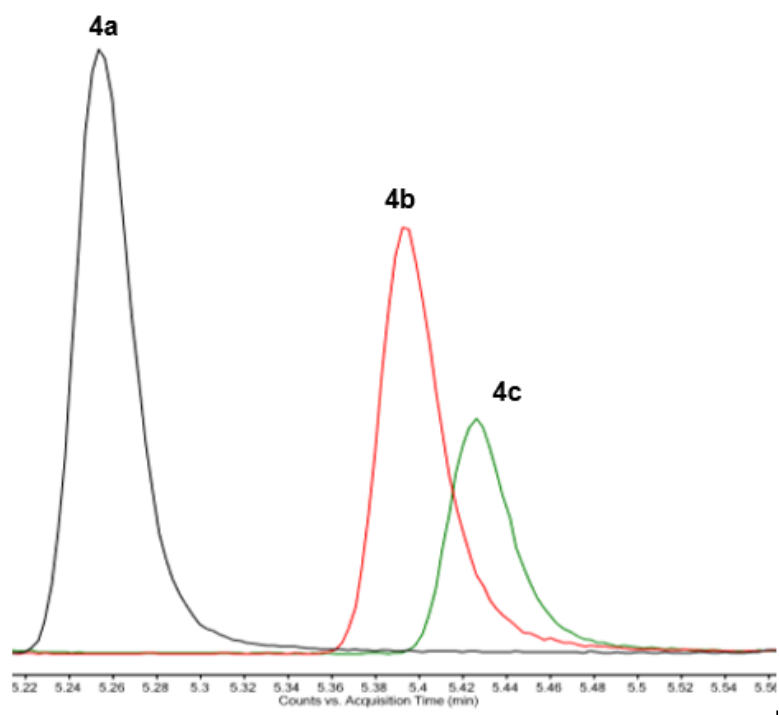


**Figure 40:** Superimposed GC chromatographs of the three fluoroamphetamine (**4a–4c**) regioisomers

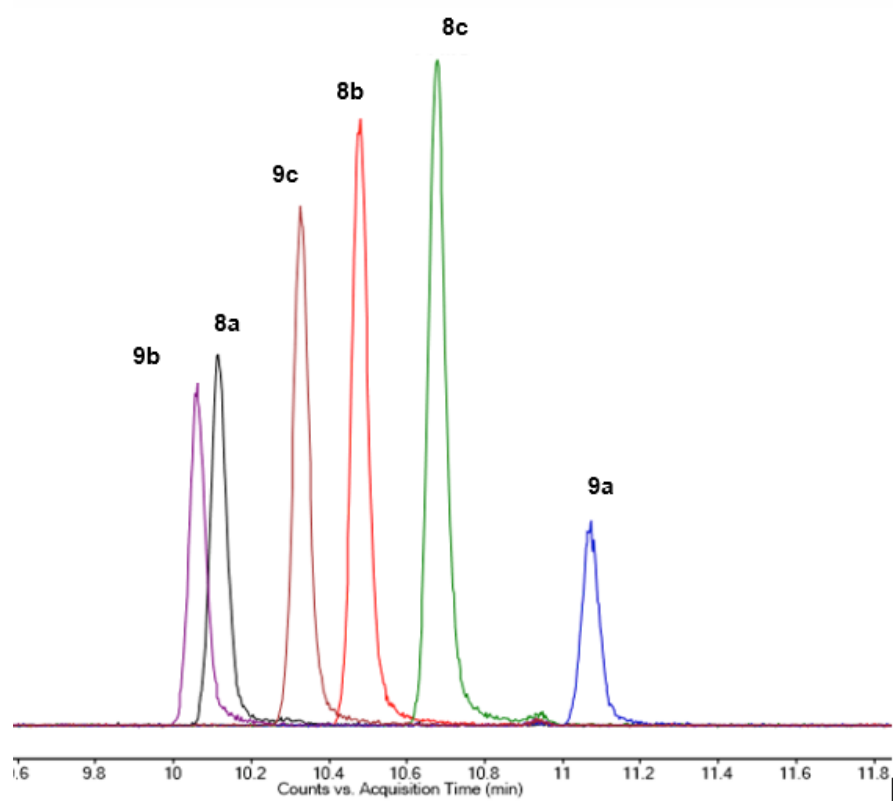


**Figure 41:** Superimposed GC chromatographs for the fluoromethcathinone (FMC, **8a–8c**) and trifluoromethylmethcathinone (TFMMC, **9a–9c**) regioisomers

**Table 20:** Validation values for the FMC (**8a–8c**) and TFMMC (**9a–9c**) regioisomers including LOD, LOQ and %RSD for all calibration standards

Analyte	Correlation coefficient (R <sup>2</sup> )	LOD (µg mL <sup>-1</sup> )	LOQ (µg mL <sup>-1</sup> )	Precision (%RSD) n = 6				
				100 µg mL <sup>-1</sup>	200 µg mL <sup>-1</sup>	300 µg mL <sup>-1</sup>	400 µg mL <sup>-1</sup>	500 µg mL <sup>-1</sup>
<b>2-FMC, 8a</b>	0.994	14.19	40.96	0.94	4.91	3.10	0.38	0.26
<b>3-FMC, 8b</b>	0.992	15.96	44.22	2.82	2.05	1.92	0.63	0.38
<b>4-FMC, 8c</b>	0.990	8.05	24.21	4.35	4.18	2.43	0.83	0.44
<b>2-TFMMC, 9a</b>	0.993	11.50	33.82	2.48	3.30	1.92	2.80	1.88
<b>3-TFMMC, 9b</b>	0.993	8.89	25.63	0.98	1.00	1.20	0.47	1.33
<b>4-TFMMC, 9c</b>	0.994	8.88	26.72	1.63	1.41	1.37	0.50	1.03

The mass spectroscopy data can also be used to help identify the compound present with the FMC, TFMMC and FA classes all producing different spectra. The mass spectroscopy data cannot, however, be used to distinguish between isomers within a class. The spectra for each of the three classes can be seen in Figure 45 – Figure 46. The FA isomers shows a base peak of  $m/z = 44.1$ , which represents an ion containing the  $^+CH_2CH_3$  chain bonded to the amine, along with a secondary peak of 109 representing a fluorine substituted tropylium cation (Figure 42).

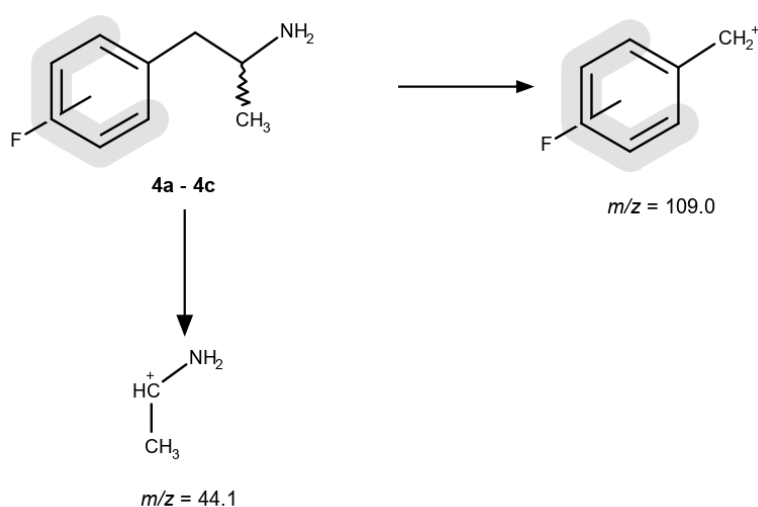


**Figure 42:** MS fragmentation for the fluoroamphetamine (FA, **4a–4c**) regioisomers

The FMC isomers show a primary base peak with an  $m/z$  of 58 representing the amine bonded to the methyl group and a  $^+CH_2CH_3$  similar to the fluoroamphetamine fragmentation. The secondary base peak of  $m/z$  95.0 is produced from the phenyl ring with the fluorine substituent. There is also a peak with an  $m/z$  charge of 123.0 representing the substituted phenyl with the addition of the carbonyl group (Figure 43)

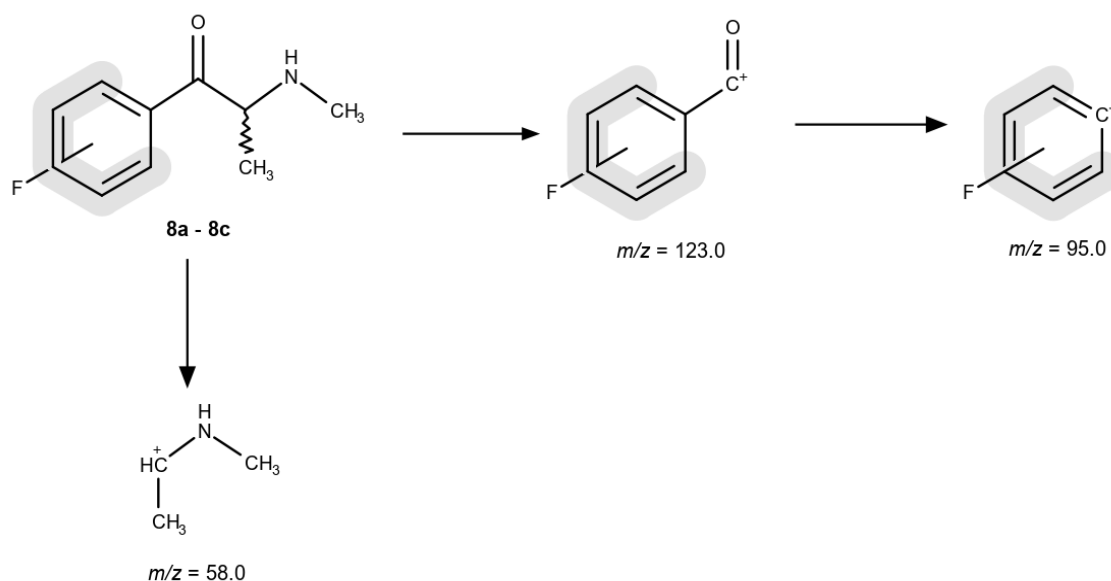


**Figure 43:** MS fragmentation for the fluoromethcathinone (FMC, **8a–8c**) regioisomers

The TFMMC isomers have a similar mass spectroscopy fragmentation pattern to the FMC isomers with a base peak of *m/z* 58 and a peak at *m/z* 95.0. However, the main difference with the TFMMC isomers is that the secondary base peak has an *m/z* value of 145.0. This represents the phenyl cation with the trifluoromethyl group substituent (Figure 44).

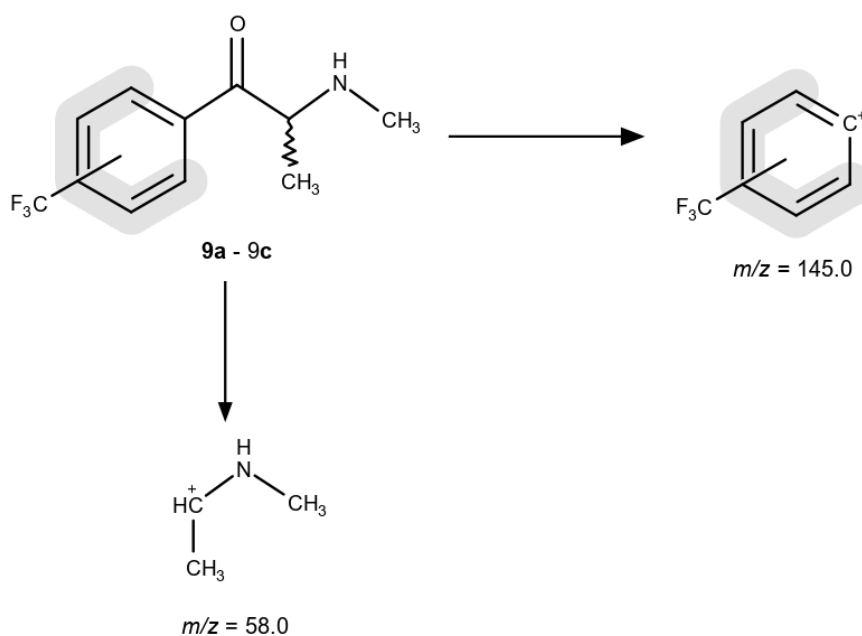


**Figure 44:** MS fragmentation pattern for the trifluoromethylmethcathinone (TFMMC, **9a-9c**) regioisomers

The differences in the mass spectroscopy helps to identify the class of compound present with the retention times helping to identify which isomer is present. It is also seen in the chromatographs of all compounds that there is no tailing due to thermal degradation with symmetry shown in all peaks. This could be a result of using higher split ratios or lower injection volumes and inlet temperatures.

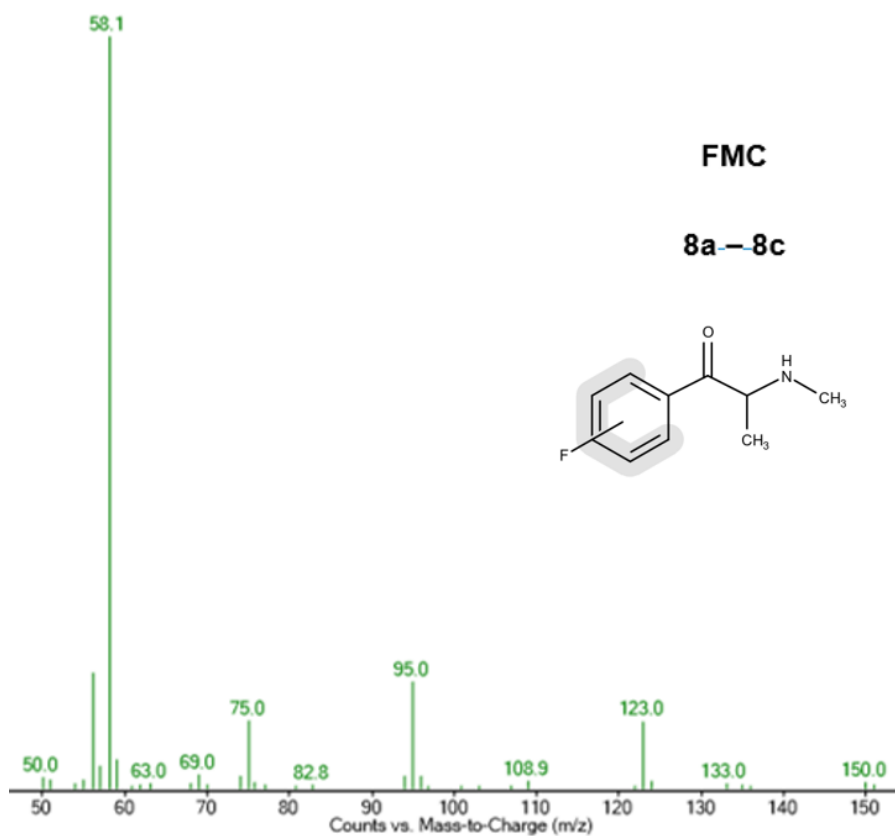
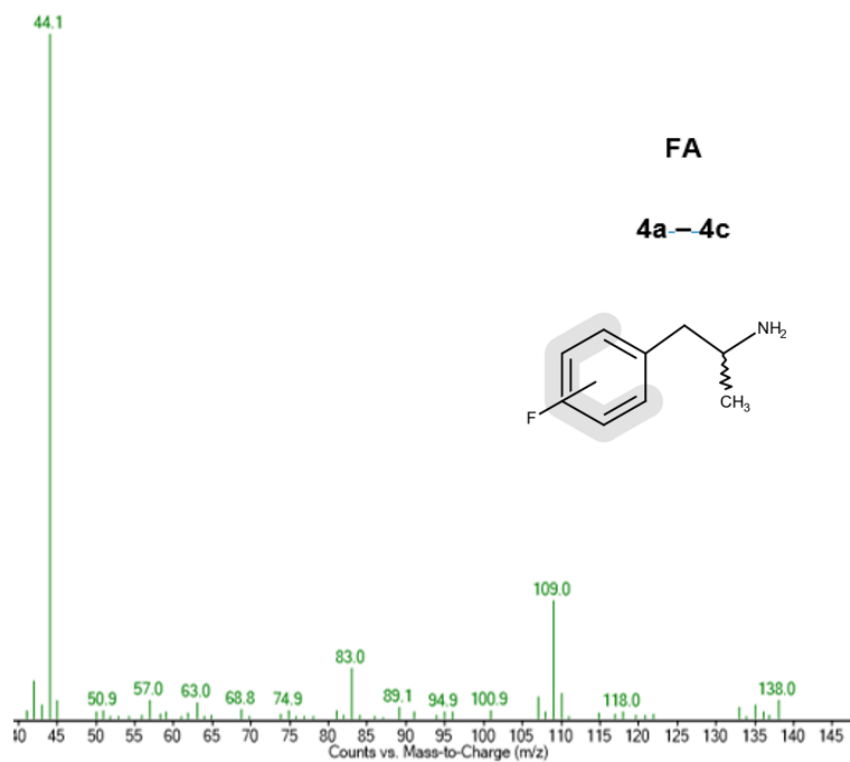


**Figure 45:** Mass spectra for the fluoroamphetamine (**4a–4c**) and fluoromethcathinone (**8a–8c**)

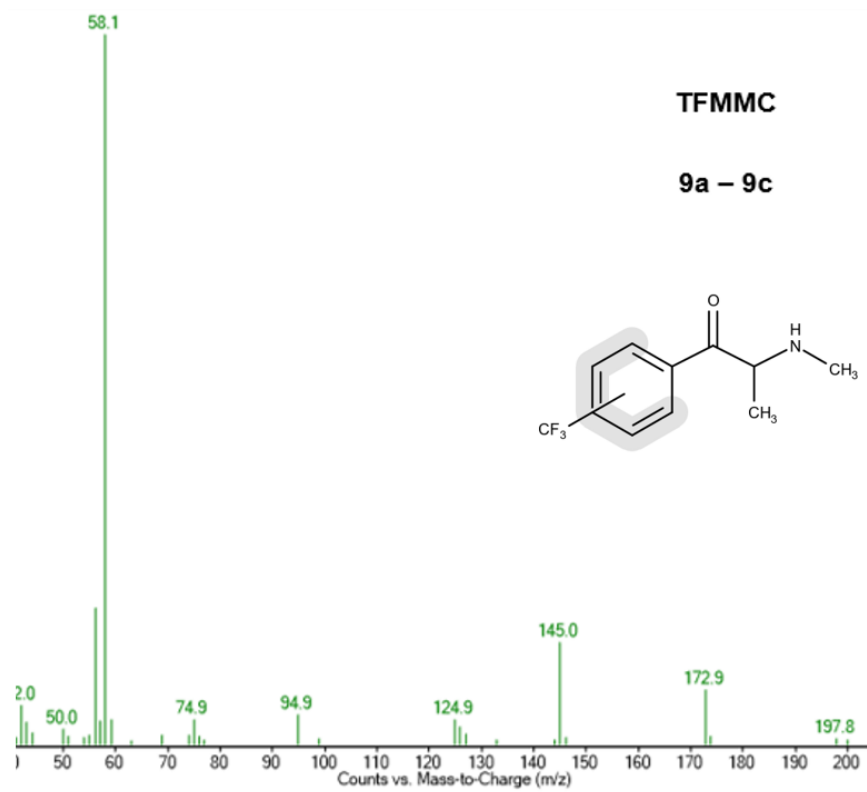


**Figure 46:** Mass spectrum for the trifluoromethylmethcathinone (**9a–9c**) regioisomers



### 3.5. 60 MHz NMR presumptive testing

All fluorinated amphetamines and cathinones were run on a 60 MHz Pulsar NMR instrument to acquire  $^1\text{H}$  and  $^{19}\text{F}$  NMR data. This was done in order to show the possibility of identifying these compounds in unknown street samples. The spectra produced for both the  $^1\text{H}$  and  $^{19}\text{F}$  NMR experiments produce very similar characteristic patterns to those produced when structurally elucidating compounds synthesised, using a 400 MHz instrument. The splitting patterns can still be seen, however the resolution is reduced due to the reduced power of the external magnetic field. Due to the reduced resolution peaks appear broader, however comparison of spectra can still show differences between isomers within a class. This means that the 60 MHz instrument can be used as a presumptive test by providing structural information to enable regioisomers to be distinguished by eye.

All spectra were run in  $\text{DMSO-d}_6$  ( $\delta$  ppm = 2.50) in order to provide a clear reference point for all spectra which could then be stacked to facilitate ease of comparison. In the case of  $^{19}\text{F}$  experiments, trifluoroacetic acid was added as an internal standard ( $\delta$  ppm = -76.55) in order to produce accurate sample chemical shift values. In all  $^1\text{H}$  cases a water peak is seen at a chemical shift of 3.30 ppm. In the case of the fluoroamphetamine regioisomers (Figure 47) all peaks observed when characterisation data was acquired are present in the 60 MHz spectra. The  $\text{CH}_3$  is seen as a clear doublet at 1.13 ppm, showing that splitting patterns can still be seen. The  $\text{CH}_2$  and  $\text{CH}$  peaks can also be seen at the same chemical shifts as with the 400 MHz instrument. When stacked the three FA regioisomers show matching aliphatic regions with the aromatic regions showing clear differences based on the splitting caused by the fluorine substituent moving around the benzene ring.

The fluoromethcathinone (Figure 48) and trifluoromethylmethcathinone (Figure 49) regioisomers show matching spectral patterns to the 400 MHz characterisation with matching aliphatic regions for both sets of classes. This is due to the only difference occurring in the substituent group concerning fluorine is that the fluorine in the FMC isomers contrasts with a  $\text{CF}_3$  group for

the TFMMC isomers. This means that the only differences observed for the regioisomers occurs in the aromatic regions of the spectra. There are also clear differences between the FMC and TFMMC compounds when the substituent is in matching positions of the benzene ring. The differences in the spectra for all nine compounds shows that the technique can be used to identify unknown samples.

The  $^{19}\text{F}$  NMR experiments for all compounds show matching chemical shifts to those seen when using 400 MHz instruments, however the peak widths are increased. The table containing all  $^{19}\text{F}$  NMR chemical shifts can be seen in Table 21 with the stacked spectra of all trifluoromethylmethcathinone isomers seen in Figure 50. The monofluorinated cathinone and amphetamine regioisomers are seen in a similar region, however the stacked  $^{19}\text{F}$  NMR spectra (Figure 51) shows that each compound can be distinguished based on its chemical shift value. This can help to aid in the identification of unknown active components in seized street samples. This means that clear differences can be seen using the 60 MHz instrument for three regioisomers using two different experiments in just 30 minutes.

**Table 21:**  $^{19}\text{F}$  NMR chemical shift values for all fluorinated amphetamine and cathinone derivatives run on a 60 MHz instrument

Compound no.	Compound	$^{19}\text{F}$ chemical shift ( $\delta$ ppm)
<b>4a</b>	2-fluoroamphetamine	-117.58
<b>4b</b>	3-fluoroamphetamine	-113.03
<b>4c</b>	4-fluoroamphetamine	-115.69
<b>8a</b>	2-fluoromethcathinone	-110.35
<b>8b</b>	3-fluoromethcathinone	-111.70
<b>8c</b>	4-fluoromethcathinone	-102.02
<b>9a</b>	2-trifluoromethylmethcathinone	-58.34
<b>9b</b>	3-trifluoromethylmethcathinone	-63.65
<b>9c</b>	4-trifluoromethylmethcathinone	-64.17

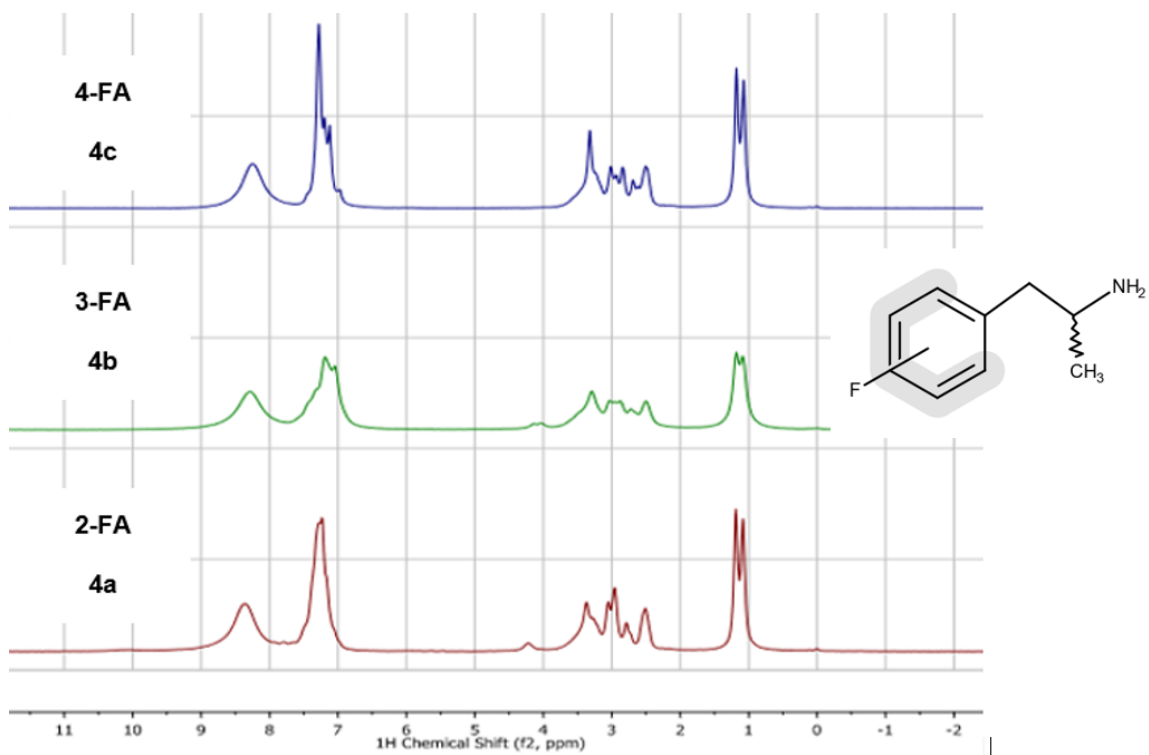


**Figure 47:** <sup>1</sup>H NMR spectra for the fluoroamphetamine regioisomers (FA, **4a–4c**), run on a 60 MHz instrument in DMSO-d<sub>6</sub> (δ ppm = 2.50)

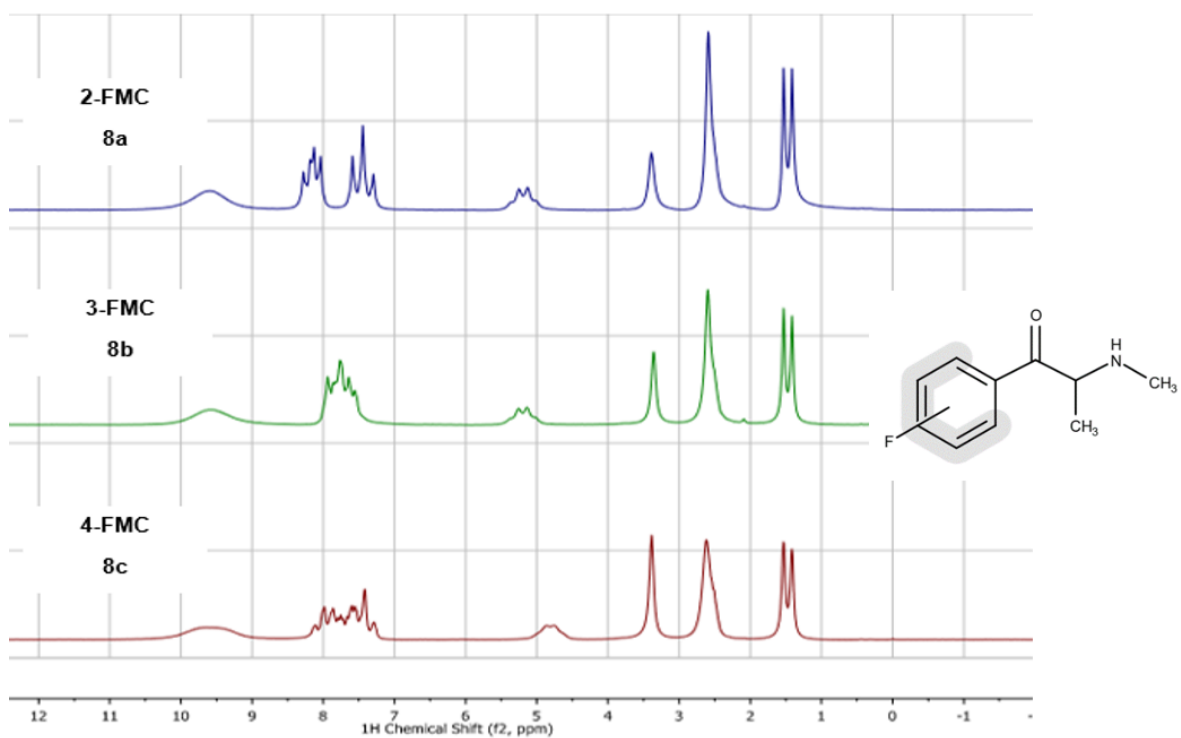


**Figure 48:** <sup>1</sup>H NMR spectra for the fluoromethcathinone regioisomers (FMC, **8a–8c**), run on a 60 MHz instrument in DMSO-d<sub>6</sub> (δ ppm = 2.50)

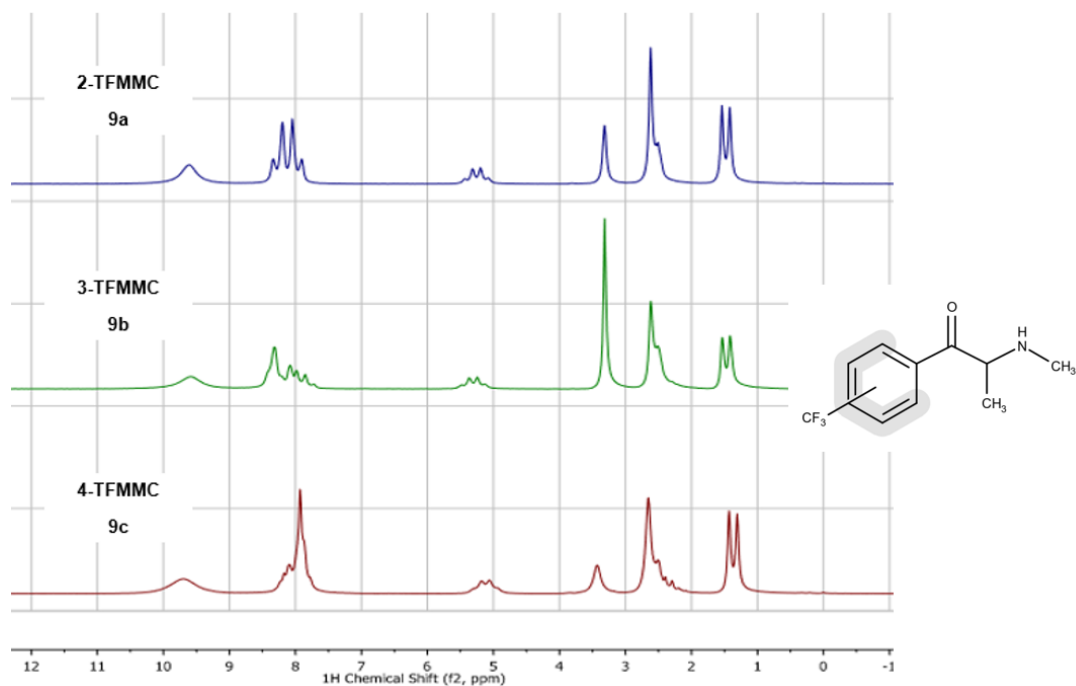


**Figure 49:**  $^1\text{H}$  NMR spectra for the trifluoromethylmethcathinone regioisomers (TFMMC, **9a**–**9c**), run on a 60 MHz instrument in  $\text{DMSO-d}_6$  ( $\delta$  ppm = 2.50)

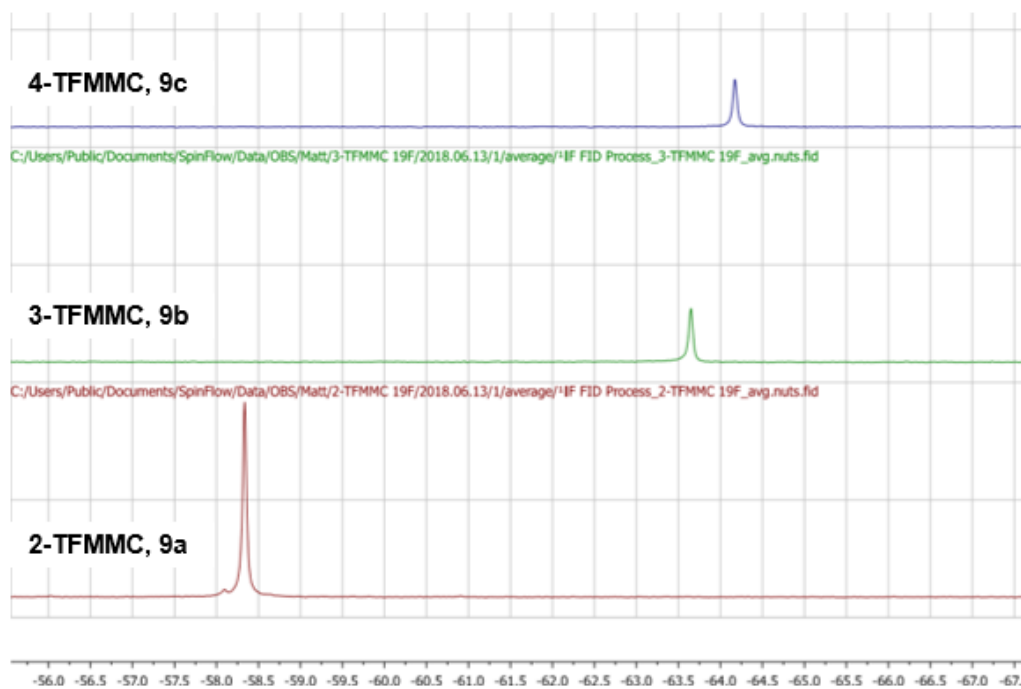


**Figure 50:** Stacked  $^{19}\text{F}$  NMR spectra for the trifluoromethylmethcathinone regioisomers

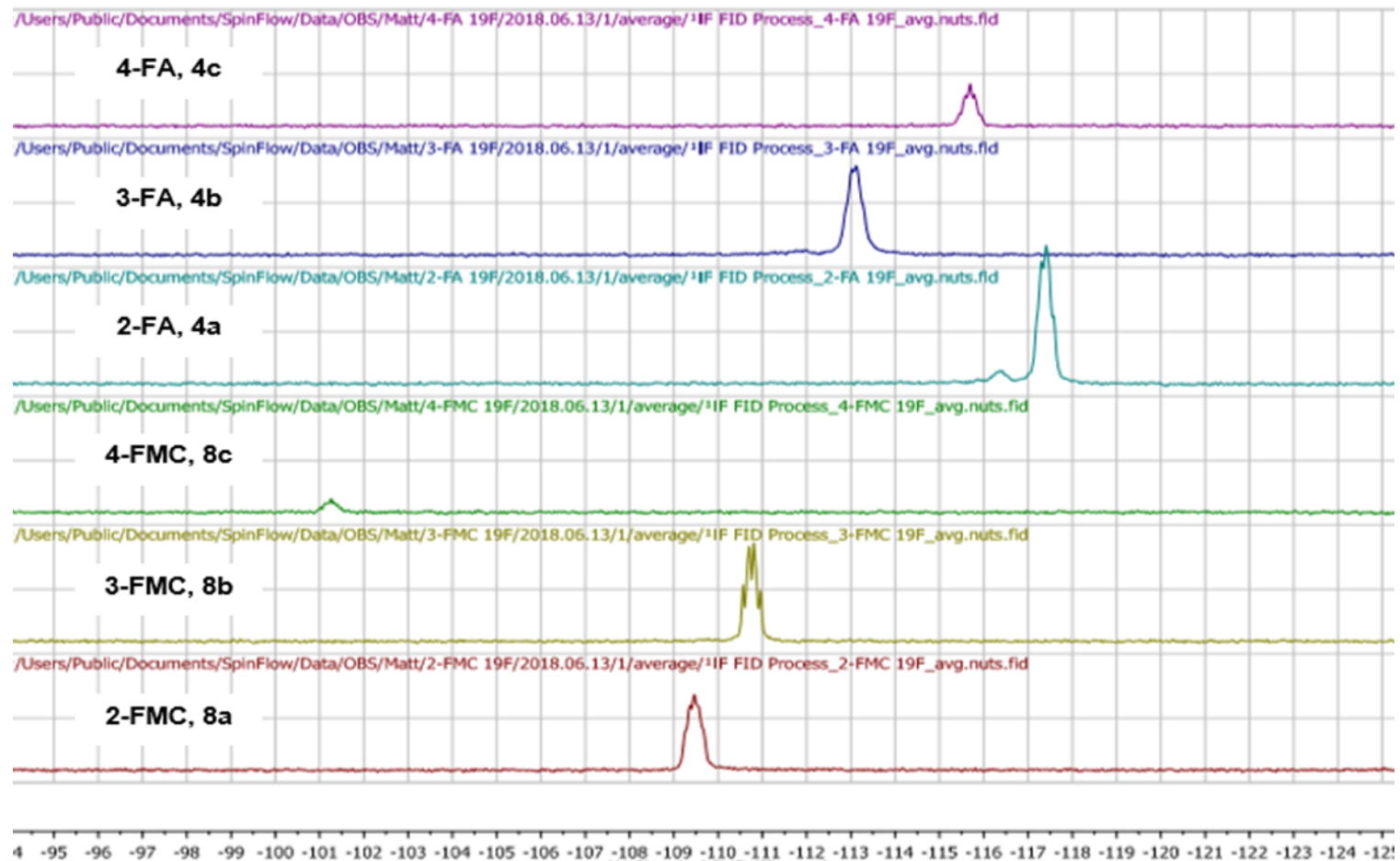


**Figure 51:** Stacked  $^{19}\text{F}$  NMR spectra for all fluoroamphetamine (FA, **4a–4c**) and fluoromethcathinone (FMC, **8a–8c**) regioisomers

### 3.6. GC-MS and 60 MHz NMR quantitative analysis

Based on the acquisition of street samples from Greater Manchester Police (GMP), presumed to contain fluoroamphetamine, calibration series were created for the three fluoroamphetamine isomers using both GC-MS and  $^{19}\text{F}$  NMR spectroscopy on a 60 MHz instrument. This was done in order to be able to provide information on how much active ingredient is present in the street samples tested in section 3.7.

A calibration series was created for all three FA regioisomers on the GC-MS using standards in the concentration range  $100\ \mu\text{g mL}^{-1}$  –  $500\ \mu\text{g mL}^{-1}$  with each concentration run in triplicate. An extra calibration standard was run for the 3-FA standard at a concentration of  $50\ \mu\text{g mL}^{-1}$  in order to show that positive correlation was achieved through the origin. Eicosane was used at a constant concentration of  $100\ \mu\text{g mL}^{-1}$  for all standards and integrated area ratios calculated between sample peaks and the eicosane peaks. The developed GC-MS method used in section 3.4 was used to run all calibration samples. The calibration graph containing each isomer can be seen in Figure 522 and shows a correlation coefficient ( $R^2$ ) greater than 0.99 in the case of the 2-FA (**4a**) and 4-FA (**4c**) isomers. The 3-FA (**4b**) isomers showed positive correlation with a coefficient only slightly below 0.99 (0.9874). This shows that the GC-MS method can be used for quantitative analysis of street samples. Based on the standard deviation and the response of the slope LOD and LOQ values were calculated for all three isomers. The 2-FA sample gave an LOD and LOQ of 20 and  $68\ \mu\text{g mL}^{-1}$  respectively. The 3-FA and 4-FA isomers gave LOD and LOQ values of 25 – 23  $\mu\text{g mL}^{-1}$  and 80 – 75  $\mu\text{g mL}^{-1}$  respectively. When compared to MDMA tablets this would be below the average amounts of active component that would be present in street samples so is acceptable for analysis. Average MDMA tablets contain 100 -150  $\mu\text{g mL}^{-1}$ , with weak tablets containing around 70  $\mu\text{g mL}^{-1}$ .<sup>144</sup> As long as a controlled substance or NPS is detected then a prosecutor can be convicted so if there are extra minor components, trace levels of other compounds or cutting agents that fall below the LOD, within a sample, then these are not considered within analysis. The relative standard deviation percentage (RSD%), for the triplicate runs, with all concentration standards is below the acceptable 5%.

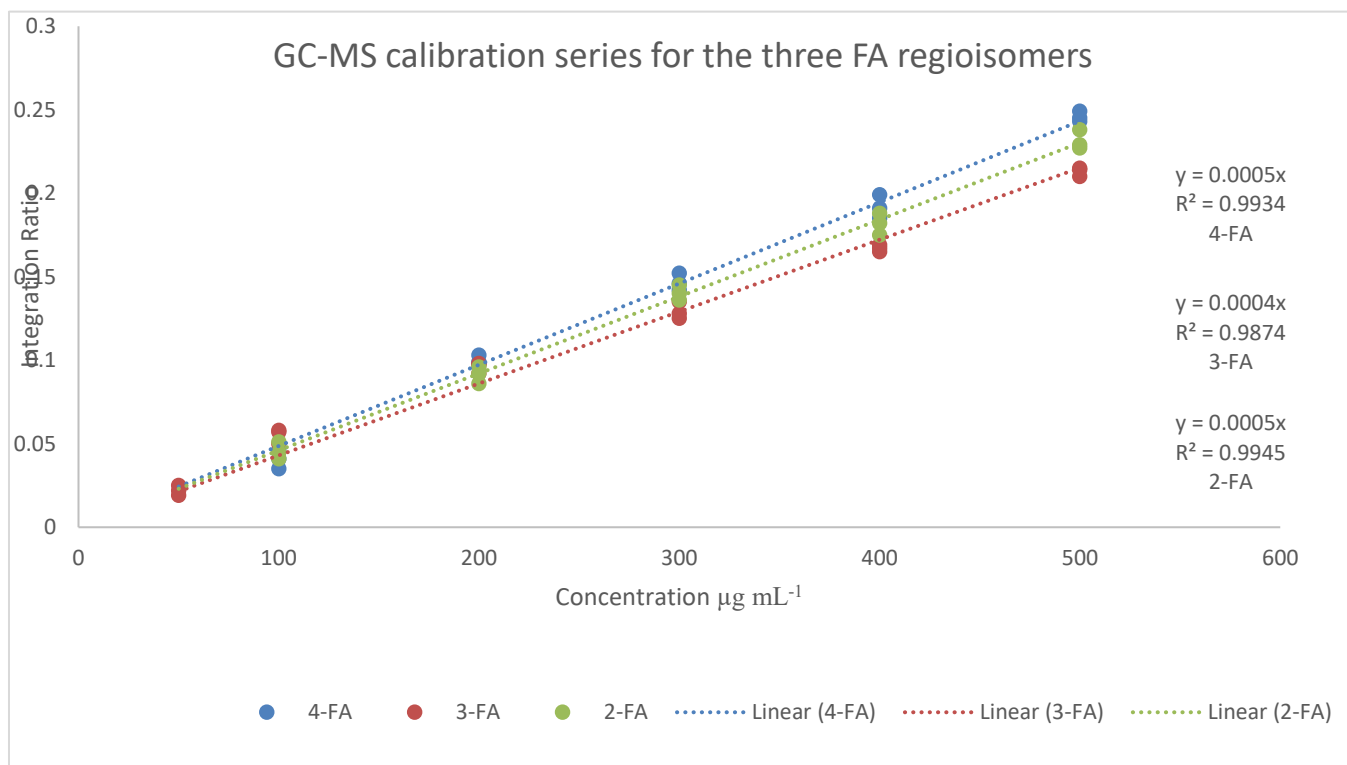


**Figure 52:** Calibration series performed using GC-MS on all three fluoroamphetamine (FA, **4a-4c**) regioisomers

A calibration series for all three of the FA isomers was also performed on the 60 MHz NMR using a  $^{19}\text{F}$ -based NMR experiment. Calibration standards were prepared over the concentration range  $5 \text{ mg mL}^{-1}$  –  $15 \text{ mg mL}^{-1}$  with trifluoroacetic acid (TFA) added as an internal standard at a concentration of 0.1% v/v of DMSO used. 16 scans was used with a 3 second relaxation delay. Calibration graphs were then produced by calculating the integrated area ratio between sample peaks and TFA peaks and plotting against concentration. The calibration graphs can be seen in Figure 53.

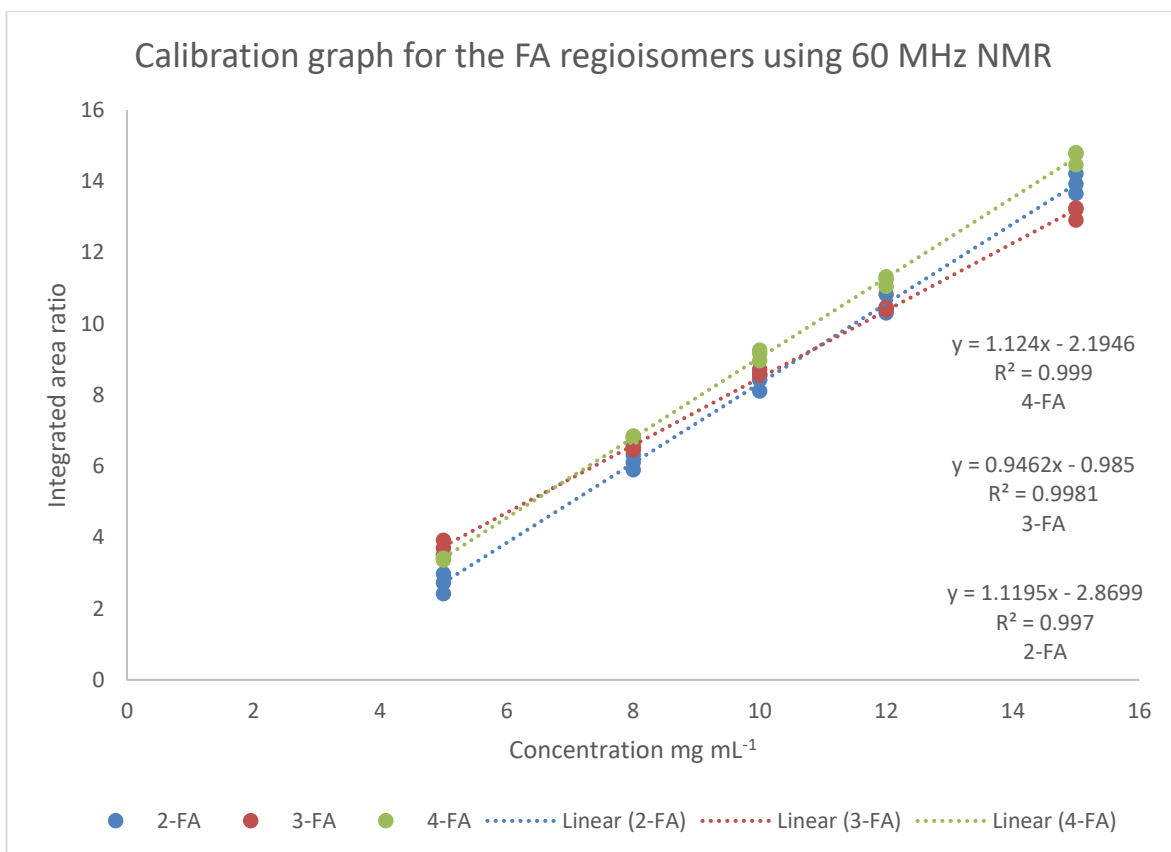


**Figure 53:** Calibration graphs for the FA regioisomers using <sup>19</sup>F NMR experiments on a 60 MHz NMR

The three isomers show acceptable correlation (>0.99) meaning the method can be used to perform quantitative analysis. The LOD and LOQ for the three regioisomers can be seen in Table 22 and shows that the highest LOQ is below 2 mg mL<sup>-1</sup>. This is acceptable as the majority of street samples will have active components greater than 2 mg per sample. The RSD % of the triplicate readings for each calibration standard is higher than those produced from GC-MS, however they are still lower than the acceptable 5%. The calibration graphs for the NMR analysis does not go through the origin, due to the increased noise of the baseline compared to other analytical techniques. The integrated values for the baseline around each signal can be averaged and deducted from the integrated values of the signal and reference peak prior to performing the ratio calculations. This would then allow the calibration series to go through the origin, however the process would be complicated for untrained users, who the system is aimed towards. It is also clear that positive correlation is achieved without the baseline average and subtraction and



concentrations can be determined using this method. The 60 MHz instrument is more favourable due to the ease of data processing and the quicker run time from around 40 minutes with the GC-MS to 5 minutes per run for the NMR.

**Table 22:** LOD and LOQ values for the three FA (**4a–4c**) regioisomers from the calibration series produced on the 60 MHz NMR instrument

Sample	LOD (mg mL <sup>-1</sup> )	LOQ (mg mL <sup>-1</sup> )
2-FA	0.49	1.63
3-FA	0.33	1.10
4-FA	0.28	0.93

### 3.7. Street samples analysis

Two tablets (SS1 and SS2, Figure 544) were seized by Greater Manchester Police (GMP) initially thought to contain MDMA based on appearance. However after initial analysis performed using the GC-MS general screening method, the resulting GC trace did not produce the corresponding  $R_t$  for MDMA or a mass spectrum fragmentation pattern resembling MDMA. Consequently, samples were tested using presumptive colour test reagents, GC-MS again (using the method developed in this chapter) and 60 MHz NMR. The two tablets were weighed and masses of 275.2 and 248.0 mg recorded. As well as determining the active component in the tablet, qualitative analysis was also performed on the two tablets.



**Figure 54:** Image of the seized street sample (SS1)

The two street samples were both tested using the full range of presumptive test reagents used when testing the reference materials. Both tablets were dissolved in water ( $10 \text{ mg mL}^{-1}$  solutions) and a couple of drops of test reagent were added to a couple of drops of the sample solution. Both solutions produced the same colour changes when each reagent was added. No colour changes were observed when Mandelin's and Scott's reagents were added, however none of the FA, FMC or TFMMC reference materials changed colour with these reagents so this does not help in distinguishing isomers. In a similar manner the solution changed to an orange colour with the Marquis reagent, however this occurred with all nine of the fluorinated compounds. A negative reaction was seen with the Zimmerman reagent, meaning it is possible that the unknown street samples are not cathinones. There was also a positive

reaction with the Robadope's reagent with the solution changing to a brown colour in a similar manner to the fluoroamphetamine regioisomers.

The street samples were then run on the 60 MHz NMR instrument using matching  $^1\text{H}$  and  $^{19}\text{F}$  experiments to the reference materials. Both street samples gave matching spectra to each other on both the  $^1\text{H}$  and  $^{19}\text{F}$  experiment. The spectra can be seen in Figure 55. The  $^1\text{H}$  NMR spectra for the street sample shows a doublet peak, representing three protons at 1.15 ppm and two multiplet peaks, representing one proton each, in the region of 2.80–3.20 ppm. There is also an amine singlet peak at 8.20 ppm representing two protons. This is similar to the aliphatic region of the FA isomers with a peak for DMSO and water at 2.50 and 3.30 ppm respectively.

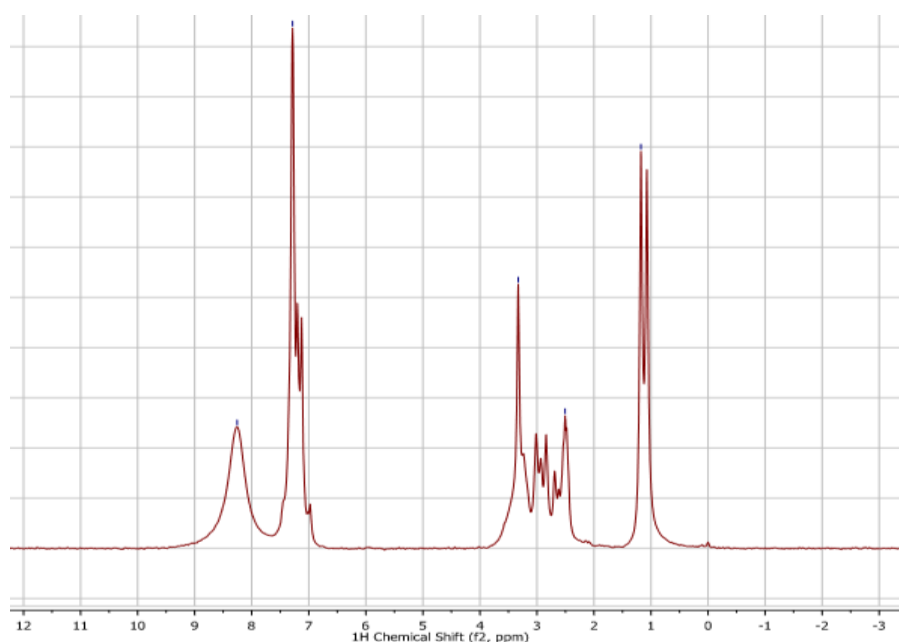


**Figure 55:**  $^1\text{H}$  NMR spectra for the street sample run in  $\text{DMSO-d}_6$  ( $\delta$  ppm = 2.50)

This region matches the aliphatic region of the FA isomers produced when the reference materials were run on a 60 MHz instrument. The aromatic regions for the street samples were then matched to the three FA isomers and a close match is seen with the 4-FA isomer.

The  $^{19}\text{F}$  NMR spectra (Figure 56) for the street sample produced a sample chemical shift of -115.60 ppm. This is very close (-0.09 ppm) to the chemical

shift produced from the  $^{19}\text{F}$  NMR spectra of the 4-FA reference material and when added to the result for the  $^1\text{H}$  NMR experiment strongly suggests the possibility of the street sample having 4-FA as an active component. Both the  $^1\text{H}$  and  $^{19}\text{F}$  NMR spectra suggest that there is only the one active ingredient in the street samples.

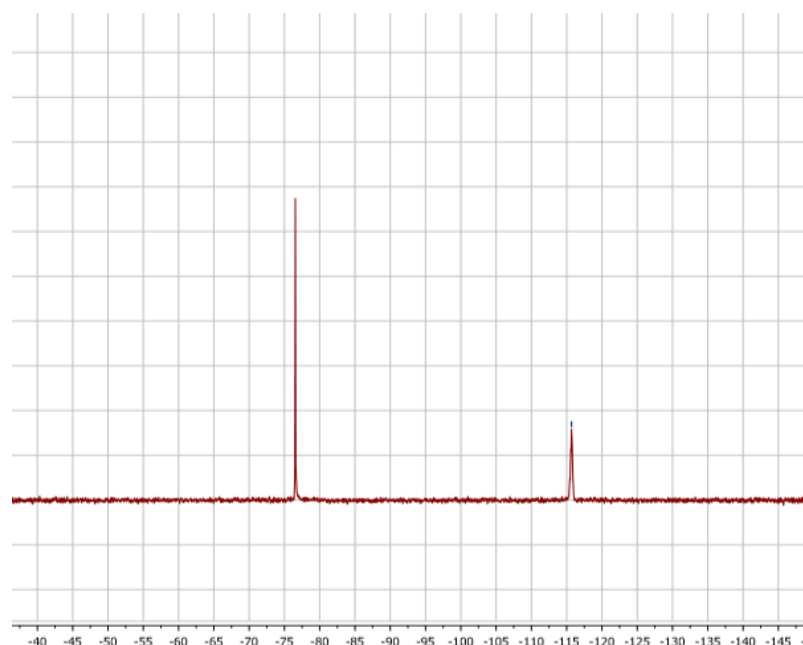


**Figure 56:**  $^{19}\text{F}$  NMR spectrum for the street samples with TFA added as an internal reference ( $\delta$  ppm = -76.55)

After analysis of the two street samples had been performed on the 60 MHz NMR spectrometer, GC-MS was used to confirm the active component as 4-FA. The developed method was used to analyse both street samples. The two chromatographs can be seen in Figure 57 with the mass spectra produced seen in Figure 58. The two street samples produced retention times of 5.43 and 5.42 mins respectively, which both match up to the retention time for the 4-FA isomer and the mass spectra produced matches that for all fluoroamphetamine regioisomers.

The data acquired, its subsequent analysis, confirm that both street samples contain 4-FA as the single active component with no further adulteration or cutting agents added.

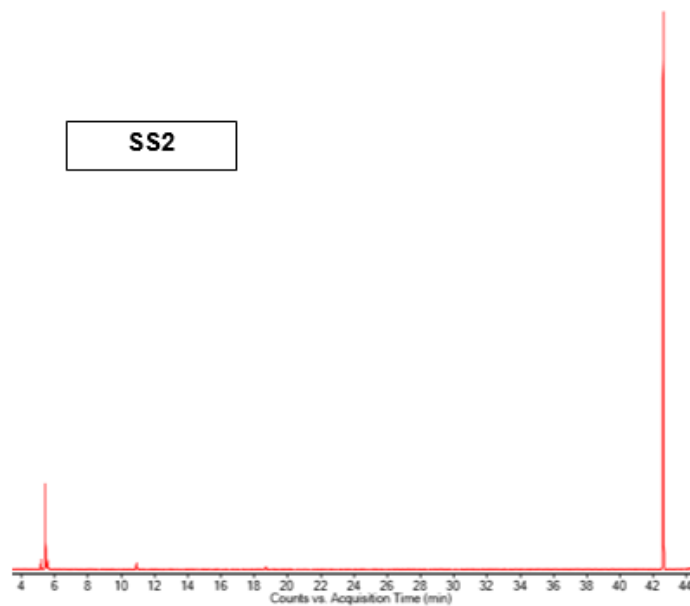
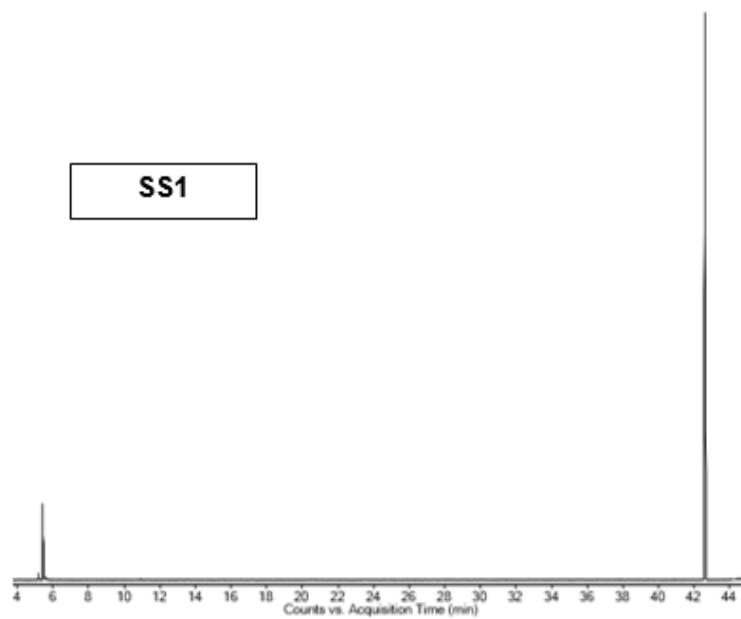


**Figure 57:** GC-MS chromatographs for the two street samples run with eicosane added as an internal standard ( $R_t = 30.85$  mins)

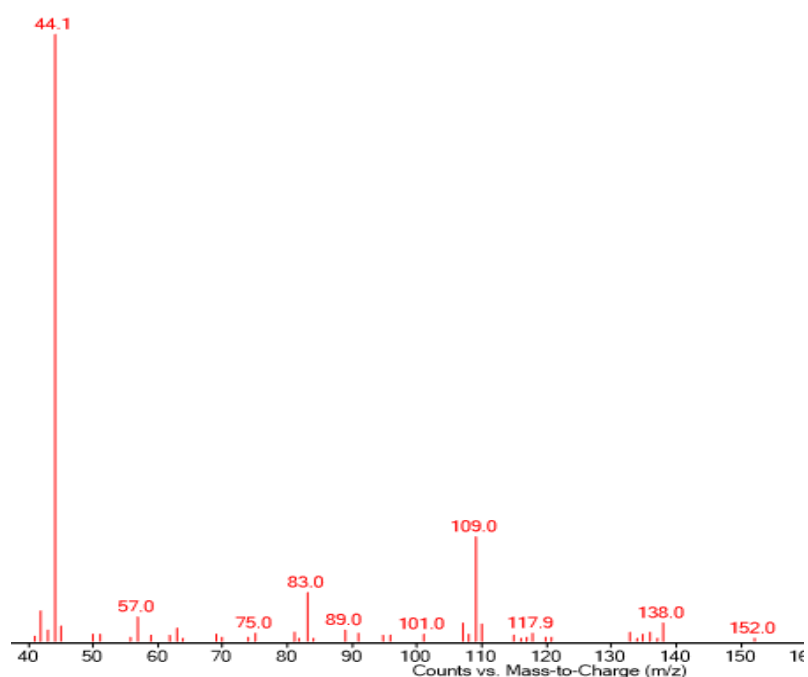


**Figure 58:** Mass spectrum produced for the two street samples

Based on the knowledge that both street samples contain 4-FA, qualitative analysis was performed using the calibration series created in section 3.6, using both GC-MS and 60 MHz NMR. Two samples for both street samples were made for GC-MS analysis firstly at a concentration of  $300 \mu\text{g mL}^{-1}$  in order to fall in the centre of the calibration series. The two solutions for each street sample were both run in duplicate with the calculated concentrations, based on the equation of the calibration graph shown in Figure 52. These concentrations were then converted to weight of active ingredient and percentage weight per tablet based on original tablet weights and dilution factors.

The GC-MS (Table 23) showed that SS1 contained 40% w/w active ingredient with the two samples differing by an acceptable 2%. SS2 gave a % weight of 49% w/w. This equates to weights of 109–123 mg of 4-FA in the two street samples. This would not be considered a high amount of substance per tablet based on the common dosages found in MDMA, where a weight of around 240 mg would be considered high.<sup>145</sup>

**Table 23:** Quantification results for active component, 4-FA, in the two street samples from GC-MS analysis

Sample	Integrated area Ratio (IAR)		Concentration of diluted solution ( $\mu\text{g mL}^{-1}$ )		Active component weight in tablet (mg)			% weight (% w/w)
	Run 1	Run 2	Run 1	Run 2	Run 1	Run 2	Average	
SS1 sample 1	0.053	0.055	118.0	121.4	108.20	111.36	109.78	39.9
SS1 sample 2	0.057	0.056	124.6	123.8	114.26	113.60	113.93	41.4
SS2 sample 1	0.067	0.070	144.6	151.4	119.50	125.18	122.34	49.3
SS2 sample 2	0.071	0.065	153.0	141.0	126.48	116.56	121.52	49.0

**Table 24:** Quantification results for active component, 4-FA, in the two street samples from 60 MHz NMR analysis

Sample	Integrated area Ratio (IAR)		Concentration of NMR sample ( $\text{mg mL}^{-1}$ )		Active component weight in tablet (mg)			% weight (% w/w)
	Run 1	Run 2	Run 1	Run 2	Run 1	Run 2	Average	
SS1 sample 1	5.17	5.08	6.55	6.47	120.20	118.72	119.46	43.4
SS1 sample 2	5.00	5.06	6.40	6.45	117.44	118.35	117.90	42.8
SS2 sample 1	5.93	6.09	7.23	7.37	119.51	121.83	120.67	48.7
SS2 sample 2	6.16	6.06	7.43	7.34	122.82	121.33	122.08	49.2

The street samples were then analysed quantitatively using the 60 MHz NMR calibration through the  $^{19}\text{F}$  experiments. Based on the knowledge from the GC-MS results the NMR street samples were made at a concentration of  $15\text{ mg mL}^{-1}$  in order to ensure the sample integrated area ratio (IAR) would fall within the linear range of the calibration graph. Two samples from both street samples were prepared using 0.1% TFA v/v in a similar manner to the calibration series with the IAR for each sample reported in Table 24. The table also shows calculations for the concentration of 4-FA in the NMR sample and the weight of FA in the original tablets based on original weights of the tablets and conversion factors.

From the results both percentage weight compositions for both street samples is within 2% for the two runs. SS2 shows a very similar percentage composition and weight of 4-FA in the sample, while SS1 appear to produce a %weight slightly higher to that reported using GC-MS. The mean difference is 1.4% between the GC-MS and NMR techniques, which equates to 5–10 mg. This amount would not make a significant difference when reporting to healthcare services.

The similarity of the results obtained from the two instrumentation methods shows the possibility of using 60 MHz NMR as a technique in law enforcement to determine active components of street sample not only qualitatively but quantitatively also. When compared to the GC-MS analysis the results both provide the same outcome, however the 60 MHz instrument produces the results 6 times quicker (5 mins compared to 30) with the same level of precision (both <5%). The quantitative analysis provides the same percentage composition, within 10 mg (4%) for the street samples under the same number of repeats, however for each run the 60 MHz is performing 32 scans which could be considered extra repeats.



### 3.8. Conclusions

In conclusion regioisomers of fluoroamphetamine, fluoromethcathinone and trifluoromethylmethcathinone were taken and fully characterised allowing them to be used for further analysis.

Presumptive colour tests have shown that the Zimmerman reagent is a clear indicator to the presence of cathinones with the Simon's reagent allowing indication of a methcathinone (secondary amine). The Robadope's reagent allows indication as to the presence of the fluoroamphetamine, however it does not allow the three regioisomers to be distinguished. The fluoromethcathinone regioisomers can be distinguished using both the Zimmerman and Simon's reagents, however the combination does not distinguish between the trifluoromethylmethcathinone regioisomers. This means that the presumptive colour tests can only be used to narrow down possibilities of these compounds being present and if a specific compound needs to be known this technique cannot provide this information.

A GC-MS method was developed which enabled all fluorinated amphetamines and cathinones to be distinguished from one another, although baseline separation has not been achieved for the 3' and 4' fluoroamphetamine isomers. All peaks were shown to have good symmetry with no fronting or tailing, which has reported previously through thermal degradation.<sup>4</sup> The developed GC-MS runs do not separate all the regioisomers, it would be considered that the run time of 24 minutes is too long.

60 MHz NMR was shown to provide a possible presumptive test for determination of unknown sample identification. This is possible due to spectra produced matching those produced on a 400 MHz system and still showing distinguishing features for differing reference materials. All regioisomers can be separated from one another so if law enforcement need an initial statement as to what an unknown sample is the 60 MHz instrument can provide this information. Quantitative analysis was performed using both the developed GC-MS method and <sup>19</sup>F NMR experiments on the 60 MHz NMR instrument.

Both techniques showed good linearity ( $R^2 > 0.99$ ) and repeatability of triplicated runs (RSD < 5%). This again shows the benefits of the 60 MHz as it can perform quantitative analysis in a quicker manner than the GC-MS instrumentation, which is currently considered the optimum technique, with no great loss to limits of detection, precision or accuracy.

Street sample analysis was performed on two tablets originally thought to contain MDMA based on appearance. Both were shown to contain 4-FA based on GC-MS and NMR analysis using qualitative analysis. Further quantitative analysis via GC-MS and 60 MHz NMR analysis proved the two tablets contained 4-FA at a level of 40% and 49% respectively. This would equate to 109 – 123 mg per tablet. The two techniques differ by 1.4% (mean value), which equates to 5–10 mg. This again shows that 60 MHz instrumentation can be used for street sample analysis as it provides the same result for the active ingredients of the tablets, as the GC-MS analysis, with percentage composition also matching. This is a key factor if the instrument is to be utilised in locations such as police custody and festivals, where samples can be identified correctly, rapidly (5 mins) by officers with little training, due to the ease of sample preparation and processing. The only disadvantage seen with the 60 MHz instrument in this instance is a higher LOD (0.5 mg max) but common tablet concentrations for MDMA have shown to be higher than this, with a weak tablet considered to contain around 100 mg. <sup>144</sup>As long as a fluorinated amphetamine or cathinone is detected then a conviction can be made so it does not matter if other cutting agents or trace products are within the sample.

## 4. Chapter 4 - Separation and identification of diphenidine derivatives using GCMS analysis results

### 4.1. Overview

In the past few years diphenidine (**13a**) and its methoxy-substituted derivatives, 4-methoxyphenidine (4-MXP, **13d**), have increased in popularity on the recreational drugs market. This danger was enhanced with a number of fatalities in both Europe and Asia in both their pure forms and in combination with synthetic cannabinoids.<sup>97, 98, 112</sup> Wallach *et al.* and McLaughlin *et al.* have already published characterisation data on diphenidine and the methoxyphenidine regioisomers respectively.<sup>34, 102</sup> Techniques have been developed for the toxicological screening of 2-methoxyphenidine (2-MXP, **13b**) in blood (using HPLC, LC-MS-MS or UPLC-QTOF-MS) and urine (using HPLC, LC-MS, LC-MS-MS or UPLC-QTOF-MS), due to recent fatalities and intoxications.<sup>99, 103</sup> The increased use of diphenidine-derived dissociatives has required the development of rapid testing methods for the identification and quantification of these substances. There is a current lack of such methods in the literature, especially for new and emerging derivatives of currently available compounds.

This chapter of work will seek to address the current gap in the literature and will report presumptive colour tests, thin layer chromatographic and GC-MS data for thirteen new diphenidine derivatives encountered by law enforcement. A validated GCMS method will be reported which, for the first time, will provide both a general screening method for the thirteen derivatives and quantification of the active components for seized solid samples, both in their individual pure forms and as mixtures containing common cutting agents and adulterants. Reference spectra and data will be produced from characterisation through <sup>1</sup>H NMR, <sup>13</sup>C NMR and <sup>19</sup>F NMR for the compounds synthesised and prepared in this study. This will also provide a comparison for laboratories or environments that are engaged in the routine analysis of these compounds.

## 4.2. Synthesis

Samples of thirteen diphenidine derivatives (**13a–13m**) were prepared as their corresponding hydrochloride salts prior to the project at Manchester Metropolitan University. All target compounds were synthesised, as racemic mixtures, using a modification of the previously reported methods from the prerequisite aromatic aldehydes (Figure 61).<sup>34, 102</sup>

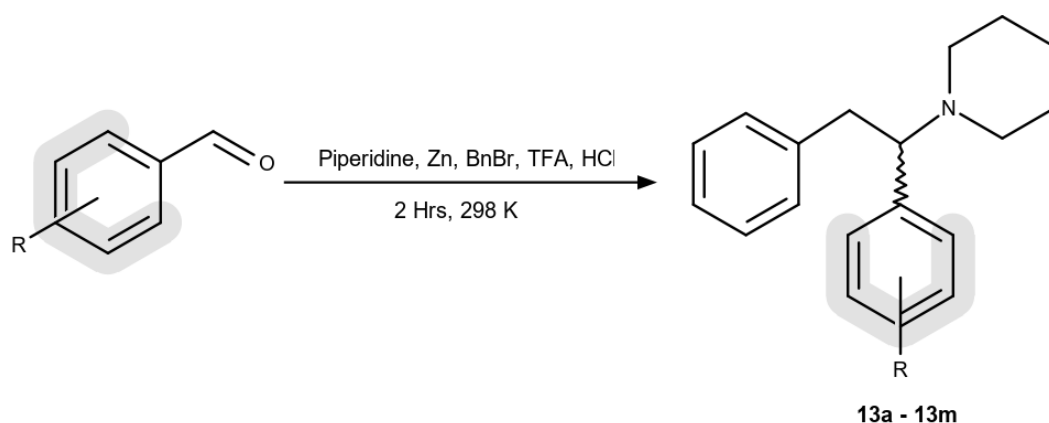


**Figure 59:** Reaction scheme for the synthesis of the diphenidine derivatives

Reference materials were produced as stable, colourless to off-white powders with overall yields ranging from 21-77%. The hydrochloride salts were determined to be soluble ( $10 \text{ mg mL}^{-1}$ ) in deionised water, methanol, dichloromethane and dimethylsulfoxide. To ensure the authenticity of the materials utilised in this study the synthesised compounds were fully structurally characterized, to produce reference spectra, by  $^1\text{H}$  NMR (Figure 63-Figure 71),  $^{13}\text{C}$  NMR (supplementary data: Figure 1-Figure 13), and FTIR (supplementary data: Figure 50-Figure 62).  $^{19}\text{F}$  NMR was also run on the relative compounds (**13e–13g**) and the respective chemical shifts can be seen in Table 25. The purity of all samples was checked by elemental analysis and shown to be >95% in all cases.

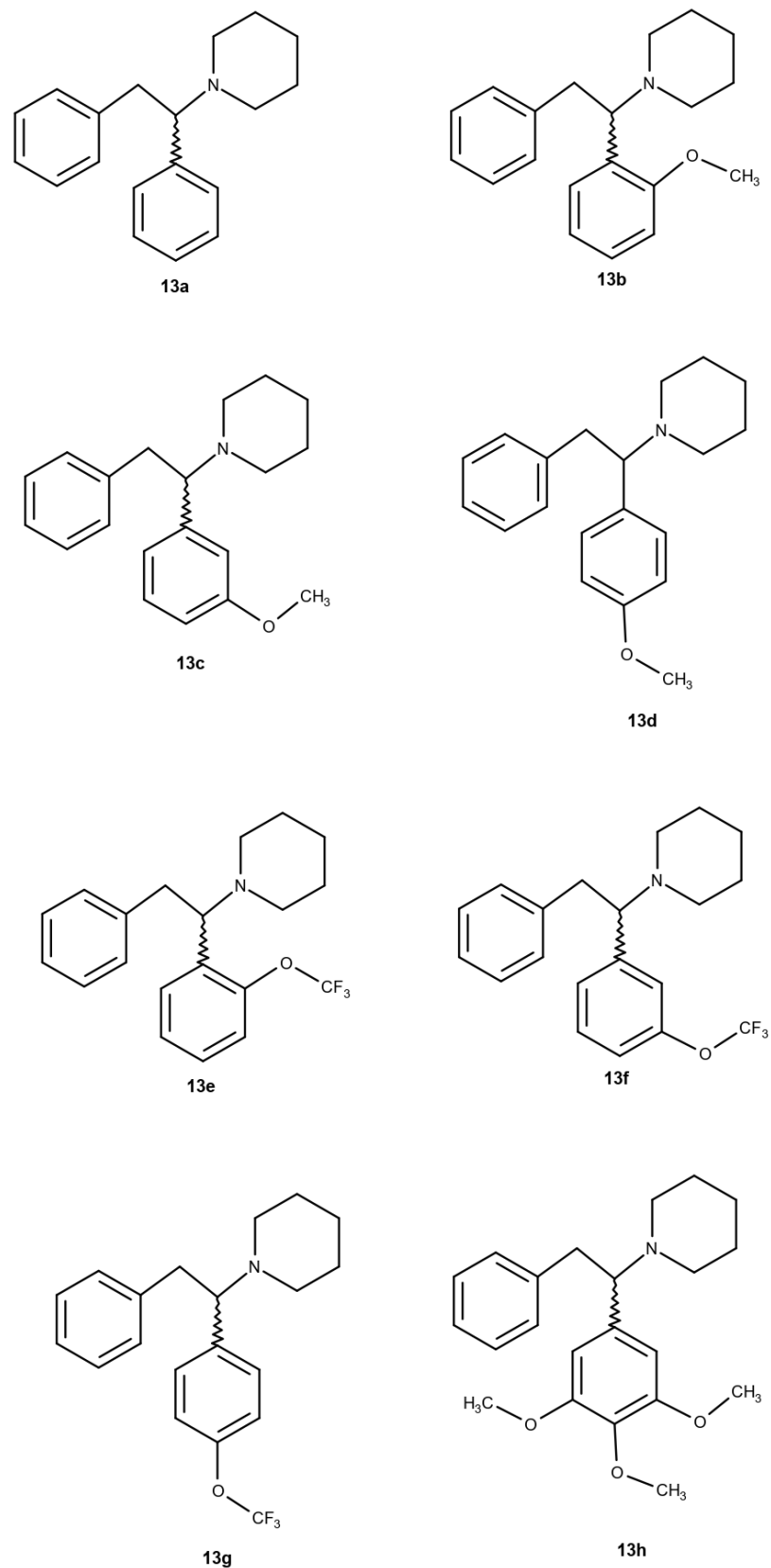


**Figure 60:** Chemical structures for diphenidine (**13a**), the three methoxyphenidines (MXP, **13b–13d**) and trifluoromethoxyphenidines (TFMXP, **13e–13f**) regioisomers along with the 2,3,4-trimethoxyphenidines (mescphenidine, **13h**) derivative

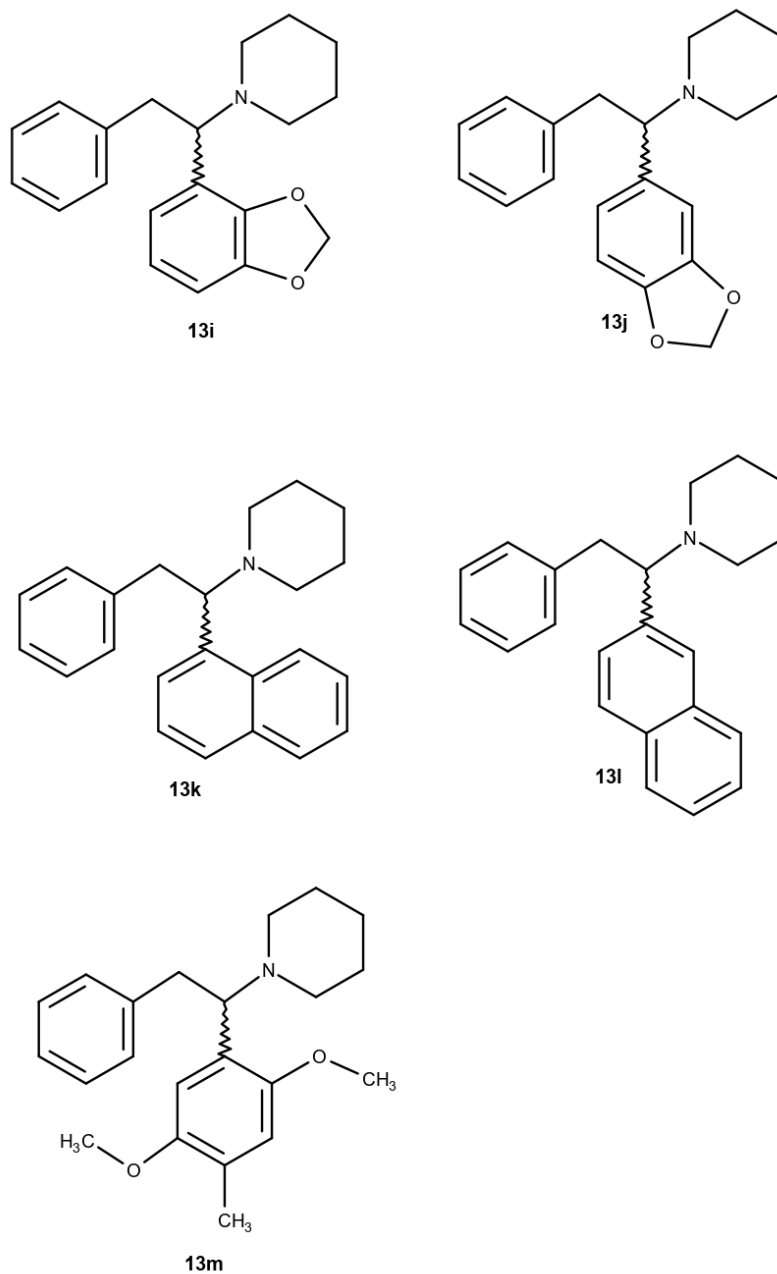


**Figure 61:** Chemical structures for the methylenedioxyphenidine (MDDP, **13i–13j**), naphthenidine (NPD, **13k–13l**) and the IAS-013 (**13m**) derivatives

Due to the variation in chemical structures between each of the diphenidine derivatives there are slight differences in the  $^1\text{H}$  NMR spectra that is produced especially in the aromatic regions. Diphenidine (**13a**) provides the base structure for all the other derivatives and therefore spectra can be compared to that of diphenidine to help with identification (figure 61). In some cases acetone and water were present in the  $^1\text{H}$  NMR spectra produced at around 2.2 ppm and 3.3 ppm respectively. All samples were run in deuterated dichloromethane ( $\text{CD}_2\text{Cl}_2$ ) with a solvent peak at 5.32 ppm.

Diphenidine contains thirteen aliphatic protons, ten of which come from the aliphatic piperidine ring. The remaining three aliphatic protons come from the chiral centre proton and the two protons on the adjacent carbon. 8 of the 10 piperidine protons can be seen in the diphenidine spectra between 1.27 ppm – 3.47 ppm, with some overlap of peaks making splitting patterns hard to distinguish. The remaining two protons in the piperidine ring can be seen at 3.40 ppm and 3.57 ppm. All protons in the piperidine ring clearly seem to exist in different chemical environments due to the differences in chemical shifts with most peaks showing multiplicity in the splitting. This could be due to the rotation of the compound and the interaction that the protons may experience from the nearby aromatic groups and potential induced magnetic fields.

The piperidine protons were all linked together using the 2D Correlation Spectroscopy (COSY) NMR experiment, as all the protons in this piperidine ring showed coupling to one another where appropriate. Protons adjacent to the nitrogen showed coupling to two other protons as well as the amine proton. All other protons in the ring showed coupling to four other protons due to two lots of  $\text{CH}_2$  groups on either side. Due to some aliphatic protons bonded to the same carbon having different chemical shifts and chemical environments, a HMQC experiment was performed in order to confirm the coupling shown in the COSY experiment. The peaks at 3.46 ppm and 3.99 ppm represent the  $\text{CH}_2$  group, on the carbon adjacent to the chiral centre carbon, and is shown by both  $^1\text{H}$  NMR peaks showing coupling to the same carbon in the HMQC and coupling to the proton at 4.25 ppm in the COSY experiment, which represents the chiral centre proton.

All aromatic peaks fall between 7 ppm and 8 ppm and integrate to 10 protons which fits with the proposed structure of diphenidine with six peaks present due to the symmetrical nature of the aromatic regions. The peak representing the proton bonded to the nitrogen in the amine is present at 12.59 ppm as a singlet peak.

The main significant peak that is produced in the three methoxyphenidine derivatives (**13b–13d**, figure 64), that provides a clear difference to the diphenidine spectra is the methoxy substituted group on the phenyl ring that is shown through the singlet peak at 3.80 ppm in the three spectra with an integration of 3 protons. The main difference between the three methoxyphenidine regioisomers comes in the aromatic region (figure 65). The 2-MXP isomer appears to produce a difference with the chiral proton, compared to diphenidine, with the splitting pattern changing from a doublet of doublets to a broad singlet, possibly caused by coupling to the OCH<sub>3</sub> group with rotation. All three compounds have 9 aromatic protons, compared to the 10 of diphenidine, with the 2-MXP isomer having an individual peak at 7.75 ppm, which will be the proton adjacent to the carbon bonded to the OCH<sub>3</sub> group. The 3-MXP spectra also contains more peaks in the aromatic region compared to that of the 4-MXP due to the non-symmetrical nature of the phenyl group in the 3-MXP compound.

The three-trifluoromethoxyphenidine regioisomers (**13e–13g**, figure 66 – figure 67) <sup>1</sup>H NMR spectra appears very similar to the methoxyphenidine spectra. There is no clear difference with the aliphatic peaks and both sets of regioisomers contain nine aromatic protons, however there is no OCH<sub>3</sub> peak as this is replaced by the OCF<sub>3</sub> group and doesn't produce a signal in the <sup>1</sup>H-NMR spectrum. In order to show this substituent group is present, a <sup>19</sup>F NMR spectrum was obtained. The resulting <sup>19</sup>F chemical shifts are reported in Table 255. It is not possible to distinguish between the 3' and 4' positional isomers using just the fluorine signals, however the 2-TFMXP isomers provides a distinguishable signal.



**Table 25:**  $^{19}\text{F}$  NMR chemical shifts for the three trifluoromethoxyphenidine regioisomers (**13e** – **13g**) run in DMSO

Sample	Abbreviation	$^{19}\text{F}$ Chemical Shift (ppm)
2'-trifluoromethoxyphenidine	2-TFMXP	-57.47
3'-trifluoromethoxyphenidine	3-TFMXP	-58.82
4'-trifluoromethoxyphenidine	4-TFMXP	-58.69

The 2,3,4-trimethoxyphenidine (**13h**, mescphenidine, figure 68 – figure 69) compound provides a significant difference in the proton spectra through the singlet peak at 3.91 ppm that represents the nine  $\text{OCH}_3$  protons present in the same chemical environment. There is a slight shift in the chemical shifts of some of the aliphatic protons within the piperidine ring due to the difference in electron density caused by the new substituted methoxy groups. However, this is not significant enough to distinguish between mescphenidine and diphenidine. Mescphenidine also only contains seven aromatic protons compared to the ten of diphenidine and the nine of the MXP regioisomers.

The two MDDP isomers (**13i**–**13j**, figure 68 – figure 69) shows a significant difference to the other diphenidine derivatives due to the two methylenedioxy protons and only having eight aromatic protons. The two  $\text{CH}_2$  protons present in the methylenedioxy substituted group can be seen at between 5.86 ppm – 5.97 ppm for the 2,3-MDDP isomer while the peak for the 3,4-MDDP isomer can be seen at 5.99 ppm. This matches previous literature for substances such as MDMA where the two methylenedioxy protons appear at 5.83 ppm.

The two naphthenidine isomers both contain the same aliphatic region as diphenidine and a number of its derivatives, however the main difference is the aromatic region as both isomers contain twelve aromatic protons and can be distinguished from one another, due to the difference in chemical environments that the protons exist (figure 70 – figure 71). A stacked image of the aromatic regions of naphthenidine show the clear difference between the two isomers (figure 62).

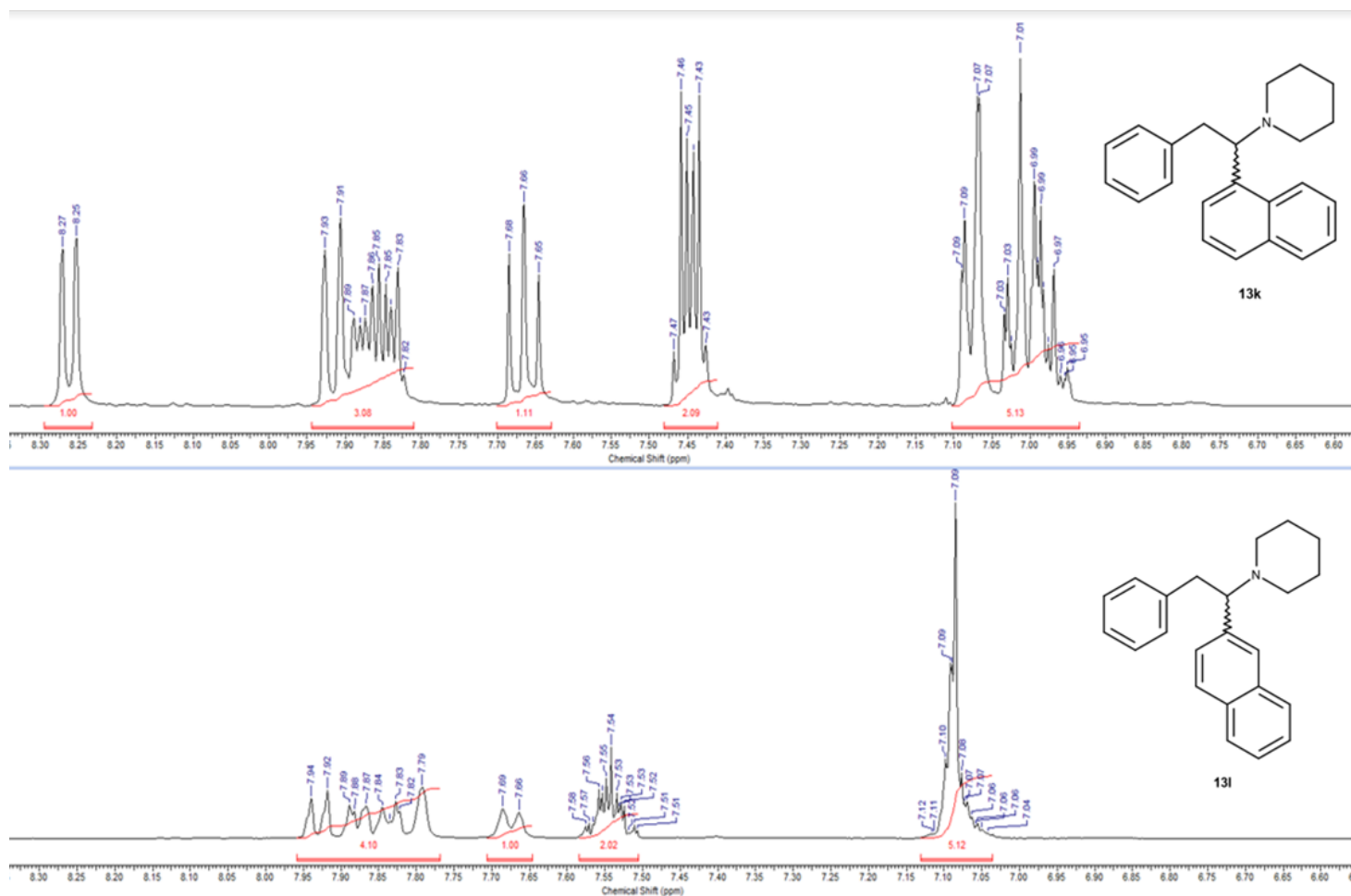


**Figure 62:** Stacked  $^1\text{H}$  NMR aromatic region for the two-naphthenidine regioisomers (NP, **13k** (top) – **13l** (bottom))

Finally, the IAS-013 compound is easily distinguishable based on its seven aromatic protons and the two  $\text{OCH}_3$  groups along with the  $\text{CH}_3$  group (figure 70 – figure 71). Three peaks, each representing three protons, at different chemical shifts, show this. This shows each group containing the three protons is in a different chemical environment and that no protons are on the neighbouring carbon of the benzene ring, due to each peak appearing as a singlet.

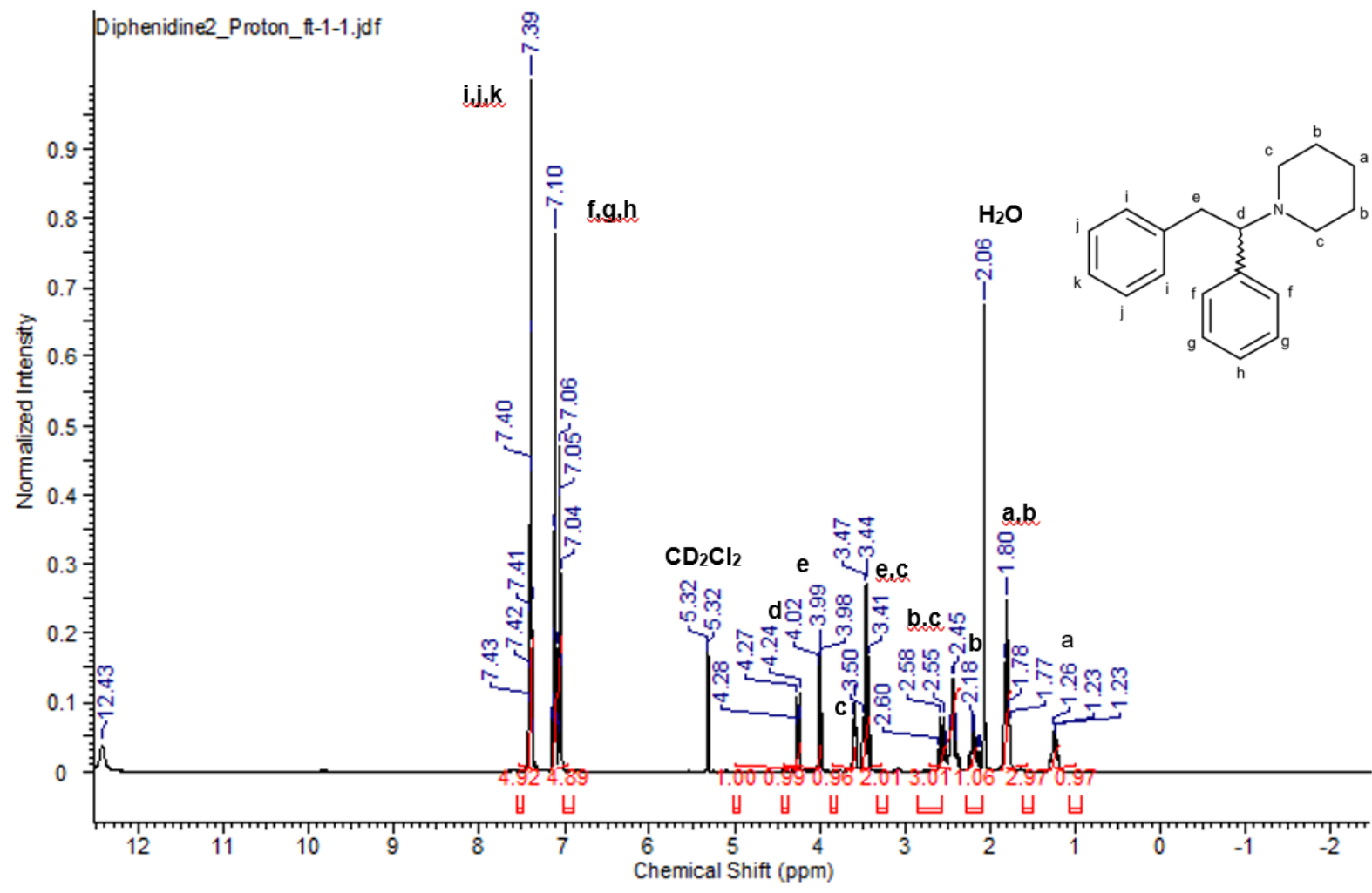
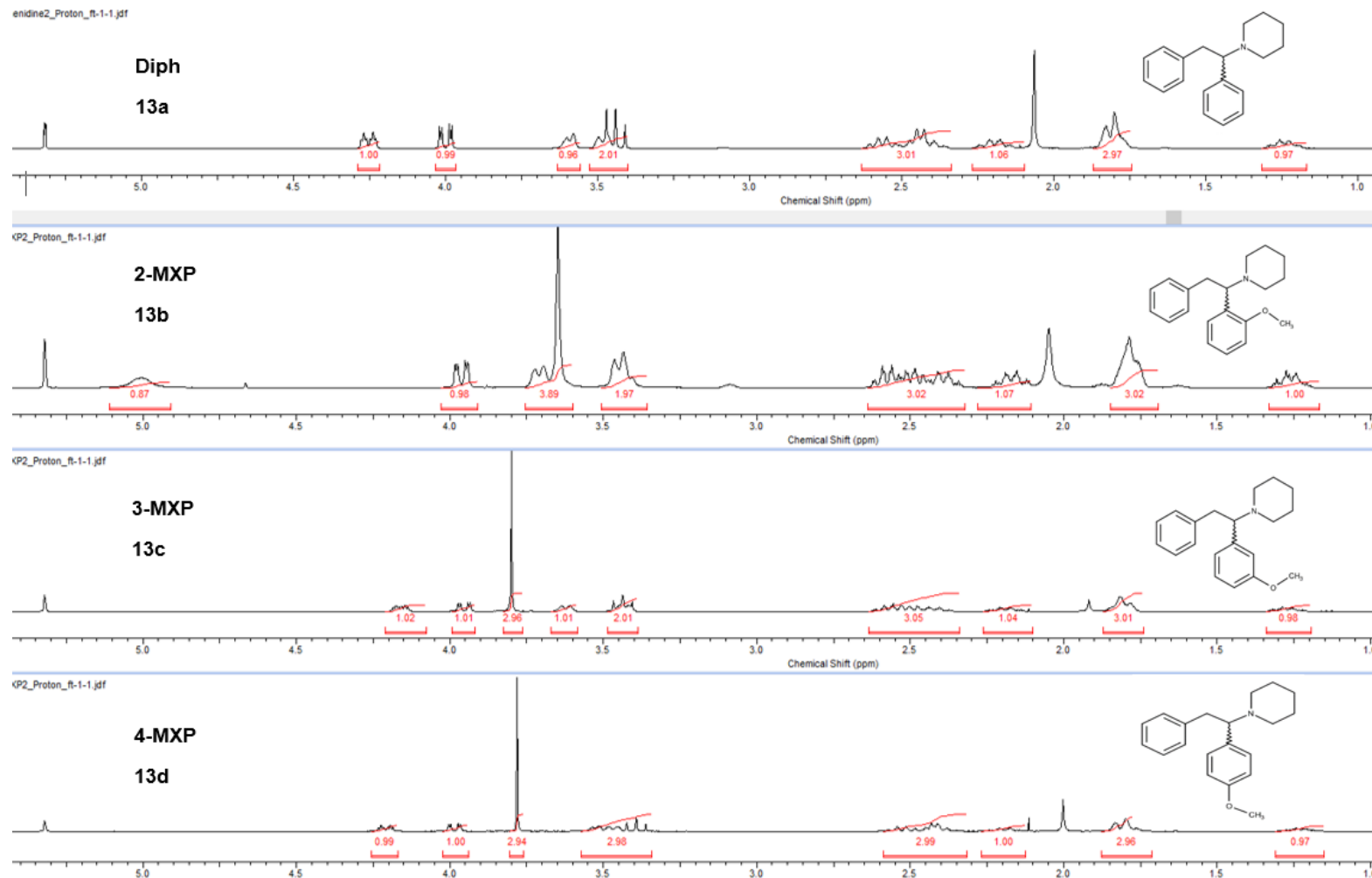
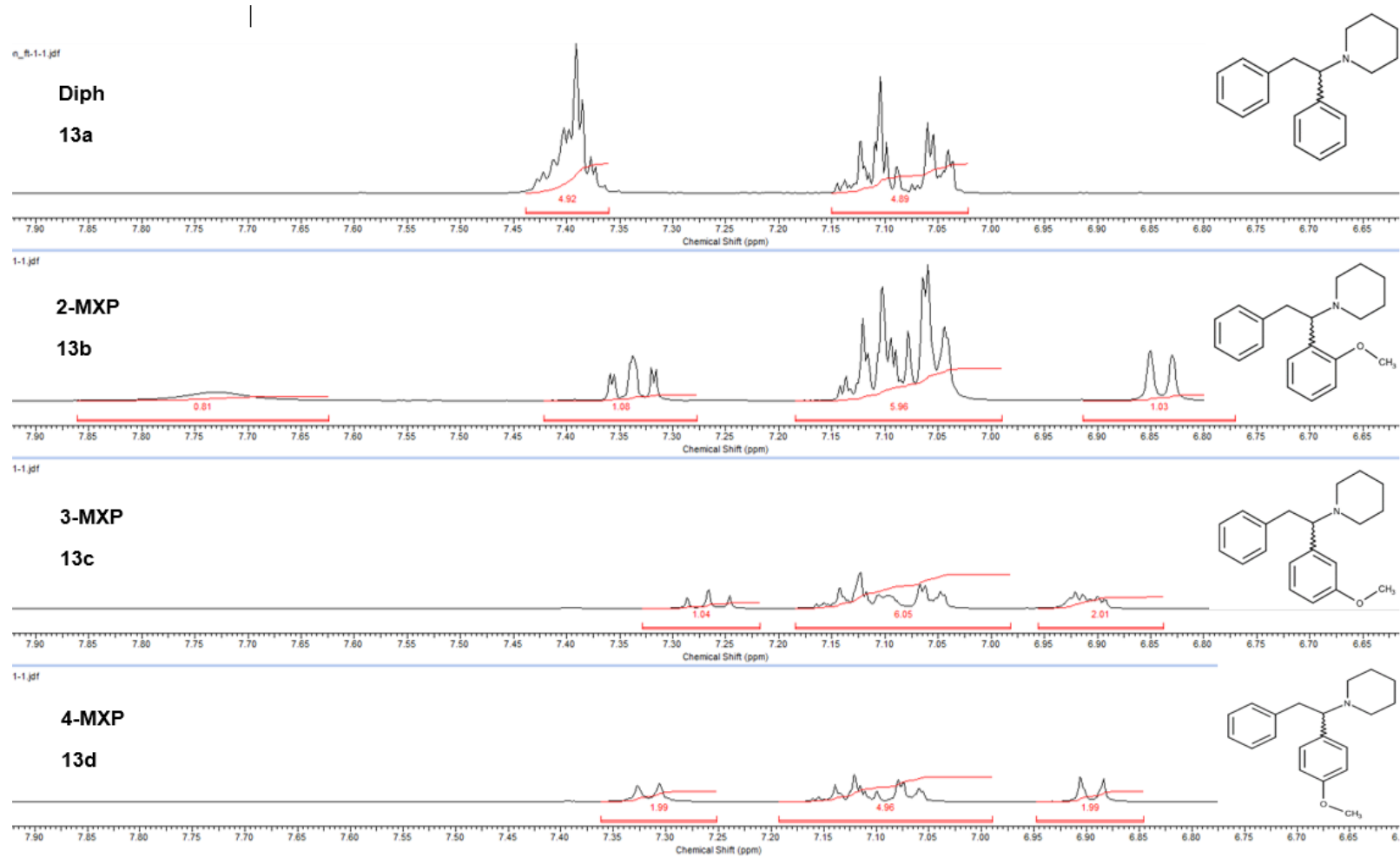


Figure 63: <sup>1</sup>H NMR (400 MHz, CD<sub>2</sub>Cl<sub>2</sub>) spectrum of diphenidine hydrochloride (13a)



**Figure 64:** Stacked <sup>1</sup>H NMR spectra for the aliphatic region of diphenidine (**13a**), 2-MXP (**13b**), 3-MXP (**13c**) and 4-MXP (**13d**)



**Figure 65:** Stacked <sup>1</sup>H NMR spectra for the aromatic region of diphenidine (**13a**), 2-MXP (**13b**), 3-MXP (**13c**) and 4-MXP (**13d**)

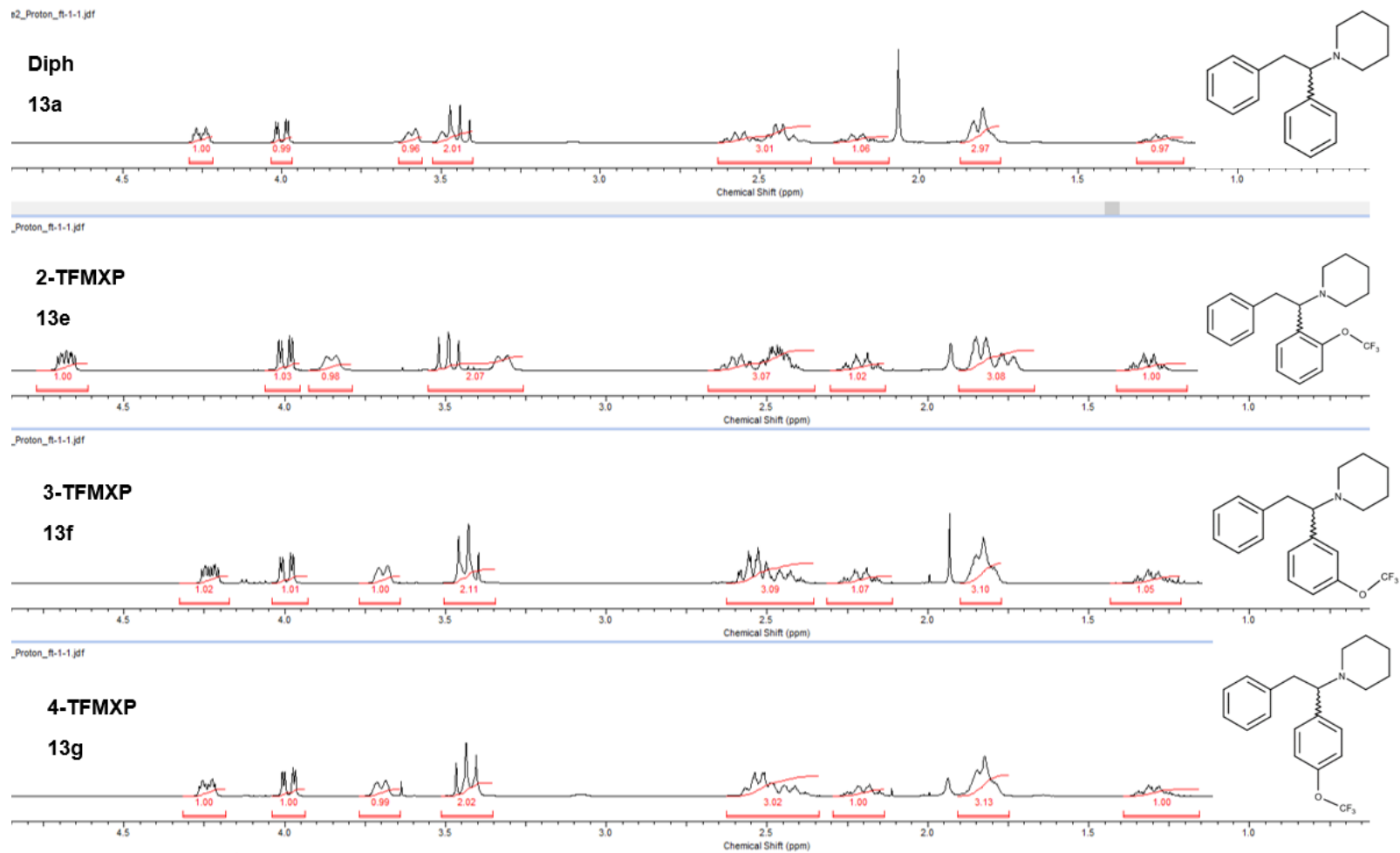


**Figure 66:** Stacked  $^1\text{H}$  NMR spectra for the aliphatic region of diphenidine (**13a**), 2-TFMXP (**13e**), 3-TFMXP (**13f**) and 4-TFMXP (**13g**)

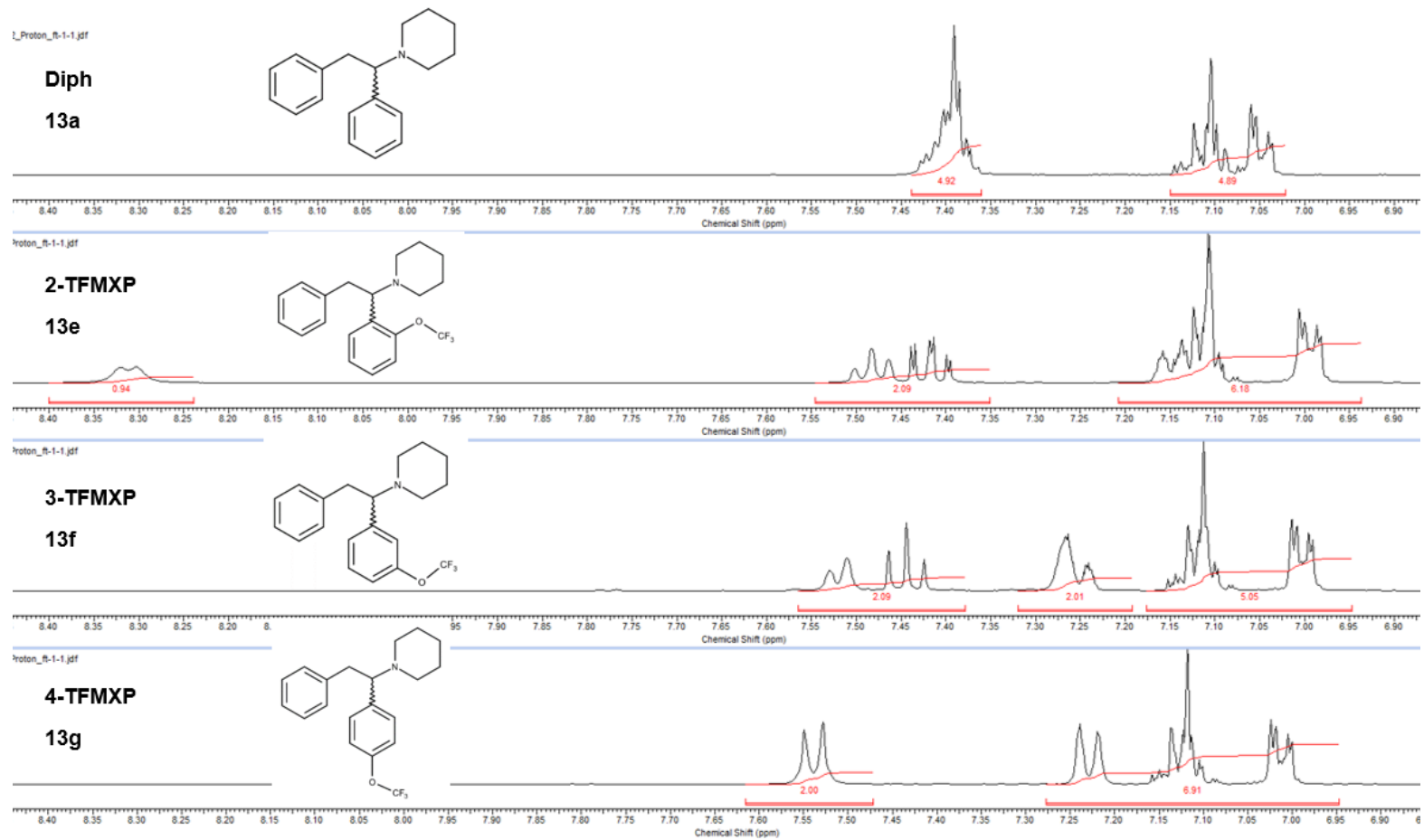


**Figure 67:** Stacked <sup>1</sup>H NMR spectra for the aromatic region of diphenidine (**13a**), 2-TFMXP (**13e**), 3-TFMXP (**13f**) and 4-TFMXP (**13g**)

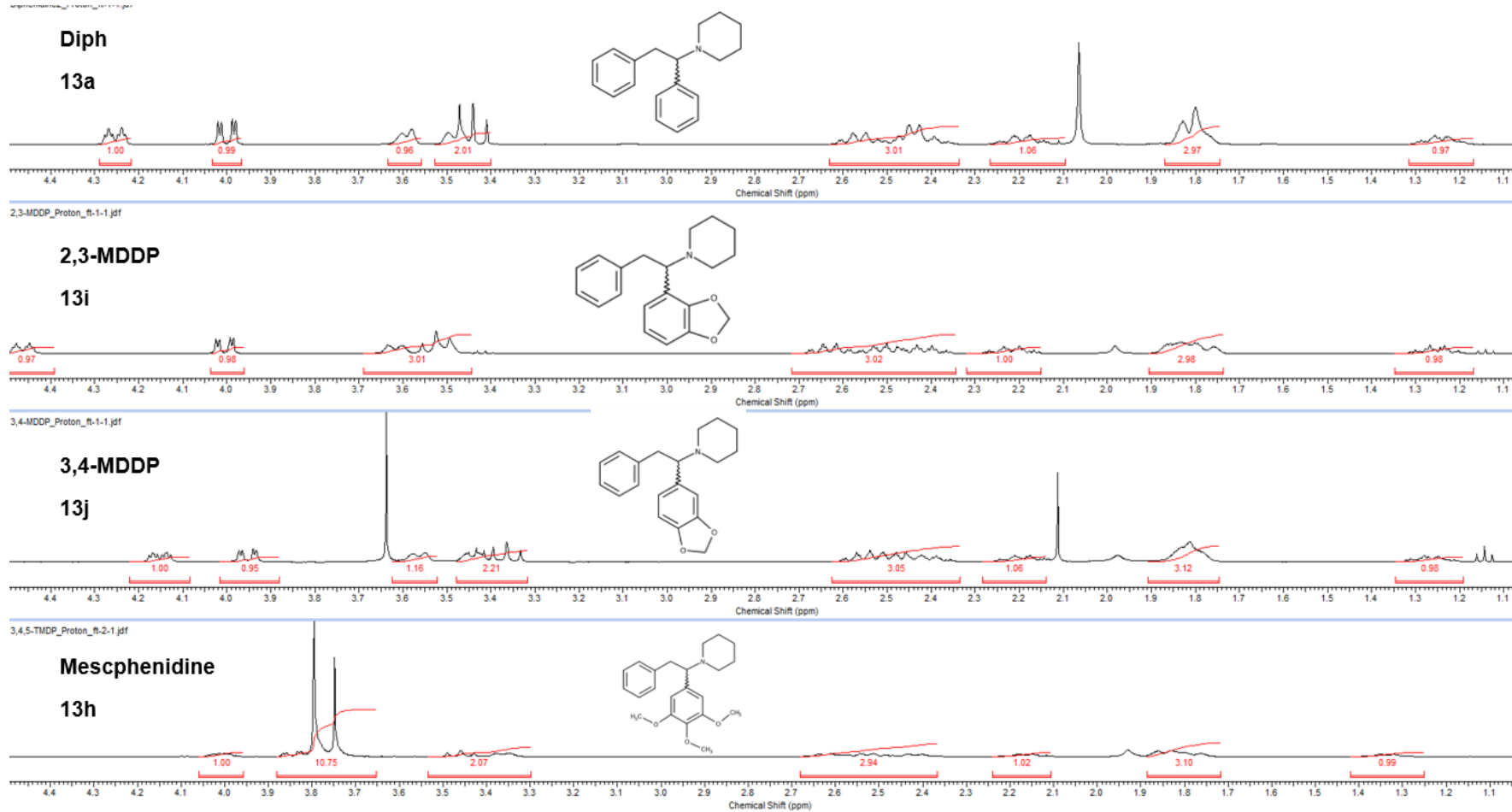


**Figure 68:** Stacked  $^1\text{H}$  NMR spectra for the aliphatic region of diphenidine (**13a**), 2,3-MDDP (**13i**), 3,4-MDDP (**13j**) and mescphenidine (**13h**)



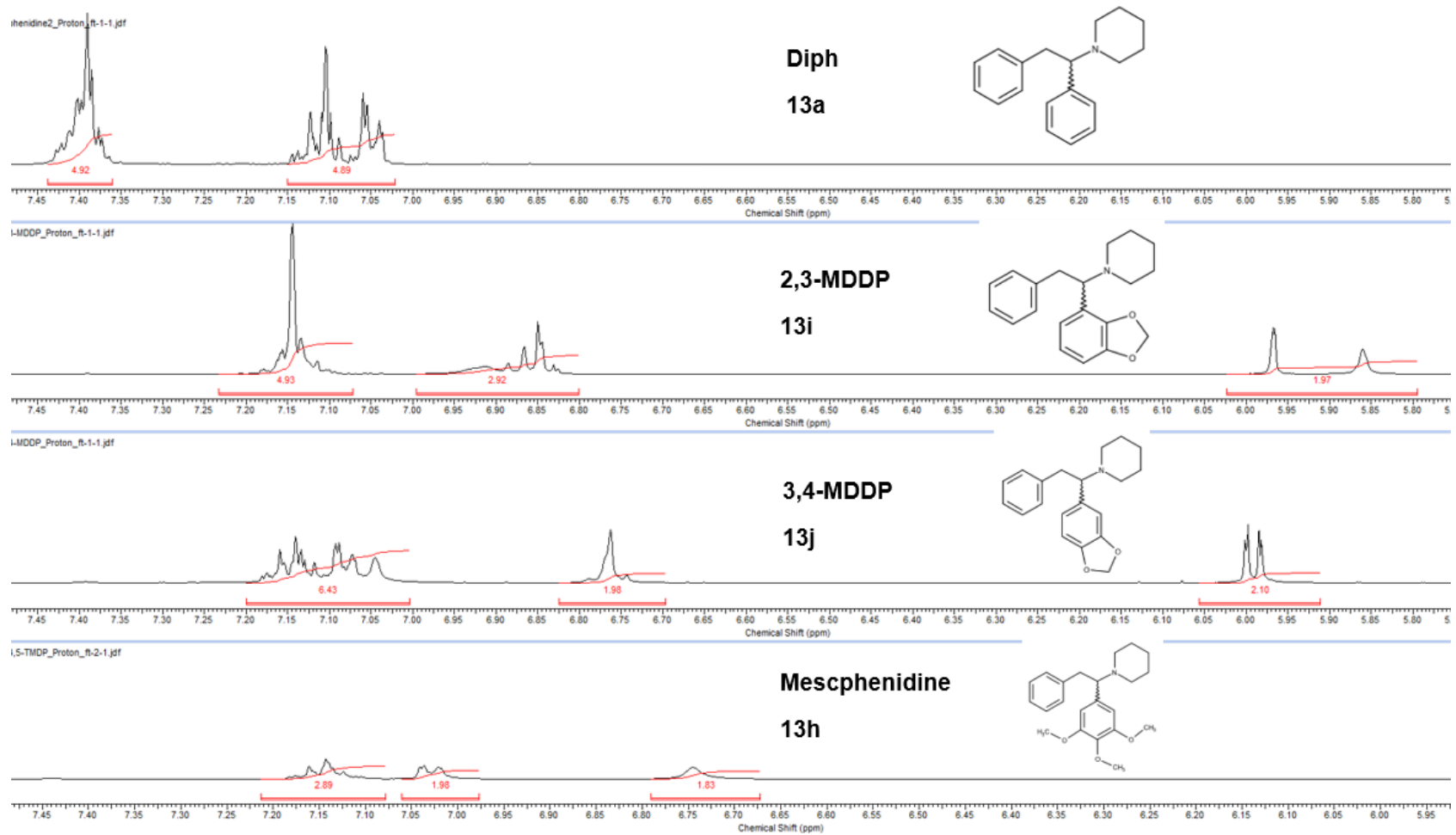


**Figure 69:** Stacked <sup>1</sup>H NMR spectra for the aromatic region of diphenidine (13a), 2,3-MDDP (13i), 3,4-MDDP (13j) and mescphenidine (13h)

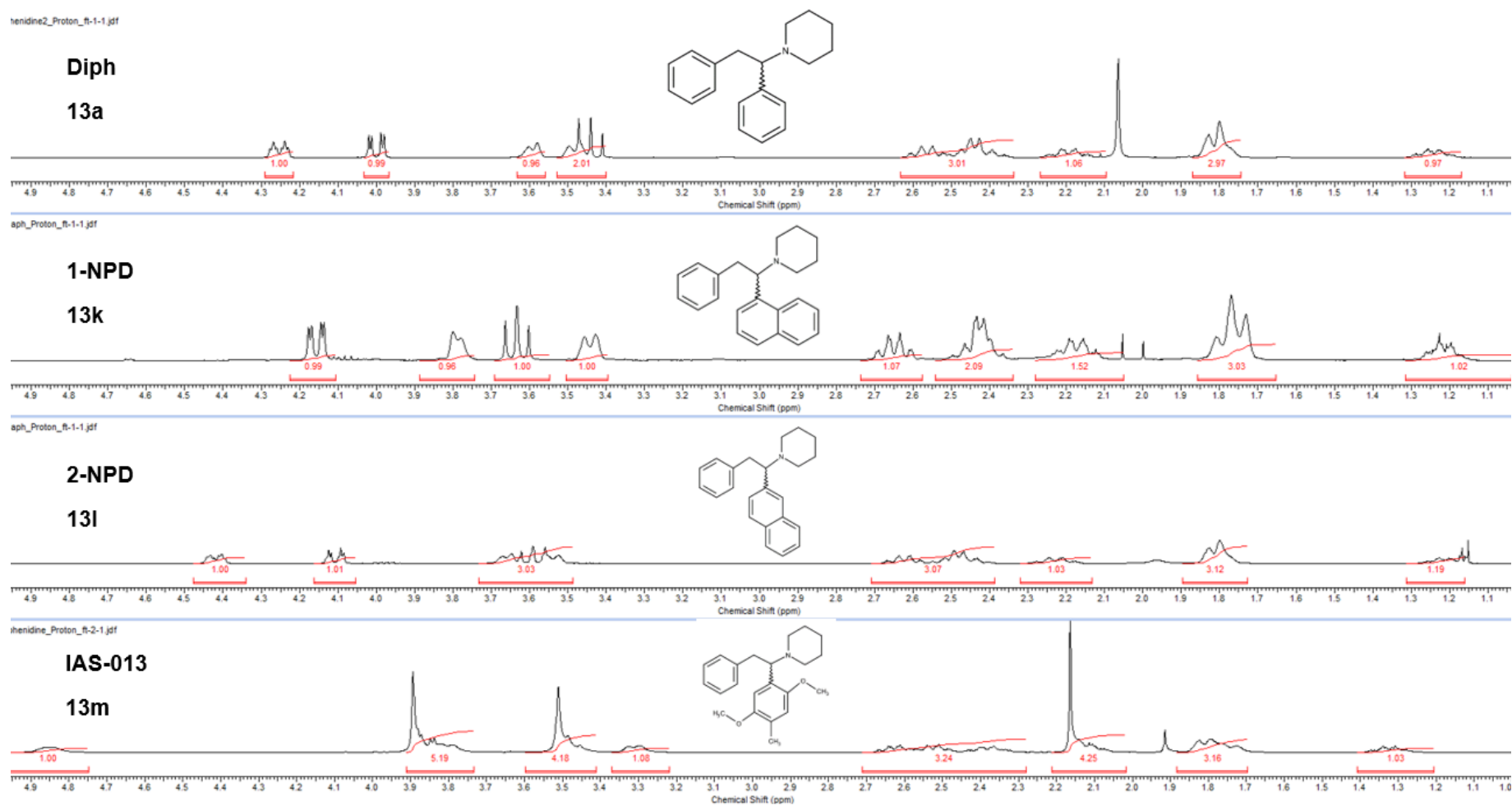


**Figure 70:** Stacked  $^1\text{H}$  NMR spectra for the aliphatic region of diphenidol (**13a**), 1-NPD (**13k**), 2-NPD (**13l**) and IAS-013 (**13m**)

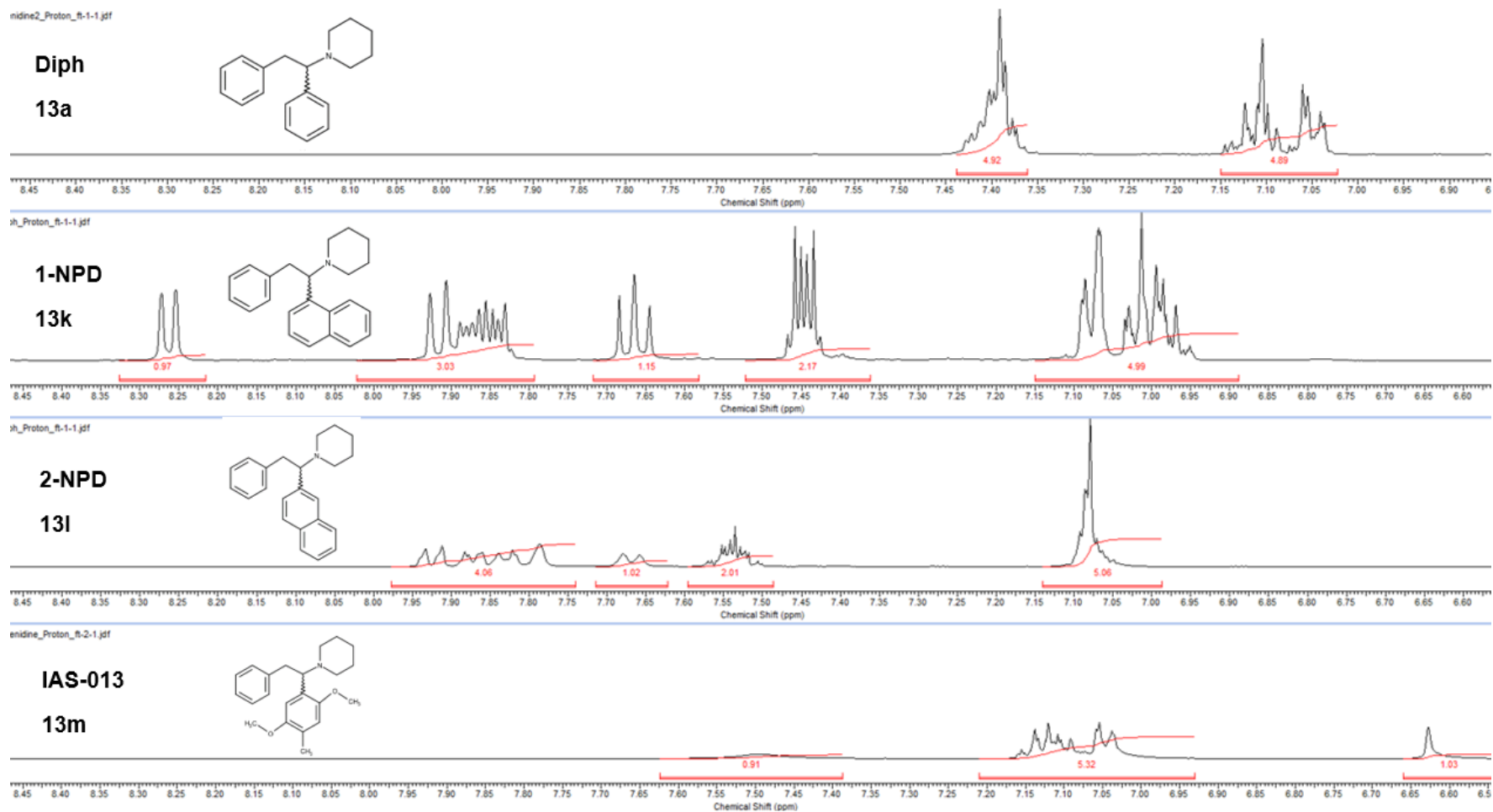
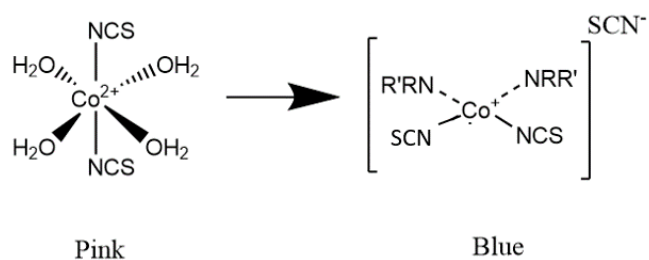


Figure 71: Stacked  $^1\text{H}$  NMR spectra for the aromatic region of diphenidine (**13a**), 1-NPD (**13k**), 2-NPD (**13l**) and IAS-013 (**13m**)

### 4.3. Presumptive Testing

The presumptive colour tests for all thirteen diphenidine derivatives (**13a-13m**) was carried out according to the United Nations recommended guidelines.<sup>118</sup> Literature regarding the presumptive testing of diphenidine and its substituted derivatives is limited, therefore a range of presumptive tests were applied to this study: (i) Marquis test; (ii) Mandelin test; (iii) Scott's test and (iv) Zimmerman test. The preparation of the reagents is detailed in the experimental section (section 2.2). A solution of each reference standard (10 mg mL<sup>-1</sup>) was prepared in deionised water and a couple of drops placed into a dimple well of a spotting tile. The required presumptive test reagent (1-2 drops) was then added and any colour change upon initial addition of the reagents were noted and observations were made again after a five minute time period (Table 26).

Marquis, Mandelin, Scott's and Zimmerman's reagents were the only test to provide a positive reaction and noticeable colour change when reacted with sample solutions. All samples were dissolved in deionised water in order to yield desired colour changes, however, methanol was initially tried but didn't produce a colour change to the solution. Instead, evaporation of the methanol and sample was observed with a colour change beginning on the outer walls of the wells, rather than in solution. The order of addition also appeared vital as sample solution added to the test reagent yielded no colour change for any test. All diphenidine derivatives, that contain a tertiary amine, gave a positive reaction with the Marquis and Scott's reagents, however, a gradual loss of intensity of the initial colour with Marquis reagent was observed over the five minute period. In the case of the Scott's test, which is employed in the screening of cocaine, the coloured products may result from the coordination of the tertiary amines to the pink Co(II) octahedral complex affording the blue Co(II) tetrahedral complex.<sup>146</sup>(Figure 72)



**Figure 72:** Proposed scheme for the colour change in the Scott's reagent

The colour change that is observed when the Marquis reagent is used, may be afforded to the reaction of the drug molecules with sulfuric acid, in a similar way to that of the mechanism of MDMA (figure 73).<sup>3</sup> The gradual loss of colour over 5 minutes may suggest that this product is not stable under the test conditions used.

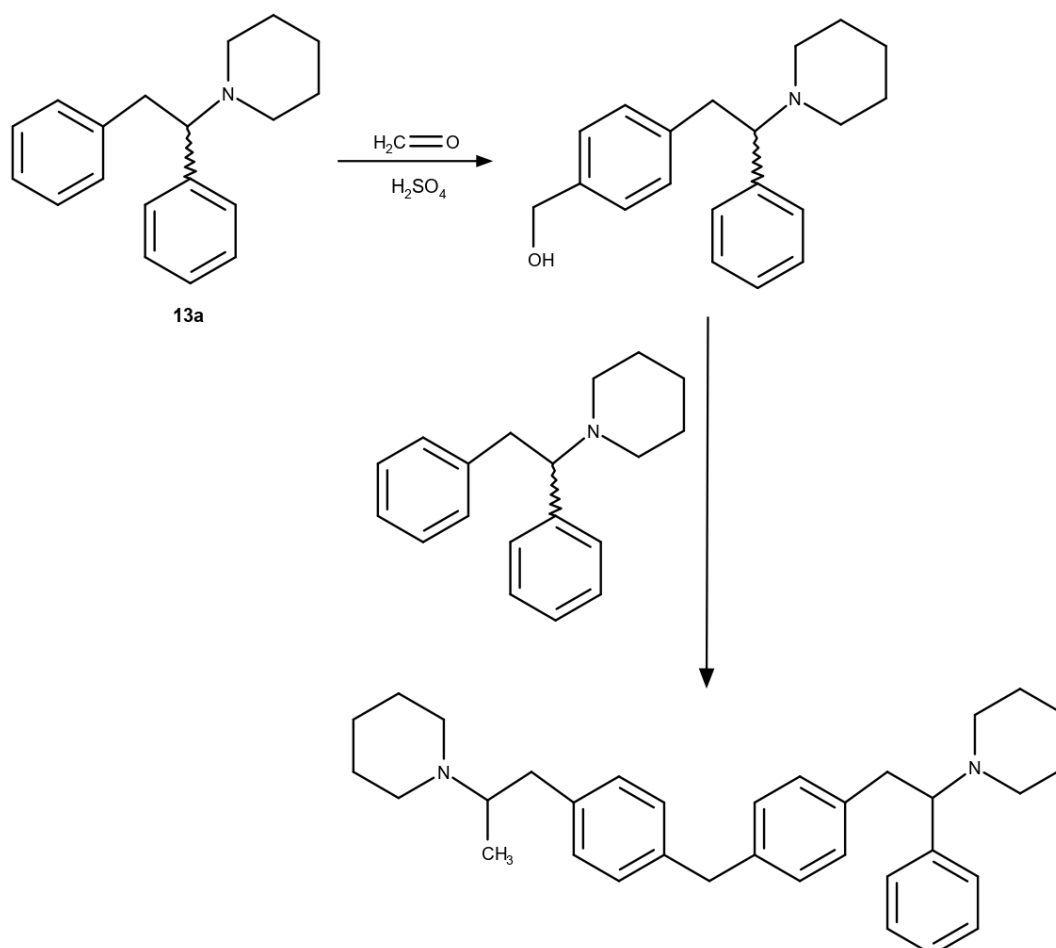


**Figure 73:** Proposed reaction scheme for the Marquis reagent with diphenidine

The Mandelin reagent (acidified ammonium metavanadate) gave a positive reaction to all diphenidine derivatives, except for both the 3-

trifluoromethoxydiphenidine (**13f**) and 4-trifluoromethoxydiphenidine (**13g**). Due to the lack of literature on both diphenidines and their presumptive testing, there is no readily available explanation as to why there is a lack of response for both **13f** and **13g**. The slightly different coloured products obtained with the MXP isomers [2-MXP (**13b**, dark yellow); 3-MXP (**13c**, brown) and 4-MXP (**13d**, pale yellow) respectively] could be potentially used to discriminate between these three positional isomers.



**Figure 74:** Reaction scheme for the positive colour change in the Mandelin reagent

When the diphenidine derivatives are tested against the Zimmerman reagent a white or pale yellow precipitate forms. This precipitate is believed to be the free-base form of the corresponding tertiary amines, which are insoluble in water, rather than a positive reaction of the substrates with the Zimmerman test.<sup>147</sup> A positive test for the Zimmerman reagent usually relies on the presence of an activated methylene group, which can react with 1,3-dinitrobenzene to give a positive colour change based on the Meisenheimer complex formed. This reaction has been previously reported for the identification of cathinone derivatives.<sup>143</sup>

The observed colour changes reported for all diphenidine samples (Table 26) indicate that Scott's reagent could provide a simple and rapid test for these materials. Cocaine also forms a blue Co(II) tetrahedral complex with Scott's reagent, however, it does not give a positive reaction with the Marquis reagent. Therefore, in order to identify diphenidine samples the two presumptive tests (Marquis and Scott's) should be employed together to discriminate between cocaine and these novel diphenidine-derived NPS. Presumptive testing provides difficulty in separating the isomers as colour changes would appear different to different observers and all positional isomers having identical UV  $\lambda_{\text{max}}$  values when analysed through UV analysis.

**Table 26:** Colour changes observed with presumptive test reagents for 13 diphenidine derivatives (**13a-13m**) immediately after addition and after 5 minutes of addition

	Marquis		Mandelin		Scott's		Zimmerman	
	Immediate colour change	Colour after 5 minutes	Immediate colour change	Colour after 5 minutes	Immediate colour change	Colour after 5 minutes	Immediate colour change	Colour after 5 minutes
<b>13a</b>	orange	pale brown	dark yellow	yellow green	blue	blue	- pale yellow ppt	- pale yellow ppt
<b>13b</b>	pink	colourless	dark yellow	dark yellow	blue	blue	- pale yellow ppt	- pale yellow ppt
<b>13c</b>	red brown	colourless	brown	brown	blue	blue	- pale yellow ppt	- pale yellow ppt
<b>13d</b>	pale pink	colourless	pale yellow	pale yellow	blue	blue	- pale yellow ppt	- pale yellow ppt
<b>13e</b>	pale yellow	colourless	light yellow	light yellow	blue	blue	- white ppt	- white ppt
<b>13f</b>	orange	colourless	-	-	blue	blue	- white ppt	- white ppt
<b>13g</b>	orange	colourless	-	-	blue	blue	- pale yellow ppt	- pale yellow ppt
<b>13h</b>	pale orange	pale pink	pale green	pale green	blue	blue	- pale yellow ppt	- pale yellow ppt
<b>13i</b>	pale brown	colourless	brown	brown	blue	blue	- pale yellow ppt	- pale yellow ppt
<b>13j</b>	purple	colourless	brown	brown	blue	blue	- pale yellow ppt	- pale yellow ppt
<b>13k</b>	beige	pale brown	dark yellow	brown	blue	blue	- pale yellow ppt	- pale yellow ppt
<b>13l</b>	grey blue	colourless	brown	brown	blue	blue	- pale yellow ppt	- pale yellow ppt
<b>13m</b>	pale orange	colourless	green/yellow	green/yellow	blue	blue	- pale yellow ppt	- pale yellow ppt

#### 4.4. Thin Layer Chromatography

It has previously been demonstrated by McLaughlin *et al.* that a specific test using TLC has been developed for the analysis of the three MXP isomers (**13b-13d**). All 13 diphenidine derivatives were analysed using TLC and all isomers produced an identical blood-red coloured spot when viewed with modified Dragendorff-Ludy-Tenger reagent.<sup>102</sup> The examination of the Retention Factors ( $R_f$ ) demonstrates separation of the compounds based upon this measure, particularly of the three MXP isomers (2-MXP (**13b**), 3-MXP (**13c**) and 4-MXP (**13d**):  $R_f = 0.76, 0.87$  and  $0.79$  respectively) – which correlates with previously reported data. Separation is slightly less clear-cut for other isomeric derivatives: 2,3-MDDP (**13i**,  $R_f = 0.78$ ) vs. 3,4-MDDP (**13j**,  $R_f = 0.84$ ); 1-NPD (**13k**,  $R_f = 0.91$ ) vs. 2-NPD (**13l**,  $R_f = 0.85$ ) and in the case of the TFMXP isomers (**13e – 13g**) the three compounds co-eluted. The TLC data for each compound, including their  $R_f$  and Relative Retention Factor ( $RR_f$ ), with respect to diphenidine (**13a**), are presented in Table 27.



**Table 27:** Thin Layer Chromatography data for diphenidine (**13a**) and its substituted derivatives (**13b-13m**)

	Compound name	Spot colour under UV light (254 nm)	Spot colour after staining with modified Dragendorff-Ludy-Tenger Reagent	R <sub>f</sub> value	RR <sub>f</sub> <sup>a</sup>
<b>13a</b>	Diphenidine	Black spot	Blood-red spot	0.85	1.00
<b>13b</b>	2-methoxyphenidine	Black spot	Blood-red spot	0.76	0.89
<b>13c</b>	3-methoxyphenidine	Black spot	Blood-red spot	0.87	1.02
<b>13d</b>	4-methoxyphenidine	Black spot	Blood-red spot	0.79	0.95
<b>13e</b>	2-trifluoromethoxyphenidine	Black spot	Blood-red spot	0.94	1.11
<b>13f</b>	3-trifluoromethoxyphenidine	Black spot	Blood-red spot	0.93	1.09
<b>13g</b>	4-trifluoromethoxyphenidine	Black spot	Blood-red spot	0.92	1.08
<b>13h</b>	Mescphenidine	Black spot	Blood-red spot	0.84	0.99
<b>13i</b>	2,3-(Methylenedioxy)diphenidine	Black spot	Blood-red spot	0.78	0.92
<b>13j</b>	3,4-(Methylenedioxy)diphenidine	Black spot	Blood-red spot	0.84	0.99
<b>13k</b>	1-Naphthenidine	Black spot	Blood-red spot	0.91	1.07
<b>13l</b>	2-Naphthenidine	Black spot	Blood-red spot	0.85	1.00
<b>13m</b>	IAS-013	Black spot	Blood-red spot	0.74	0.87

**Key:** <sup>a</sup> Relative Retention Factor (RR<sub>f</sub>) with respect to diphenidine (**13a**)

## 4.5. Gas Chromatography – Mass Spectrometry

The qualitative GC-MS method used required an extremely straightforward dissolution of the samples in methanol ( $1 \text{ mg mL}^{-1}$ ) followed by direct injection into the instrument. No derivatisation step was required. All thirteen diphenidine derivatives were resolved from each other and from three common adulterants: caffeine, benzocaine and procaine. An exemplar chromatogram is presented in Figure 75.

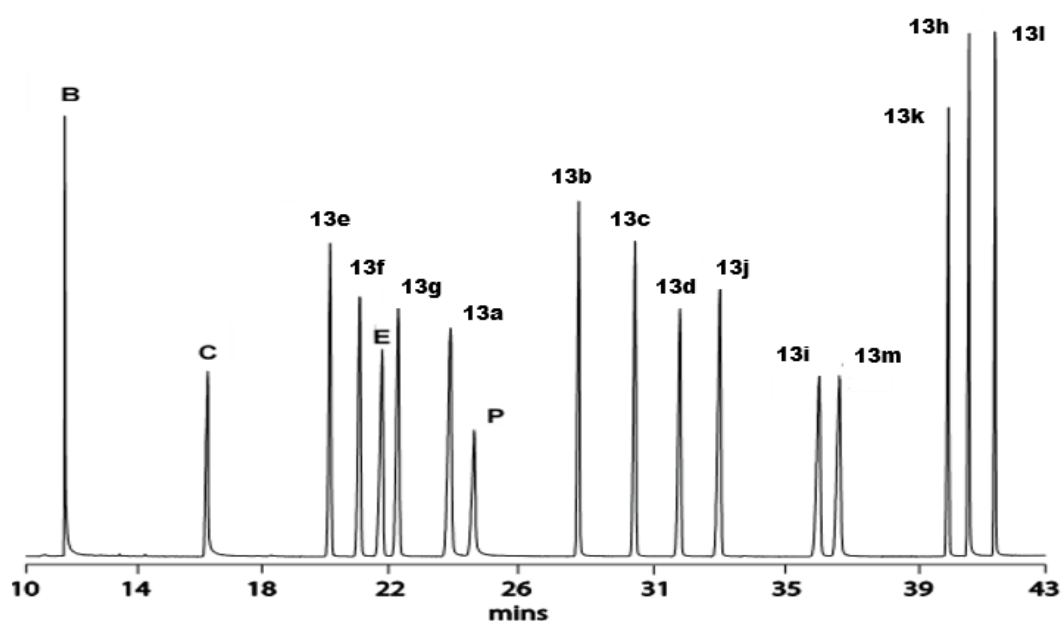


**Figure 75:** GC-MS chromatogram demonstrating the separation of the thirteen diphenidine derivatives (**13a–13m**) along with the relevant adulterants: benzocaine (**B**); caffeine (**C**) and procaine (**P**), with eicosane (**E**) added as an internal standard.

Research has been on going into the possibilities of utilising GC-MS for the separation of diphenidine and the methoxphenidine regioisomers mainly in cases where solid samples have been seized at a crime scene. However, the issue with these reports is the lack of a validated quantitative chromatographic method (or limits of detection and quantification), which provides a general screening tool. This prevents the quantification of component psychoactive substances detected in forensic bulk samples.

Calibration standards were prepared and all thirteen substituted diphenidines demonstrated a linear response ( $r^2 = 0.996 - 0.998$ ) over a  $25.0 - 250.0 \mu\text{g mL}^{-1}$  range with satisfactory repeatability ( $\text{RSD} = 1.29 - 14.02\%$ ,  $n = 6$ ). The limits of detection and quantification for the analytes were determined, based on the standard deviation of the response and the slope, as being  $4.23 - 5.99$  and  $12.83 - 17.51 \mu\text{g mL}^{-1}$  respectively. The method was also suitable for the detection and quantification of the three common adulterants (benzocaine, caffeine and procaine), demonstrating linear response ( $r^2 = 0.996 - 0.998$ ) over the same concentration range with reasonable repeatability ( $\text{RSD} = 1.80 - 10.41\%$ ,  $n = 6$ ). The limits of detection and quantification were also determined, for the adulterants, and found to be  $5.97 - 11.82 \mu\text{g mL}^{-1}$  and  $18.10 - 35.82 \mu\text{g mL}^{-1}$  respectively. The validation parameters for the method are summarised in Table 28. The accuracy (percentage recovery study) of the assay was determined from spiked samples prepared in triplicate at three levels over a range of  $80 - 120\%$  of the target concentration ( $100 \mu\text{g mL}^{-1}$ ). Though the repeatability ( $\% \text{RSD}$ ) of the method was significantly lower than expected, which is believed to be a result of the manual injection of the calibration standards, the percentage recovery ( $\% \text{ assay}$ ) and  $\% \text{RSD}$  calculated for each of the three replicate samples demonstrated excellent recoveries for all thirteen analytes within the desired concentration range. All results are within acceptable limits ( $100 \pm 2\%$ ) and the validated GC-MS method was deemed suitable for the analysis of street samples.

The use of GC-MS also facilitated the visualization of the mass spectral data for each individual compound and these are presented in figure 82 and figure 83. For all compounds a peak at a mass to charge ratio  $m/z$  of 91 is present,

which represents the benzyl cation, produced from the phenyl group being separated and any substituent group removed (Figure 76).

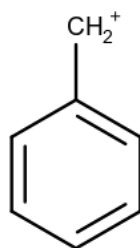


**Figure 76:** structure of the benzyl cation

All diphenidine derivatives have a similar structural backbone to diphenidine and therefore the fragmentation patterns for all derivatives can be compared to that of diphenidine. Diphenidine (**13a**) has a base peak of  $m/z = 174$ , which comes from the removal of the benzyl group to leave the piperidine ring and phenyl ring as shown in Figure 77. The secondary base peak in the diphenidine mass spectrum is then the benzyl cation mentioned earlier which comes from the further removal of the piperidine ring.

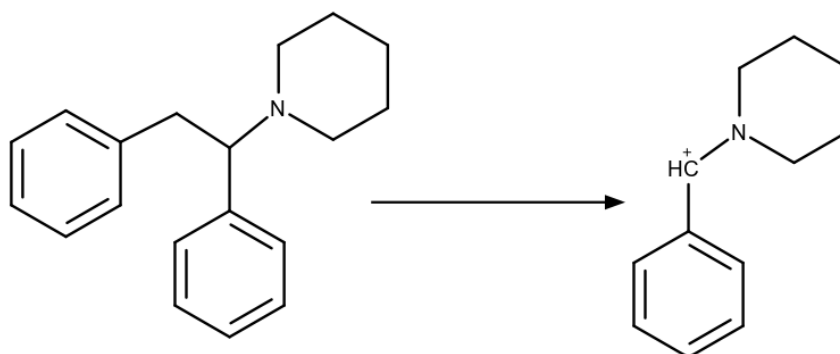


**Figure 77:** GC-MS fragmentation for diphenidine (**13a**) base peak

All other diphenidine derivatives fragment in a similar way to diphenidine with methoxphenidine and trifluoromethoxphenidine regioisomers losing the benzyl group before losing the piperidine ring to produce base and secondary peaks of  $m/z = 204$  and  $m/z = 121$  respectively for the MXP isomers and 258 and 175 respectively for the TFMXP isomers (Figure 78). The peak at  $m/z$  of 91 is present in both cases.

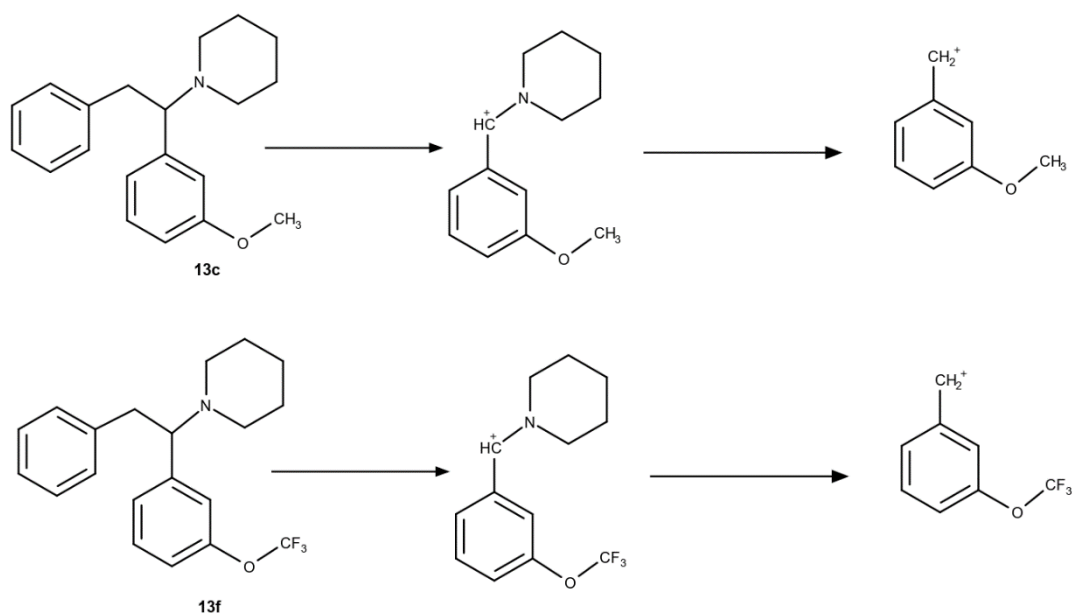


**Figure 78:** GC-MS fragmentation of the MXP (**13b–13d**) and TFMXP (**13e–13g**) regioisomers

The methylenedioxy and naphthyl derivatives of diphenidine also produce characteristic base and secondary peaks from the mass spectrometer with  $m/z$  values of  $m/z = 218$  and  $m/z = 136$  respectively for MDDP and  $m/z = 224$  and  $m/z = 141$  respectively for the NP regioisomers. The fragmentation ions can be seen in Figure 79.

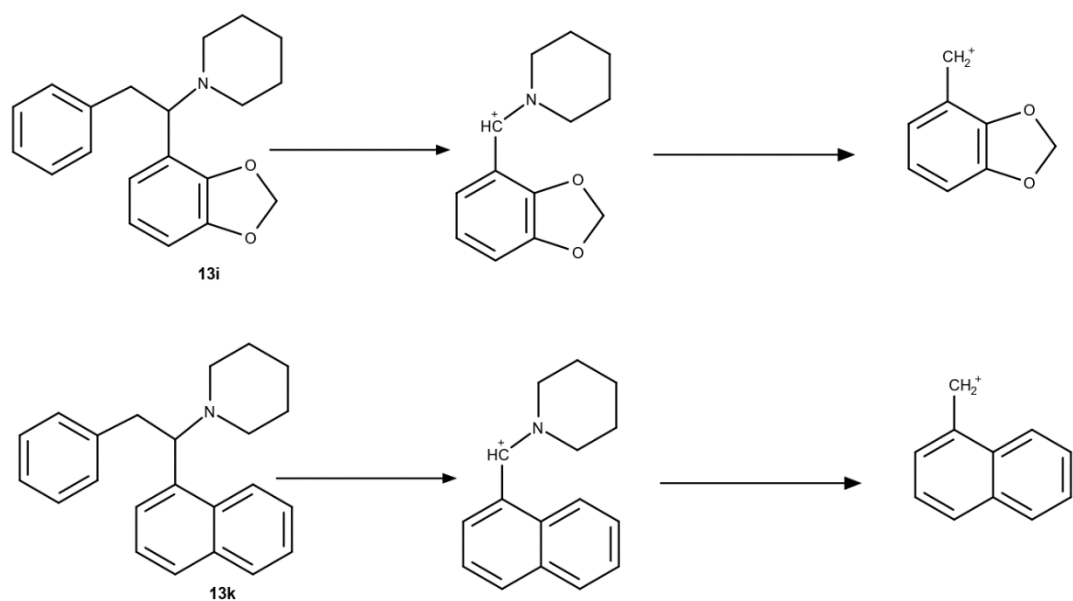


**Figure 79:** GC-MS fragmentation of the MDDP (**13i–13j**) and NP (**13k–13l**) regioisomers

The TMXP and IAS-013 compound are the only main difference to the fragmentation pattern observed by diphenidine and its other derivatives due to the removal of OCH<sub>3</sub> and CH<sub>3</sub> groups from the base peak ion. These produce smaller peaks in the mass spectra due to the instability of the ions created meaning the benzyl cation becomes the secondary base peak for these two compounds. The fragmentation pattern including the secondary base peak ion for both compounds can be seen in figure 80 and figure 81.

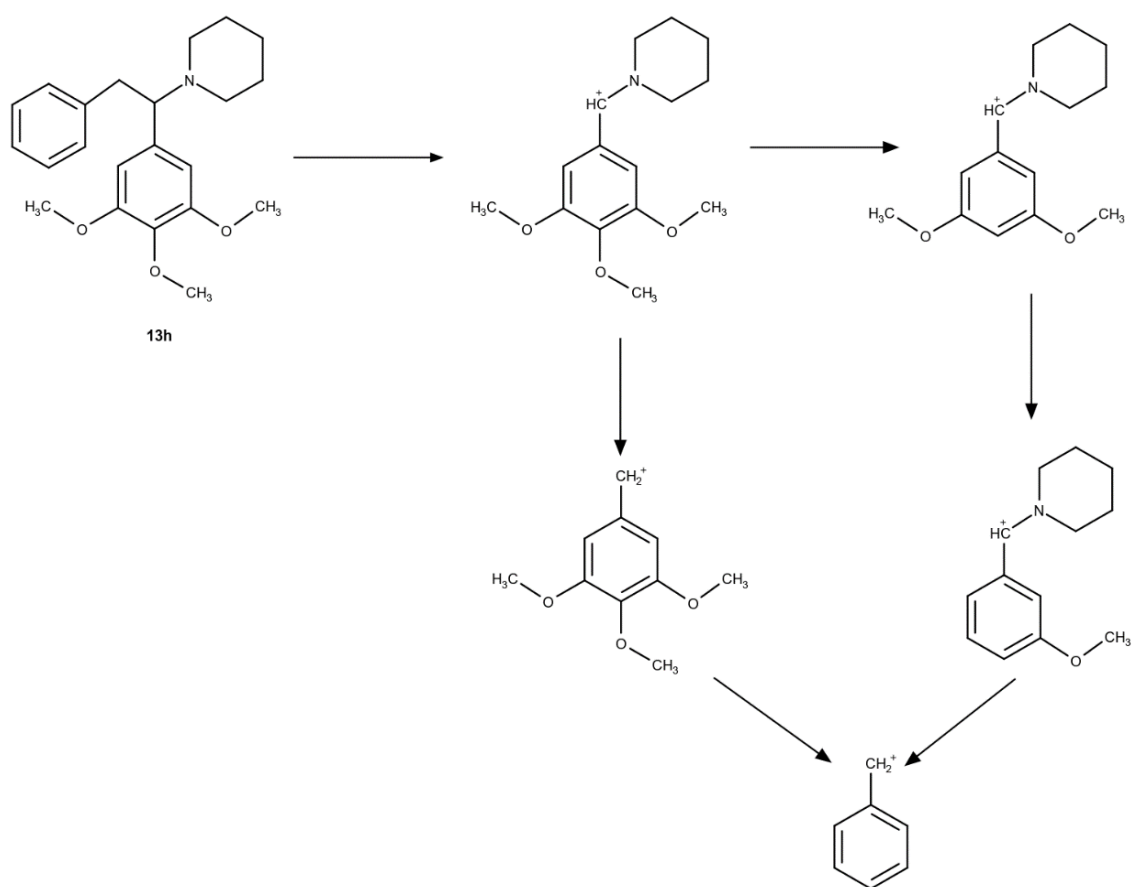


**Figure 80:** GC-MS fragmentation pattern for TMXP (13h)

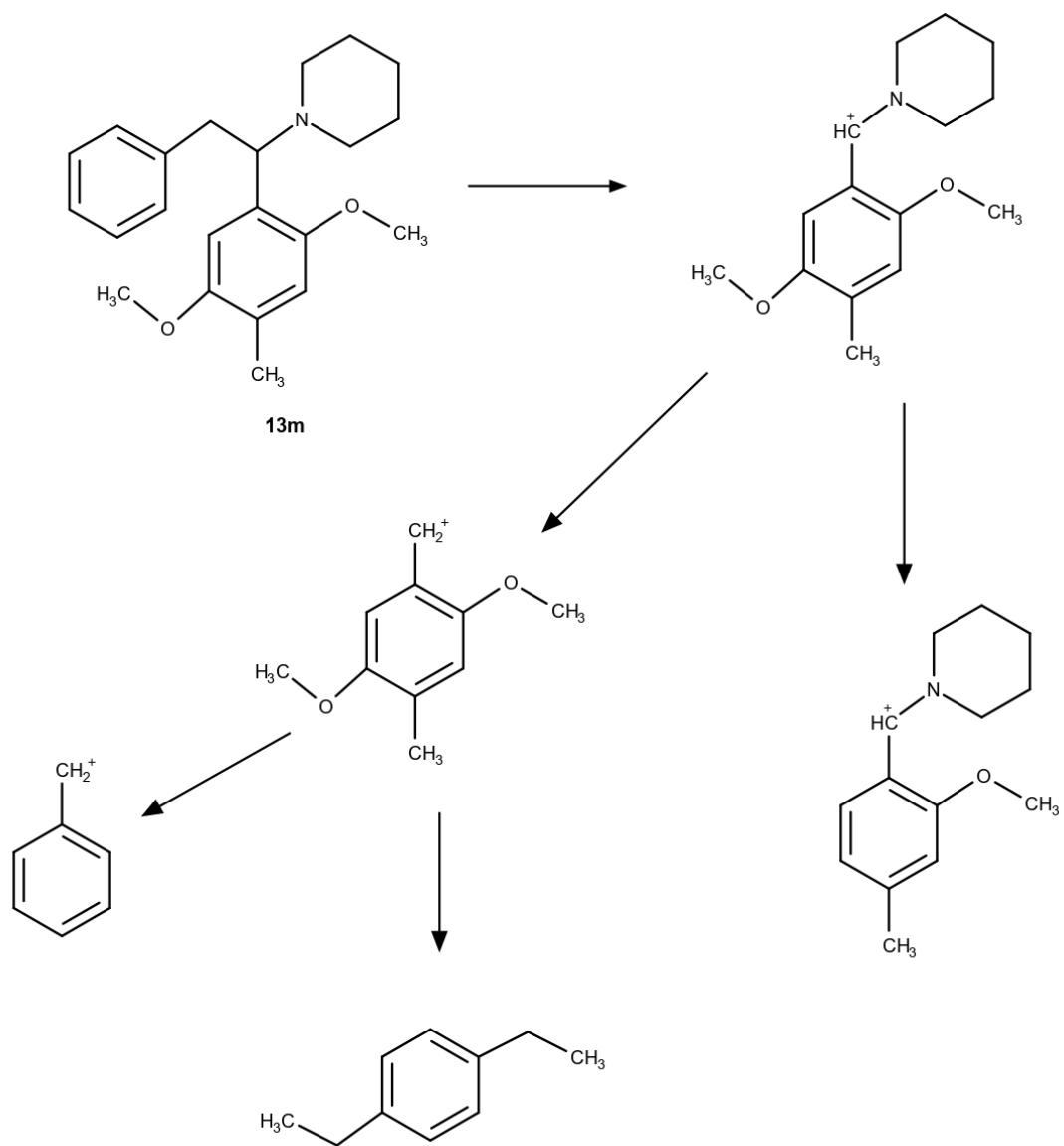


**Figure 81:** GC-MS fragmentation pattern for IAS-013 (**13m**)

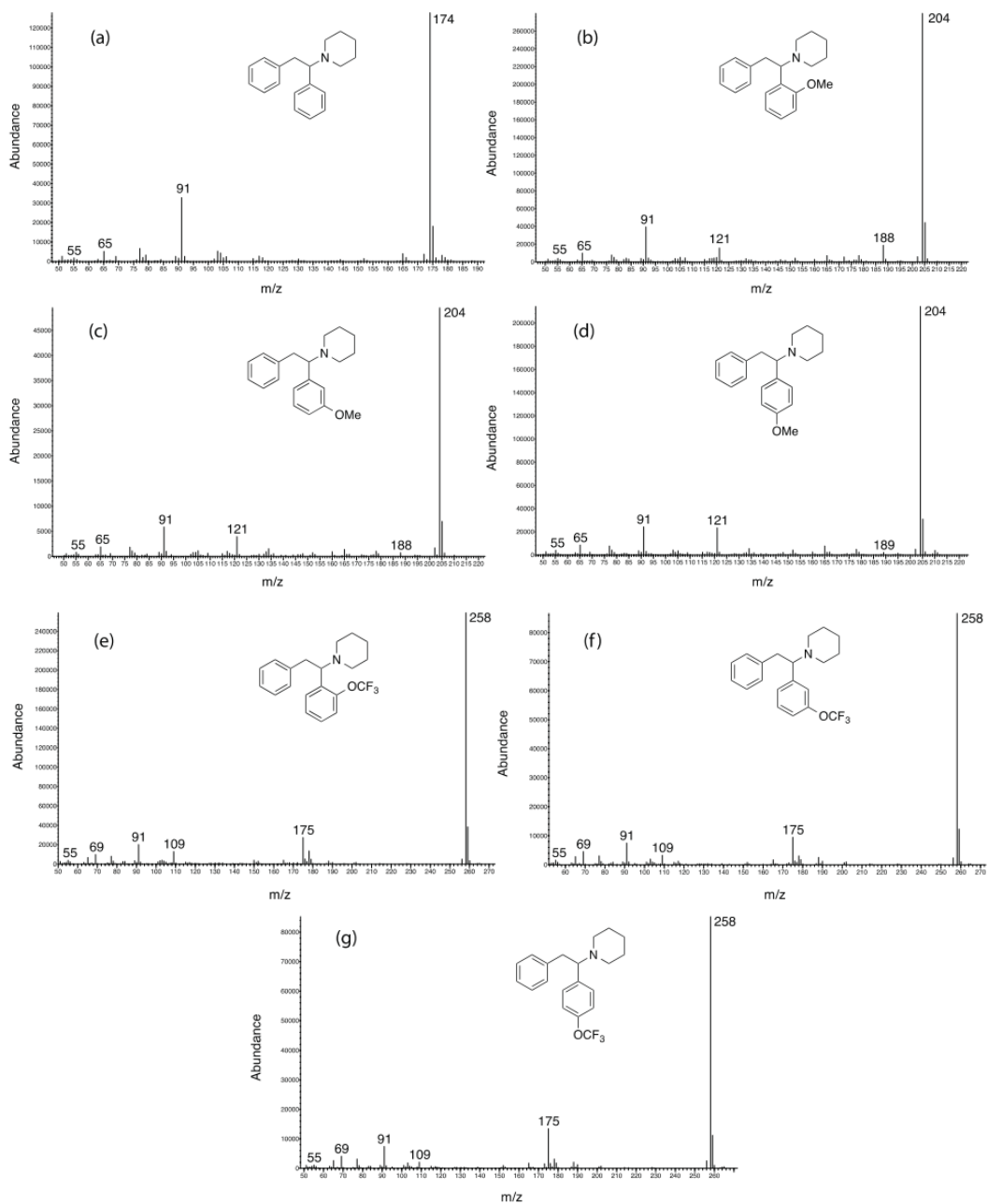


**Figure 82:** EI-MS spectra of (a) diphenidine (**13a**) and its substituted derivatives (b) 2-methoxyphenidine (2-MXP, **13b**); (c) 3-methoxyphenidine (3-MXP, **13c**); (d) 4-methoxyphenidine (4-MXP, **13d**); (e) 2-trifluoromethoxyphenidine (2-TFMXP, **13e**); (f) 3-trifluoromethoxyphenidine (3-TFMXP, **13f**) and (g) 4-trifluoromethoxyphenidine (4-TFMXP, **13g**).



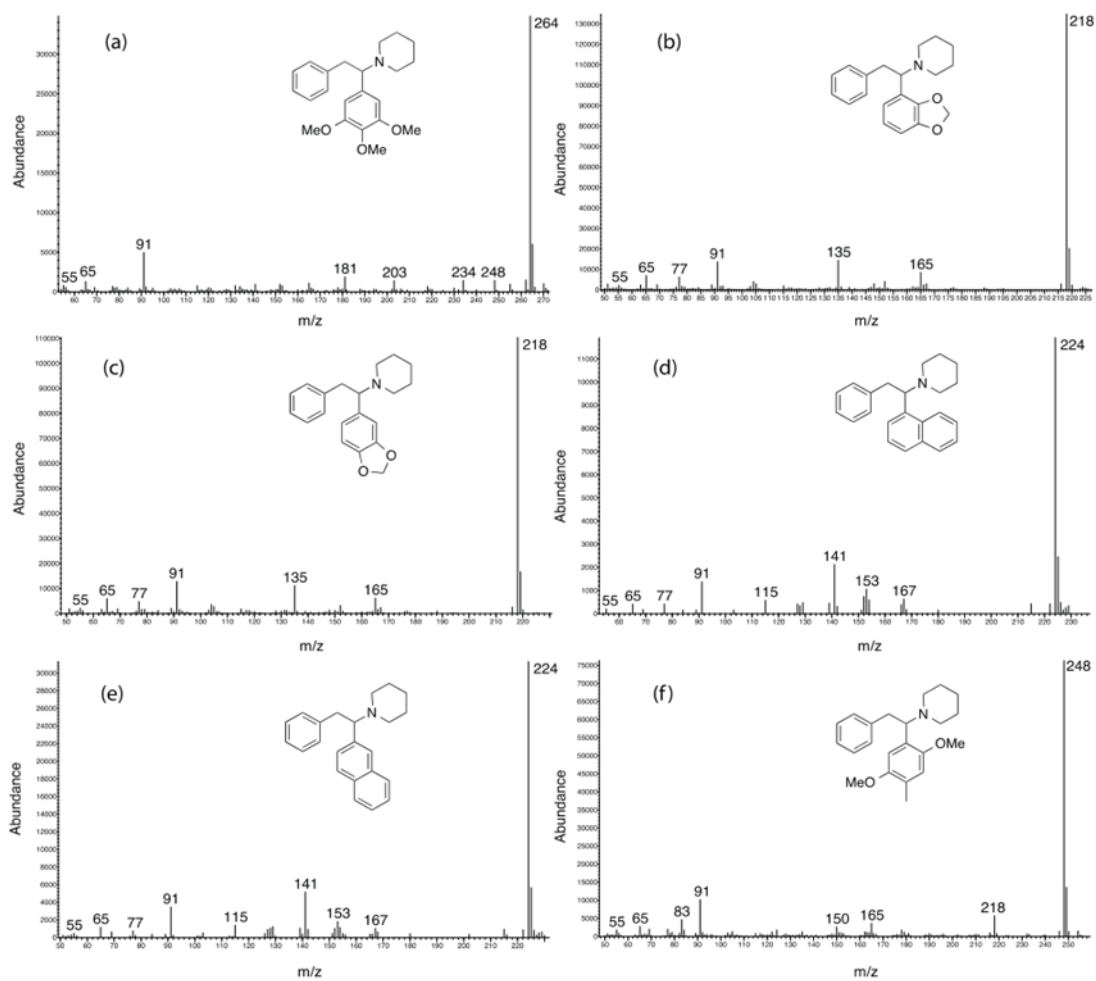


**Figure 83:** EI-MS spectra of (a) mescphenidine (3,4,5-TMXP, **13h**); (b) 2,3-(methylenedioxy)diphenidine (2,3-MDDP, **13i**); (c) 3,4-(methylenedioxy)diphenidine (3,4-MDDP, **13j**); (d) 1-naphthenidine (1-NPD, **13k**); (e) 2-naphthenidine (2-NPD, **13l**); (f) IAS-013 (**13m**).

**Table 28:** Summary of GC-MS validation data for the quantification of diphenidine (**13a**) and its substituted derivatives (**13b–13m**). NB.  $R_t$  (eicosane) = 21.55 min. See Figure 75 for representative chromatogram.

Analyte	Rt (min)	RRT	Regression co-efficient	LOD ( $\mu\text{g mL}^{-1}$ )	LOQ <sup>s</sup> ( $\mu\text{g mL}^{-1}$ )	Precision (%RSD, $n = 6$ )				
						25 $\mu\text{g mL}^{-1}$	50 $\mu\text{g mL}^{-1}$	100 $\mu\text{g mL}^{-1}$	200 $\mu\text{g mL}^{-1}$	250 $\mu\text{g mL}^{-1}$
<b>Benzocaine</b>	10.98	0.46	0.996	5.97	18.10	7.81	7.81	5.25	4.13	2.19
<b>Caffeine</b>	15.68	0.66	0.998	11.82	35.82	10.41	5.54	4.79	2.99	3.16
<b>10e</b>	19.80	0.83	0.998	4.23	12.83	3.53	1.29	1.79	2.25	2.47
<b>10f</b>	20.77	0.88	0.998	4.61	13.97	4.30	1.52	2.16	2.69	2.77
<b>10g</b>	22.02	0.93	0.997	5.31	16.10	5.82	2.44	2.63	3.01	3.09
<b>10a</b>	23.72	1.00	0.997	5.08	15.39	4.39	2.34	2.33	3.49	3.00
<b>Procaine</b>	24.25	1.02	0.996	6.24	18.92	9.05	3.30	5.29	1.80	2.86
<b>10b</b>	28.06	1.18	0.997	5.22	15.81	9.36	3.85	3.68	3.22	3.52
<b>10c</b>	29.94	1.26	0.998	4.58	13.88	9.06	3.73	3.52	2.92	2.77
<b>10d</b>	31.40	1.32	0.996	5.71	17.30	9.88	3.60	3.52	3.37	3.69
<b>10j</b>	32.76	1.38	0.997	4.86	14.74	8.15	3.29	3.11	3.57	2.82
<b>10i</b>	36.03	1.52	0.996	5.99	18.16	11.20	4.41	4.35	3.27	4.08
<b>10m</b>	36.70	1.55	0.996	5.70	17.29	13.12	5.98	3.92	4.12	3.00
<b>10k</b>	40.43	1.70	0.997	5.13	15.54	9.83	4.06	3.79	3.66	3.02
<b>10h</b>	41.13	1.73	0.996	5.78	17.51	14.02	5.99	4.63	4.31	3.31
<b>10l</b>	42.00	1.77	0.997	4.81	14.57	12.72	3.54	4.19	3.98	2.17

## 4.6. Forensic application

A sample of diphenidine (SS-1) and methoxphenidine (SS-2) were bought from “Buy Research Chemicals UK” (<http://www.brc-chemicals.com>, September 2015) and both were reported to be >99% pure and to contain 1 g of either diphenidine (**13a**, SS-1 Figure 84) or 2-methoxyphenidine (**13b**, SS-2 Figure 84).

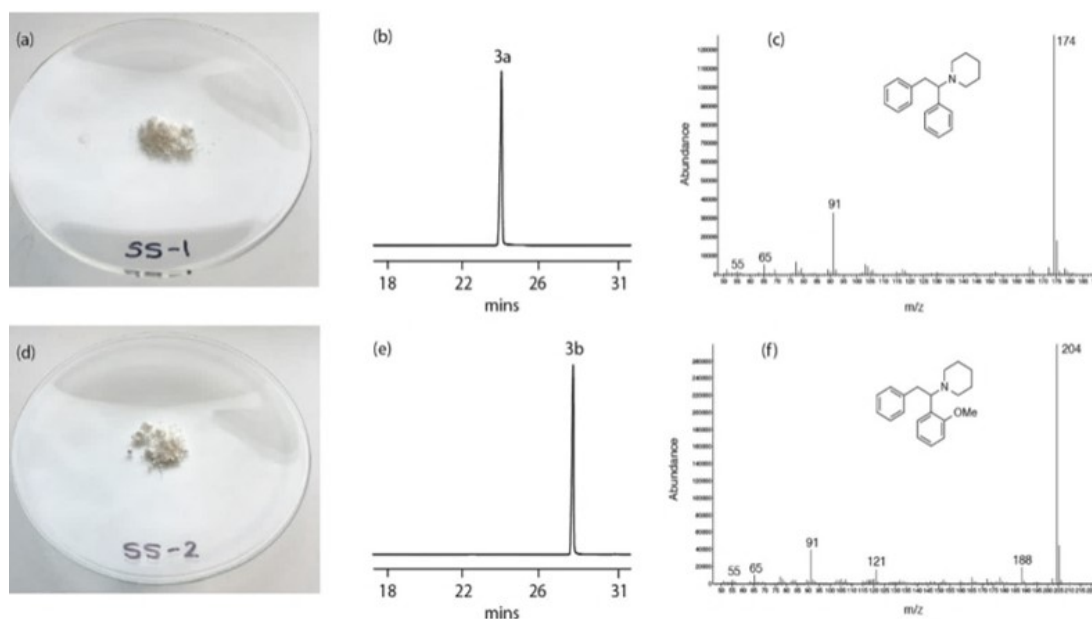


**Figure 84:** GC-MS analysis of the two street samples SS-1 and SS-2

Initially, presumptive tests were carried out using the same procedures reported for the reference materials. The diphenidine sample (SS-1) gave a positive result to the Marquis (orange), Mandelin (dark yellow) and Scott's (blue) tests to indicate the possible presence of diphenidine (**13a**). SS-2 also gave similar results to these tests producing the same positive colours with the Mandelin and Scott's reagents, however a pink colour was obtained with the Marquis reagent leading to the possibility of the presence of 2-methoxyphenidine (2-MXP, **13b**). Thin Layer Chromatographic (TLC) analysis of the two samples utilizing a silica gel stationary phase and a mobile phase consisting of dichloromethane-methanol (9:1 v/v) containing 0.8% ammonia (7 N in methanol) indicated that both samples contained single components (SS-1,  $R_f = 0.84$  and SS-2,  $R_f = 0.77$ ). Comparison of the samples with the

reference materials confirmed the presence of diphenidine (**13a**,  $R_f = 0.85$ ) and 2-methoxyphenidine (**13b**,  $R_f = 0.76$ ) respectively.

Qualitative analysis using GC-MS confirmed the presence of diphenidine and 2-MXP for SS-1 and SS-2 respectively. This was shown due to a match in retention time and fragmentation pattern from the mass spectrometer (SS-1:  $R_t = 23.72$  min,  $m/z$  (base peak) = 174  $[M+H]^+$ , **13a**, figure 86 and SS-2:  $R_t = 28.06$  min,  $m/z$  (base peak) = 204  $[M+H]^+$ , **13b**, figure 86). The two samples appeared to contain no further adulteration and this purity was confirmed with  $^1\text{H}$  NMR analysis.  $^1\text{H}$  NMR (400 MHz,  $\text{CD}_2\text{Cl}_2$ ) analysis and comparison with standards of diphenidine (**13a**) and 2-methoxyphenidine (**13b**) showed that the samples were essentially pure and confirmed the absence of any adulterants or diluents within the samples (Figure 85).

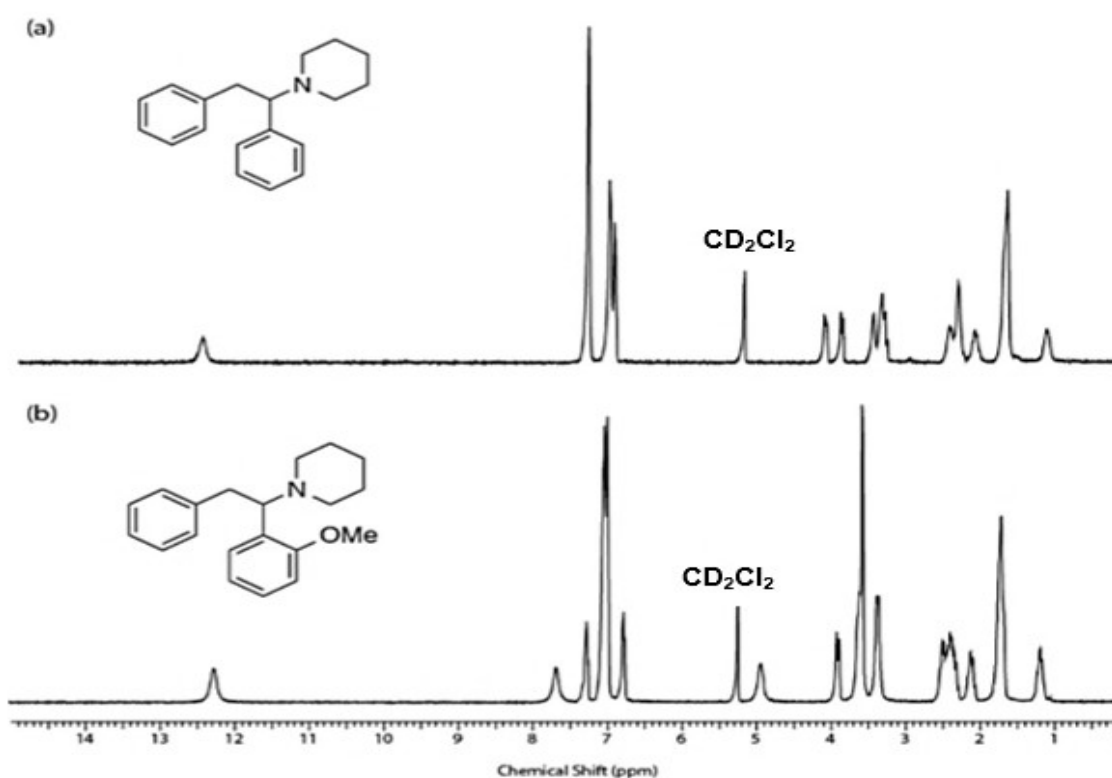


**Figure 85:**  $^1\text{H}$  NMR analysis of SS-1 (a) and SS-2 (b) run in  $\text{CD}_2\text{Cl}_2$  (10 mg  $\text{mL}^{-1}$ )

With substantial evidence, supporting a quantitative GC-MS approach for detecting various substituted diphenidine derivatives in street samples, the

viability of the proposed protocol was tested. The samples were reanalysed (in triplicate) using the validated GC-MS method at a concentration of  $100 \mu\text{g mL}^{-1}$ . The GC-MS results (Figure 86), confirm that the samples only contained the two alleged components (SS-1:  $R_t = 23.72$  min, **10a**, 100.3% w/w, % RSD = 0.21%,  $n = 3$ ) and SS-2:  $R_t = 28.06$  min, **10b**, 99.5% w/w, % RSD = 1.37%,  $n = 3$ ). The majority of NPS that are encountered on the drugs market usually contain some sort of adulteration or inaccurate composition information of the packaging. However, these samples appeared to both comply with the vendors claims (in terms of principal ingredient), be of high purity (>99% w/w) and there was no evidence (confirmed by  $^1\text{H NMR}$ ) that either contained any additional NPSs or commonly used diluents and/or adulterants.

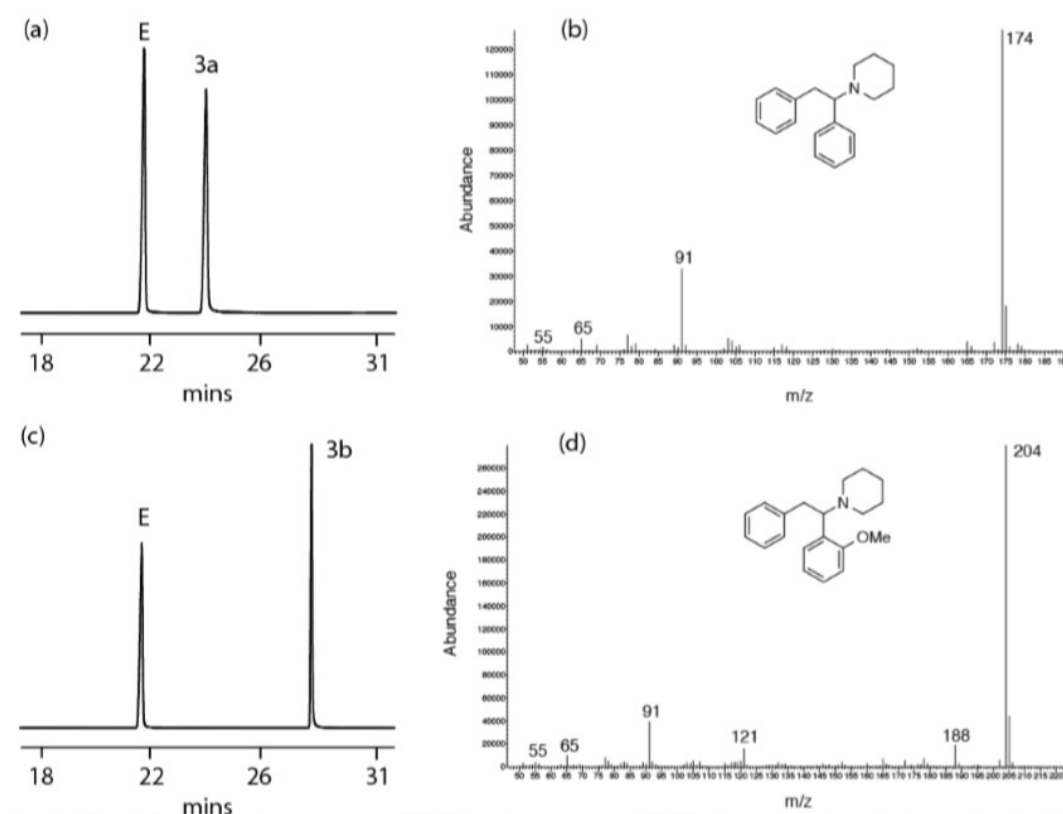


**Figure 86:** Quantitative GC-MS analysis containing both GC chromatographs and mass spectra data of SS-1 (a and b) and SS-2 (c and d) ( $0.1 \text{ mg mL}^{-1}$  in methanol containing  $0.1 \text{ mg mL}^{-1}$  eicosane, E)

## 4.7. Conclusions and future work

Based on the appearance of diphenidine and its methoxy substituted derivatives on the recreational drugs market a range of 13 derivatives have been synthesised. Yields were 21–77 %, showing an ease of production, with each synthesis only taking 2 hours, in clandestine labs with all purities appearing >95% by elemental analysis. Samples were analysed using  $^1\text{H}$  NMR,  $^{13}\text{C}$  NMR,  $^{19}\text{F}$  NMR (where necessary) in order to confirm their chemical identity and provide reference spectra to aid forensic laboratories and other organisations involved in trying to identify these compounds on a regular basis.

Presumptive colour tests have been performed on all reference materials with Marquis and Mandelin reagents both providing a positive colour change. Scott's reagent also produces a positive colour change for all diphenidine derivatives with a clear change from red to blue making it the optimum reagent to use for the detection of diphenidines. However, it also shows the potential for diphenidines to provide a false positive in the initial test for cocaine as that also turns Scott's reagent blue. The production of so many false positives in relation to cocaine produces a big issue when determining a drug controlled by the Misuse of Drugs Act (1971) to a drug controlled by the Psychoactive Substances Act (2016). This is due to the differences in penalties when convicted under either law. If the colour tests continue to be used somebody could be in possession of diphenidine, which would be conviction under the Psychoactive Substances Act (2016), but penalised under the Misuse of Drugs Act (1971).

Thin Layer Chromatography (TLC) analysis provided some initial separation of compounds and positional isomers. A 45-minute GC-MS method was developed in order to allow separation and identification of the thirteen diphenidine derivatives to be achieved. This method was validated, in order to provide a general screening method for qualitative analysis and general triaging of samples, but also a quantitative method, for both pure, individual component samples, and samples cut with common adulterants.

Two samples obtained from online vendors were analysed and shown to contain the active components (95–100% w/w) stated (diphenidine and 2-methoxohenidine) with no adulteration.

## 5. Chapter 5 – Halogenated diphenidine derivatives

### 5.1. Overview

Based on the increased popularity of the diphenidine derivatives<sup>96, 98, 112</sup> and the difficulty experienced in keeping ahead of the increasing number of derivatives produced, it is important to enhance the library of compounds closely resembling the structure of diphenidine. Literature has already shown the increased metabolic stability of compounds with the inclusion of fluorine, through the greater stability of the C-F bond compared to the C-H bond and the increased lipophilicity of fluorine compared to hydrogen.<sup>2</sup> Therefore, the three monofluorinated derivatives have been prepared along with the remaining halogenated substituted derivatives (**20a–20l**). This helps to increase the library of samples available for testing in order to improve the speed and reliability of compound identification in samples encountered by law enforcement.

This chapter will include all characterisation data for all the halogenated diphenidine derivatives, through <sup>1</sup>H NMR, <sup>13</sup>C NMR, <sup>19</sup>F NMR, ATR-FTIR, melting points and TLC experiments. A validated GC-MS method is reported which, for the first time, provides a general screening method for all of the halogenated derivatives. This GC-MS method is employed for the qualitative analysis of two street samples as well as the identification of adulterants and cutting agents.

Presumptive testing through commonly used colour testing reagents will be performed in order to show the difficulty in initially identifying active components in samples. It will also highlight the increase in false-positive results for commonly controlled substance, under the Misuse of Drugs Act, as the number of clandestinely produced NPS increases. 60 MHz NMR will also be utilised in order to provide a possible new presumptive testing instrument that will provide more distinguishable features in results produced, while still being a rapid testing method with easy sample preparation.



## 5.2. Synthesis of the halogenated diphenidine derivatives

Halogenated diphenidine derivatives (**20a–20l**) were synthesised as hydrochloride salts. All target compounds were prepared as racemic mixtures, using similar methods used to synthesize of diphenidine.<sup>34</sup> The only difference in the synthesis method between the different halogenated derivatives was the prerequisite aldehyde used, with *ortho*-, *para*- and *meta*-substituted halogen functional groups added. Reference materials were produced as stable, colourless to off-white powders with overall yields ranging from 26-61%. A table containing all yields can be seen in Table 29.

**Table 29:** Percentage yields for the halogenated regioisomers (**20a–20l**)

Compound no.	Compound Name	Abbreviation	Yield (%)
<b>20a</b>	2-fluphenidine	2-FP	40
<b>20b</b>	3-fluphenidine	3-FP	33
<b>20c</b>	4-fluphenidine	4-FP	44
<b>20d</b>	2-chlophenidine	2-CP	43
<b>20e</b>	3-chlophenidine	3-CP	54
<b>20f</b>	4-chlophenidine	4-CP	49
<b>20g</b>	2-brophenidine	2-BP	47
<b>20h</b>	3-brophenidine	3-BP	49
<b>20i</b>	4-brophenidine	4-BP	61
<b>20j</b>	2-iodophenidine	2-IP	26
<b>20k</b>	3-iodophenidine	3-IP	54
<b>20l</b>	4-iodophenidine	4-IP	60

The hydrochloride salts were determined to be soluble (at the level of 10 mg mL<sup>-1</sup>) in deionised water, methanol, dichloromethane and dimethylsulfoxide. To ensure the authenticity of the materials utilised in this study the synthesised compounds were fully structurally characterized, to produce reference spectra, by <sup>1</sup>H NMR, <sup>13</sup>C NMR (supplementary data: Figure 20-Figure 31), and FTIR (supplementary data: Figure 78-Figure 89). <sup>19</sup>F NMR was also run on the relative compounds (**20a–20c**) and the respective chemical shifts can be seen in Table 30. The purity of all samples was checked, using the NMR

experiments and GC-MS analysis, with internal standards and were shown to be >95% in all cases.

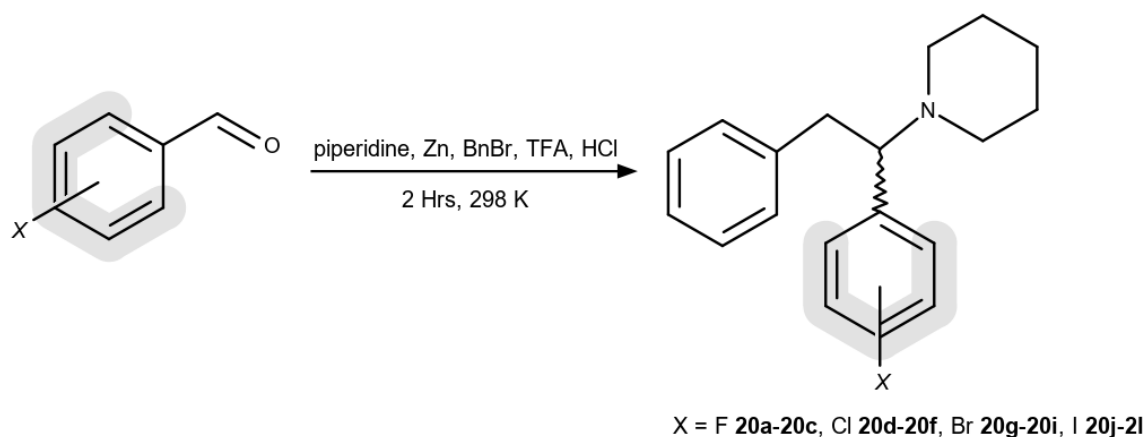


**Figure 87:** Reaction scheme for the synthesis of the halogenated diphenidine derivatives (**20a-20l**)

The structures of all the halogenated diphenidine samples are very closely related to diphenidine (**13a**).  $^1\text{H}$  NMR spectrum was previously acquired for diphenidine in deuterated DCM (figure 63) in chapter 4. In order to show a direct comparison to the halogenated derivatives, which were run in  $\text{DMSO-d}_6$ , the diphenidine sample was repeated in  $\text{DMSO-d}_6$ .

The spectrum produced from the deuterated DMSO shows slight differences to the deuterated DCM spectrum and can be seen through the stacked spectra (figure 88). The DMSO spectrum (figure 89) shows a greater splitting, regarding the proton environments of the aromatic and piperidine regions, with clearer splitting patterns from coupling. There is a slight change in the chemical shift values of the  $^1\text{H}$  NMR spectrum, as the solvent is changed from  $\text{DCM-d}_2$  to  $\text{DMSO-d}_6$ , with the amine peak shifted more upfield and the chiral proton shifted more downfield. The assignment of protons still matches, with the change of solvent, with the chiral proton (4.64 ppm) still coupled to the two  $\text{CH}_2$  protons (3.86 ppm and 3.53 ppm) in the  $^1\text{H}$ - $^1\text{H}$  COSY spectra. The peak at 3.73 ppm belongs to the piperidine ring with coupling to the peak at 3.52 ppm in the  $^1\text{H}$ - $^1\text{H}$  COSY spectra and showing coupling to the same carbon in the  $^1\text{H}$ - $^{13}\text{C}$  HMQC spectra. This also shows that there is overlap at 3.52 ppm

with two different proton environments being superimposed on one another in this region. The  $^1\text{H}$  NMR signal for water is also seen at 3.33 ppm so may coalesce with peaks representing piperidine protons, should this be present in a sample.

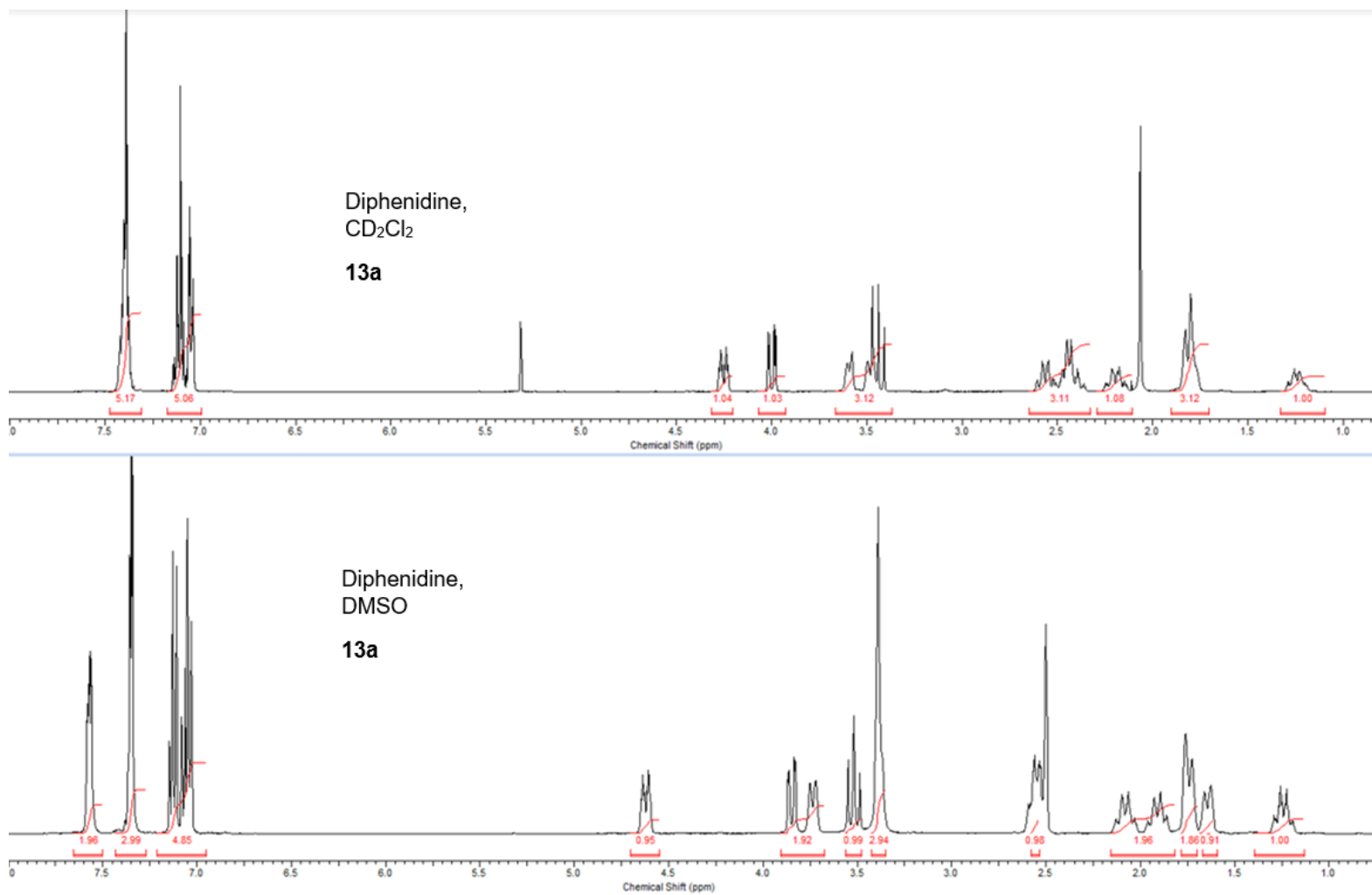


**Figure 88:** Stacked <sup>1</sup>H-NMR spectra of diphenidine (**13a**) run in DMSO-d<sub>6</sub> (δ ppm = 2.50) and CDCl<sub>3</sub> (δ ppm = 7.26)

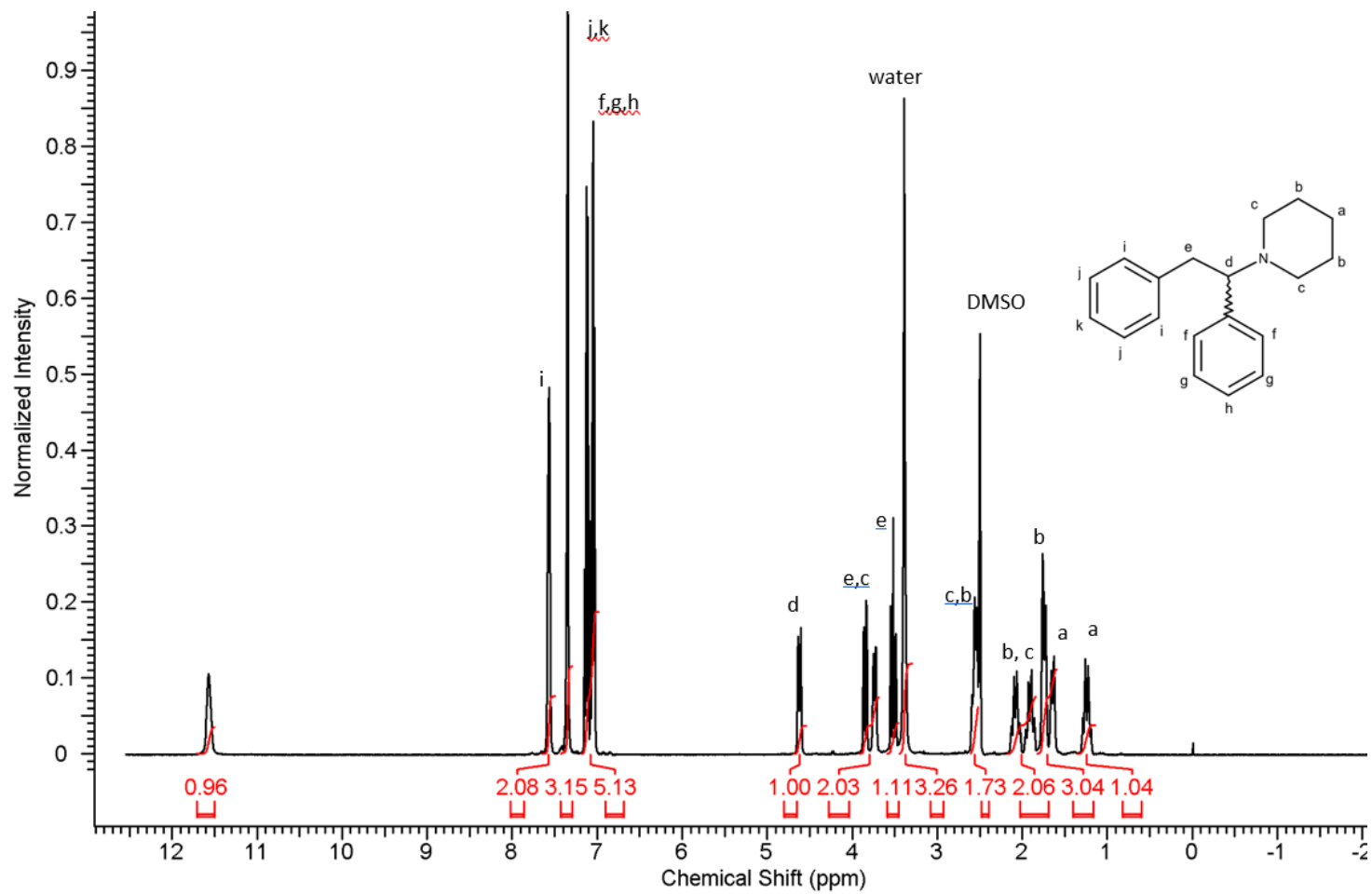


**Figure 89:**  $^1\text{H-NMR}$  spectrum of diphenidine (13a) run in  $\text{DMSO-d}_6$  ( $\delta$  ppm = 2.50)

The  $^1\text{H}$  NMR spectrum for diphenidine allows direct comparisons to be made with the corresponding spectra of the halogenated derivatives, in order to show whether any distinguishable features are present and whether each isomer can be distinguished from one another. All halogenated derivatives show a very similar aliphatic region, showing that it is possible to detect the class of compound based on this region. There are very slight differences in this region between both the *meta*- and *para*-substituted derivatives, in each halogenated substituent, compared to the *ortho*-substituted isomers. The halogenated substituent being situated on the 2' position of the phenyl group alters two proton environments in the piperidine ring, with 2 peaks moving downfield from 2.09 and 1.84 ppm to 2.76 and 2.68 ppm respectively and also the chiral centre proton shifts from 4.68 ppm to 4.995 ppm. The change in the chemical shift values is linked to the de-shielding of the shifted protons, through the addition of an electronegative atom, drawing electron density away from those regions. The 3' and 4' positional isomers produce aliphatic regions that are identical to one another. The difference between the 3' and 4' isomers compared to the 2' isomer can be visualised in figure 90.

The aromatic regions for each halogenated regioisomer shows significant differences in the number and chemical shifts of proton peaks. The splitting patterns, in the aromatic region, are unique for each compound showing that each halogen atom produces a slightly different effect in the neighbouring protons. It also shows the power of NMR to help identify specific compounds and the possibility of using  $^1\text{H}$  NMR experiments as an initial test for the detection of halogenated diphenidine regioisomers. The stacked spectra for the *ortho*-, *meta*- and *para*-positional isomers of the fluorinated derivatives shows the difference in the  $^1\text{H}$  NMR shifts in the aliphatic regions between positional isomers (figure 90), along with an enlargement of the differences in the aromatic region (figure 91). The enlarged stacked spectra (figure 91–figure 94) of the aromatic region for all positional isomers has also been produced to show the clear differences observed in the aromatic region of each spectrum. All spectra were run in  $\text{DMSO-d}_6$  with a residual peak at 2.50 ppm. All spectra also contained residual peaks at 3.30 ppm for water. All

aromatic regions integrate to nine protons for the halogenated regioisomers compared to ten present in the  $^1\text{H}$  NMR spectrum for diphenidine.

$^{19}\text{F}$  NMR was also performed on the 400 MHz instrument to complete NMR characterisation for the three fluphenidine regioisomers (**20a–20c**). Trifluoroacetic acid (TFA) was added as an internal standard in order to achieve an accurate chemical shift value for the sample. The chemical shifts for the three compounds can be seen in Table 30. These show the similarity between the shifts for the 3' and 4' positional isomers, although they can be distinguished using 400 MHz instrument, with the 2' positional isomer providing a much different chemical shift value (+5 ppm).

**Table 30:**  $^{19}\text{F}$  NMR chemical shift values for the fluphenidine regioisomer (FP, **20a–20c**)

Compound	$^{19}\text{F}$ chemical shift ( $\delta$ ppm)
<b>20a</b>	-115.71
<b>20b</b>	-110.96
<b>20c</b>	-110.78

When the halogenated substituents are checked through a computational program and the substituent is changed from fluorine to iodine the log P values increase. This means that the lipophilicity is increased for iodine compared to fluorine. The iodine compounds can have the potential for an increased permeability in the blood brain barrier. This can also have an increased effect on the potency of these isomers. No significant difference was seen in the log P values between different positional isomers. However, the log P values of both the bromine and iodine substituents are both  $> 5$  and this can result in a higher metabolic turnover, low solubility and poor oral absorption meaning these drugs may not be very effective. Highly lipophilic compounds tend to bind to hydrophobic targets other than the desired target, and, therefore, there is an increased risk of promiscuity and toxicity.<sup>138</sup> No current toxicology experiments have been performed on any of the halogenated derivatives.

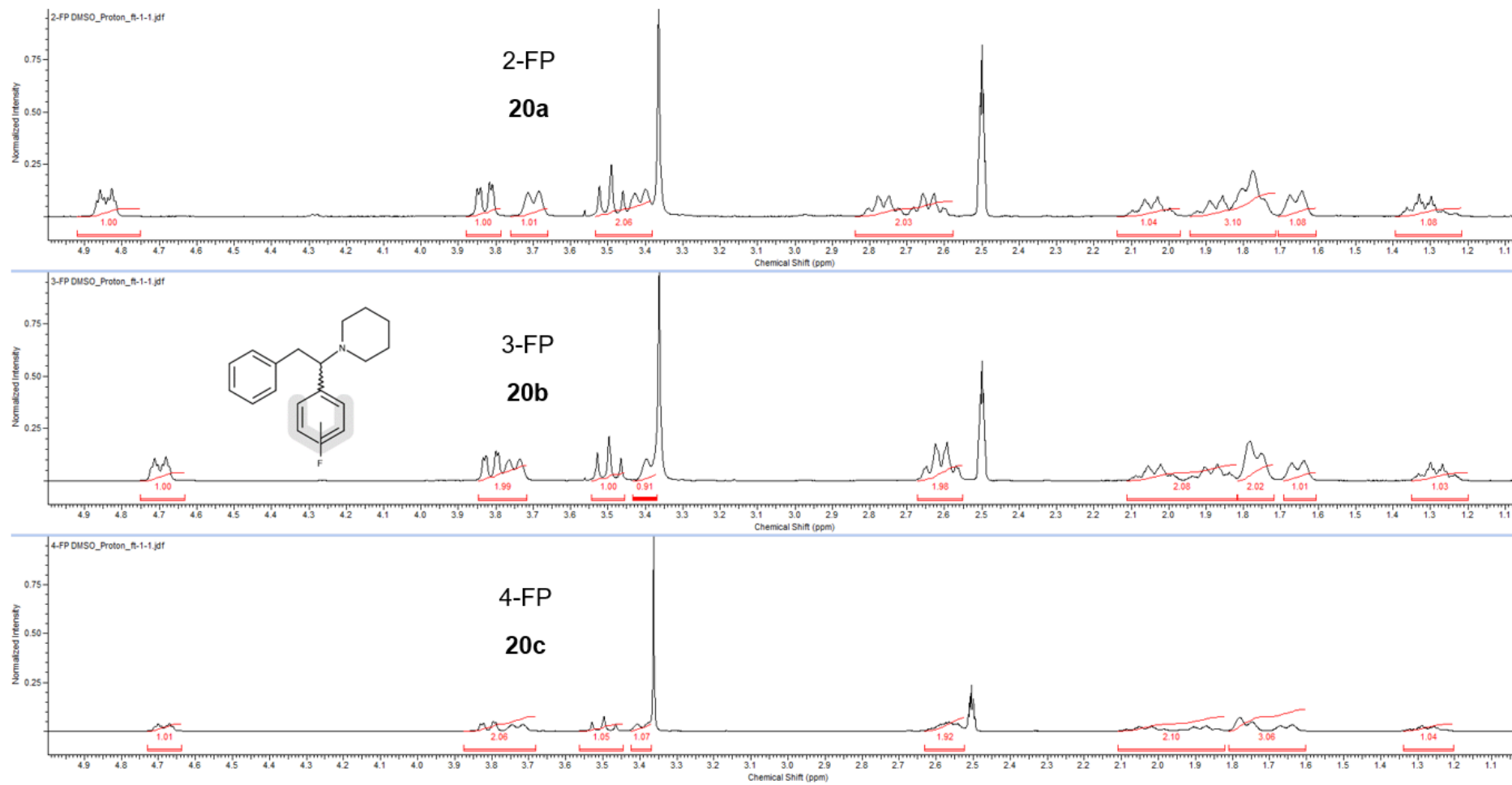


**Figure 90:** Stacked  $^1\text{H-NMR}$  spectra for the fluphenidine regioisomers (**20a–20c**) run in  $\text{DMSO-d}_6$  ( $\delta$  ppm = 2.50)



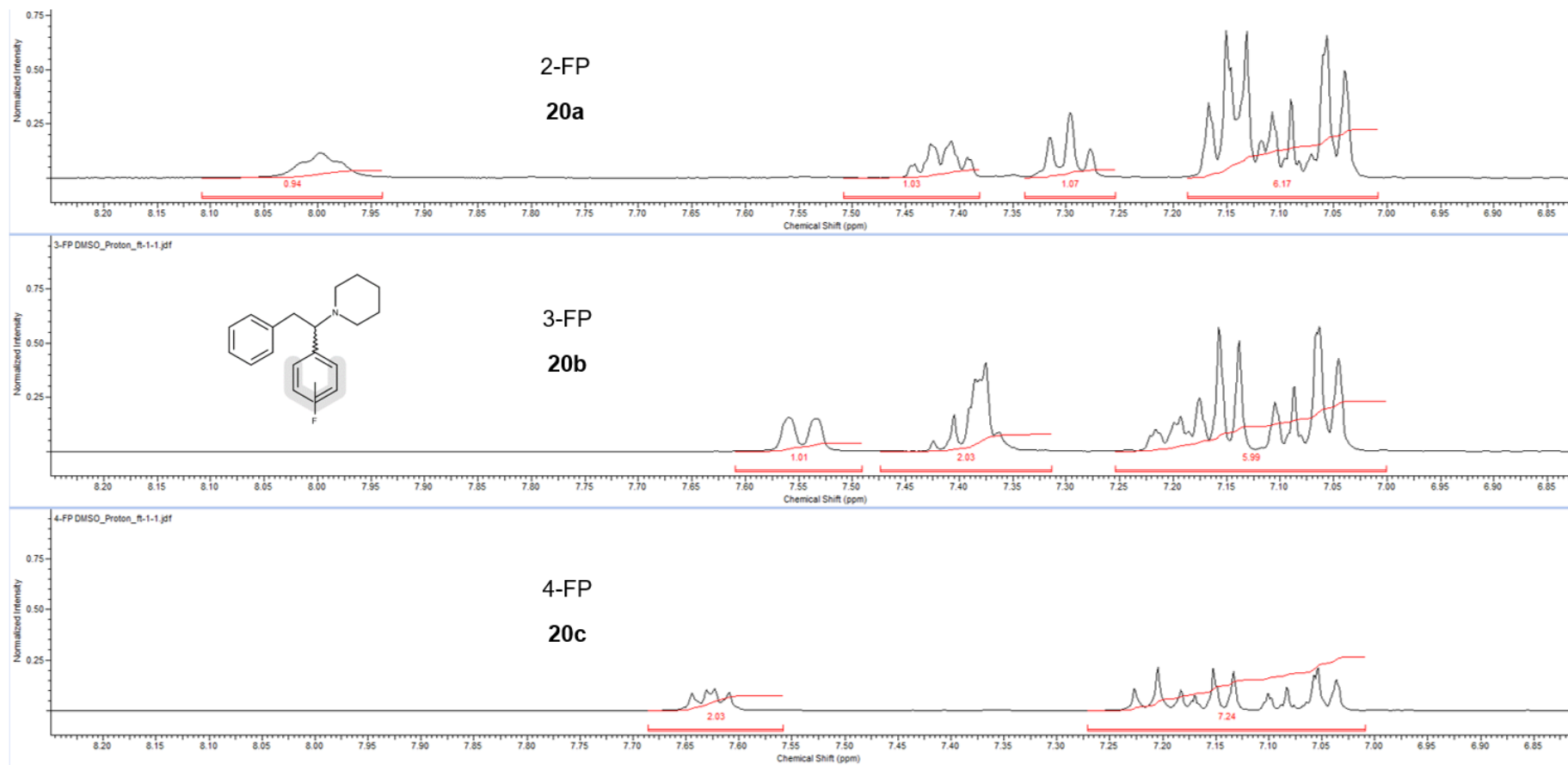


**Figure 91:** Stacked <sup>1</sup>H NMR spectra showcasing the aromatic region of the fluphenidone regioisomers (20a–20c)

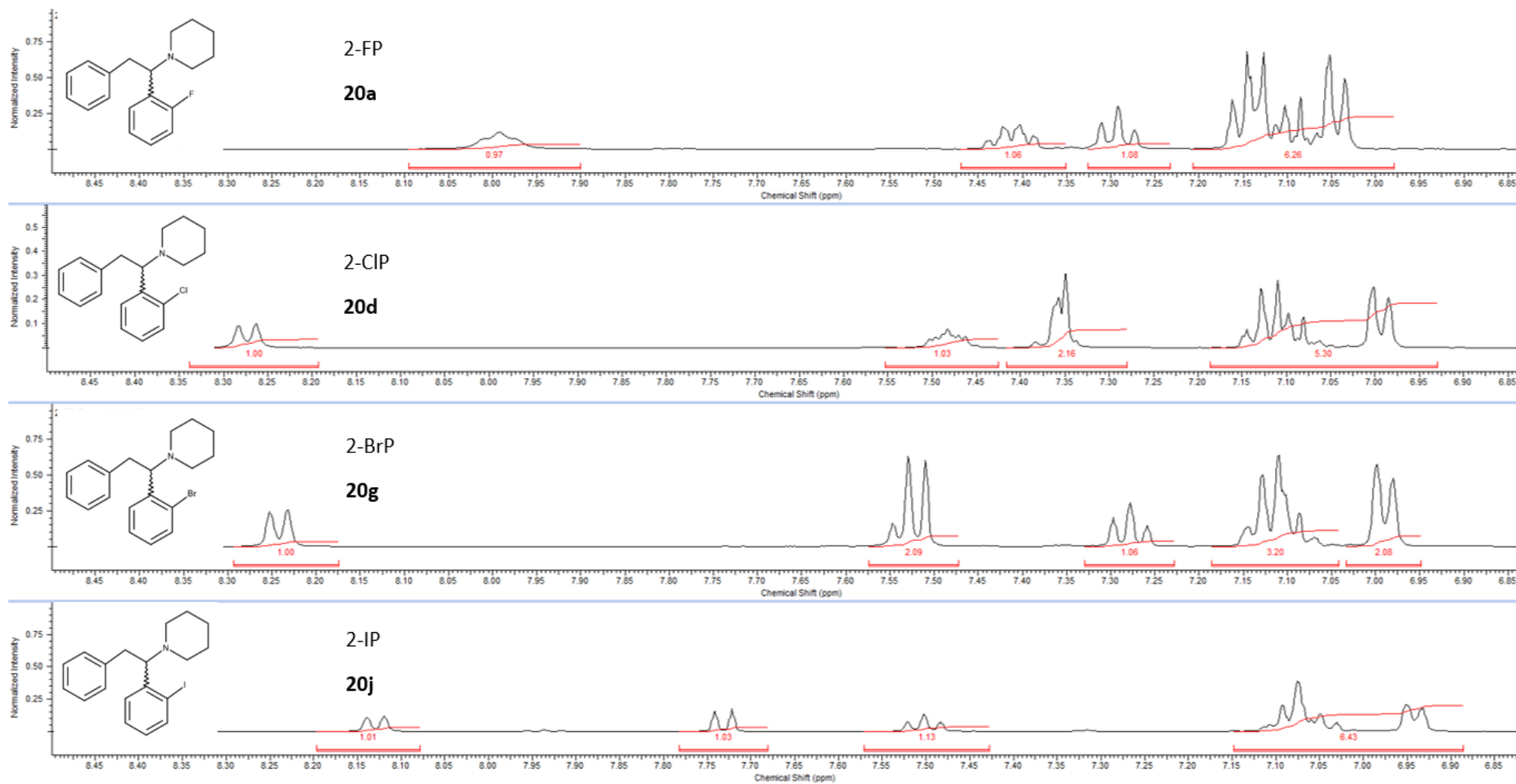


**Figure 92:** Stacked <sup>1</sup>H NMR spectra showcasing the aromatic region of the 2'-positional isomers of the halogenated diphenidines

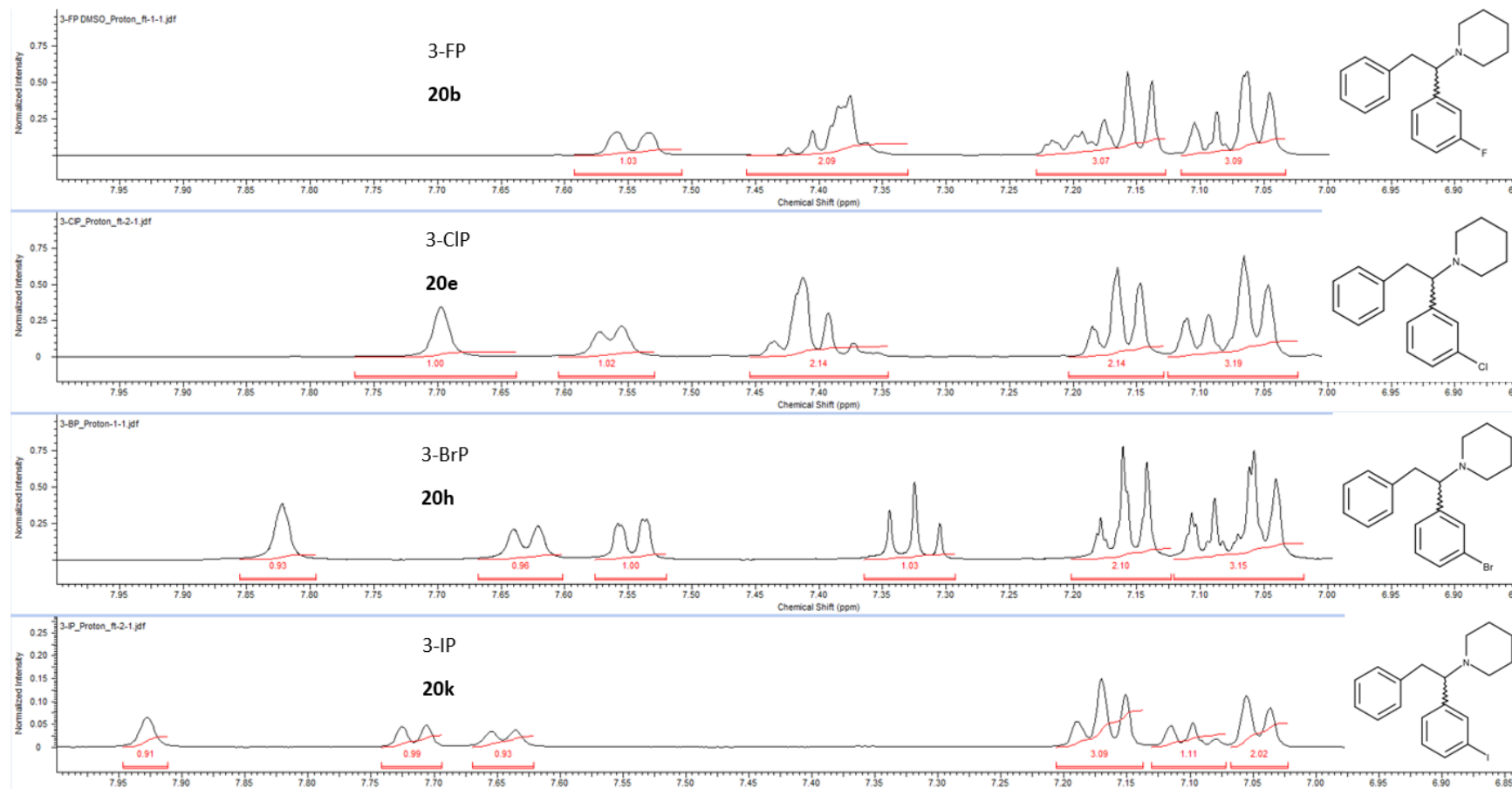


**Figure 93:** Stacked <sup>1</sup>H NMR spectra showcasing the aromatic region of the 3'-positional isomers of halogenated diphenidines

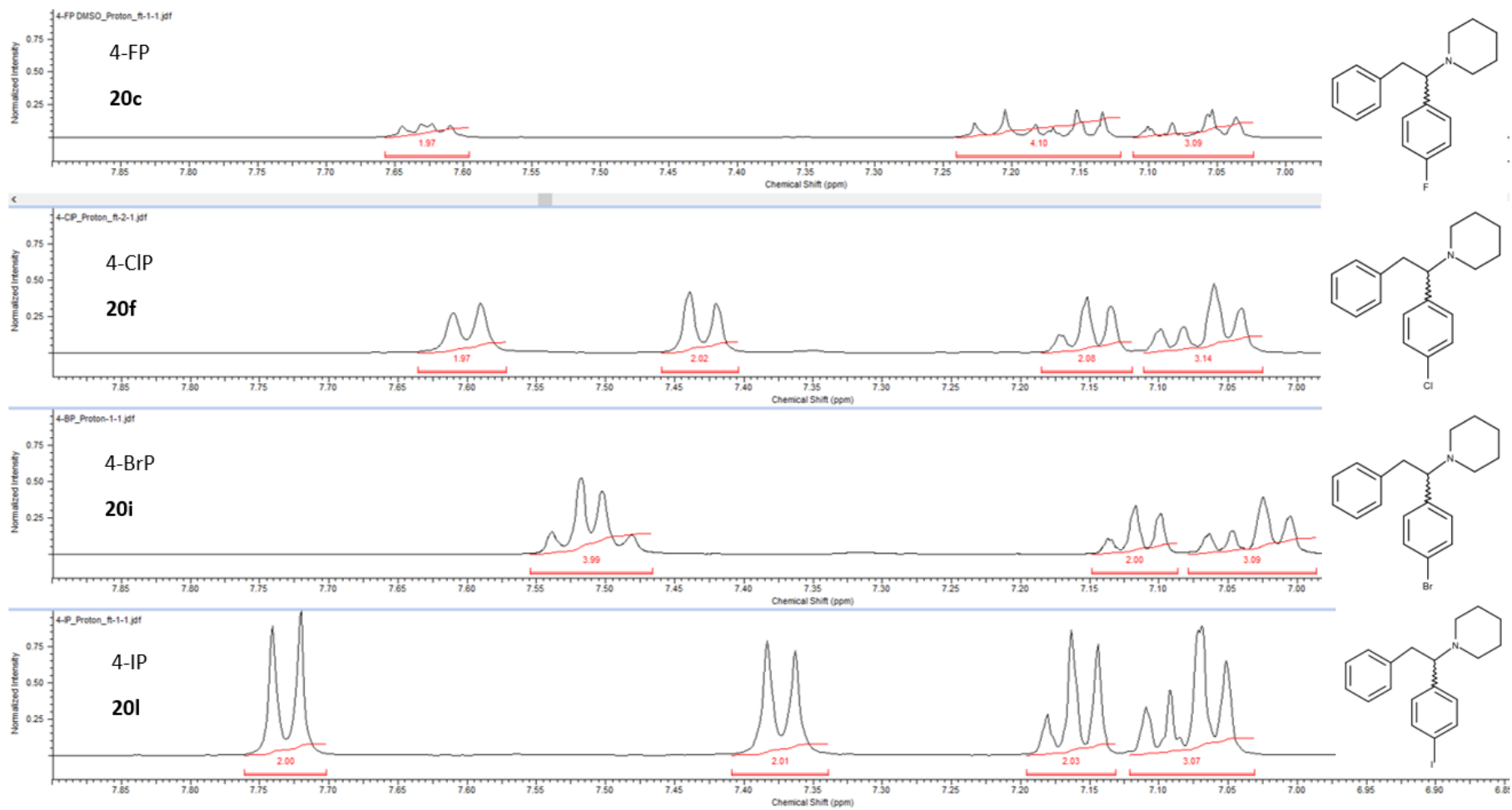


**Figure 94:** Stacked <sup>1</sup>H NMR spectra showcasing the aromatic region of the 4'-positional isomers of halogenated diphenidines

### 5.3. Presumptive Testing

Presumptive testing was carried out on all of the halogenated diphenidine derivatives (**20a–20l**) using the United Nations recommended guidelines.<sup>118</sup> No previous presumptive testing has been reported for any of the halogenated diphenidines, so a range of test reagents were used to fully detail possible colour changes. (i) Marquis test; (ii) Mandelin test; (iii) Simon's test; (iv) Robadope's test; (v) Scott's test and (vi) Zimmerman test reagents were prepared and used based on the procedures detailed in section 2.2. A solution of each reference standard ( $10 \text{ mg mL}^{-1}$ ) was prepared in deionised water and a couple of drops placed into a dimple well of a spotting tile. The required presumptive test reagent (1-2 drops) was then added and any colour change upon initial addition of the reagents were noted, with observations being made again after a five-minute period. Blank solutions of deionised water were used in order to show the natural colour of the test reagents prior to being added to sample solution.

The Marquis, Mandelin and Scott's reagents were the only reagents to provide a positive colour change with the halogenated diphenidines and the colour changes can be seen in Table 3131. The Scott's test reagent turned all halogenated compounds blue, with the colour remaining constant after a five-minute observation. This reaction matches that of all the diphenidine derivatives, with the coordination of the tertiary amines to the pink Co(II) octahedral complex affording the blue Co(II) tetrahedral complex.<sup>146</sup> In a similar manner to all the diphenidine derivatives, the halogenated regioisomers also provide a false-positive for cocaine for the Scott's test, increasing the confusion of identification between substances controlled by the Misuse of Drugs Act (1971) and those controlled by the Psychoactive Substances Act (2016).

The reaction of the halogenated derivatives with the Marquis and Mandelin reagents is also similar to that of diphenidine. The intense yellow/orange change with the Mandelin reagent also loses its intensity similar to diphenidine.

The colour changes observed when the Marquis and Mandelin reagents are used vary slightly in intensity from one halogenated isomer to another and provide slightly different colours to the non-halogenated diphenidine derivatives. The stability of the product formed with the Mandelin test does not show stability, however, as the intense colour produced initially fades over five minutes. The iodine substituents still keep a higher colour intensity, with the Marquis reagent, compared to the remaining halogenated substituents. The colour change for the Scott's reagent is consistent for all halogenated diphenidines, meaning identification of specific isomers is impossible even with the full range of presumptive tests. However, combining the Scott's test with the Marquis test will help to show the initial possibility of a halogenated diphenidine being present.

**Table 31:** Colour changes observed with presumptive test reagents for the 12 halogenated diphenidine derivatives (**20a–20l**) immediately after addition and after 5 minutes of addition

	Marquis		Mandelin		Scott's	
	Immediate colour change	Colour after 5 minutes	Immediate colour change	Colour after 5 minutes	Immediate colour change	Colour after 5 minutes
<b>20a</b>	orange	light orange	dark yellow	yellow	blue	blue
<b>20b</b>	light orange	light orange	dark yellow	yellow	blue	blue
<b>20c</b>	light orange	light orange	dark yellow	yellow	blue	blue
<b>20d</b>	dark orange	light orange	dark yellow	yellow	blue	blue
<b>20e</b>	orange	light orange	dark yellow	yellow	blue	blue
<b>20f</b>	orange	light orange	dark yellow	yellow	blue	blue
<b>20g</b>	orange	light orange	dark yellow	yellow	blue	blue
<b>20h</b>	orange	light orange	dark yellow	yellow	blue	blue
<b>20i</b>	orange	light orange	dark yellow	yellow	blue	blue
<b>20j</b>	dark orange	orange	dark yellow	yellow	blue	blue
<b>20k</b>	dark orange	orange	dark yellow	yellow	blue	blue
<b>20l</b>	dark orange	orange	dark yellow	yellow	blue	blue

## 5.4. Thin Layer Chromatography (TLC)

Thin layer chromatography has been performed on all 12 of the halogenated diphenidine regioisomers, using the same method and mobile phase composition, as used for the thirteen diphenidine derivatives (see section 4.4). Average  $R_f$  values are reported (Table 32) based on the averages from six repeats. Based on  $R_f$  values it is difficult to separate each regioisomer from one another. There is a slight pattern with the halogenated substituent present as the more polar fluphenidine regioisomers move more slowly on the TLC plate, as the interaction with the silica is stronger than that observed for the iodophenidine regioisomers. The  $R_f$  values do not allow the regioisomers of each substituted halogen to be distinguished from one another.

**Table 32:** Thin Layer Chromatography data for the halogenated diphenidine regioisomers (20a–20l)

	Compound name	Spot colour under UV light (254 nm)	Spot colour after staining with modified Dragendorff-Ludy-Tenger Reagent	$R_f$ value
<b>20a</b>	2-fluphenidine	Black spot	red spot	0.65
<b>20b</b>	3-fluphenidine	Black spot	red spot	0.61
<b>20c</b>	4-fluphenidine	Black spot	red spot	0.62
<b>20d</b>	2-chlophenidine	Black spot	red spot	0.71
<b>20e</b>	3-chlophenidine	Black spot	red spot	0.73
<b>20f</b>	4-chlophenidine	Black spot	red spot	0.73
<b>20g</b>	2-brophenidine	Black spot	red spot	0.80
<b>20h</b>	3-brophenidine	Black spot	red spot	0.77
<b>20i</b>	4-brophenidine	Black spot	red spot	0.79
<b>20j</b>	2-iodophenidine	Black spot	red spot	0.83
<b>20k</b>	3-iodophendine	Black spot	red spot	0.80
<b>20l</b>	4-iodophenidine	Black spot	red spot	0.84



## 5.5. Gas chromatography – mass spectroscopy

The twelve halogenated diphenidine derivatives were all injected into the GC-MS after simple dissolution of the sample in methanol (1 mg mL<sup>-1</sup>) and a tenfold dilution (100 µg mL<sup>-1</sup>). No derivatisation step was required. All halogenated derivatives (**20a–20l**) were run individually initially, before being run as a mixture, in order to determine retention times. Retention times (R<sub>t</sub>) and relative retention times (RR<sub>t</sub>), in relation to the diphenidine (**13a**), can be seen in Table 33.

**Table 33:** GC retention times for the 12 halogenated diphenidine derivatives (**20a–20l**) including relative retention time (RR<sub>t</sub>) relative to diphenidine (**13a**, R<sub>t</sub> = 15.262 mins) with eicosane (**E**) added as an internal standard (R<sub>t</sub> = 14.464, RR<sub>t</sub> = 0.95)

Compound no.	Compound Abbreviation	Compound retention time (R <sub>t</sub> /mins)	Relative Retention time (RR <sub>t</sub> )
<b>20a</b>	2-FP	15.52	1.02
<b>20b</b>	3-FP	15.22	1.00
<b>20c</b>	4-FP	15.26	1.00
<b>20d</b>	2-CP	18.01	1.18
<b>20e</b>	3-CP	17.96	1.18
<b>20f</b>	4-CP	18.50	1.21
<b>20g</b>	2-BP	19.67	1.29
<b>20h</b>	3-BP	19.92	1.31
<b>20i</b>	4-BP	20.85	1.37
<b>20j</b>	2-IP	21.99	1.44
<b>20k</b>	3-IP	22.85	1.50
<b>20l</b>	4-IP	24.59	1.61

The relative retention times from the developed method show the difficulties in trying to separate the fluorinated derivatives of diphenidine (**20a–20c**). This is a problem with the increasing popularity of fluorinated compounds being produced. There is also co-elution of the *ortho*- and *meta*-chlorine substituted isomers (**20d**, **20e**), showing there may be an issue with the polarity of compounds when trying to separate the compounds on a commonly used non-

polar column. No experiments were performed on a polar column, so possible interactions between a polar stationary phase and polar compounds could not be tested. With a polar column it would be expected that the more polar fluorinated compounds would produce stronger interactions, with the polar column, eluting later than the less polar iodinated compound. However, when the diphenidine derivatives were ran on a polar column the isomeric pairings reacted in the same manner, with retention times altering by the same difference.

The relative retention times ( $RR_t$ ) compared to diphenidine (**13a**) for the bromo- and iodo-substituted derivatives (**20g–20l**) shows clear separation that would provide baseline separation if the BP and IP regioisomers were to be run all as a mixture. Rather than all samples being run as a mixture, three mixtures were prepared containing all positional isomers. Each positional isomer shows clear baseline separation from one another when included as an isomeric mixture (figure 96–figure 98) Diphenidine was included in the three isomer mixtures to show where the compound would elute and shows that baseline separation is not possible between diphenidine and each of the fluorinated derivatives ( $RR_t = 1$ ). This means that diphenidine cannot be included as an internal standard for quantification and calculation of relative retention, so eicosane must be used.

As well as the separation in the retention times for diphenidine derivatives with different halogenated substituents, there are clear differences between the mass spectroscopy data of each differing substituent. The main difference is seen in the base peaks produced, with all adulterants and cutting agents producing different mass spectra as well. All spectra are shown in figure 99–figure 105 with the common base peak structure for all derivatives shown in figure 95. There is also a clear difference with the chloro- and bromo-compounds based on the number of active isotopes present for each atom. Chlorine contains two active isotopes,  $^{35}\text{Cl}$  and  $^{37}\text{Cl}$ , which appears in a 3:1 ratio and causes each mass fragmentation peak to appear in a 3:1 ratio in the spectra as well, with different masses for each different isotope. The bromine

atom also contains two active isotopes,  $^{79}\text{Br}$  and  $^{81}\text{Br}$ , in an abundance ratio of 1:1, meaning two peaks are produced for each fragmentation with equal intensities. Fluorine and iodine are both considered monoisotopic. This feature with the halogen substituents can help aid with the identification of street samples.

The main problem with using the mass spectrometry data for identification purposes comes when looking at the regioisomers from each substituted halogen, with each producing identical spectra.

Method validation was performed for all three of the isomer mixtures, without the inclusion of diphenidine, in order to show the linearity and repeatability of the developed method. Five calibration standards were prepared between the region of  $100\ \mu\text{g mL}^{-1}$  and  $300\ \mu\text{g mL}^{-1}$  and run using the matching method to the previous mixtures. All 12 halogenated derivatives, along with the three additional adulterants; benzocaine (B); caffeine (C) and paracetamol (P), demonstrated a linear response between this concentration range ( $R^2 \geq 0.99$ ). The limits of detection and quantification for the analytes were determined, based on the standard deviation of the response and the slope, as being 0.5–2.1 and  $1.6\text{--}6.2\ \mu\text{g mL}^{-1}$  respectively. All samples showed acceptable repeatability, with 6 repeats performed, producing a relative standard deviation percentage (%RSD) range from 0.8–5.8%. The only two samples that produced slightly higher deviations were the paracetamol and 4-IP samples (10.4% and 9.9% respectively). This was only seen with the  $100\ \mu\text{g mL}^{-1}$  standards, however, due to the small change in concentration injection creating bigger alterations in the peak areas created. These %RSD values are still much lower than the values reported for the diphenidine derivatives (section 4.5) and this can be explained through the use of an automated injection system, compared to a manual injector, removing any possible errors in injection volume.

Accuracy for the method was performed using three spiked samples ranging from 80-120% of the targeted value. In this case the target value was set at  $200\ \mu\text{g mL}^{-1}$ , meaning percentage recovery samples were prepared at  $160\ \mu\text{g mL}^{-1}$ .

$\text{mL}^{-1}$ ,  $200 \mu\text{g mL}^{-1}$  and  $240 \mu\text{g mL}^{-1}$ .  $200 \mu\text{g mL}^{-1}$  was chosen due to the ease of sample preparation as well as the concentration falling at the centre of linearity for calibration standard range. All percentage recovery results for the triplicate runs at each concentration, for all compounds, are contained within the supplementary, (Supplementary information: Table S23-Table S34). All samples showed acceptable percentage recovery (% assay) with calculated concentrations falling within  $\pm 2\%$  of the prepared sample and acceptable %RSD values all falling below 2%. The 4'-position isomers showed the highest percentage recovery values with the closest values to 102%. Based on the accuracy and precision experiments it is considered acceptable that street samples can be tested both qualitatively and quantitatively using GC-MS analysis.

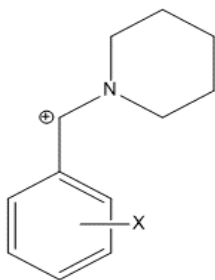


**Figure 95:** Base peak fragmentation for all the halogenated diphenidine regioisomers

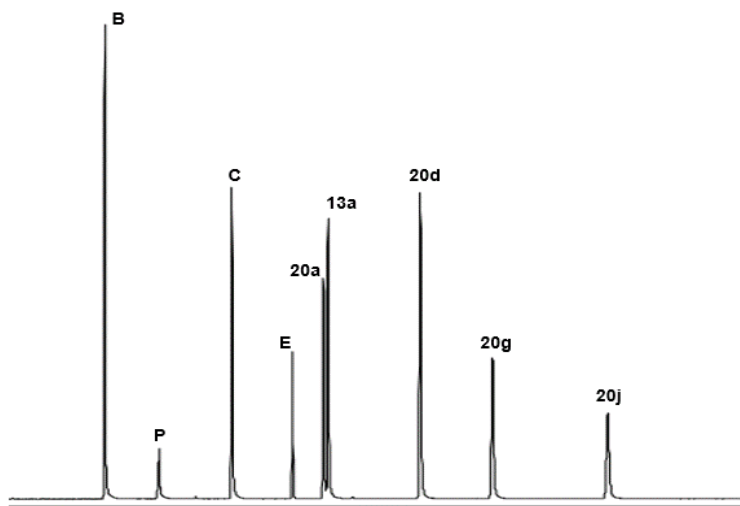


**Figure 96:** GC chromatogram for the mixture of 2'-positional halogenated diphenidine compounds with the inclusion of common adulterants: benzocaine (**B**); paracetamol (**P**); caffeine (**C**) and the internal standard eicosane (**E**)

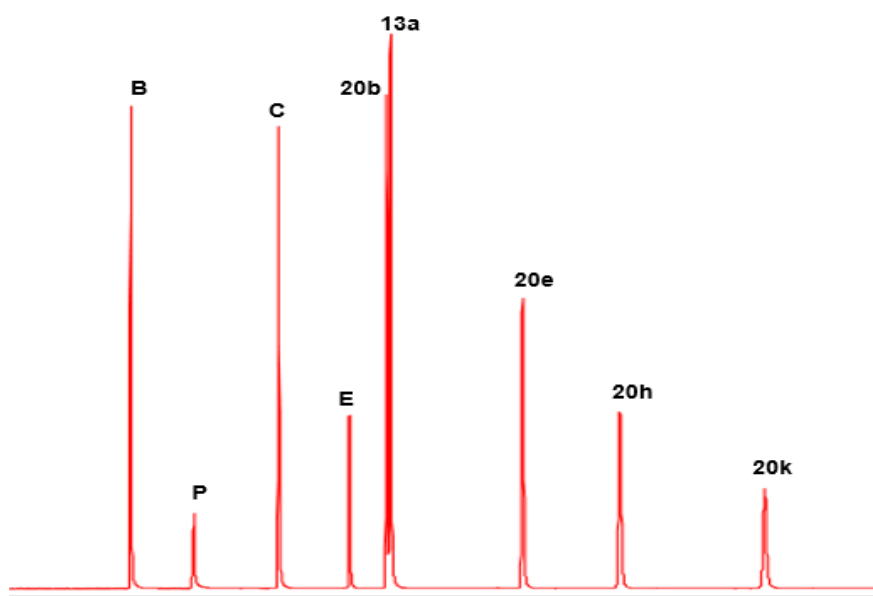


**Figure 97:** GC chromatogram for the mixture of 3'-positional halogenated diphenidine compounds with the inclusion of common adulterants: benzocaine (**B**); paracetamol (**P**); caffeine (**C**) and the internal standard eicosane (**E**)

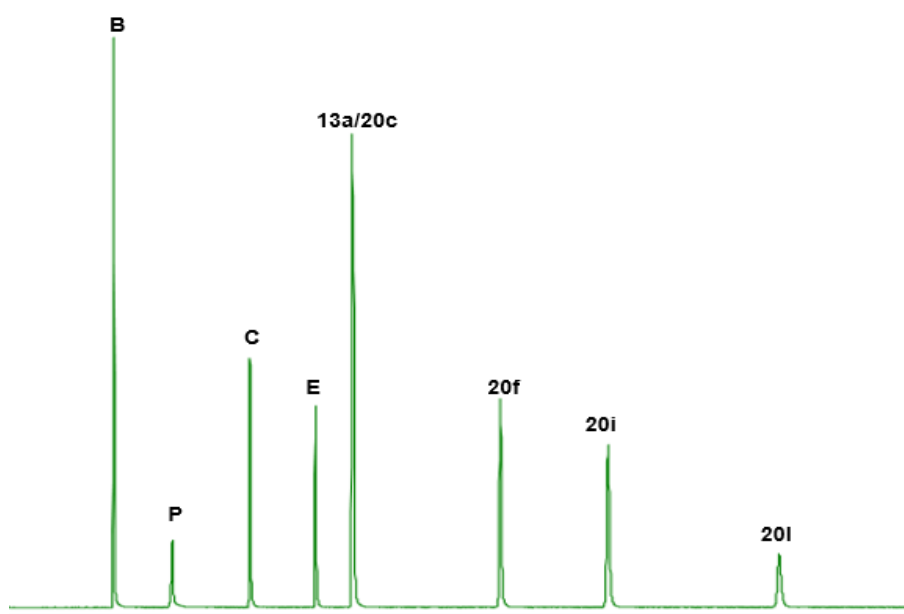


**Figure 98:** GC chromatogram for the mixture of 4'-positional halogenated diphenidine compounds with the inclusion of common adulterants: benzocaine (**B**); paracetamol (**P**); caffeine (**C**) and the internal standard eicosane (**E**)

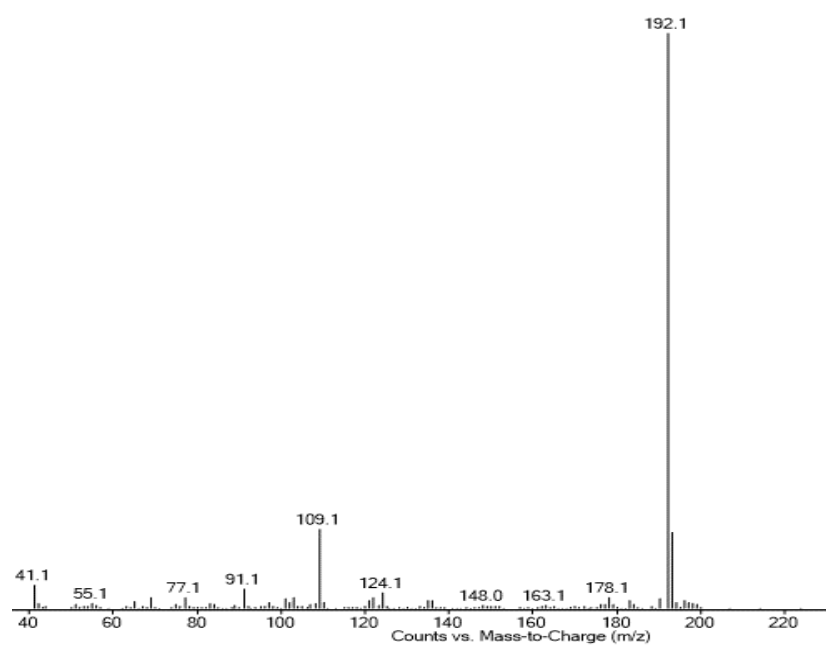


**Figure 99:** Mass spectrum for all fluphenidone regioisomers (20a-20c)

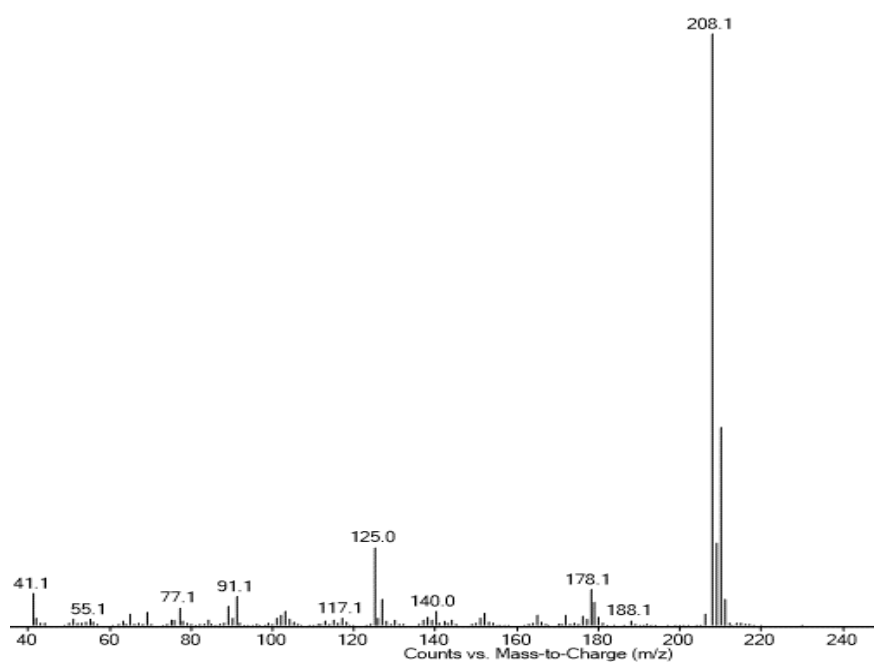


**Figure 100:** Mass spectrum for all chlorphenidone regioisomers (20d-20f)

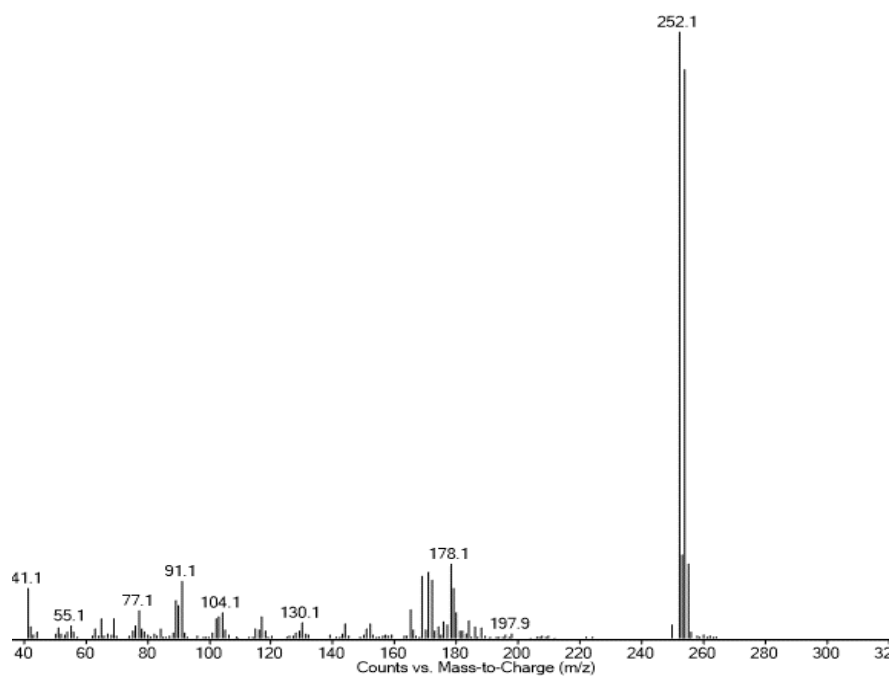


**Figure 101:** Mass spectrum for all brophenidine regioisomers (20g–20i)

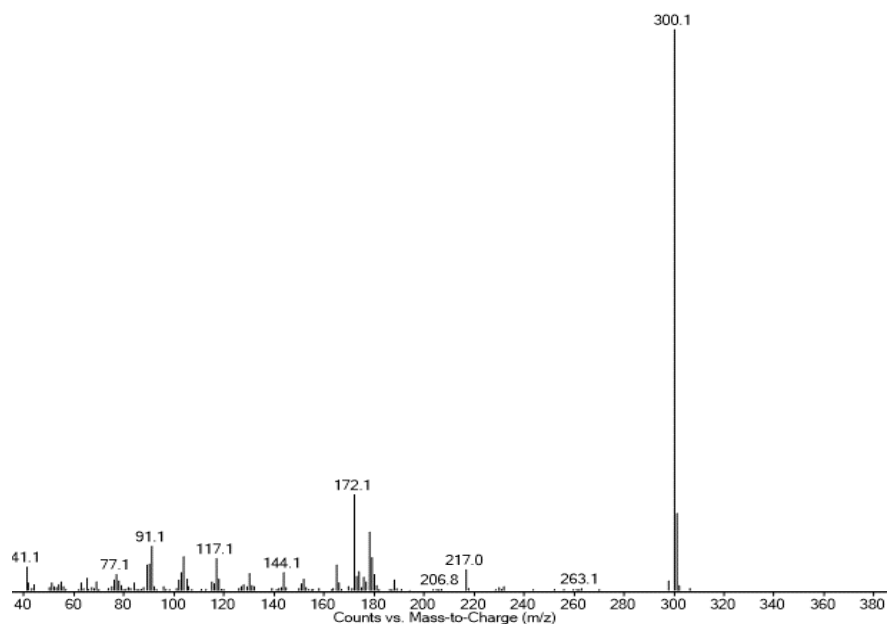


**Figure 102:** Mass spectrum for all iodophenidine regioisomers (20j–20l)

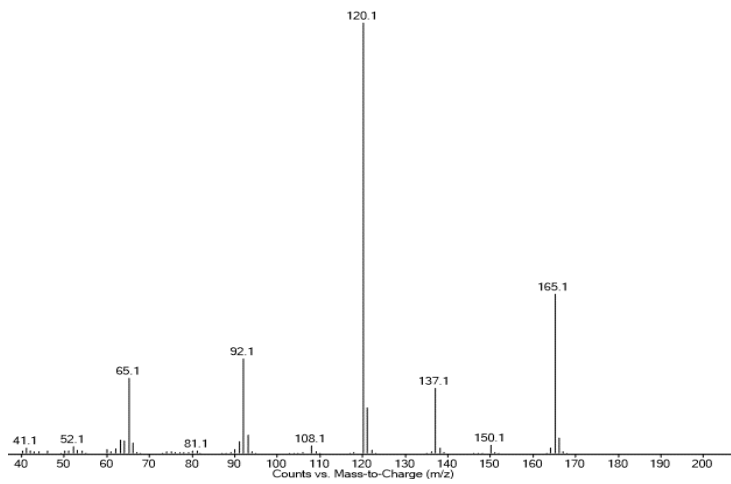


**Figure 103: Mass spectrum for benzocaine (B)**

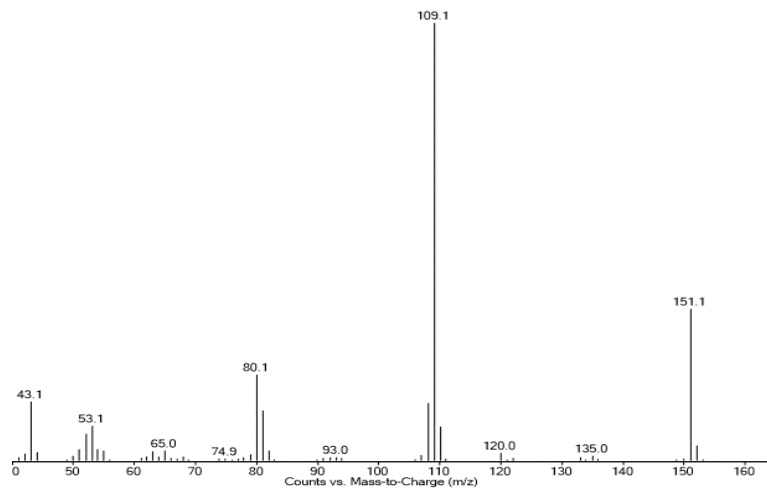


**Figure 104: Mass spectrum for paracetamol (P)**

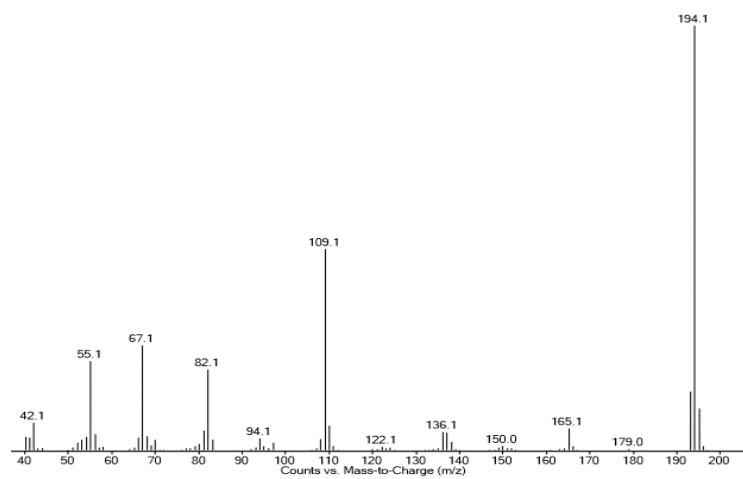


**Figure 105: Mass spectrum for caffeine (C)**



**Table 34:** GC-MS validation figures for the halogenated diphenidine derivatives (**20a-20l**) and the three added adulterants: benzocaine (**B**); paracetamol (**P**) and caffeine (**C**). Key: <sup>x</sup>Relative Retention time with respect to eicosane (**E**, R<sub>t</sub> = 14.464 min)

Analyte	R <sub>t</sub> (mins)	RR <sub>t</sub> <sup>x</sup>	Regression Coefficient (R <sup>2</sup> )	LOD (µg mL <sup>-1</sup> )	LOQ (µg mL <sup>-1</sup> )	Precision (%RSD) n=6				
						100 µg mL <sup>-1</sup>	150 µg mL <sup>-1</sup>	200 µg mL <sup>-1</sup>	250 µg mL <sup>-1</sup>	300 µg mL <sup>-1</sup>
<b>Benzocaine</b>	10.05	0.69	0.992	0.66	2.01	1.46	1.43	3.33	2.14	2.93
<b>Paracetamol</b>	11.32	0.78	0.997	1.65	5.01	10.41	3.30	2.59	2.70	1.09
<b>Caffeine</b>	13.03	0.90	0.991	1.13	3.42	5.27	3.38	1.66	1.37	2.74
<b>20a</b>	15.52	1.07	0.993	0.91	2.76	2.30	2.49	3.96	3.53	1.62
<b>20b</b>	15.22	1.05	0.990	1.73	5.24	3.87	0.86	0.43	2.14	1.38
<b>20c</b>	15.26	1.06	0.990	2.05	6.22	2.19	2.63	2.10	2.58	2.03
<b>20d</b>	18.01	1.25	0.994	0.53	1.60	3.44	3.66	4.14	1.17	2.51
<b>20e</b>	17.96	1.24	0.990	1.66	5.03	2.78	4.00	0.80	2.61	1.63
<b>20f</b>	18.50	1.28	0.993	1.62	4.90	5.23	2.96	2.82	1.82	0.84
<b>20g</b>	19.67	1.36	0.991	0.86	2.61	3.97	4.68	3.29	4.75	2.03
<b>20h</b>	19.92	1.38	0.993	1.91	5.78	3.56	3.02	0.89	3.23	1.93
<b>20i</b>	20.85	1.44	0.993	0.99	3.00	5.06	3.79	1.81	0.90	2.20
<b>20j</b>	21.99	1.52	0.992	0.96	2.91	4.89	4.42	2.42	4.96	2.12
<b>20k</b>	22.85	1.58	0.994	1.81	5.49	5.32	3.47	0.90	3.88	1.08
<b>20l</b>	24.59	1.70	0.994	1.66	5.03	9.87	4.56	3.10	2.33	1.33

## 5.6. 60 MHz NMR presumptive testing

The 60 MHz Pulsar instrument was used to obtain  $^1\text{H}$  NMR experiments on all the halogenated diphenidine derivatives (**20a–20l**). The spectra produced showed very similar patterns to those produced when characterising compounds synthesised, using 400 MHz instruments. The 60 MHz measurements allows similar structural information to be attained, as with the 400 MHz instruments, with less expense and less expertise required to perform experimentation. The  $^1\text{H}$  NMR spectra were obtained at a concentration of  $10\text{ mg mL}^{-1}$ . Samples were prepared in the same manner as those used to obtain spectra on the 400 MHz instrument and each spectrum was acquired using 8 scans.

In a similar manner to the 400 MHz spectra, the 60 MHz  $^1\text{H}$  NMR experiment produces a matching aliphatic region for all the *ortho*-substituted derivatives as seen in figure 106, with the aromatic region providing the major clear difference. The  $^1\text{H}$  NMR spectra acquired at 60 MHz are equivalent to those acquired on the 400 MHz instrument, with the only difference being the splitting patterns produced. The peaks appear broader, with a loss of resolution due to a weaker magnetic field when measurements are conducted on a 60 MHz instruments compared to the 400 MHz. As well as the aromatic regions for all the 2'-substituted positions showing significant differences, there are also clear modifications in the  $^1\text{H}$  NMR spectra when looking at the aromatic regions of the *ortho*-, *meta*- and *para*-positions of the same substituted halogens. The stacked aromatic regions for the three regioisomers for each of the substituted halogens can be seen in figure 107–figure 110.

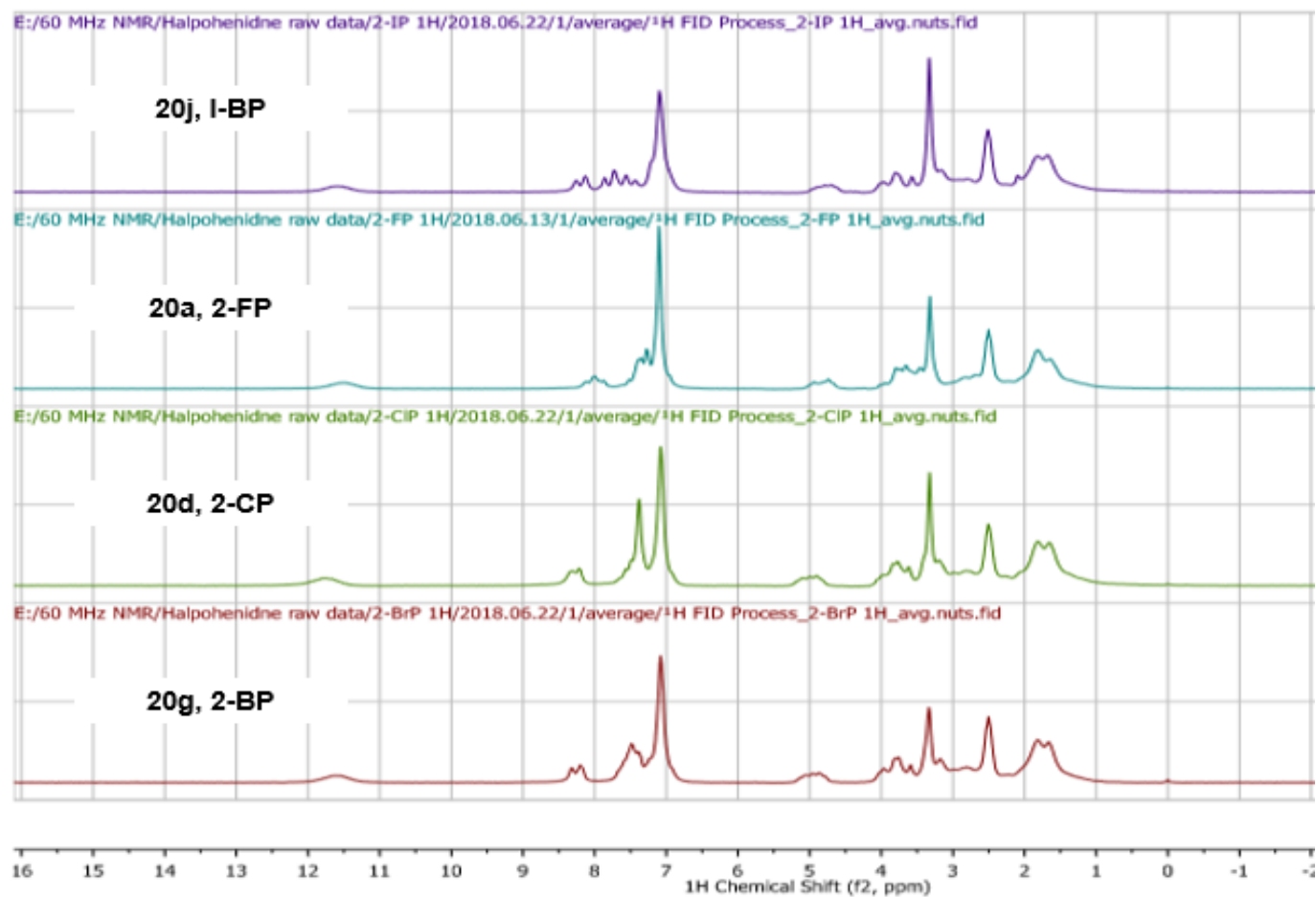


**Figure 106:** 60 MHz <sup>1</sup>H NMR spectra for the 2'-positional halogenated derivatives acquired in DMSO-d<sub>6</sub> (δ ppm = 2.50)

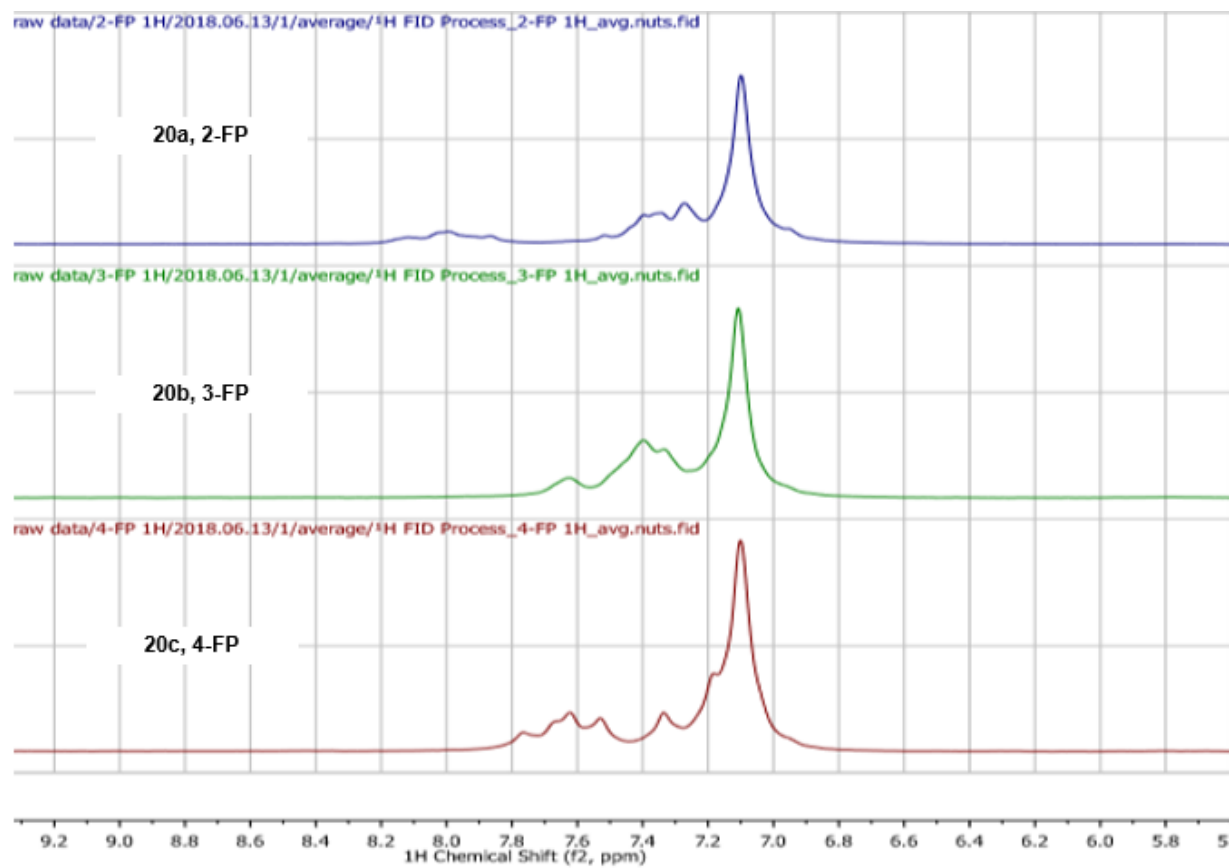


**Figure 107:** <sup>1</sup>H NMR spectra showing the aromatic region only of the fluphenidone regioisomers (**20a–20c**) acquired on a 60 MHz instrument

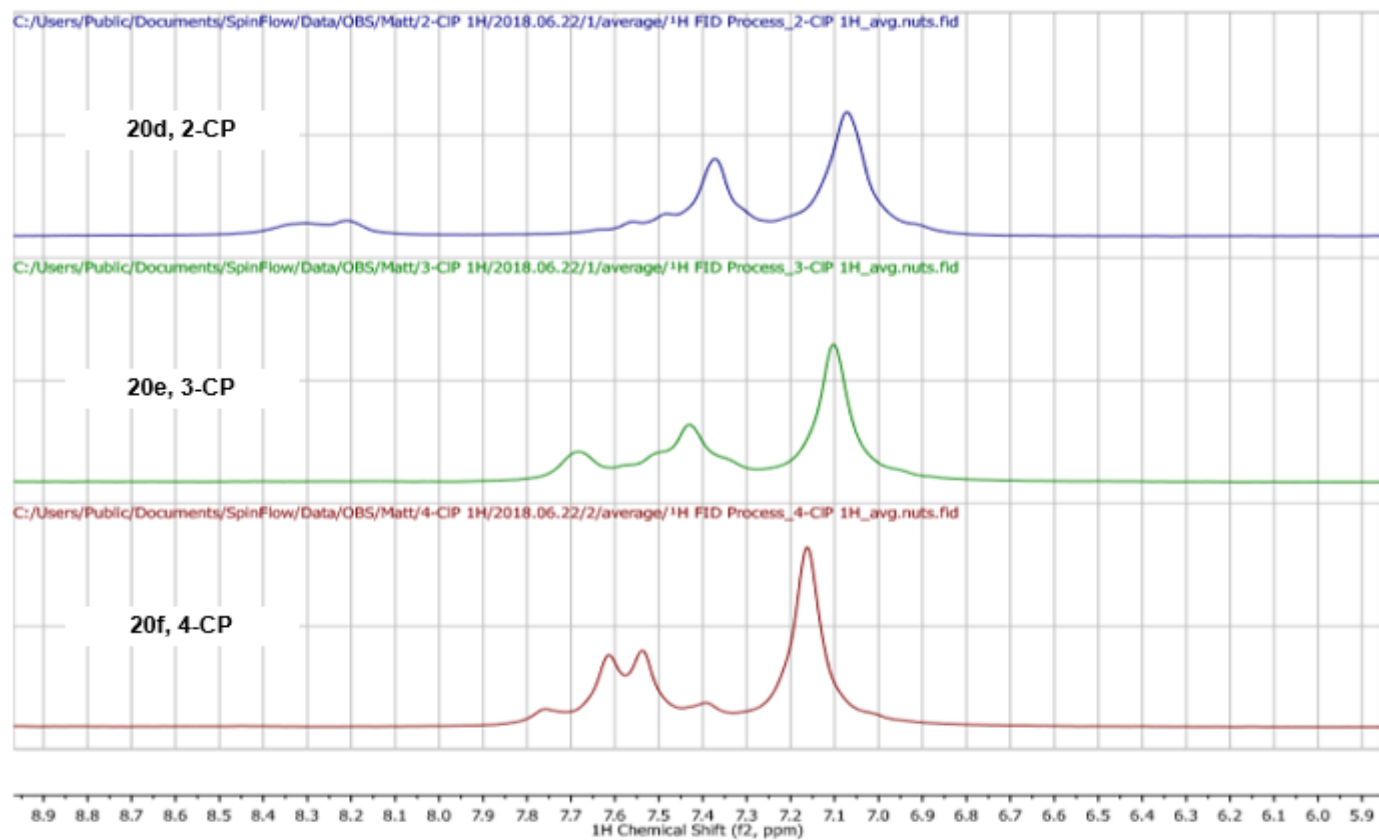


**Figure 108:** <sup>1</sup>H NMR spectra showing the aromatic region only of the chlophenidine regioisomers (**20d–20f**) acquired on a 60 MHz instrument

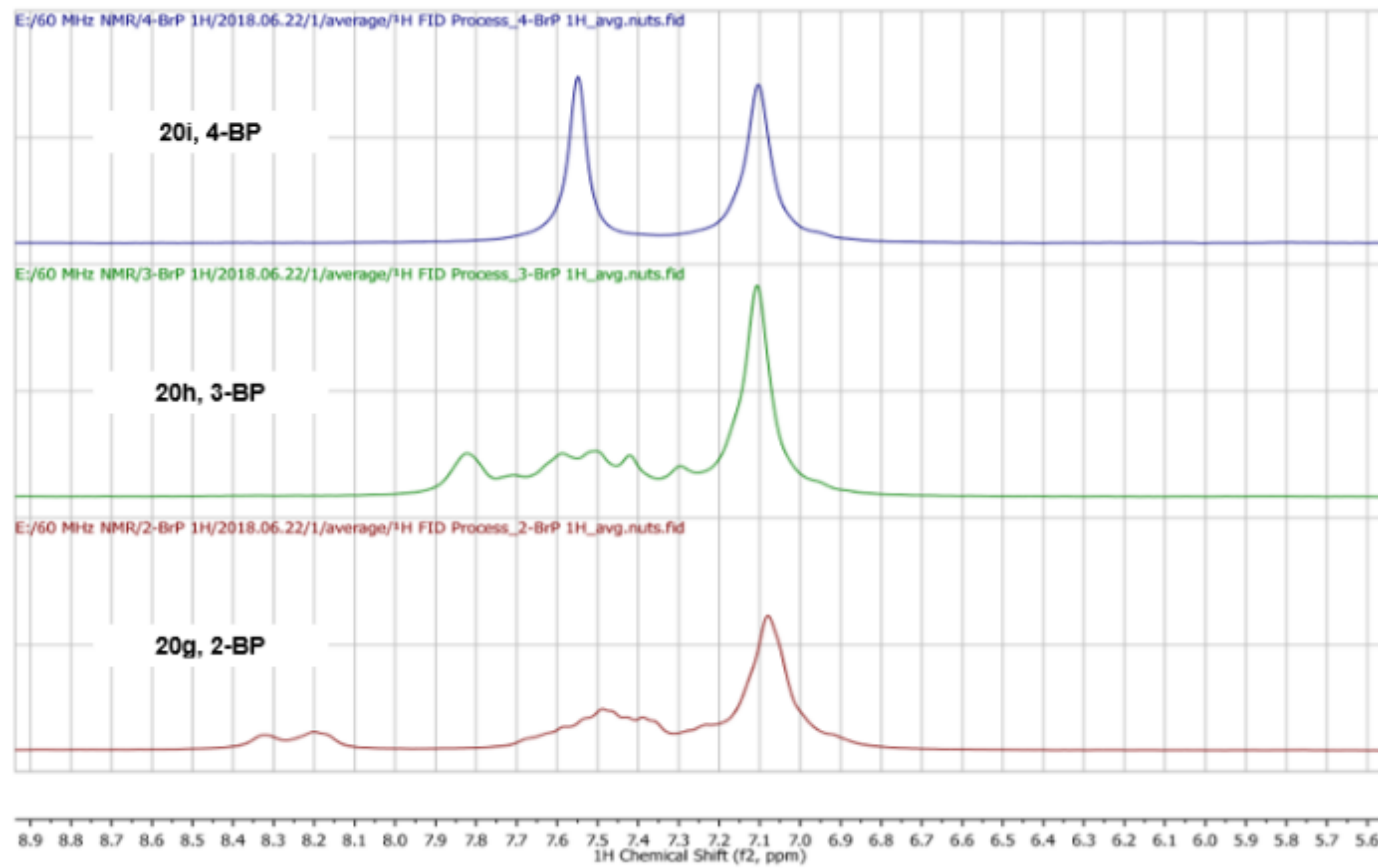


**Figure 109:** <sup>1</sup>H NMR spectra showing the aromatic region only for the brophenidine regioisomers (**20g–20i**) acquired on a 60 MHz instrument

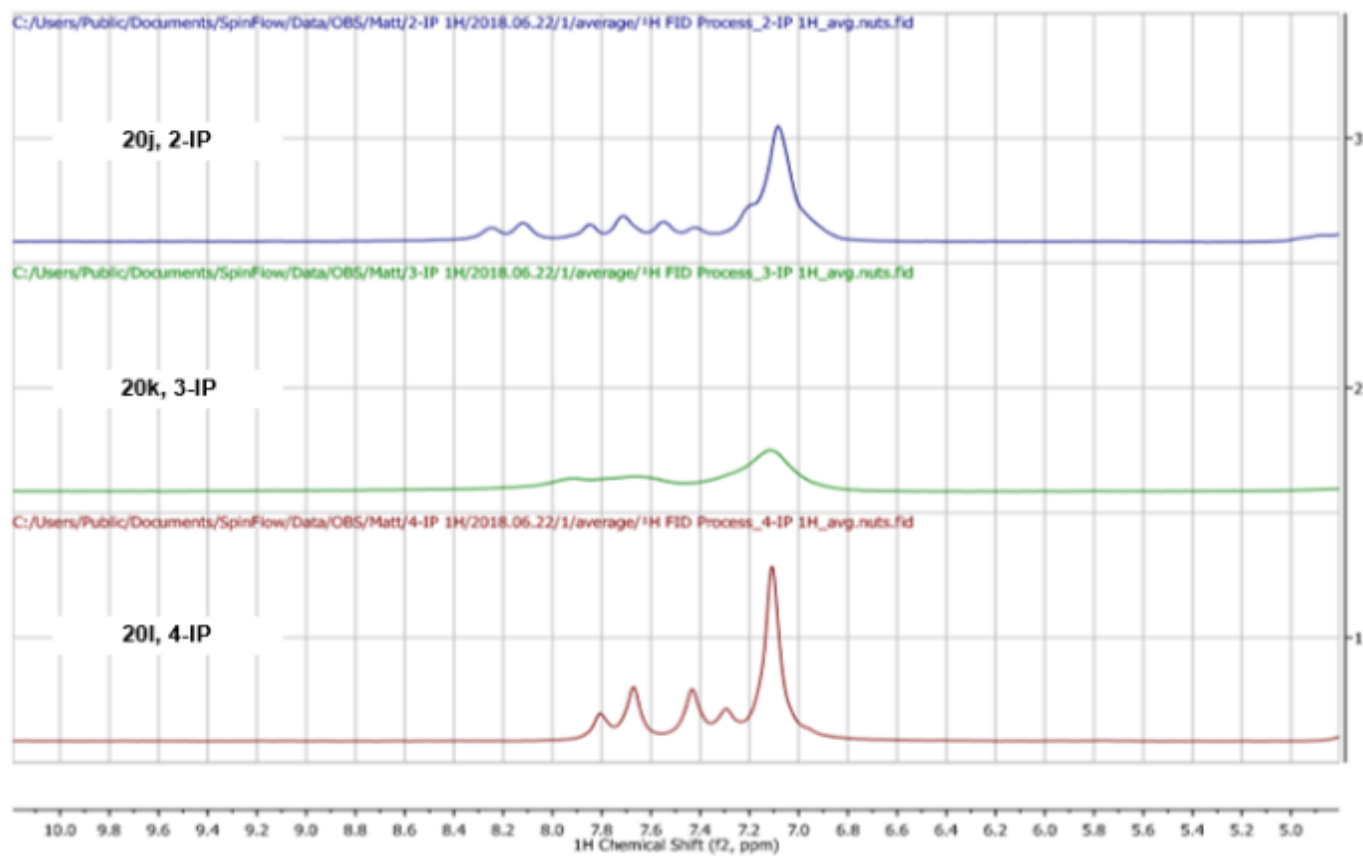


**Figure 110:** <sup>1</sup>H NMR spectra showing the aromatic region only for the iodophenidine regioisomers (**20j–20l**) acquired on a 60 MHz instrument

<sup>19</sup>F NMR measurements were also performed on a 60 MHz Pulsar instrument, on the relevant fluorinated substances (**20a-20c**), in order to show possible distinguishable features in the spectra. The stacked fluorinated spectra (figure 111) show the possibility of easily distinguishing **20a** from **20b** and **20c**, however the latter two regioisomers cannot be distinguished from one another. The chemical shift values can be seen in Table 35, which are referenced to trifluoroacetic acid (0.01% v/v) which has a chemical shift value of -76.55 ppm.

**Table 35:** Table containing <sup>19</sup>F NMR chemical shift data for the fluphenidine regioisomers (**20a-20c**) run on a 60 MHz instrument

<b>Compound no.</b>	<b>Compound name</b>	<b><sup>19</sup>F chemical shift (δ ppm)</b>
<b>20a</b>	2-fluphenidine	-115.71
<b>20b</b>	3-fluphenidine	-110.90
<b>20c</b>	4-fluphenidine	-110.81

With the ease of sample preparation and distinguishable features in the aromatic regions of the <sup>1</sup>H spectra, it is possible for the 60 MHz instrumentation to act as a presumptive test to identify the presence of a halogenated diphenidine regioisomer. The <sup>19</sup>F NMR data also helps to aid with possible identification of the fluorinated derivatives. Current literature suggests that no prior measurements have been made into the detection of halogenated derivatives using NMR instrumentation as a presumptive test.



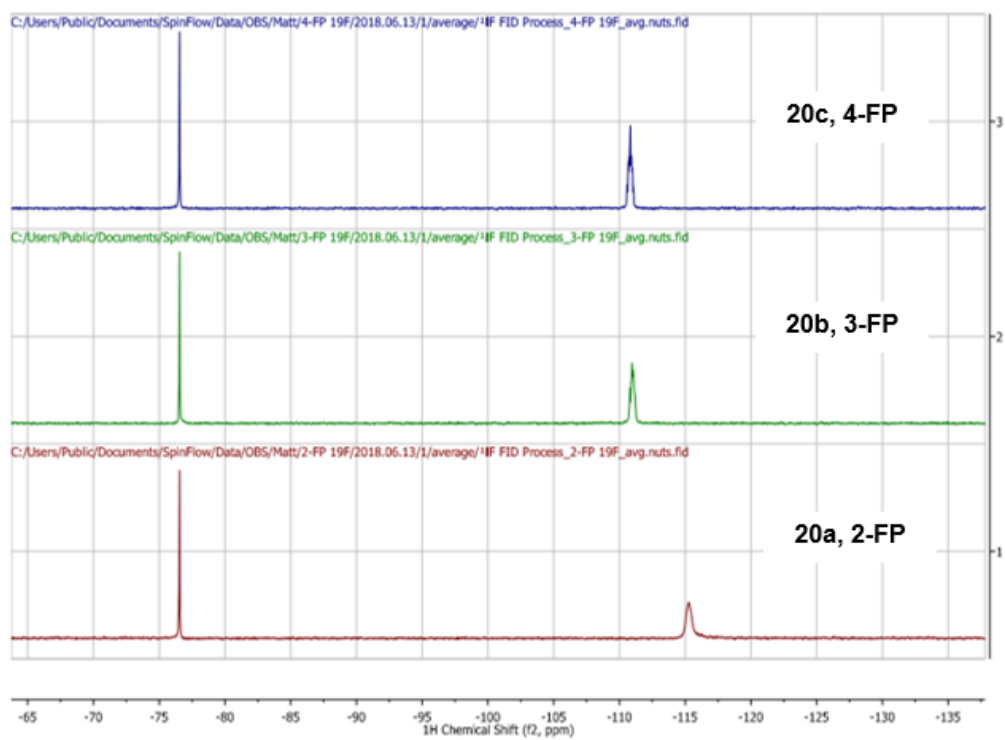


**Figure 111:** Stacked  $^{19}\text{F}$  NMR spectra for the fluphenidone regioisomers run in DMSO with the inclusion of trifluoroacetic acid (TFA,  $\delta$  ppm = -76.55)

## 5.7. Forensic application

Two unknown, white powder samples (SS-H1 and SS-H2) were analysed in order to show the possibility of using the 60 MHz NMR and GCMS instruments to detect the presence of halogenated regioisomers.

Initially, presumptive tests were carried out using the same procedures reported for the reference materials (section 2.2). Both street samples presented a positive reaction when tested with the Marquis and Mandelin reagents, changing to a dark orange and dark yellow colour respectively. When the Scott's test was employed, a blue colour was observed for both compounds showing the possible presence of a diphenidine derivative, as all diphenidine reference materials change the Scott's reagent from a red to a blue colour. Although the colour tests do not show the exact compound that is present in the street samples, it helps to narrow down possibilities with the 2-CP isomer and all the iodophenidines regioisomers reacting in a similar manner with the Marquis and Mandelin reagents.

Thin layer chromatographic (TLC) analysis of the two samples utilizing a silica gel stationary phase and a mobile phase consisting of dichloromethane-methanol (9:1 v/v) containing 0.8% ammonia (7 N in methanol) indicated that street sample 1 contained a single component (SS-H1,  $R_f = 0.71$ ), while the second street sample appeared to contain two components with the second spot not appearing as clearly under UV as the primary spot (SS-H2,  $R_f = 0.70$  and  $0.55$ ). The  $R_f$  values for the two street samples appears to fall within the range created when the chlorphenidine regioisomers are analysed using a matching experimental setup. The spot created at a retention factor of  $0.55$  does not appear to matchup with any of the halogenated regioisomers.

Both street samples were then analysed using the 60 MHz NMR instrument using a matching  $^1\text{H}$  and  $^{19}\text{F}$  experiment to the ones performed with the reference material. In both cases the  $^{19}\text{F}$  experiments were performed with TFA as reference ( $\delta$  ppm =  $-76.55$ ) and no sample peaks were generated. This shows that the street samples cannot be a fluorinated substituted substance,

narrowing down the possible compounds present in a 5 minute experiment. A matching  $^1\text{H}$  experiment was performed subsequent to this and the two spectra can be seen in figure 112.

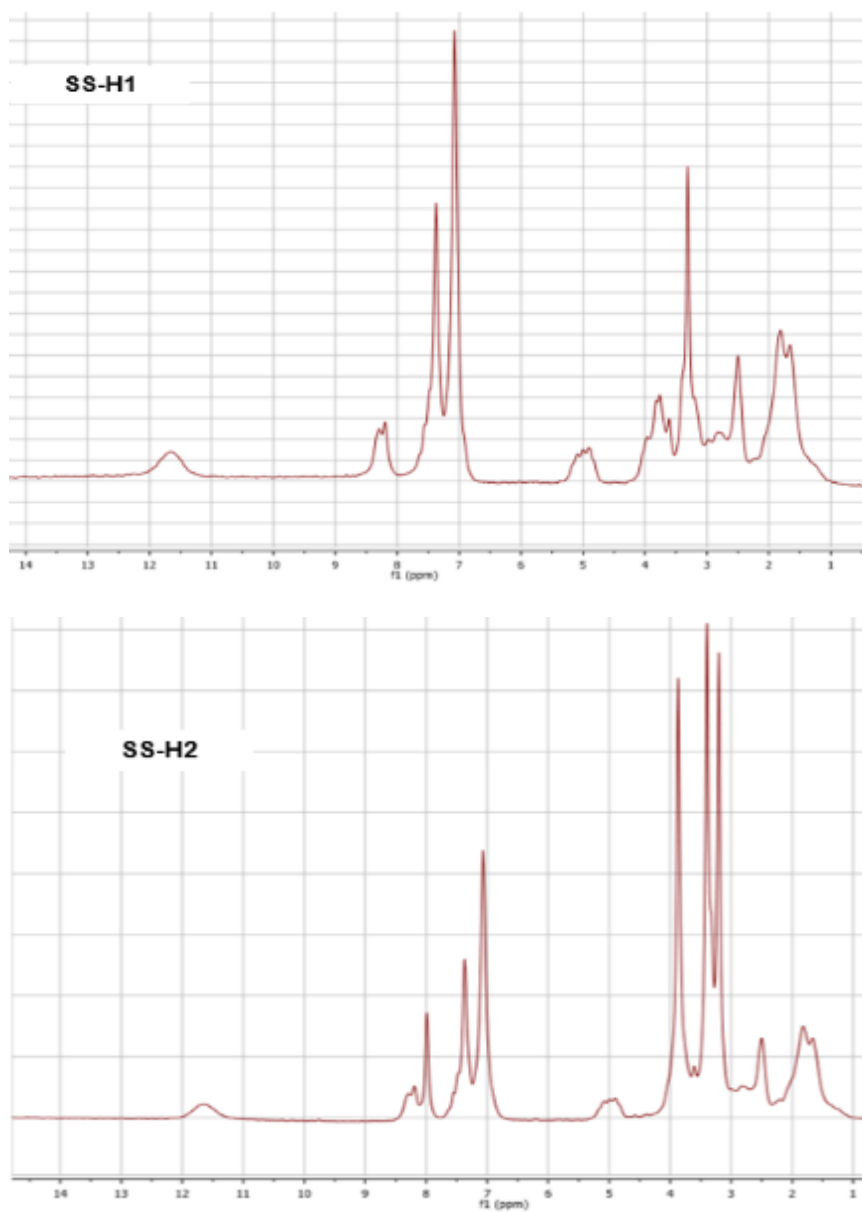


**Figure 112:**  $^1\text{H}$  NMR spectra run in DMSO ( $\delta$  ppm = 2.50), measured on a 60 MHz instrument for the two street samples (SS-H1 and SS-H2)

SS-H1 shows very similar pattern matching in the aliphatic region with all the halogenated diphenidine derivatives. It then also shows a very similar pattern to the 2-Cl isomer (figure 113) in the aromatic region.

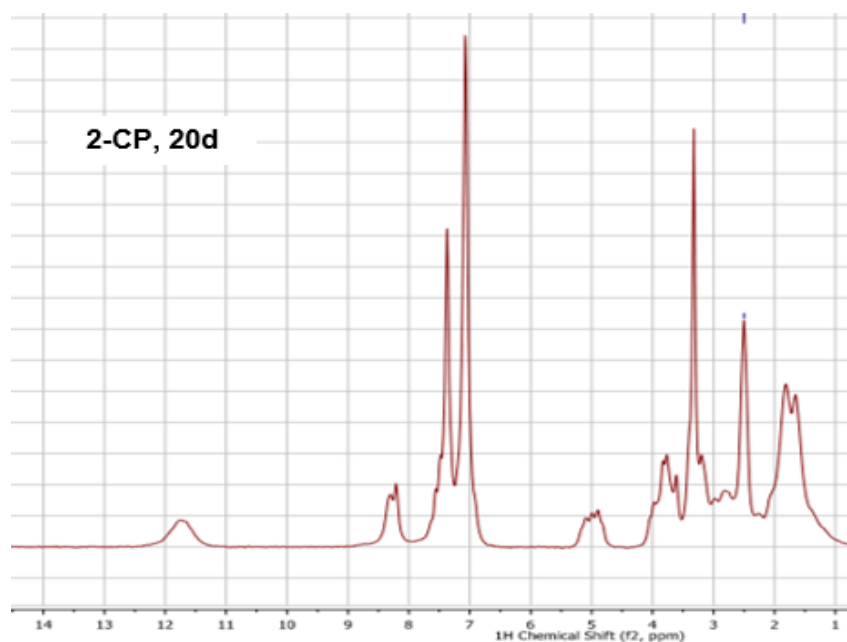


**Figure 113:** Full <sup>1</sup>H NMR spectrum for the 2-CP standard (**20d**), performed on a 60 MHz instrument in DMSO-d<sub>6</sub> ( $\delta$  ppm = 2.50)

The second street sample (SS-H2) shows a very similar pattern, however there are additional peaks in the aliphatic region compared to all halogenated diphenidine derivatives. This is seen at 3.2 ppm with a peak that appears to overlap just below 4 ppm. The peaks at 1.65 ppm and 5 ppm do show a very similar splitting pattern between SS-H2 and SS-H1, with the reference materials, which suggests that the second street sample could be a halogenated diphenidine derivative with slight impurities, or a compound with a very similar chemical structure. The aromatic region for SS-H2 still also shows a very similar pattern to the 2-CP isomer's aromatic region with an additional peak at 8.1 ppm. This could again be due to a slight adulterant in the street sample as the remaining peaks and pattern matches to the reference material. In both cases the 60 MHz NMR provides a good initial indication as to the active component present, suggesting a match to the 2-CP isomer, and allows easier identification to be made with the common confirmatory tests.

Both SS-H1 and SS-H2 were then tested on the GC-MS in order to confirm the active ingredients present in the samples. The two samples were prepared at a concentration of  $100 \mu\text{g mL}^{-1}$ , through dissolution in methanol and dilution, to match the qualitative analysis of the reference materials. The two chromatograms produced are shown in figure 114 and figure 115.

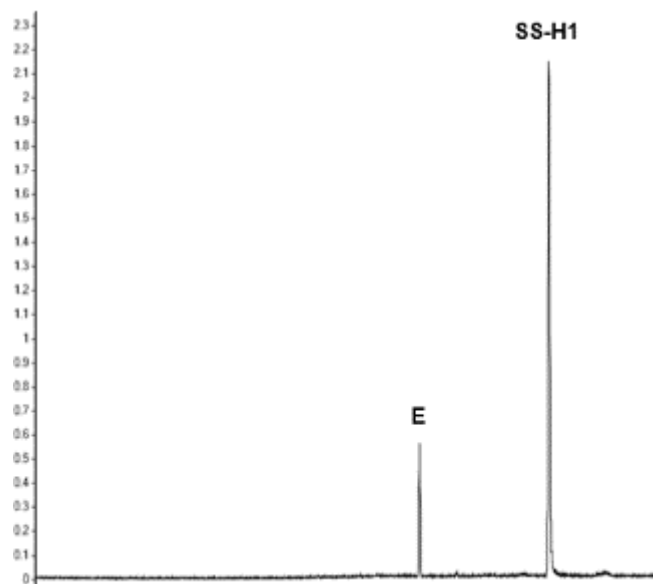


**Figure 114:** GC-MS chromatograph for SS-H1 with the inclusion of internal reference eicosane (**E**,  $R_t = 14.464$  min)

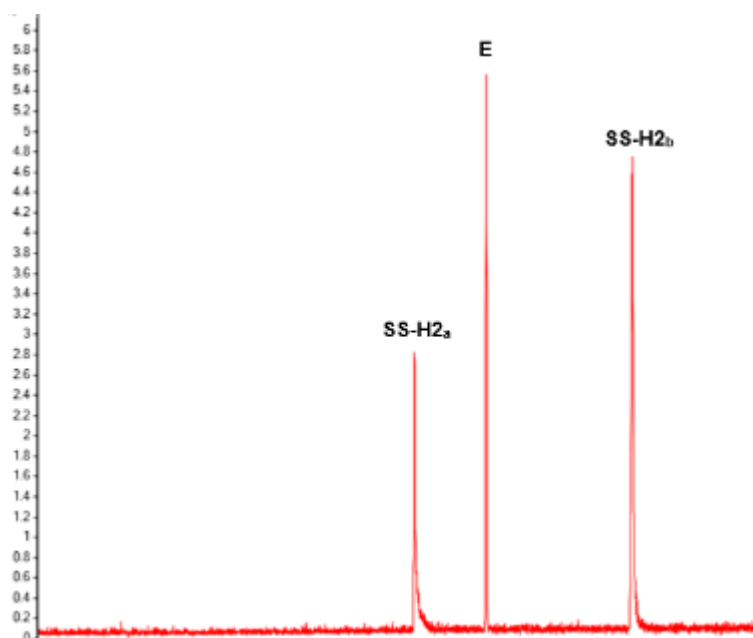


**Figure 115:** GC-MS chromatograph for SS-H2 with the inclusion of internal reference eicosane (**E**,  $R_t = 14.464$  min)

One sample peak was produced for SS-H1, while SS-H2 yielded two sample peaks, showing the possibility of either two active components or the addition of an adulterant / cutting agent, which matches observations made from the  $^1\text{H}$  NMR spectrum. Both street samples included eicosane as an internal reference standard in order to calculate relative retention times ( $\text{RR}_t$ ) for comparison with the reference compounds. The eicosane peak for both street samples appears at 14.468 min with both samples producing a sample peak at 17.9 and 17.9 min respectively. These peaks create an  $\text{RR}_t$  of 1.24, which matches closely to the  $\text{RR}_t$  values of both **20d** and **20e**. This would suggest that the active component is 2-CP as the  $^1\text{H}$  NMR spectrum produced for the presumptive testing does not match in the aromatic region to the 3-CP isomer, however it does create a close match to that of 2-CP. The mass spectrum was obtained for the sample peaks on both street samples and shows the same fragmentation masses (figure 116), however this would not help distinguish between 2-CP and 3-CP as both isomers produce matching spectra as mentioned previously.

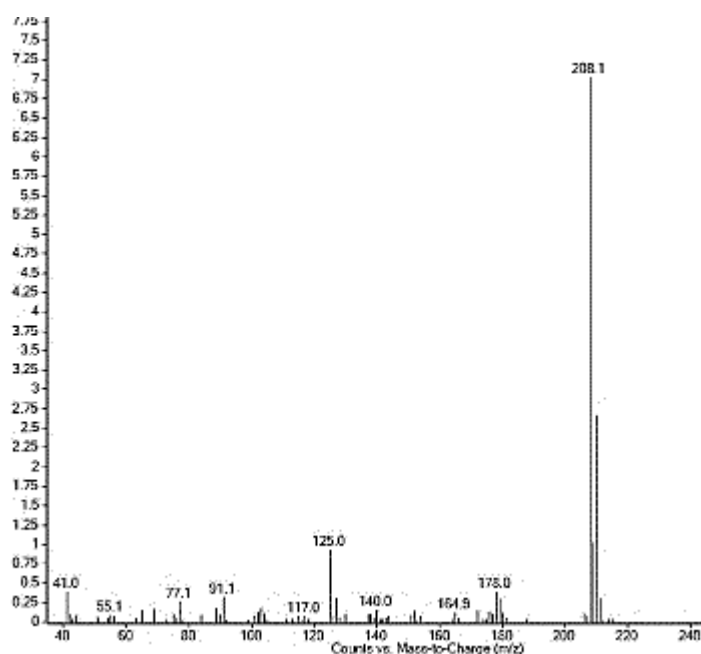


**Figure 116:** Mass spectrum for the sample peak produced in both SS-H1 and SS-H2

The second sample peak produced from SS-H2 elutes at 13.028 min with an  $RR_t$  of 0.90 when compared with eicosane. This matches the  $RR_t$  for caffeine and would account for the extra proton peaks seen, in the aromatic and aliphatic regions, of the 60 MHz NMR measurements. The mass spectrum produced also matches that of the caffeine reference.

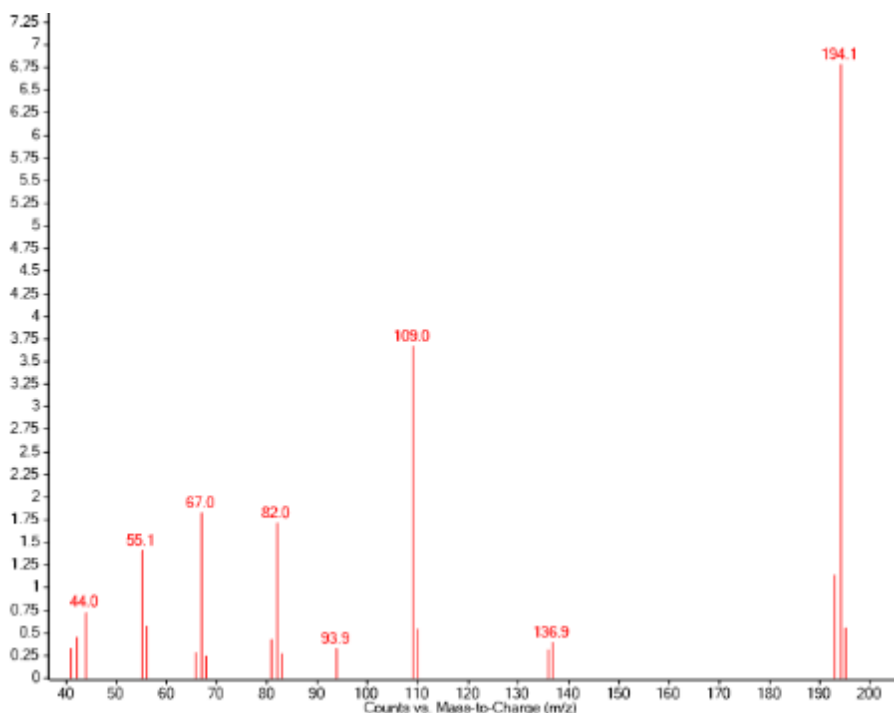


**Figure 117:** Mass spectrum produced for the adulterant peak of SS-H2

The two street samples were also run on the 400 MHz instrument in order to confirm the presence of 2-CP in both samples. The comparison spectra for the 2-CP with SS-H1 and SS-H2 can be seen in figure 118. This appears to confirm that SS-H1 is pure 2-CP with no adulterants or impurities, while SS-H2 appears to contain 2-CP with the presence of an adulterant. There are peaks present in the  $^1\text{H-NMR}$  spectrum for SS-H1 and SS-H2 that are present due to water (3.30 ppm), however this could have come from the DMSO solvent and is not considered an impurity.

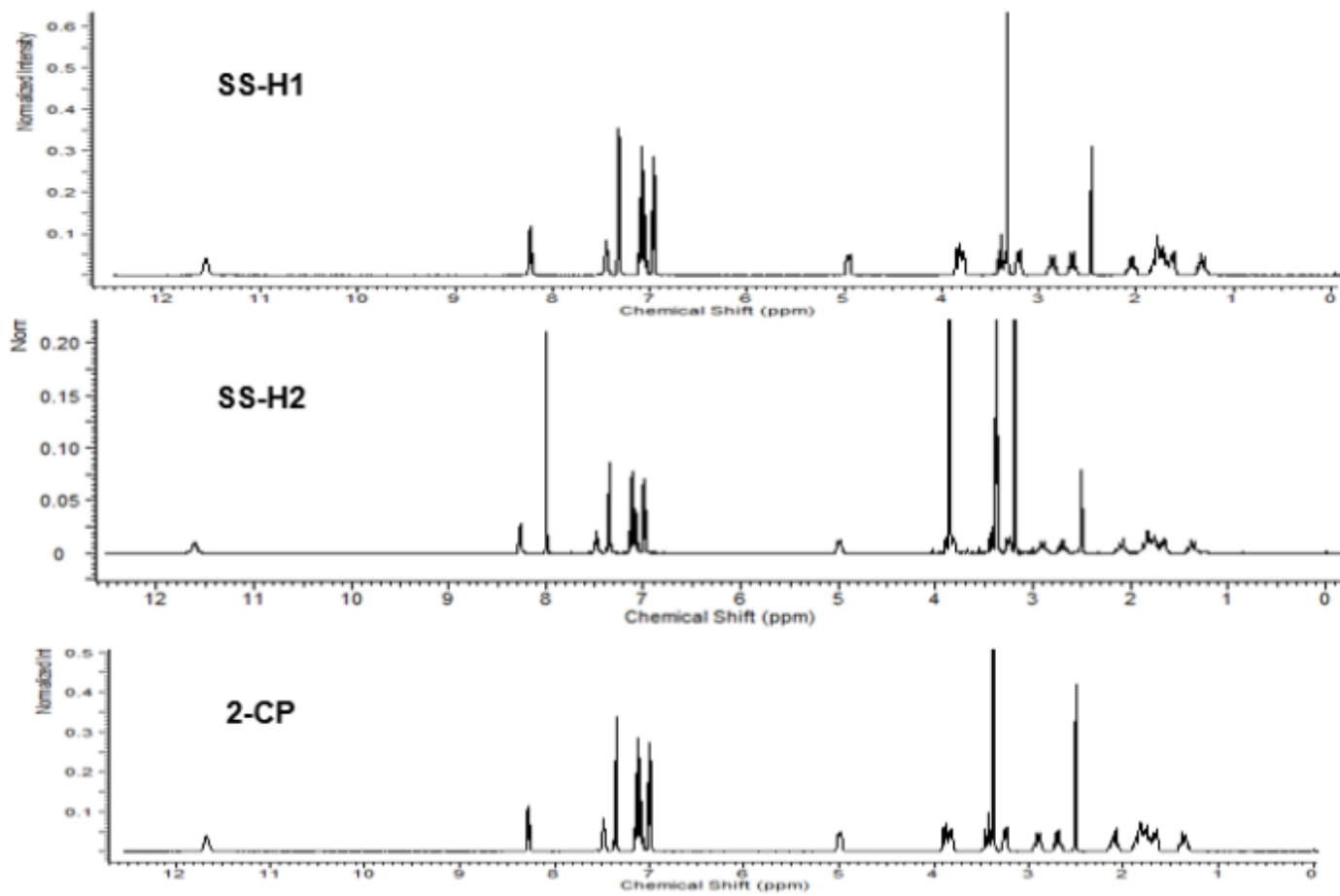


**Figure 118:** Stacked <sup>1</sup>H-NMR spectra comparison for SS-H1, SS-H2 and 2-CP run in DMSO ( $\delta$  ppm = 2.50) acquired using a 400 MHz instrument



After confirmation of the presence of 2-CP in both SS-H1 and SS-H2 and caffeine in SS-H2, qualitative analysis was performed. The two street samples were prepared at  $200 \mu\text{g mL}^{-1}$  in order to fit the middle of the calibration series for both 2-CP and caffeine. All street samples were run in triplicate in a similar manner to the percentage recovery samples and concentrations were calculated for each run based on rearrangement of the calibration graph equations (2-CP:  $y = 0.019x - 0.2916$ ; Caffeine:  $y = 0.0115x + 0.0217$ ). Tables showing integration ratios with eicosane along with concentration calculations can be seen in Table 36. Concentrations were then converted into a w/w percentage based on the original weights of the two powdered street samples (SS-H1 – 287 mg; SS-H2 – 350 mg) and averages taken.

Based on the concentrations calculated from the calibration series of both CP and caffeine it can be seen that the percentage weights of active ingredients have a combined total weight equal to the overall weight of the samples  $\pm 1\%$ . This shows that there are no additional adulterants or filling agents with street sample H1 being a pure white powder and SS-H2 a 50:50 mix of 2-CP and caffeine.

**Table 36:** Table showing concentrations and percentage weights of active ingredients in both SS-H1 and SS-H2 of caffeine and 2-CP

Sample	Integrated ratio			Concentration ( $\mu\text{g mL}^{-1}$ )			weight of active component in sample (mg) % w/w			
	Run 1	Run 2	Run 3	Run 1	Run 2	Run 3	Run 1	Run 2	Run 3	Average
SS-H1 2-CP	3.49	3.5	3.52	199.5	198.2	200.5	286.3 99.7 %	284.4 99.1 %	287.7 100.2 %	286.1 99.7 %
SS-H2 2-CP	1.56	1.61	1.59	97.5	99.8	98.9	170.6 48.7 %	174.7 49.9 %	173.1 49.5 %	172.8 49.4 %
SS-H2 Caffeine	1.13	1.15	1.17	96.4	98.4	99.7	172.2 49.2 %	168.7 48.2 %	174.5 49.8 %	171.8 49.1 %

## 5.8. Conclusions

This chapter has shown the synthesis of 12 halogenated diphenidine derivatives that have not previously been reported or analysed in order to show the possibility of detecting new compounds rapidly when NPS are created. All compounds synthesised are pure (> 95 %) with yields ranging from 26–61%, showing production can be achieved in clandestine laboratories.

Presumptive testing analysis allowed a rapid positive/negative response for the initial presence of diphenidines with Scott's test reagent. However, a positive response with the Scott's reagent could also suggest the presence of cocaine. Use of the Marquis and Mandelin reagents, in combination with the Scott's reagent, also allows identification of halogenated derivatives with slight differences between regioisomers of different substituents. However, it may be difficult to identify which isomer was present in an unknown street sample judging on just colour. The positional isomers of each halogenated substituted produce the same UV results so attachment of any UV device would not aid with separation. Some initial separation was also achieved using conventional thin layer chromatography (TLC) methods.

60 MHz NMR experiments were performed as a possible replacement presumptive test to the colour test reagents. Sample preparation for both the  $^1\text{H}$  and  $^{19}\text{F}$  experiments is simplistic with experiments carried out in under 5 minutes. Distinguishing features were shown in the aromatic region of each regioisomer in the  $^1\text{H}$  NMR spectra with a clearly identifiable pattern for diphenidine derivatives in the aliphatic region. Analysis of two street samples using 60 MHz NMR has shown that possible unknown halogenated diphenidines can be initially identified based on pattern matching of the spectra against reference spectra.

Validated GC-MS runs have been developed and validated for the first time for halogenated derivatives. All isomers in matching positions on the benzene ring have been separated in under 23 minutes. The length of the GC-MS analysis shows that presumptive 60 MHz NMR test can provide the same

result in a quicker time (5 minutes). It is also possible for non-scientists to analyse the 60 MHz NMR and compare against reference spectrum compared to the GC-MS instrumentation.

The method allows general triaging of samples, but also a quantitative method, for both pure, individual component samples, and samples cut with common adulterants. The two street samples have been analysed using the GC-MS to confirm that both contain 2-CP, with SS-H2 also containing caffeine. All active ingredients make up the full weight of the street samples ( $\pm 1\%$ ) with no further adulterations or filling agents.

## 6. Chapter 6 – Fluorinated diphenidine analogues

### 6.1. Overview

From the previous halogenated diphenidine derivatives (Chapter 4) it was observed that difficulties began when trying to separate fluorinated regioisomers. Based on this knowledge, a range of monofluorinated diphenidine analogues were prepared in order to show the ease of production and the ever changing chemical structure of NPS. Changes in chemical structures and constant appearances of NPS on the illicit drugs market provides difficulties in detection and separation through analytical techniques. Seven different amines were used, with subtle changes made between classes, to show how small changes in alkylamine sidechains can produce differences in spectra produced and possible chromatographic separation.

Characterisation was performed on all compounds in order to provide reference measurements that can be used by forensic organisations and law enforcement in order to help with rapid and easy identification when encountered in illicit samples.  $^{13}\text{C}$ ,  $^1\text{H}$  and  $^{19}\text{F}$  NMR spectroscopy was used to characterise the compounds in addition to IR and TLC. A range of presumptive tests were used to show the interactions that occur when a range of reagents, used by law enforcement, are added to the reference solutions.

Gas chromatography was used to separate mixtures of regioisomers within classes, while providing mass spectroscopy data for use as reference spectra. 60 MHz NMR was then used as a possible presumptive testing instrument, with  $^1\text{H}$  and  $^{19}\text{F}$  experiments again performed to show the ability to distinguish between classes and then isomers within a class. This could then be used as a replacement for commonly used presumptive tests.

## 6.2. Synthesis

Fluorinated diphenidine regioisomers and its analogues were synthesised as hydrochloride salts. All target compounds were prepared as racemic mixtures, using a matching method to the synthesis of diphenidine, from previously reported methods.<sup>102</sup> The synthesis of the fluorinated analogues differed through the alteration of the aldehyde and amine utilised, with the three isomeric fluorinated benzaldehydes used in each case. The different amines used along with the final products produced, abbreviations and percentage yields, can be seen in table 37. Reference materials were produced as stable, colourless to off-white powders.

**Table 37:** Percentage yields of all fluorinated diphenidine analogues showing all names, abbreviations and different amines used in synthesis

Compound no.	Compound name	Amine used	Abbreviation	Yield (%)
20a – 20c	fluphenidine	piperidine	FP	33 – 44
15a – 15c	fluoroephenidine	ethylamine	FEP	51 – 64
19a – 19c	fluorolintane	pyrrolidine	FL	51 – 59
21a – 21c	fluoromephenidine	methylamine	FMP	48 – 60
22a – 22c	fluorodimephenidine	dimethylamine	FDMP	41 – 46
23a – 23c	fluorodiephendine	diethylamine	FDEP	54 – 68
24a – 24c	flurotrifluoroephenidine	trifluoroethylamine	FTFEP	37 – 45

The percentage yields show how consistent the synthesis of these classes of compound can be and how easily clandestine labs can produce these substances. The hydrochloride salts were determined to be soluble (10 mg mL<sup>-1</sup>) in deionised water, methanol, dichloromethane and dimethylsulfoxide. To ensure the authenticity of the materials utilised in this study the synthesised compounds were fully structurally characterized, to produce reference spectra, by <sup>1</sup>H NMR (figure 121-figure 132), <sup>19</sup>F NMR (Table 43) and <sup>13</sup>C NMR

(supplementary data: Figure 32-Figure 49). The purity of all samples was checked by GC-MS and NMR analysis and shown to be >95% in all cases.

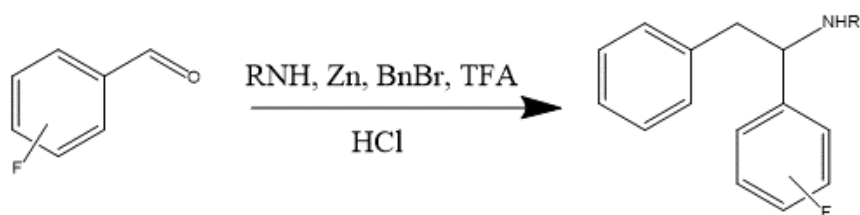


**Figure 119:** Reaction scheme for the synthesis of the fluorinated diphenidine analogues

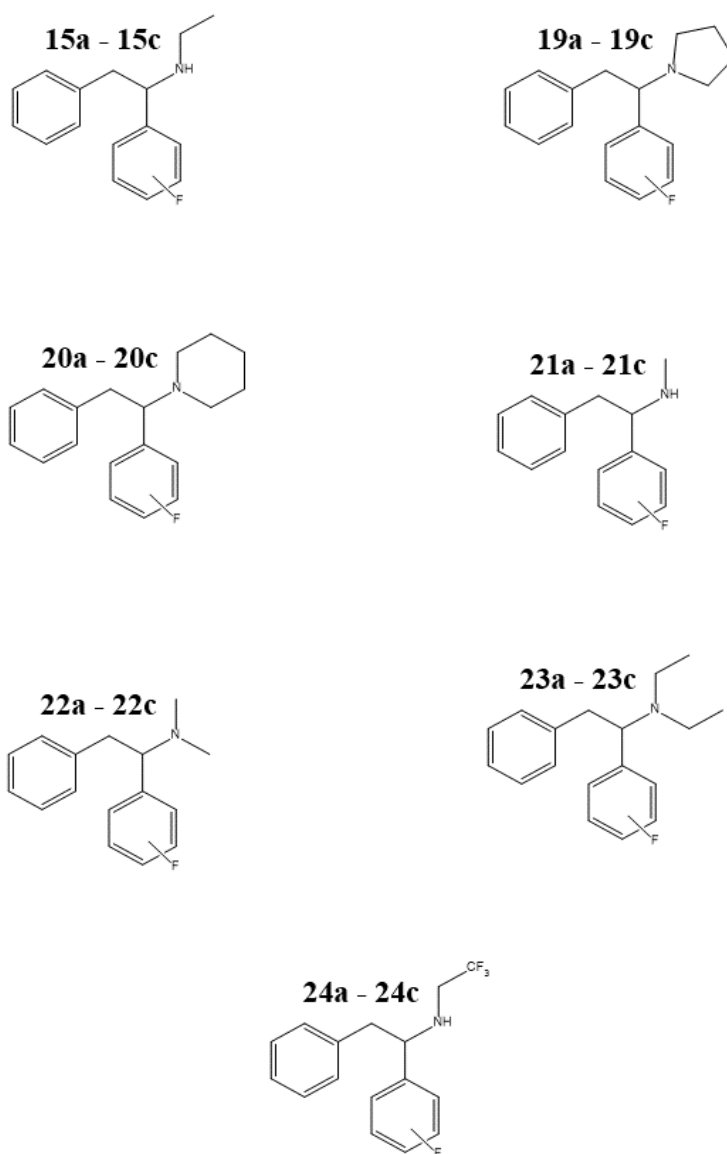


**Figure 120:** Chemical structures for all fluorinated diphenidine analogues synthesised

Although the fluorinated diphenidine analogues are closely related to the structure of diphenidine the alteration of the amine chain/group yields a different aliphatic region in the  $^1\text{H}$  NMR spectra. These clear differences can be seen for all seven of the different classes of diphenidine analogue, while each individual fluorine positional isomer, within a class, produces a different aromatic region. The difference in the aromatic regions for each class of compound can clearly be seen whilst differences are also observed between the aliphatic regions within a class, when the fluorine is substituted in the *para*-position of the phenyl ring. All proton spectra show a solvent residual peak, for DMSO- $d_6$ , at 2.50 ppm with acetone and water peaks at 2.08 and 3.33 ppm respectively. 9 aromatic protons are seen in the aromatic region for all compounds. HMQC and COSY NMR experiments were also performed for all compounds in order to identify the assignments of the aliphatic protons, which provide the spectral differences for each class.

The  $^1\text{H}$  NMR spectra for the fluphenidine regioisomers (FP, **20a–20c**) has been described in chapter 6, producing a very similar aliphatic region to that of diphenidine (**13a**), with similar splitting and chemical shift values for the piperidine ring,  $\text{CH}_2$  of the benzyl chain and proton bonded to the chiral carbon.

The fluorolintane regioisomers (FL, **19a–19c**) produce the closest similarity to the fluphenidine regioisomers regarding structures. The use of pyrrolidine instead of piperidine creates a product with a five-membered ring instead of a six-membered ring, with 8 protons rather than 10 in the region of 1.74 ppm – 3.33 ppm. The residual peak for water at 3.33 ppm also coalesces with these peaks and the multiplet at 3.64 ppm also belongs to the pyrrolidine ring, based on coupling seen in the COSY spectra and the HMQC showing it coupling to the same carbon as the proton at 3.29 ppm. The proton bonded to the chiral centre is seen as a multiplet at 4.98 ppm with coupling to the triplet and doublet of doublets peaks at 3.89 ppm and 3.47 ppm, representing the adjacent  $\text{CH}_2$  protons.

The fluoroephenidine regioisomers (FEP, **15a–15c**) show similar aliphatic regions to all the polyfluorinated ephenidine regioisomers seen in chapter 5.



The chiral centre proton is seen at 4.70, with the CH<sub>2</sub> proton peaks adjacent seen at 3.65 ppm and 3.17 ppm. The splitting observed matches that seen by all other diphenidine analogues. The CH<sub>3</sub> protons from the ethyl chain are seen at the triplet peak at 1.22 ppm, with coupling in the COSY spectrum to the multiplet peaks at 2.73 ppm and 2.89 ppm, representing the adjacent CH<sub>2</sub> protons. In a similar manner to the CH<sub>2</sub> protons of the benzyl chain, these two protons exist in different chemical environments with the proton more downfield being more deshielded due to the closeness of the fluorine substituent.

The fluoromephenidine regioisomers (FMP, **21a–21c**) contain peaks at 4.68, 3.67 and 3.17 ppm with the same assignment as the FEP regioisomers. There is also a CH<sub>3</sub> peak, however this appears as a singlet peak at 2.42 ppm as there are no other protons to couple with.

In a similar manner to the similarity between the FEP and FMP isomers, there is also the same similarity between the FDEP and FDMP regioisomers. Both compounds produce spectra with peaks at 4.92 ppm, for the chiral centre proton, and at 3.78 and 3.41 ppm for the adjacent CH<sub>2</sub> protons. The FDEP compounds show two triplet peaks at 1.19 ppm and 1.35 ppm representing the two CH<sub>3</sub> protons of the ethyl chain. The CH<sub>2</sub> protons of the ethyl chain are seen as two quartet peaks 2.73 ppm and 3.28 ppm. The FDMP compounds show a significant difference with no CH<sub>2</sub> protons, but two singlet peaks at 2.86 ppm and 2.62 ppm representing the two methyl groups bonded to the amine.

Finally, the three fluorotrifluorophenidine (FTFEP, **24a–24c**) regioisomers show significant differences in the aliphatic region to all other diphenidine analogue classes. The main difference in the FTFEP regioisomers comes in the region between 3.50 and 3.98 ppm as the multiplicity of the peaks produced becomes more complex and broader peaks are produced. The peaks observed in other spectra at 3.62 ppm, representing one of the protons on the CH<sub>2</sub> group adjacent to the chiral centre, begins to coalesce with CH<sub>2</sub> protons of the trifluoroethyl chain seen between 3.50 and 3.98 ppm. These protons split into more complex multiplet splitting patterns due to close

coupling with the fluorine atoms in the  $\text{CF}_3$  of the trifluoroethyl chain, however this provides a clear region of identification for the FTFEP regioisomers.

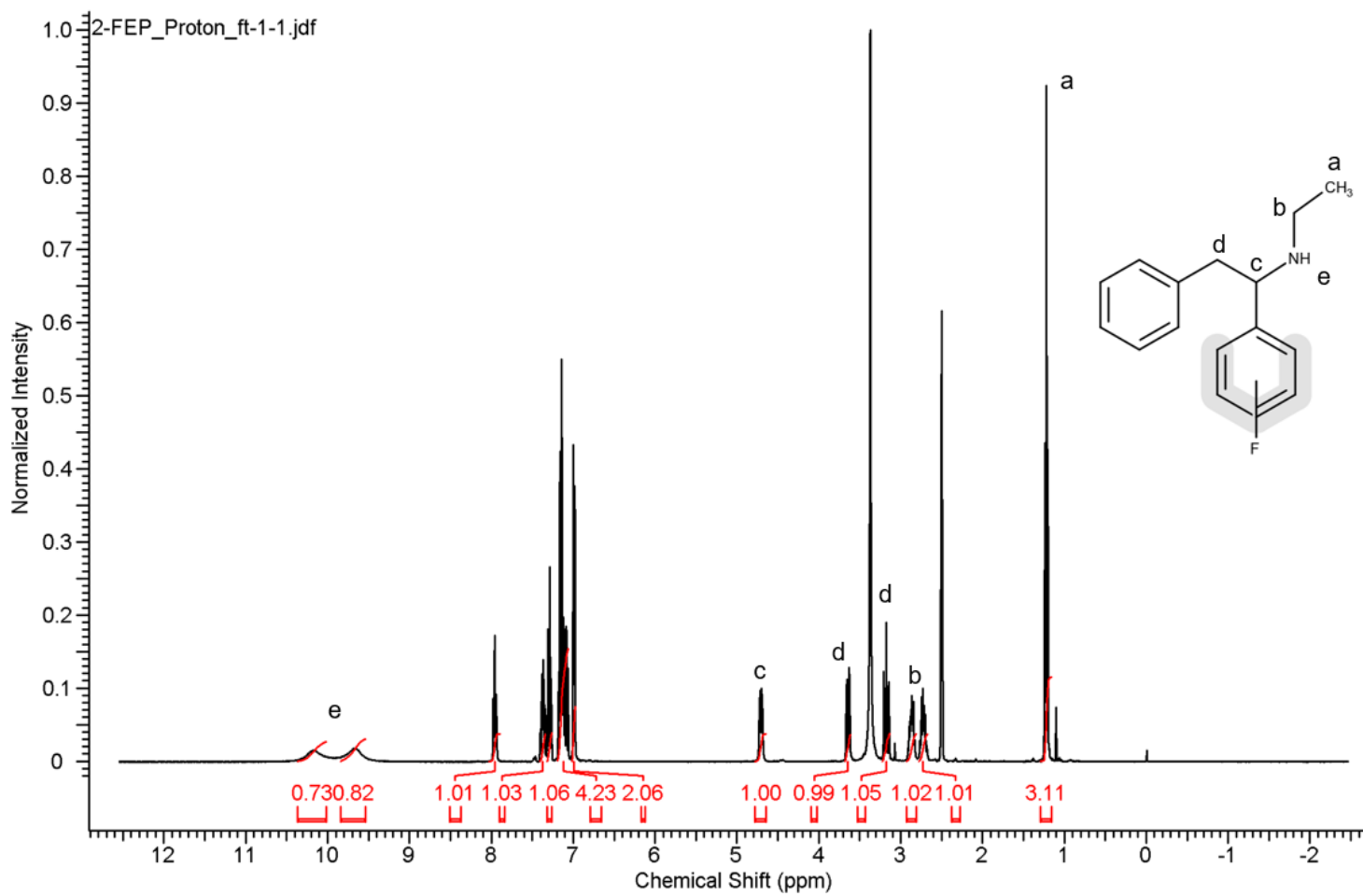


**Figure 121:** 400 MHz <sup>1</sup>H NMR spectrum for 2-fluorophenidine (2-FEP, **15a**) run in DMSO-d<sub>6</sub> ( $\delta$  ppm = 2.50)

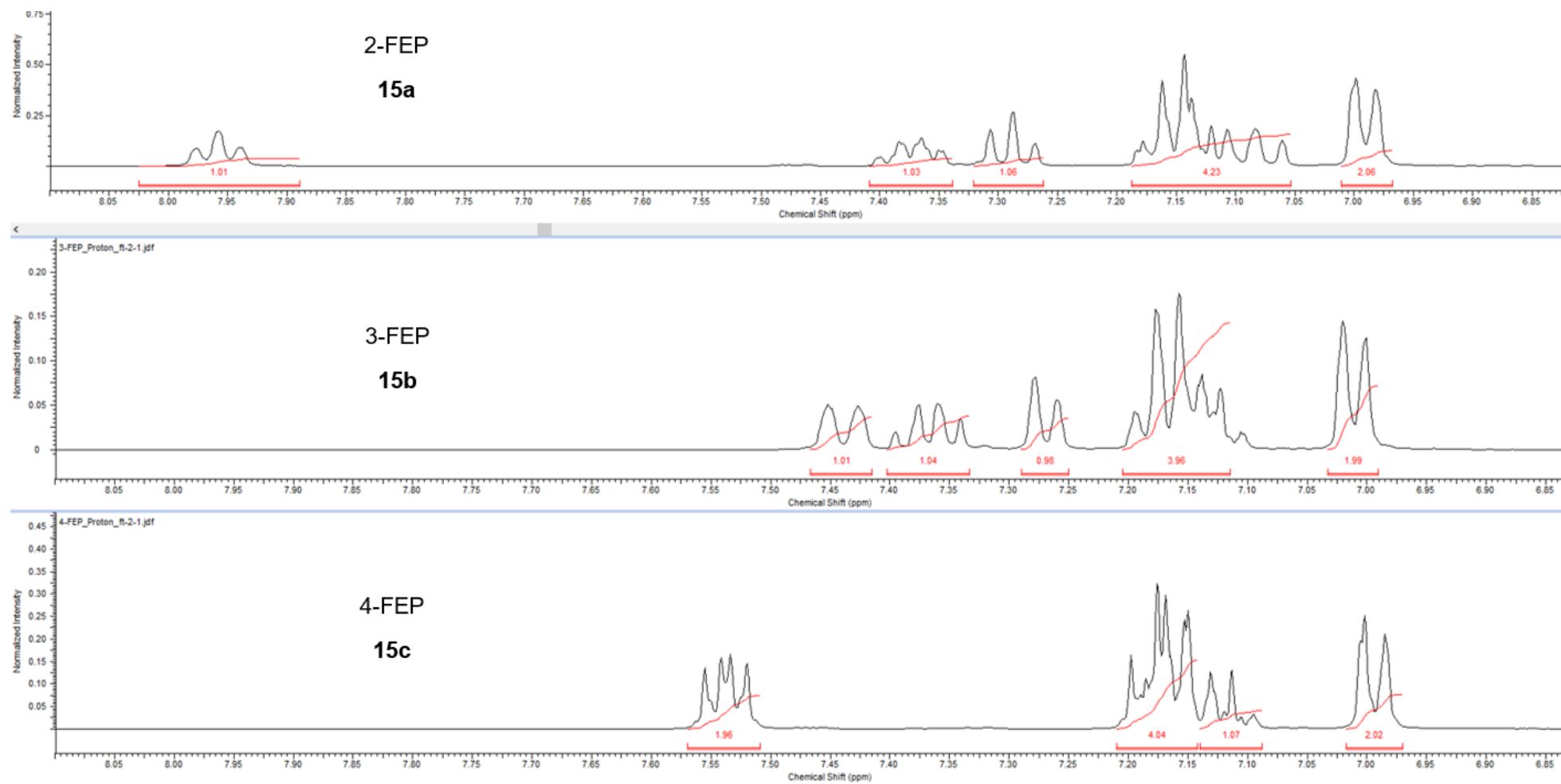


**Figure 122:** Stacked 400 MHz <sup>1</sup>H NMR spectra showing the aromatic region for the fluoroephedrine regioisomers (FEP, **15a** – **15c**)

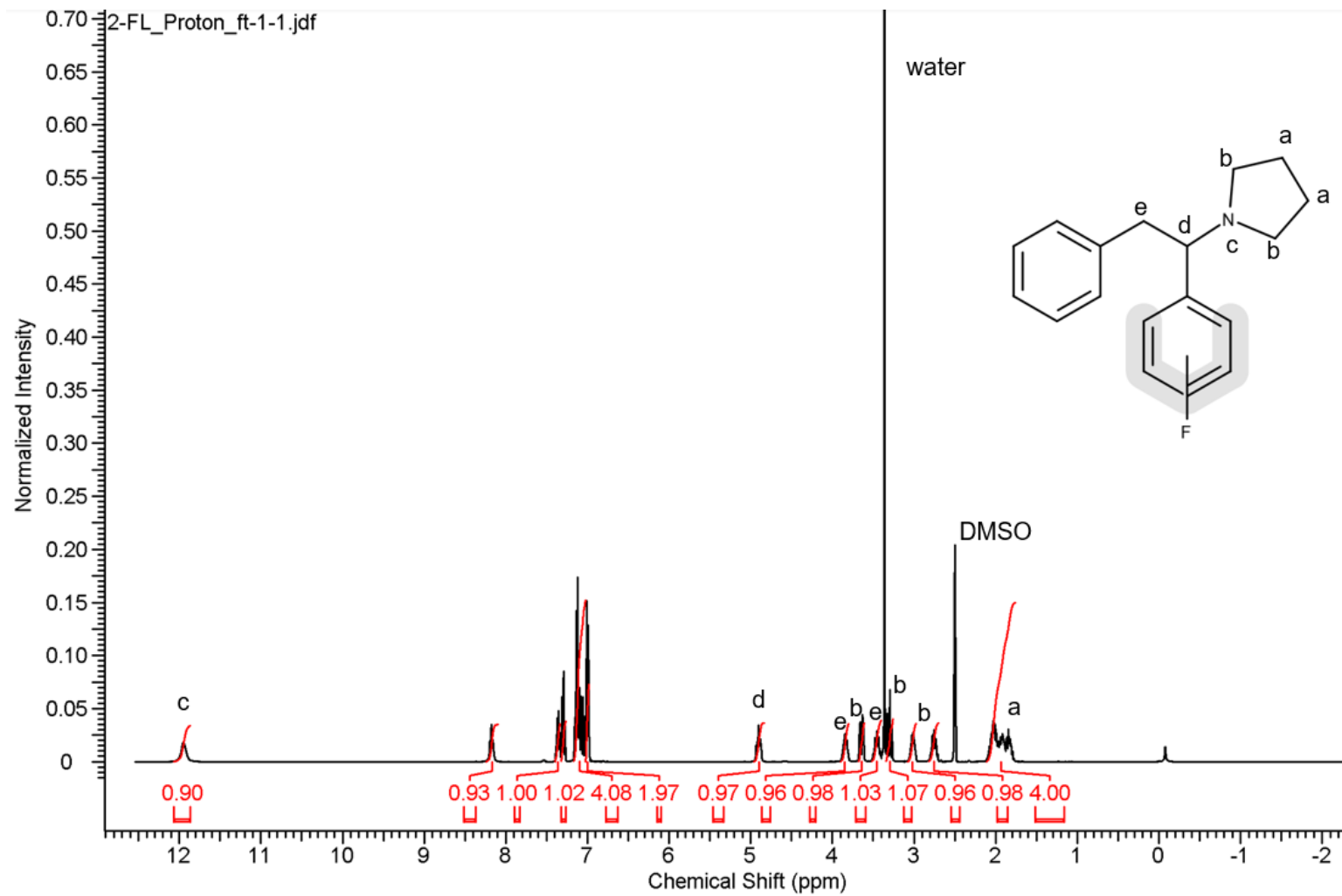


**Figure 123:** 400 MHz  $^1\text{H}$  NMR spectrum for 2-fluorolintane (2-FL, **19a**) run in DMSO- $d_6$  ( $\delta$  ppm = 2.50)

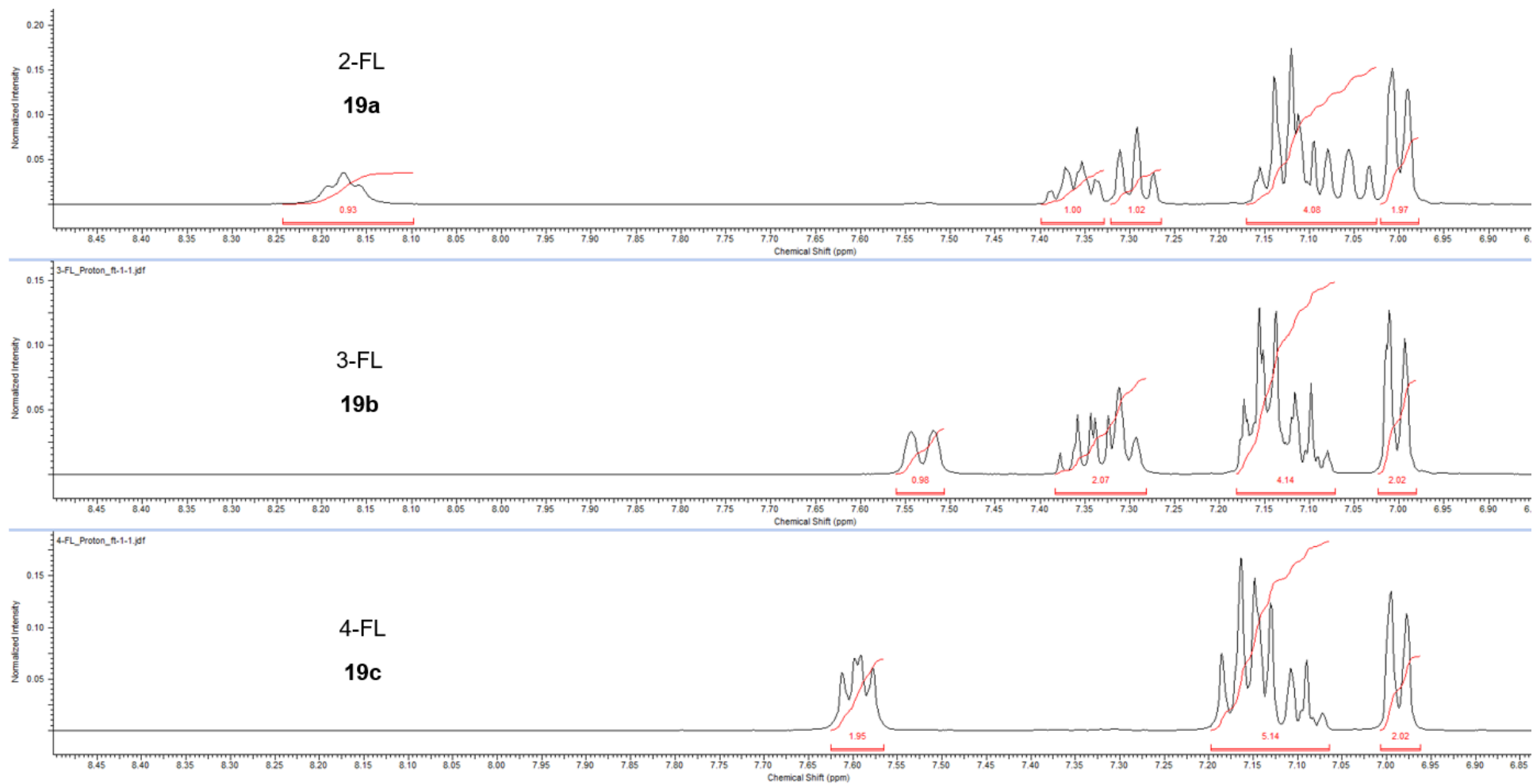


**Figure 124:** Stacked 400 MHz <sup>1</sup>H NMR spectra showing the aromatic region for the fluorolintane regioisomers (FL, **19a** – **19c**)

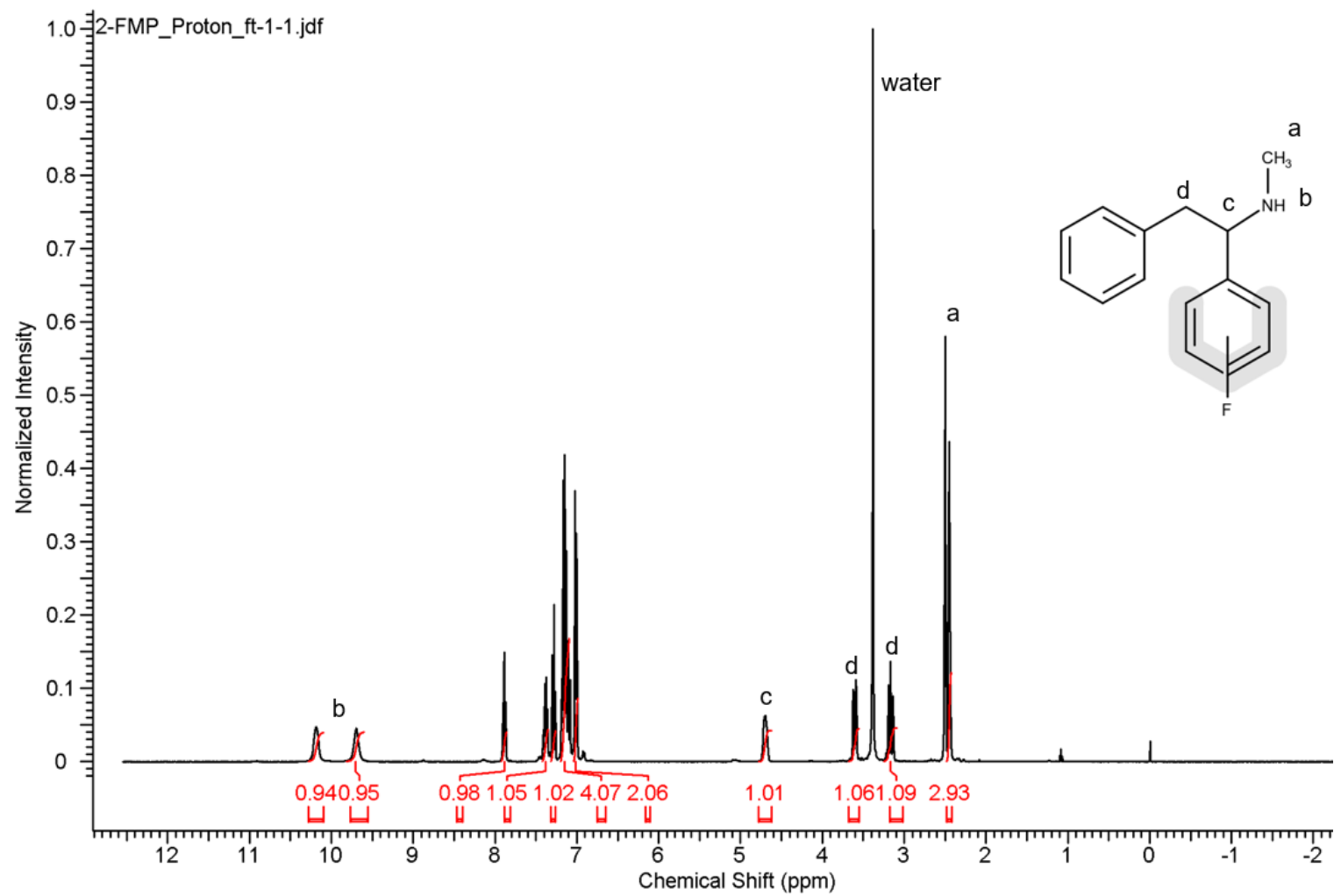


**Figure 125:** 400 MHz <sup>1</sup>H NMR spectrum for 2-fluoromephenidine (2-FMP, **21a**) run in DMSO-d<sub>6</sub> ( $\delta$  ppm = 2.50)

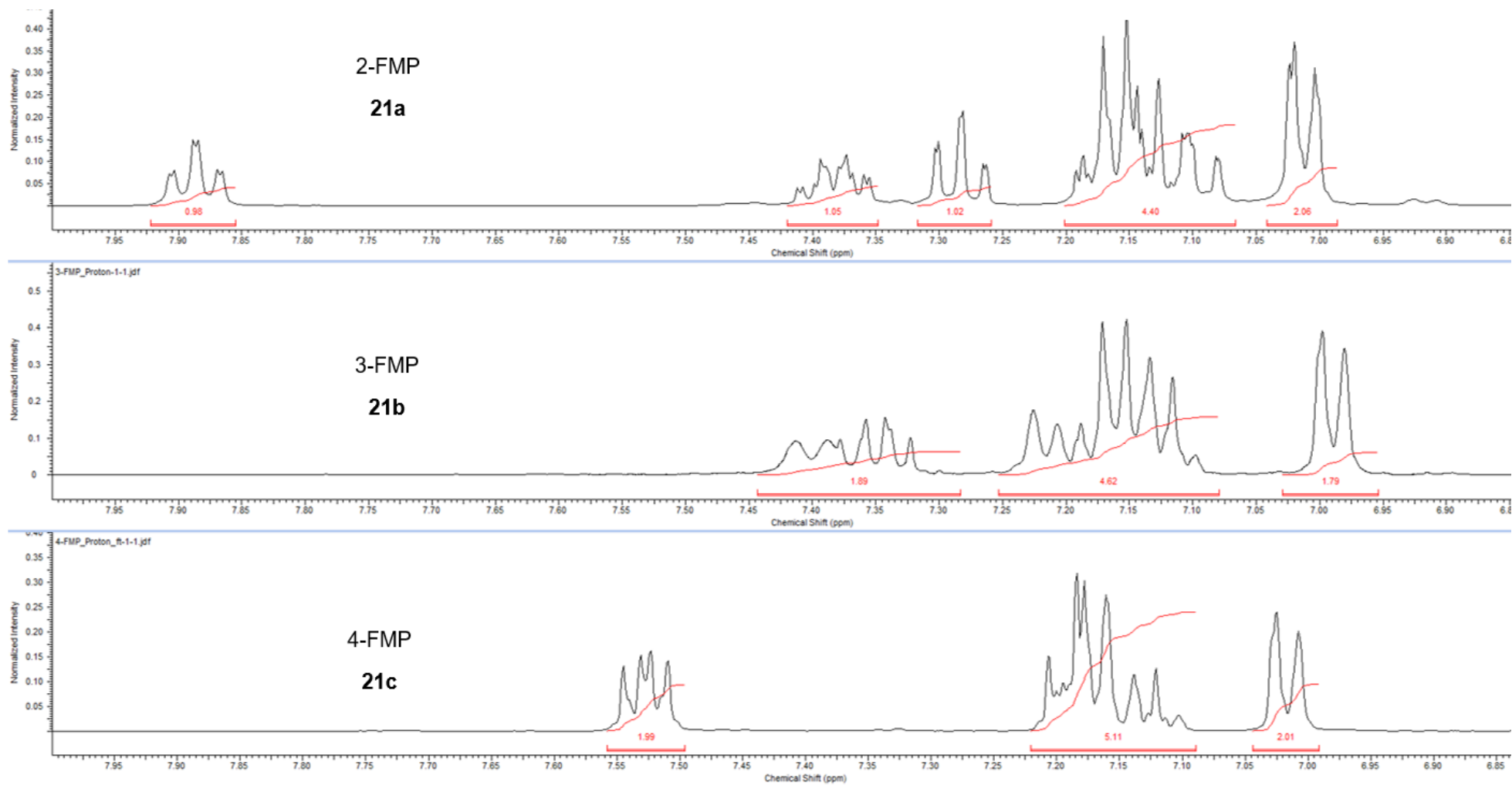


**Figure 126:** Stacked 400 MHz <sup>1</sup>H NMR spectra showing the aromatic region for the fluoromphenidine regioisomers (FMP, **21a** – **21c**)



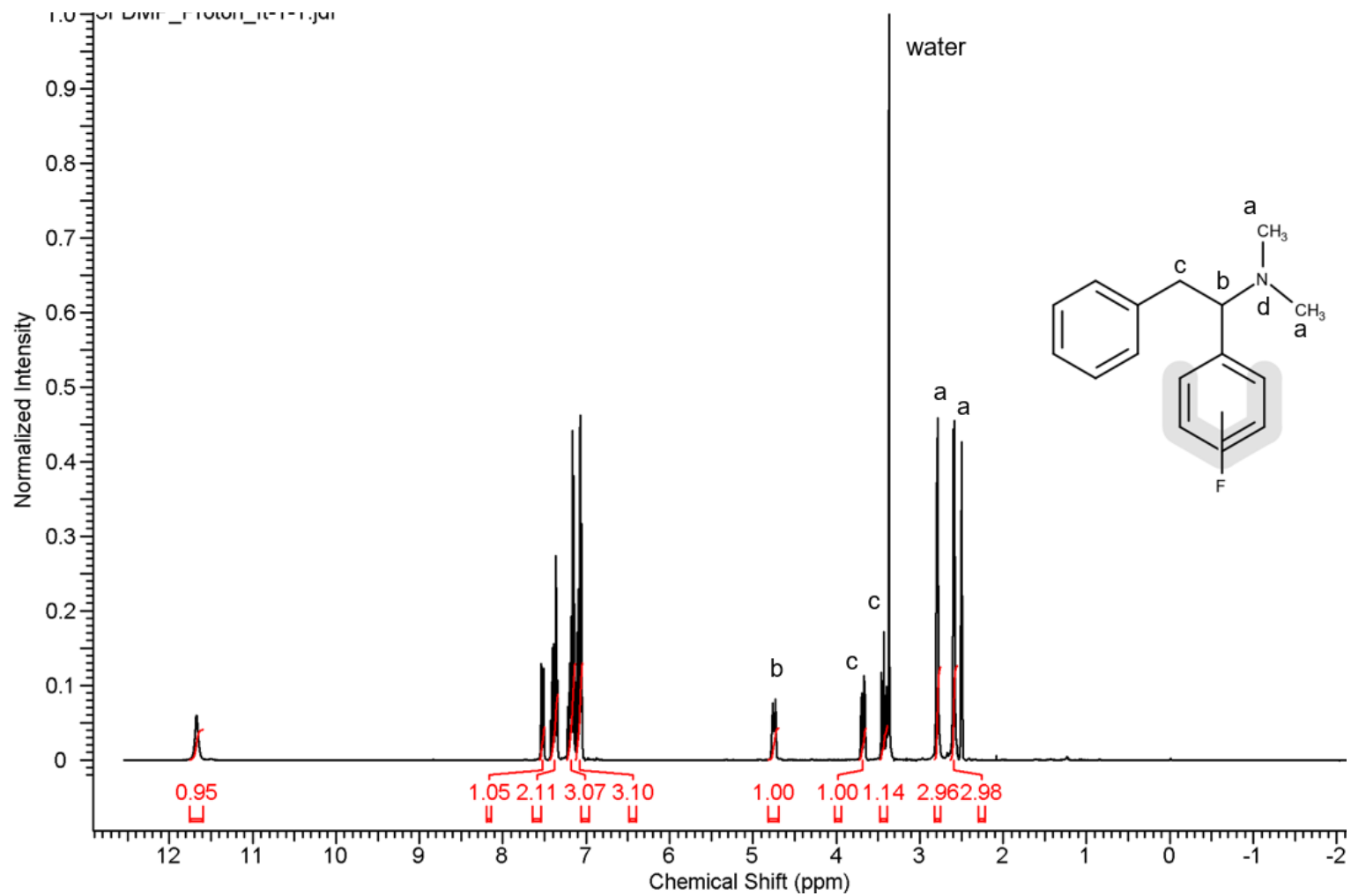


**Figure 127:** 400 MHz <sup>1</sup>H NMR spectrum for 2-fluorodimephenidine (2-FDMP, **22a**) run in DMSO-d<sub>6</sub> ( $\delta$  ppm = 2.50)

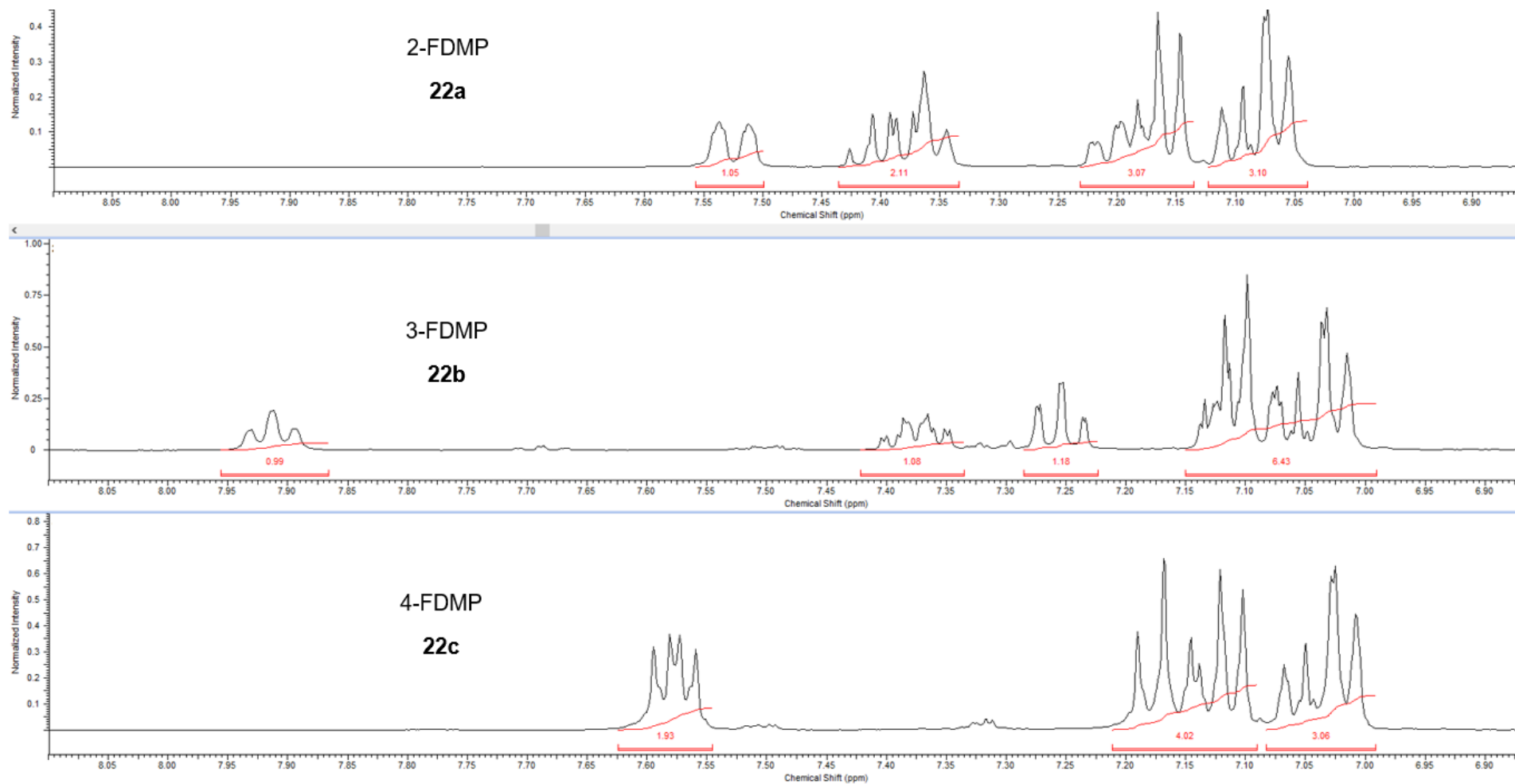


**Figure 128:** Stacked 400 MHz <sup>1</sup>H NMR spectra showing the aromatic region for the fluorodimephenidine regioisomers (FDMP, **22a** – **22c**)

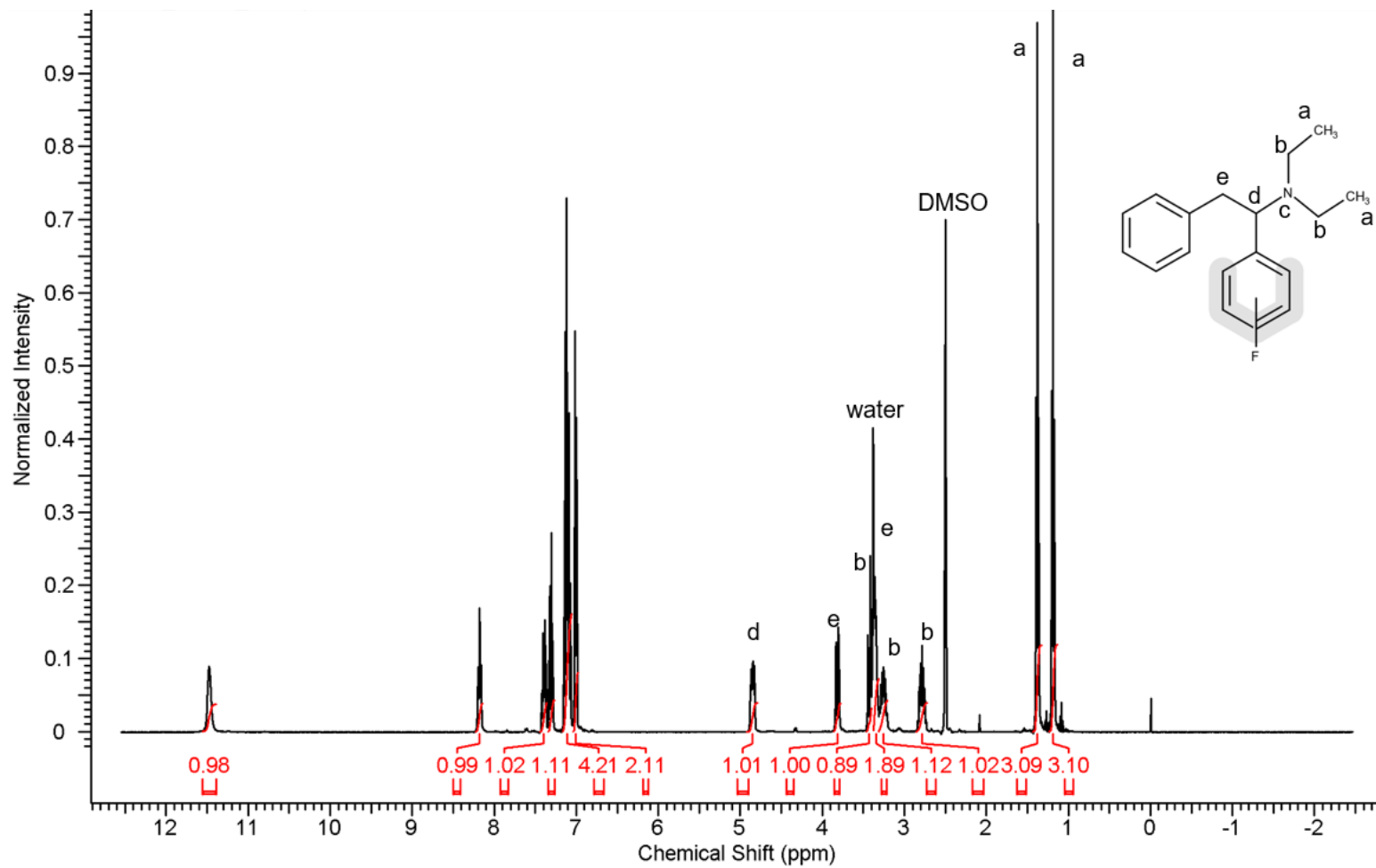


**Figure 129:** 400 MHz <sup>1</sup>H NMR spectrum for 2-fluorodiephenidine (2-FDEP, **23a**) run in DMSO-d<sub>6</sub> ( $\delta$  ppm = 2.50)

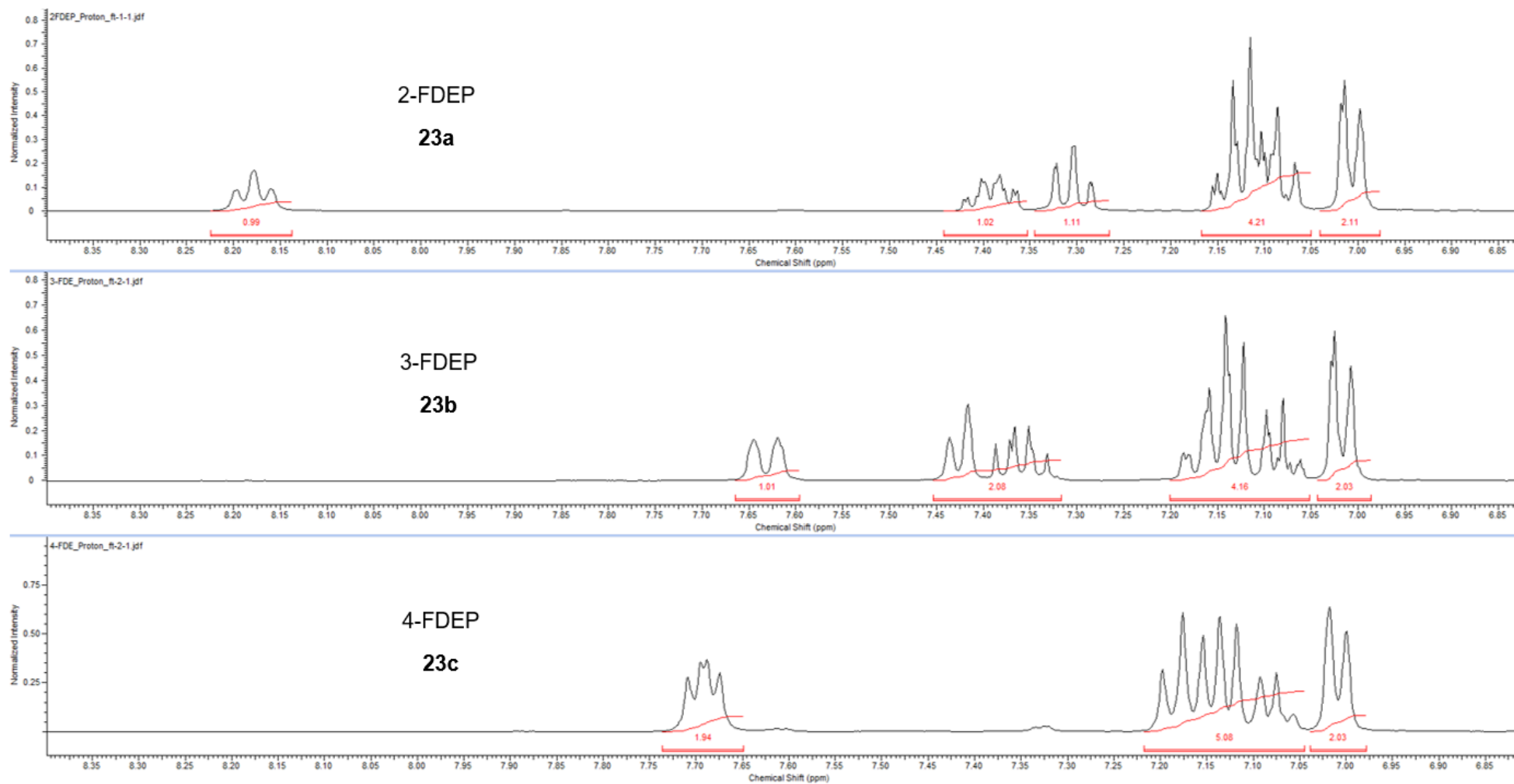


**Figure 130:** Stacked 400 MHz <sup>1</sup>H NMR spectra showing the aromatic region for the fluorodiephenidine regioisomers (FDEP, **23a** – **23c**)

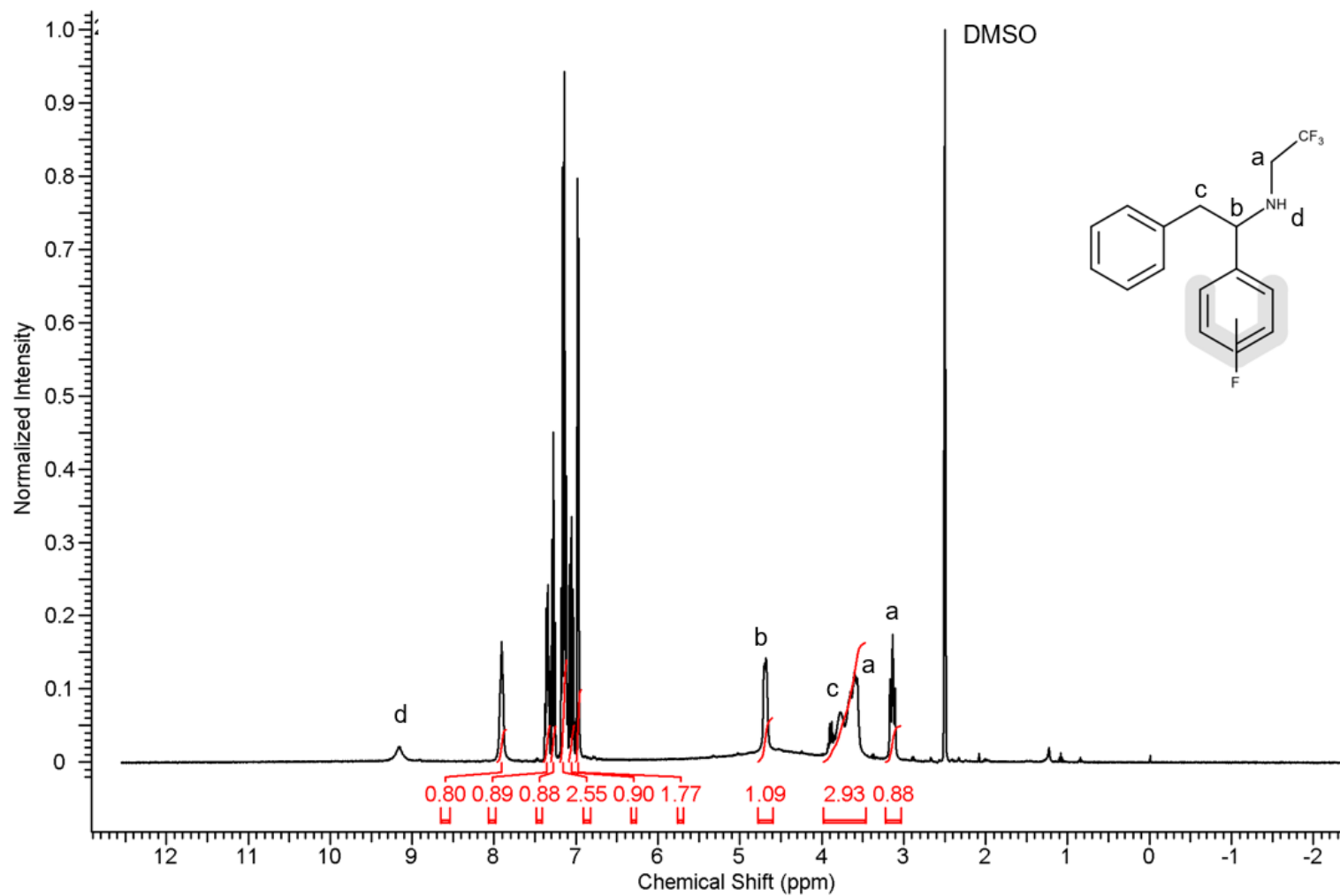


**Figure 131:** 400 MHz <sup>1</sup>H NMR spectrum for 2-fluorotrifluorophenidine (2-FTFEP, **24a**) run in DMSO-d<sub>6</sub> (δ ppm = 2.50)

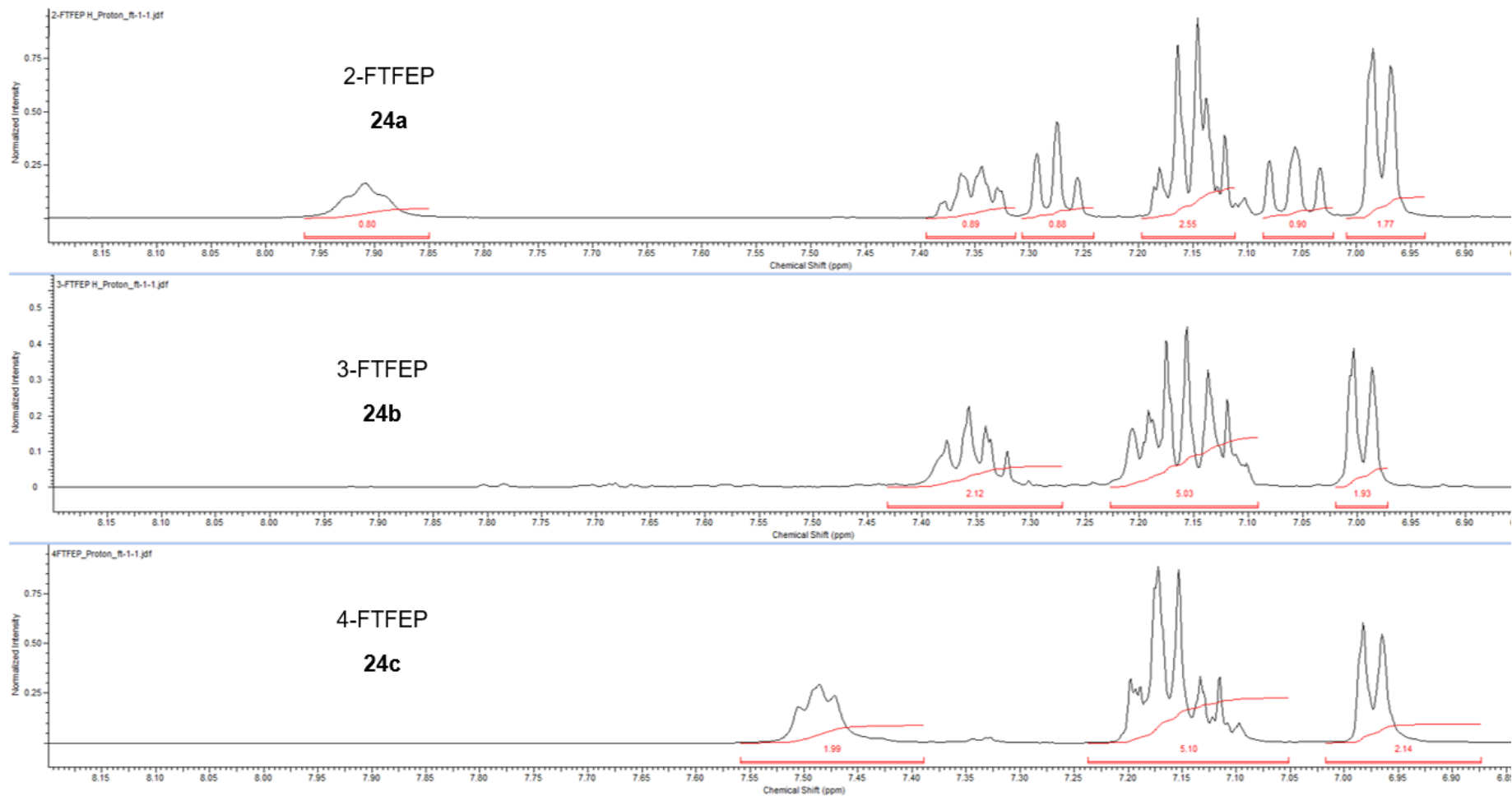


**Figure 132:** Stacked 400 MHz <sup>1</sup>H NMR spectra showing the aromatic region for the fluorotrifluoroephenidine regioisomers (FTFEP, **24a** – **24c**)

### 6.3. Presumptive testing

Presumptive testing was carried out on all of the halogenated diphenidine derivatives (**20a–20l**) using the United Nations recommended guidelines.<sup>118</sup> No previous presumptive testing has been reported for any of the halogenated diphenidines, so a range of test reagents were used to fully detail possible colour changes. (i) Marquis test; (ii) Mandelin test; (iii) Simon's test; (iv) Robadope test; (v) Scott's test and (vi) Zimmerman test reagents were prepared and used based on the procedures detailed in section 2.2. A solution of each reference standard ( $10 \text{ mg mL}^{-1}$ ) was prepared in deionised water and a couple of drops placed into a dimple well of a spotting tile. The required presumptive test reagent (1-2 drops) was then added and any colour change upon initial addition of the reagents were noted and observations were made again after a five minute time period. Blank solutions of deionised water were used in order to show the natural colour of the test reagents prior to being added to sample solution.

Due to each different class of diphenidine analogue having a different amine functional group or chain, the reactions with the testing reagents will differ in each case. This will especially be the case where the amines differ from tertiary to secondary amines. There are clear differences between different classes of analogue, however the regioisomers within a class tend to produce the same colour changes with each reagent, making identification of a specific compound difficult.

The classes of compounds that contain tertiary amines: FL; FP; FDEP and FDMP, all turn the Scott's reagent from a pink red colouration to a blue solution. This has been explained in previous chapters as the reaction of the octahedral Co(II) complex that produces the pink colour to the Co(II) tetrahedral complex. This can help to distinguish the tertiary amines from the secondary amines: FEP, FMP and FTFEP, which do not produce a reaction with Scott's reagent. However, when used alone the reagent cannot distinguish between all the classes. In order to show that secondary amines were present, Simon's reagent was used. The reaction involves the production

of the Simon-Awe complex.<sup>3</sup> This occurs through the reaction of the amine and the aldehyde to produce the enamine, which in turn reacts with sodium nitroprusside before being hydrolysed to the Simon-Awe complex. All the secondary amine compounds react with the Simon's reagent producing slightly different coloured solutions, while the tertiary amines do not react. With all the secondary amines producing slightly different colours with the Simon's reagent it helps to slightly distinguish between classes however, in a similar manner to the Scott's reagent the isomers within a class do not show significant differences in colour. The Simon-Awe usually produces a dark purple colour but in the case of the diphenidine analogues the colours range from a darker brown to brown/red colour.

In all cases the Robadope and Zimmerman's reagents do not produce a positive response. The Robadope reagent remains the peach colour that is seen in the blank sample. The Zimmerman's reagent is usually a colourless solution when both reagent solutions are added together with the water blank sample however, when the sample solutions are added a pale yellow precipitate is formed in solution. This is reported as a negative reaction in this experiment as it is believed that this is just the formation of the freebase precipitate of the samples, rather than a positive reaction with the dinitrobenzene. With all classes producing a negative response it is not advised to use either of these test reagents to help distinguish between the diphenidine analogues.

The Marquis and Mandelin reagents are both used generally as tests to detect the presence of alkaloids. The Mandelin reagent occurs as a yellow solution when prepared and appears as a light yellow solution when added to the aqueous blank, which can be explained through the dilution of the reagent colour. The FEP and FMP isomers all show a negative reaction, producing light yellow solutions. The remaining analogues produce a positive dark yellow solution however, it is not possible to distinguish the colour between classes. In all cases the dark yellow colouration fades to a lighter yellow colour after five minutes, although this yellow colour is not lost completely. This could be explained through the instability of the product formed in the reaction with the



reagent. The Marquis reagent, which begins as a colourless solution in the blank, has a positive reaction with all the analogues tested. Each class yields a slightly different colour ranging from light-yellow to orange. The fluorotrifluoroephenidine (FTFEP) regioisomers shows the biggest colour change with the Marquis reagent with a light brown solution formed. In a similar manner to the Mandelin reagent the sample solutions begin to lose their colour over 5 minutes, ending with a colourless solution or a more diluted version of the original colours produced. This means that the presumptive testing must be observed and reported upon initial addition rather than waiting before observations are made. In a similar manner to the fluorinated diphenidine derivatives (section 4.3) the regioisomers of each fluorinated analogue contain very similar  $\lambda_{\text{max}}$  values when analysed using UV instrumentation, meaning this technique is also incapable of separating isomers from one another as an alternative to colour tests.

In order to allow comparisons to be made, by distinguishing the possible classes present, the Marquis, Mandelin, Scott's and Simon's reagents should all be used. This will help to suggest the classes present for further testing to help identify the specific compound present. The presumptive tests individually would not identify the specific isomers presents, as all isomers within a class interact in a similar manner with all reagents.

**Table 38:** Reported colour changes for a range of presumptive test reagents on multiple fluorinated diphenidine analogues

	Marquis		Mandelin		Scott's		Simon's		Robadope's		Zimmerman's	
	Immediate colour change	Colour after 5 minutes	Immediate colour change	Colour after 5 minutes	Immediate colour change	Colour after 5 minutes	Immediate colour change	Colour after 5 minutes	Immediate colour change	Colour after 5 minutes	Immediate colour change	Colour after 5 minutes
<b>15a</b>	yellow	colourless	-	-	-	-	brown	light brown	-	-	- pale yellow ppt	- pale yellow ppt
<b>15b</b>	yellow	colourless	-	-	-	-	brown	light brown	-	-	- pale yellow ppt	- pale yellow ppt
<b>15c</b>	yellow	colourless	-	-	-	-	brown	light brown	-	-	- pale yellow ppt	- pale yellow ppt
<b>19a</b>	light orange	colourless	dark yellow	yellow	blue	blue	-	-	-	-	- pale yellow ppt	- pale yellow ppt
<b>19b</b>	light orange	colourless	dark yellow	yellow	blue	blue	-	-	-	-	- pale yellow ppt	- pale yellow ppt
<b>19c</b>	light orange	colourless	dark yellow	yellow	blue	blue	-	-	-	-	- pale yellow ppt	- pale yellow ppt
<b>20a</b>	orange	light orange	dark yellow	yellow	blue	blue	-	-	-	-	- pale yellow ppt	- pale yellow ppt
<b>20b</b>	light orange	light orange	dark yellow	yellow	blue	blue	-	-	-	-	- pale yellow ppt	- pale yellow ppt
<b>20c</b>	light orange	light orange	dark yellow	yellow	blue	blue	-	-	-	-	- pale yellow ppt	- pale yellow ppt
<b>21a</b>	yellow	colourless	-	-	-	-	brown	brown	-	-	- pale yellow ppt	- pale yellow ppt

<b>21b</b>	yellow	colourless	-	-	-	-	brown/red	brown/red	-	-	-	pale yellow ppt	pale yellow ppt
<b>21c</b>	yellow	colourless	-	-	-	-	brown	brown	-	-	-	pale yellow ppt	pale yellow ppt
<b>22a</b>	light yellow	colourless	dark yellow	yellow	blue	blue	no reaction	- no reaction	-	-	-	pale yellow ppt	pale yellow ppt
<b>22b</b>	light yellow	colourless	dark yellow	yellow	blue	blue	-	-	-	-	-	pale yellow ppt	pale yellow ppt
<b>22c</b>	light yellow	colourless	dark yellow	yellow	blue	blue	-	-	-	-	-	pale yellow ppt	pale yellow ppt
<b>23a</b>	orange	colourless	dark yellow	yellow	blue	blue	-	-	-	-	-	pale yellow ppt	pale yellow ppt
<b>23b</b>	orange	colourless	dark yellow	yellow	blue	blue	-	-	-	-	-	pale yellow ppt	pale yellow ppt
<b>23c</b>	orange	colourless	dark yellow	yellow	blue	blue	-	-	-	-	-	pale yellow ppt	pale yellow ppt
<b>24a</b>	light brown	colourless	dark yellow	yellow	-	-	dark brown	dark brown	-	-	-	pale yellow ppt	pale yellow ppt
<b>24b</b>	light brown	colourless	dark yellow	yellow	-	-	dark brown	dark brown	-	-	-	pale yellow ppt	pale yellow ppt
<b>24c</b>	light brown	colourless	dark yellow	yellow	-	-	dark brown	dark brown	-	-	-	pale yellow ppt	pale yellow ppt

## 6.4. Thin layer chromatography

All the monofluorinated diphenidine analogues were also analysed using thin layer chromatography (TLC). All the  $R_f$  values for each compound were measured using a matching mobile phase composition to the diphenidine regioisomers and halogenated diphenidines tested previously. Average  $R_f$  values have been reported (Table 39) based on the averages from six repeats. All compounds show only one spot using TLC, which helps to show that all reference materials are clean with no impurities, which is supported by the NMR analysis used for characterisation. The same colours are produced under UV light and with the addition of the modified Dragendorff-Ludy-Tenger reagent.<sup>102</sup> Each of the diphenidine analogues show very similar  $R_f$  values to one another making identification of a specific compound difficult. There is no clear separation in the values between different classes or in values between different isomers within classes, therefore no conclusions can be drawn on TLC data alone. The TLC data can help to aid with characterisation in order to help confirm the identify of a compound when used in combination with commonly used tests such as  $^1\text{H}$ ,  $^{13}\text{C}$  and  $^{19}\text{F}$  NMR and GC-MS.

**Table 39:** R<sub>f</sub> values for all the monofluorinated diphenidine analogues

	<b>Compound name</b>	<b>Spot colour under UV light (254 nm)</b>	<b>Spot colour after staining with modified Dragendorff-Ludy-Tenger Reagent</b>	<b>R<sub>f</sub> value</b>
<b>15a</b>	2-fluoroephenidine	Black spot	Red spot	0.56
<b>15b</b>	3-fluoroephenidine	Black spot	Red spot	0.61
<b>15c</b>	4-fluoroephenidine	Black spot	Red spot	0.58
<b>19a</b>	2-fluorolintane	Black spot	Red spot	0.64
<b>19b</b>	3-fluorolintane	Black spot	Red spot	0.64
<b>19c</b>	4-fluorolintane	Black spot	Red spot	0.67
<b>20a</b>	2-fluphenidine	Black spot	Red spot	0.65
<b>20b</b>	3-fluphenidine	Black spot	Red spot	0.61
<b>20c</b>	4-fluphenidine	Black spot	Red spot	0.62
<b>21a</b>	2-fluoromephenidine	Black spot	Red spot	0.58
<b>21b</b>	3-fluoromephenidine	Black spot	Red spot	0.50
<b>21c</b>	4-fluoromephenidine	Black spot	Red spot	0.52
<b>22a</b>	2-fluorodimephenidine	Black spot	Red spot	0.63
<b>22b</b>	3-fluorodimephenidine	Black spot	Red spot	0.64
<b>22c</b>	4-fluorodimephenidine	Black spot	Red spot	0.61
<b>23a</b>	2-fluorodiephenidine	Black spot	Red spot	0.59
<b>23b</b>	3-fluorodiephenidine	Black spot	Red spot	0.61
<b>23c</b>	4-fluorodiephenidine	Black spot	Red spot	0.64
<b>24a</b>	2-fluorotrifluoroephenidine	Black spot	Red spot	0.55
<b>24b</b>	3-fluorotrifluoroephenidine	Black spot	Red spot	0.48
<b>24c</b>	4-fluorotrifluoroephenidine	Black spot	Red spot	0.50

## 6.5. Gas chromatography – mass spectroscopy

All diphenidine analogues were analysed using Gas chromatography–mass spectroscopy (GC-MS). Samples were prepared with a simple solvation in methanol ( $1 \text{ mg mL}^{-1}$ ) and dilution ( $100 \text{ } \mu\text{g mL}^{-1}$ ) with no derivatisation required. All samples were run individually before being run as mixtures in order to determine retention times and elution orders. The three common cutting agent and adulterants: benzocaine (**B**), caffeine (**C**) and paracetamol (**P**) were also run on the initial screening method to determine where they would fit in the elution order. Retention times ( $R_t$ ) and relative retention times ( $RR_t$ ), in relation to the eicosane (**E**), can be seen in Table 40.

From the initial screening method and the Relative Retention Times ( $RR_t$ ) measured, it can be seen that classes of analogues begin to separate. However, if these compounds were to be run as a mixture, baseline separation would not be achieved for a number of the compounds, with the isomers within each class all producing very similar  $RR_t$  values. The adulterants also coelute with the reference materials when run using the initial screen. The interesting point observed in the screening method comes in the elution order and separation of the FEP, FDMP, FDEP and caffeine compounds. In the *ortho*-compounds the elution order follows: FEP  $\rightarrow$  FDMP  $\rightarrow$  FDEP  $\rightarrow$  caffeine with the 2-FEP and 2-FDMP compounds having the same  $RR_t$  values. In the *meta*-substituted compounds the elution order remains the same, but there is a much greater separation in the  $RR_t$  values. Finally, with the *para*-substituted compounds the elution order changes completely with the elution order becoming: FDMP  $\rightarrow$  FEP  $\rightarrow$  caffeine  $\rightarrow$  FDEP.

The mass spectrometry data produced for each class of compound provides another method to potentially differentiate between reference materials. All classes, aside from the FEP and FDMP classes, contain unique spectra with individual base peaks (figure 137–figure 143). The FEP and FDMP compounds contain matching mass spectra due to the matching fragmentation scheme that occurs for all the monofluorinated diphenidine analogues. The mass of the base peak fragments for both the FDMP and FEP is the same

( $m/z = 152.1$ ) due to the rearrangement of the dimethylated tertiary amine in the FDMP compound to the secondary amine with an attached ethyl chain in the FEP compounds. The differences in the mass spectrometry helps to identify the class of compound present even in the screening run where peaks may not be baseline separated. In a similar manner to previous compounds analysed the mass spectra produced for isomers within the same class are the same, meaning isomers cannot be distinguished from mass spectroscopy data alone.

Due to the screening method producing very similar  $RR_t$  values for the majority of compounds, the method was developed in order to slow the incremental rate of temperature change in order to increase separation. The retention times and relative retention times compared to eicosane for the newer developed method can be seen in Table 41. From the  $RR_t$  it can be seen that there is a greater separation in the values measured between classes. There are still similarities in the  $RR_t$  values between isomers within a class, especially in the FP and FL classes where the amine is ringed due to the use of piperidine and pyrrolidine respectively, meaning baseline separation is still not possible even with the developed method. As the ramp is already at  $1^\circ\text{C}/\text{min}$  it is not possible for this to be slowed any further to improve separation and a method was attempted with the temperature held isothermally at  $140^\circ\text{C}$  for 40 minutes. No further separation was achieved compared to the developed method used.

Mixtures were prepared, splitting all the compounds into three based on position of substitution on the benzene ring. The chromatographs (figure 134–figure 136) further show the extended separation achieved between classes. In the *meta* (3') and *para* (4') mixtures all reference materials are baseline separated, however when the adulterants are added the FMP samples coelute with paracetamol. The caffeine peak also coelutes with the FDEP in the 3' and 4' mixtures. In the *ortho* (2') mixture the adulterants are baseline separated from all the reference materials. The 2-FEP and 2-FDEP samples are the only samples in the *ortho*-mixture that are not baseline separated from one another.

Further to using the developed GC method to help distinguish compounds a single ion monitoring (SIM) mode was used for the mass spectrometer detector. This helps to target specific ion fragments based on  $m/z$  values. In this case the SIM mode was selected with all base peak fragment weights chosen, apart from in the case of paracetamol where  $m/z=151.1$  was used instead of  $m/z=109$ , as this is seen as a secondary peak in the majority of the reference material spectra. This means all samples produced two peaks when viewing chromatographs in SIM mode, one for the eicosane peak and one for sample. This helps to clearly identify individual peaks, with the only exception being the 2-FEP and 2-FDEP isomers with coelution occurring in the full scan mode and SIM mode, due to both compounds having an identical mass spectrum. When a mass of  $m/z=124.0$  is used as a fragment in SIM mode it will produce a peak for the FEP, as a secondary base peak, but not for the FDEP isomer. This is not a problem in the *meta*- and *para*-mixtures where the FEP and FDEP peaks are resolved from one another.



**Table 40:** GC retention times for the diphenidine analogues, including relative retention time (RR<sub>t</sub>) relative to eicosane (**E**, R<sub>t</sub> = 7.281 mins)

<b>Compound no.</b>	<b>Compound Abbreviation</b>	<b>Compound retention time (R<sub>t</sub> / mins)</b>	<b>Relative Retention time (RR<sub>t</sub>)</b>
<b>15a</b>	2-FEP	6.37	0.88
<b>15b</b>	3-FEP	6.42	0.88
<b>15c</b>	4-FEP	6.43	0.88
<b>19a</b>	2-FL	7.25	1.00
<b>19b</b>	3-FL	7.24	0.99
<b>19c</b>	4-FL	7.25	1.00
<b>20a</b>	2-FP	7.58	1.04
<b>20b</b>	3-FP	7.59	1.04
<b>20c</b>	4-FP	7.60	1.04
<b>21a</b>	2-FMP	6.23	0.86
<b>21b</b>	3-FMP	6.28	0.86
<b>21c</b>	4-FMP	6.27	0.86
<b>22a</b>	2-FDMP	6.37	0.88
<b>22b</b>	3-FDMP	6.86	0.94
<b>22c</b>	4-FDMP	6.40	0.88
<b>23a</b>	2-FDEP	6.82	0.94
<b>23b</b>	3-FDEP	6.85	0.94
<b>23c</b>	4-FDEP	6.86	0.94
<b>24a</b>	2-FTFEP	6.03	0.83
<b>24b</b>	3-FTFEP	6.07	0.83
<b>24c</b>	4-FTFEP	6.08	0.84
<b>P</b>	Paracetamol	6.25	0.86
<b>B</b>	Benzocaine	5.84	0.80
<b>C</b>	Caffeine	6.25	0.86

**Table 41:** GC retention times for the diphenidine analogues on the developed GC method, including relative retention time (RR<sub>t</sub>) relative to eicosane (**E**, R<sub>t</sub> = 7.281 mins)

Compound no.	Compound Abbreviation	Compound retention time (R <sub>t</sub> / mins)	Relative Retention time (RR <sub>t</sub> )
<b>15a</b>	2-FEP	18.14	0.57
<b>15b</b>	3-FEP	18.01	0.57
<b>15c</b>	4-FEP	18.83	0.60
<b>19a</b>	2-FL	28.13	0.89
<b>19b</b>	3-FL	28.00	0.89
<b>19c</b>	4-FL	28.08	0.89
<b>20a</b>	2-FP	33.64	1.07
<b>20b</b>	3-FP	33.72	1.07
<b>20c</b>	4-FP	33.91	1.07
<b>21a</b>	2-FMP	17.06	0.54
<b>21b</b>	3-FMP	17.50	0.55
<b>21c</b>	4-FMP	17.51	0.55
<b>22a</b>	2-FDMP	18.31	0.58
<b>22b</b>	3-FDMP	18.76	0.59
<b>22c</b>	4-FDMP	18.08	0.57
<b>23a</b>	2-FDEP	22.85	0.72
<b>23b</b>	3-FDEP	23.18	0.73
<b>23c</b>	4-FDEP	23.35	0.74
<b>24a</b>	2-FTFEP	16.00	0.51
<b>24b</b>	3-FTFEP	16.38	0.52
<b>24c</b>	4-FTFEP	16.36	0.52
<b>P</b>	Paracetamol	17.60	0.56
<b>B</b>	Benzocaine	14.55	0.46
<b>C</b>	Caffeine	23.26	0.74

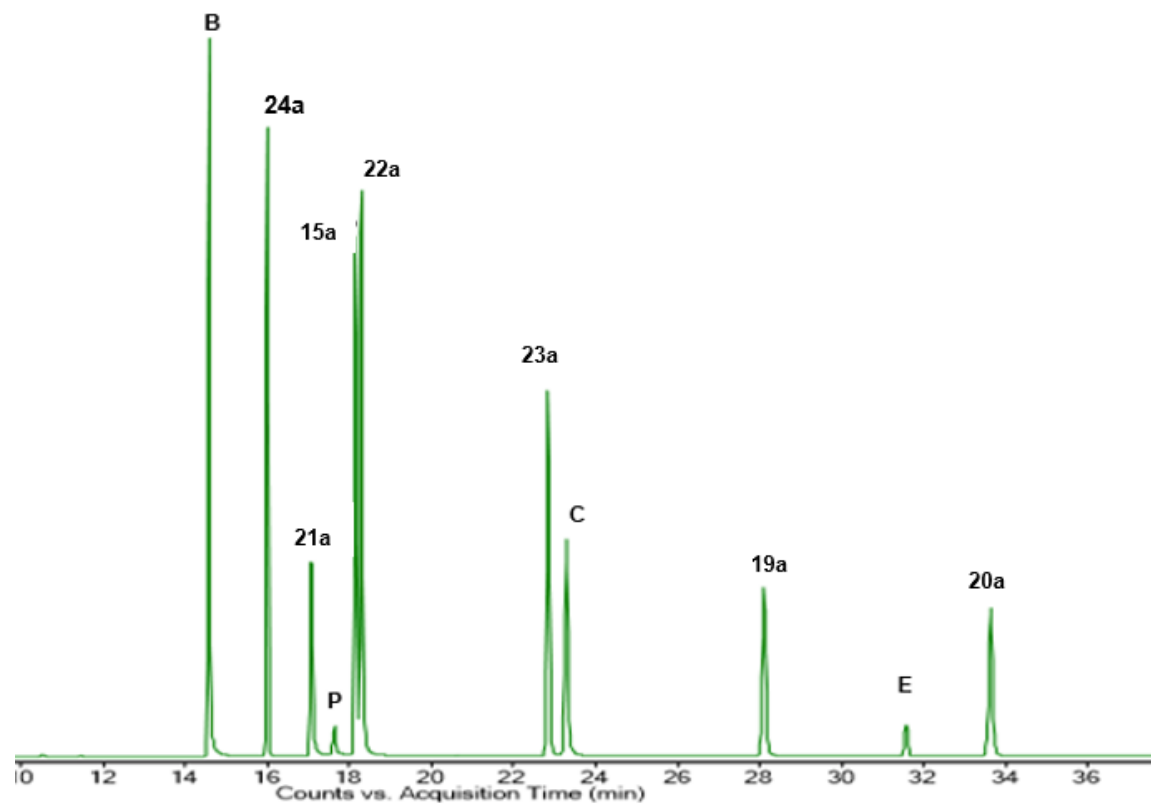


**Figure 133:** GC-MS chromatograph for the 2' positional isomers of the monofluorinated diphenidine analogues including internal standard eicosane (**E**) and common adulterants: benzocaine (**B**); paracetamol (**P**) and caffeine (**C**), run in a full scan mode.

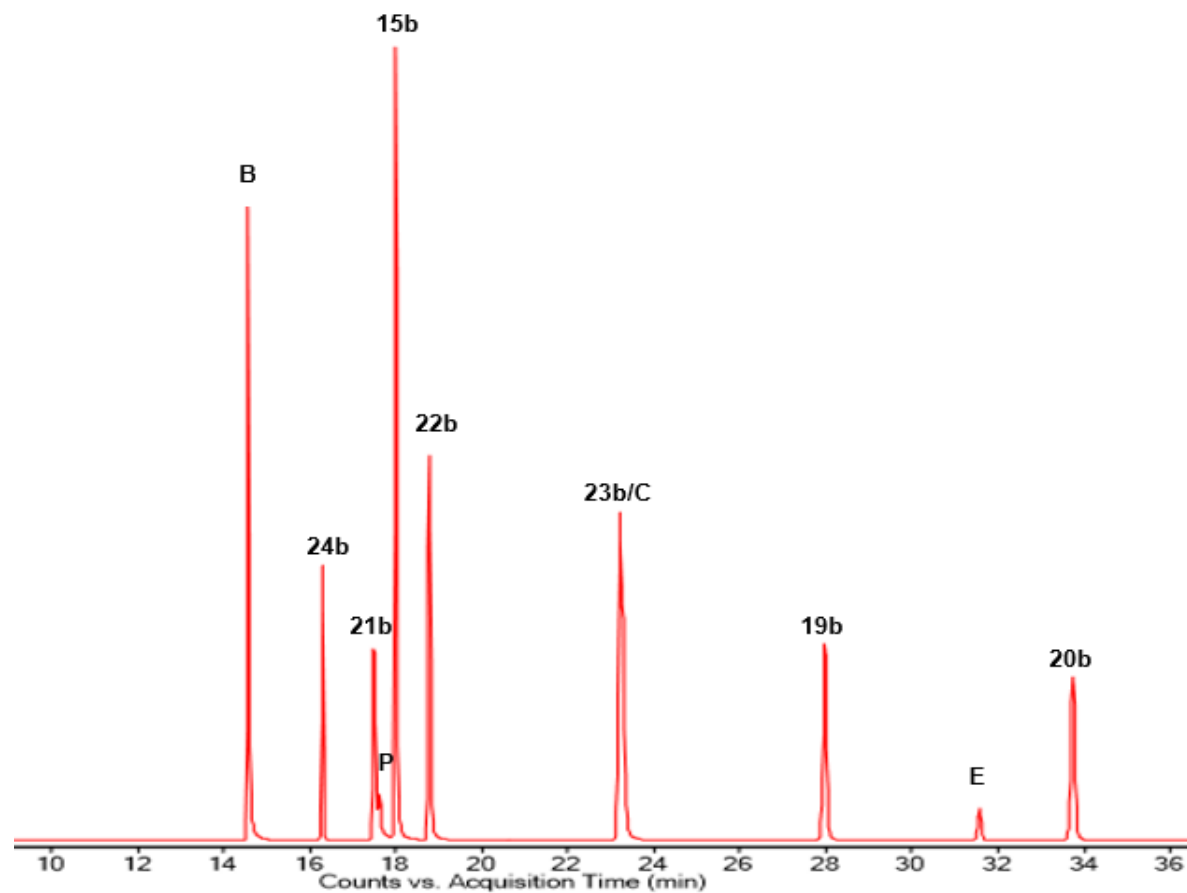


**Figure 134:** GC-MS chromatograph for the 3' positional isomers of the monofluorinated diphenidine analogues including internal standard eicosane (**E**) and common adulterants: benzocaine (**B**); paracetamol (**P**) and caffeine (**C**), run in a full scan mode.

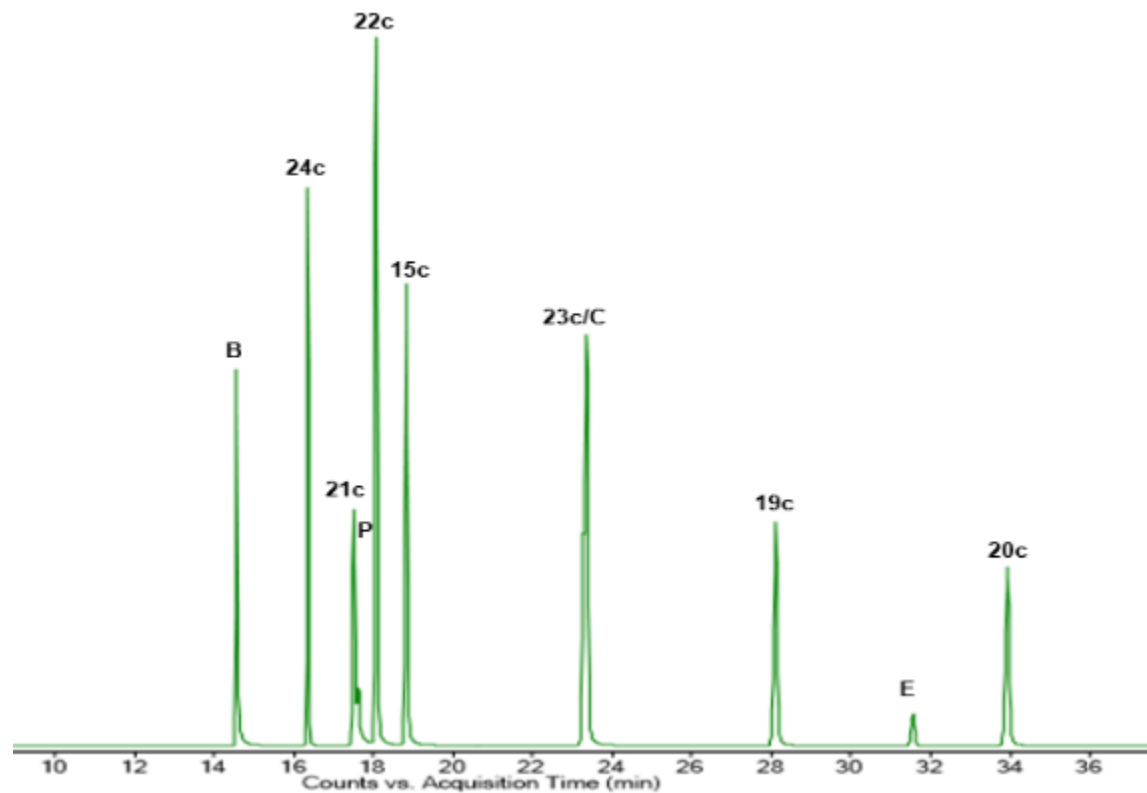


**Figure 135:** GC-MS chromatograph for the 4' positional isomers of the monofluorinated diphenidine analogues including internal standard eicosane (**E**) and common adulterants: benzocaine (**B**); paracetamol (**P**) and caffeine (**C**), run in a full scan mode.

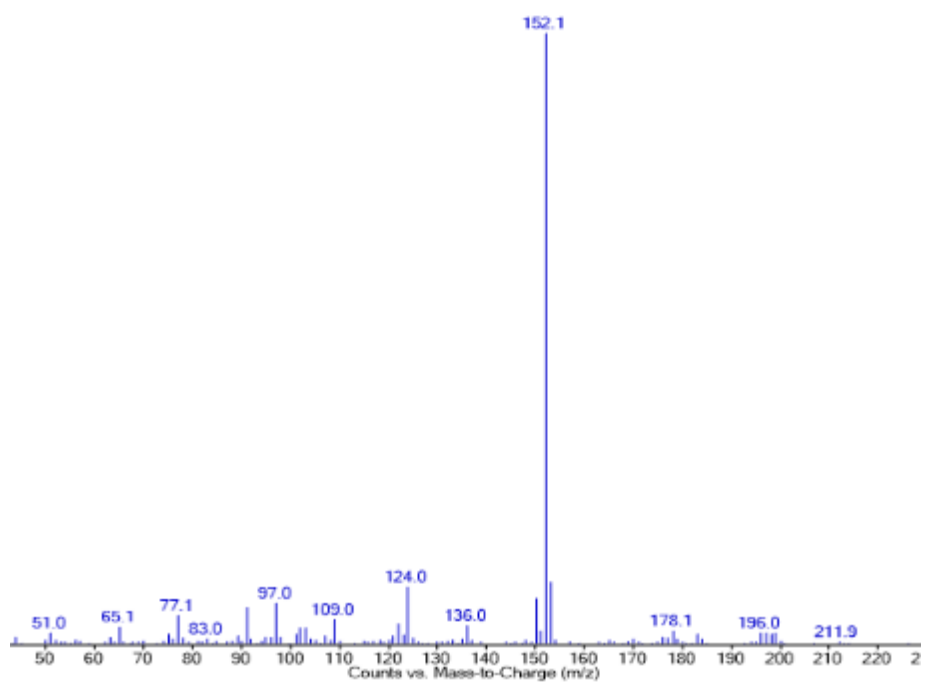


**Figure 136:** Mass spectrum for the fluoroephedrine (FEP) regioisomers (15a–15c)

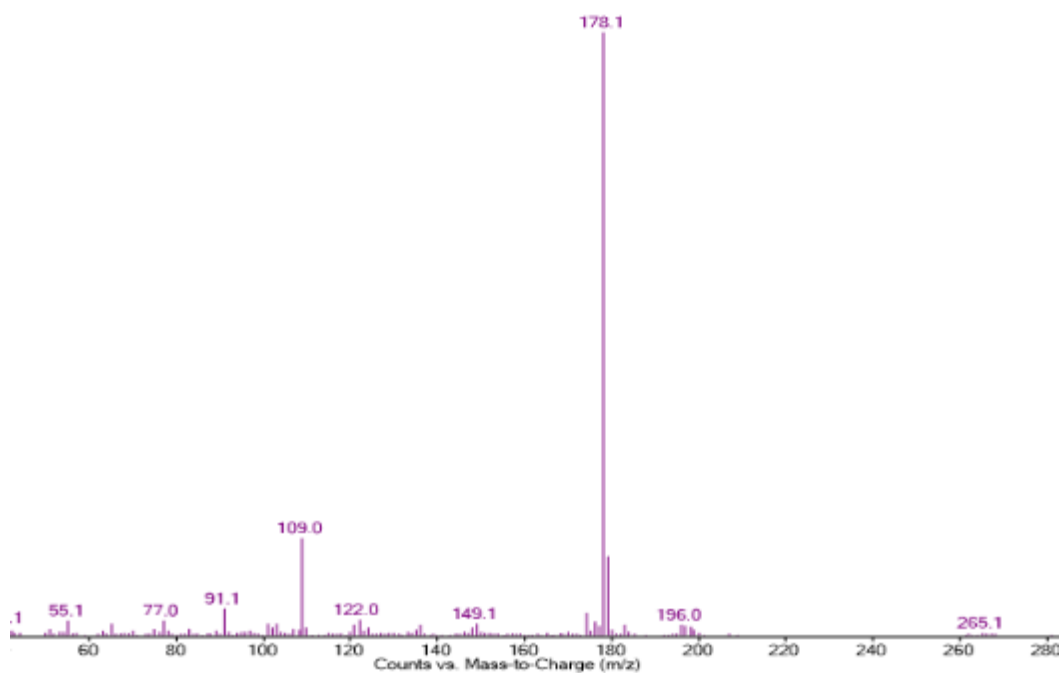


**Figure 137:** Mass spectrum for the fluorolintane (FL) regioisomers (19a–19c)

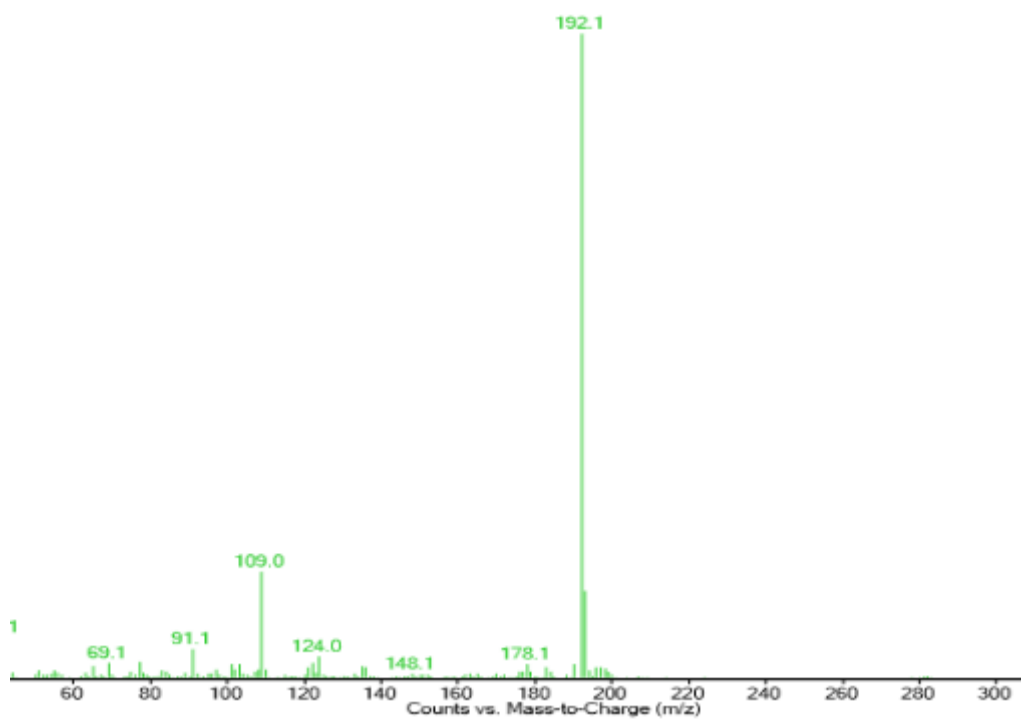


**Figure 138:** Mass spectrum for the fluphenidine (FP) regioisomers (20a-20c)

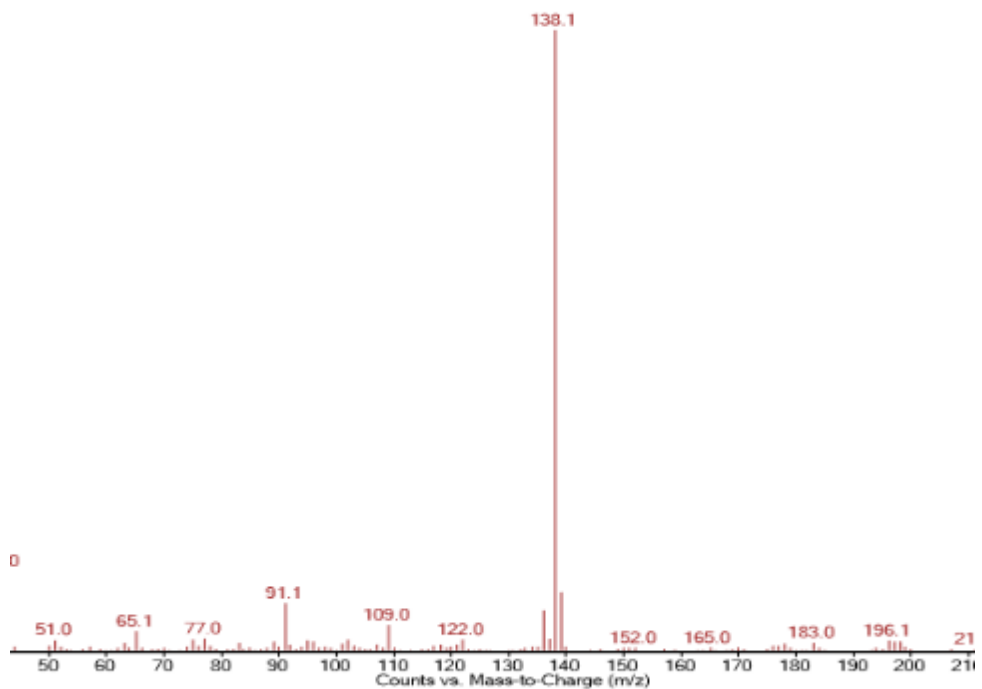


**Figure 139:** Mass spectrum for the fluoromephenidine (FMP) regioisomers (21a-21c)

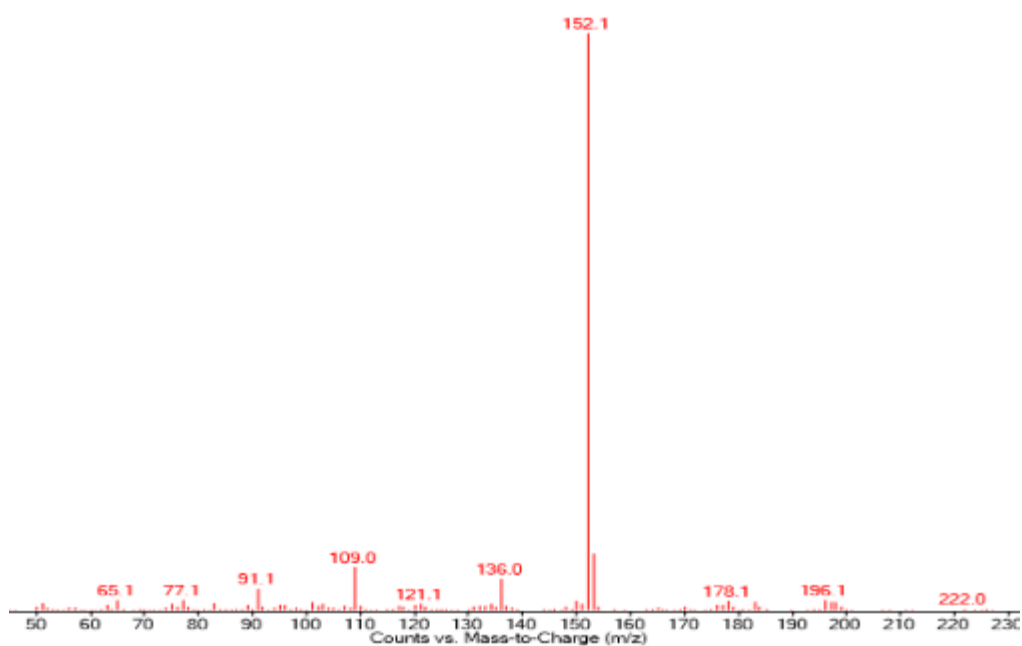


**Figure 140:** Mass spectrum for the fluorodimephenidine (FDMP) regioisomers (22a-22c)

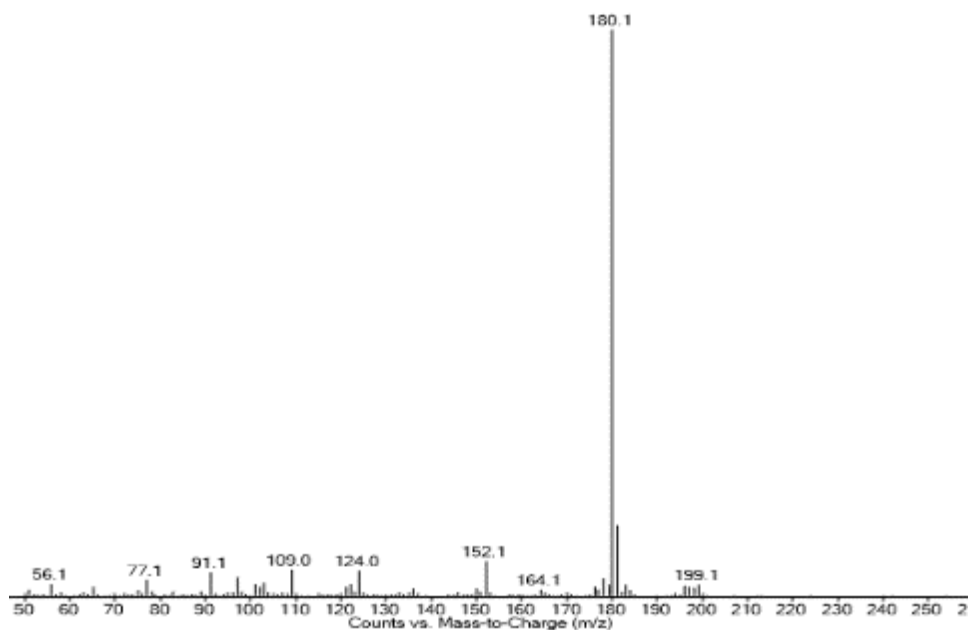


**Figure 141:** Mass spectrum for the fluorodiephenidine (FDEP) regioisomers (23a-23c)



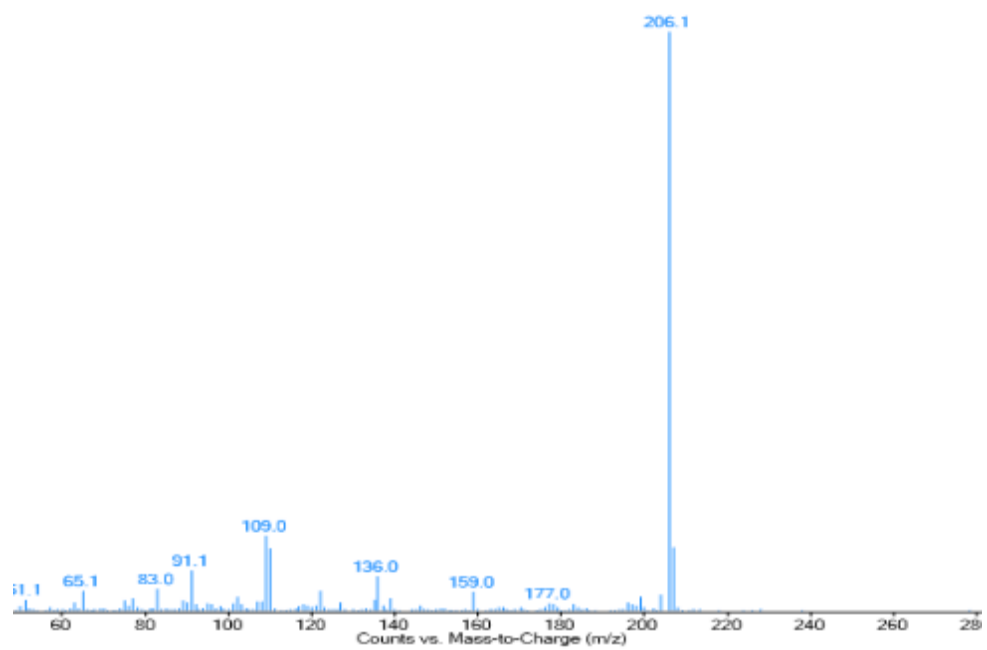


Figure 142: Mass spectrum for the fluorotrifluoroephenidine (FTFEP) regioisomers  
**(24a-24c)**

**Table 42:** GC-MS validation figures for the monofluorinated diphenidine analogues and the three added adulterants: benzocaine (**B**); paracetamol (**P**) and caffeine (**C**). Key: <sup>x</sup>Relative Retention time with respect to eicosane (**E**, R<sub>t</sub> = 31.58 min)

Analyte	R <sub>t</sub> (mins)	RR <sub>t</sub> <sup>x</sup>	Regression Coefficient (R <sup>2</sup> )	LOD (µg mL <sup>-1</sup> )	LOQ (µg mL <sup>-1</sup> )	Precision (%RSD) n=6				
						100 µg mL <sup>-1</sup>	200 µg mL <sup>-1</sup>	300 µg mL <sup>-1</sup>	400 µg mL <sup>-1</sup>	500 µg mL <sup>-1</sup>
<b>Benzocaine</b>	14.55	0.46	0.9975	6.58	19.94	1.81	2.15	0.71	0.86	0.31
<b>24a</b>	16.00	0.51	0.9951	9.25	28.03	2.04	2.13	1.20	0.29	0.08
<b>24b</b>	16.38	0.52	0.9934	10.79	32.68	3.83	2.13	1.72	0.66	0.17
<b>24c</b>	16.36	0.52	0.9987	11.81	35.81	0.69	1.35	2.15	2.79	0.06
<b>21a</b>	17.06	0.53	0.9953	9.09	27.55	2.71	1.44	0.62	0.63	3.73
<b>21b</b>	17.50	0.55	0.9939	10.37	31.42	4.22	2.60	3.50	0.32	0.04
<b>21c</b>	17.51	0.55	0.9975	11.31	34.27	1.03	4.33	2.78	3.08	0.33
<b>Paracetamol</b>	17.66	0.56	0.9906	8.01	21.46	2.18	1.75	2.26	1.53	1.88
<b>15a</b>	18.14	0.57	0.9924	11.57	35.05	3.12	1.50	0.42	0.78	2.87
<b>15b</b>	18.01	0.57	0.9918	12.05	36.50	5.28	2.75	1.41	0.27	1.62
<b>15c</b>	18.83	0.60	0.9963	12.83	38.89	0.52	3.43	1.45	4.20	0.77
<b>22a</b>	18.31	0.58	0.9954	8.96	27.14	5.20	2.21	1.51	0.28	0.12
<b>22b</b>	18.76	0.59	0.9911	12.52	37.95	5.59	2.33	0.79	0.17	0.75
<b>22c</b>	18.08	0.57	0.9919	15.14	45.88	0.71	3.04	1.42	4.04	0.91
<b>23a</b>	22.85	0.72	0.9923	11.65	35.30	4.10	2.26	0.60	0.14	0.22
<b>23b</b>	23.18	0.73	0.9906	12.92	39.14	4.03	1.14	2.51	0.08	0.09
<b>23c</b>	23.35	0.74	0.9997	14.01	42.46	0.60	3.33	1.19	3.73	0.93
<b>caffeine</b>	23.30	0.74	0.9928	8.79	26.64	5.16	3.48	0.42	0.38	0.34
<b>19a</b>	28.13	0.89	0.9933	10.92	33.08	3.52	1.93	1.56	1.05	0.25
<b>19b</b>	28.00	0.89	0.9911	12.57	38.10	3.89	1.90	1.20	0.09	0.33
<b>19c</b>	28.08	0.89	0.9953	14.44	43.76	0.18	4.09	1.45	3.26	0.30
<b>20a</b>	33.64	1.07	0.9907	12.84	38.92	3.57	1.66	0.63	0.89	0.26
<b>20b</b>	33.72	1.07	0.9910	12.63	38.27	3.78	2.39	0.36	0.22	0.44
<b>20c</b>	33.91	1.07	0.9961	14.29	33.61	0.69	4.04	1.49	3.21	0.15

Five calibration standards were prepared between the region of  $100 \mu\text{g mL}^{-1}$  and  $500 \mu\text{g mL}^{-1}$  and run using the matching developed method to the previous three mixtures. All monofluorinated diphenidine analogues, along with the three additional adulterants, benzocaine (**B**); caffeine (**C**) and paracetamol (**P**), demonstrated a linear response between this concentration range ( $R^2 \geq 0.99$ ). The limits of detection and quantification for the analytes were determined, based on the standard deviation of the response and the slope, as being 6.58–15.14 and 19.94–45.88  $\mu\text{g mL}^{-1}$  respectively (Table 42). The concentration range used was based on the response of the  $100 \mu\text{g mL}^{-1}$  due to baseline being slightly increased due to repetitive sample analysis prior to inlet clean. This had no effect on sample correlation or ratio response between sample and eicosane signals, meaning a positive correlation could still be achieved. Apart from the 3-FEP, 2FDMP and 3-FDMP  $100 \mu\text{g mL}^{-1}$  samples, all solutions showed acceptable repeatability, over 6 repeats, with RSD values  $<5\%$ .

Accuracy for the method was performed using three spiked samples ranging from 80-120% of the targeted value. In this case the target value was set at  $300 \mu\text{g mL}^{-1}$ , meaning percentage recovery samples were prepared at  $240 \mu\text{g mL}^{-1}$ ,  $300 \mu\text{g mL}^{-1}$  and  $360 \mu\text{g mL}^{-1}$ .  $200 \mu\text{g mL}^{-1}$  was chosen due to the ease of sample preparation as well as the concentration falling at the centre of linearity for the calibration standard range. All percentage recovery tables can be seen in supplementary info, (Supplementary info: Table S35-S52). All samples showed acceptable percentage recovery (% assay) with calculated concentrations falling within  $\pm 2 \mu\text{g mL}^{-1}$  of the prepared sample and %RSD values all falling below an acceptable 2%. Based on the accuracy and precision experiments it is considered acceptable that street samples can be tested both qualitatively and quantitatively using GC-MS analysis. No street samples were tested for this GC-MS method.

## 6.6. 60 MHz NMR presumptive testing

60 MHz NMR was used to obtain  $^1\text{H}$  and  $^{19}\text{F}$  NMR spectra for all the monofluorinated diphenidine analogues. The  $^1\text{H}$  NMR spectra produced showed very similar characteristic patterns to those produced when structurally elucidating the compounds synthesised, using a 400 MHz instrument. The  $^{19}\text{F}$  NMR chemical shift values produced (Table 43) also match those produced using the 400 MHz instrument.

In all cases the  $^1\text{H}$  NMR spectra were acquired in DMSO- $d_6$  ( $\delta$  ppm = 2.50) in order to provide a clear reference point for all spectra to then be stacked such that comparisons could be made easier. In a similar way to the halogenated derivatives, the spectra produced by the 60 MHz instrument still provides some splitting for peaks, although the resolution is reduced from the 400 MHz instrument. This means that peaks appear broader even though the pattern shape of the spectra will match between different powered magnets. This allows the 60 MHz instrument to be employed in a presumptive test, as it still provides vital information on the distinguishing features of the compounds investigated. The 400 MHz can then be used as a conformational tool for structural characterisation along with the GC-MS method developed to identify a specific isomer.

In all cases, each different class produced a “signature pattern” in the aliphatic region that matches with the spectra produced from the 400 MHz instrument, which can help distinguish it from other classes. The stacked spectra for all *ortho*-substituted mono-fluorinated analogues, with the aliphatic region enlarged, are seen in figure 144, to demonstrate the ease that different classes can be differentiated.

When it has been determined what class is present the three regioisomers within the class can be determined based on the aromatic region of the three regioisomers. All three positional isomers produce individual aromatic regions based on the coupling effected by the positioning of the fluorine and surrounding proton environments. The stacked aromatic regions for each

class can be seen in figure 145–figure 151, showing how easily each particular compound can be identified.

It was shown from the fluorinated diphenidine regioisomers previously that there is limited resolution between the  $^{19}\text{F}$  signals for the 3' and 4' isomers and this pattern continues in all the monofluorinated diphenidine analogues. This means that both the  $^{19}\text{F}$  and  $^1\text{H}$  NMR experiments must be used in conjunction in order to ascertain the compounds present. The only compounds to produce slightly different  $^{19}\text{F}$  NMR spectra are the FTFEP regioisomers. These produce one peak for the monofluorinated substituent in the benzene ring and another peak representing all fluorines in the  $\text{CF}_3$  of the ethyl chain. The stacked spectra for the compounds can be seen in figure 162. Trifluoroacetic acid ( $\delta$  ppm = -76.55) was added as an internal standard. The peaks representing the  $\text{CF}_3$  group appear at -66.20 ppm for each isomer, with the peaks for the fluorine in the benzene ring being similar for the 3- and 4- isomers but different for the 2- isomer.

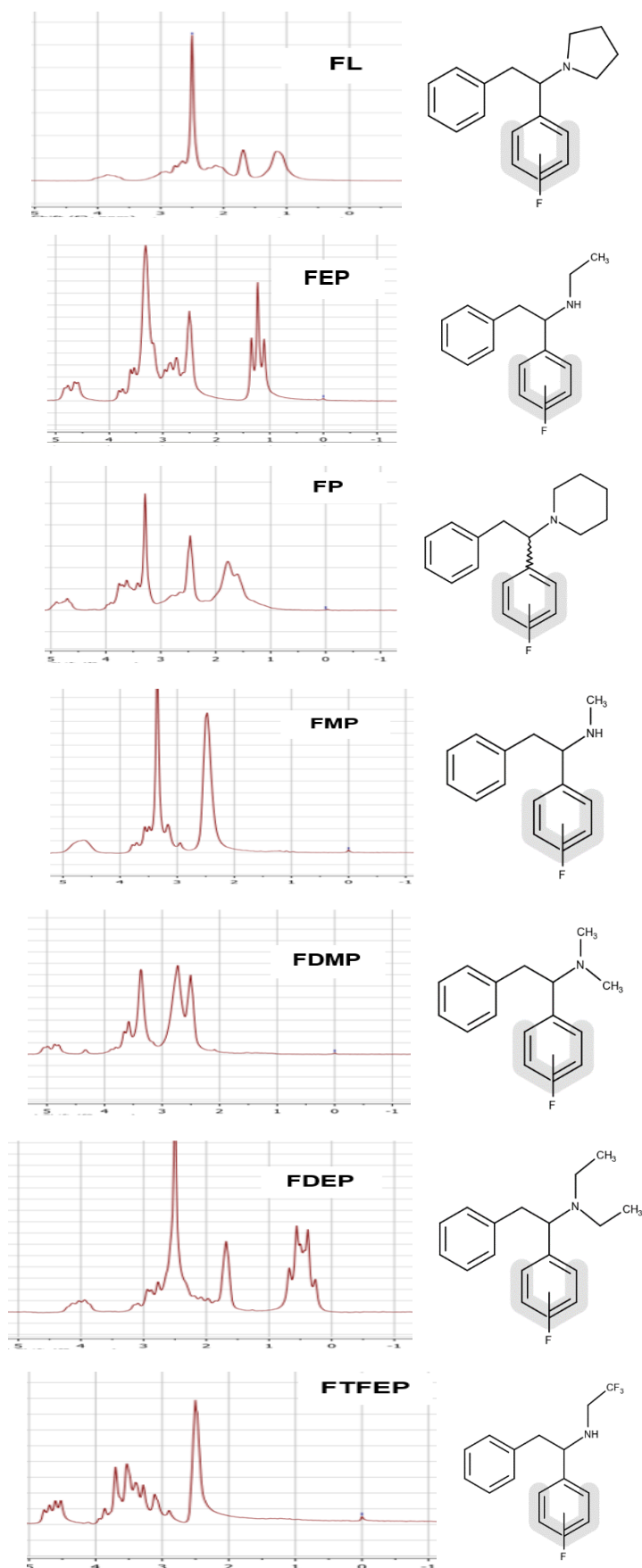


**Figure 143:** Stacked 60 MHz <sup>1</sup>H NMR spectra showcasing the aliphatic regions for the monofluorinated diphenidine analogues run in DMSO-d<sub>6</sub> (δ ppm = 2.50)

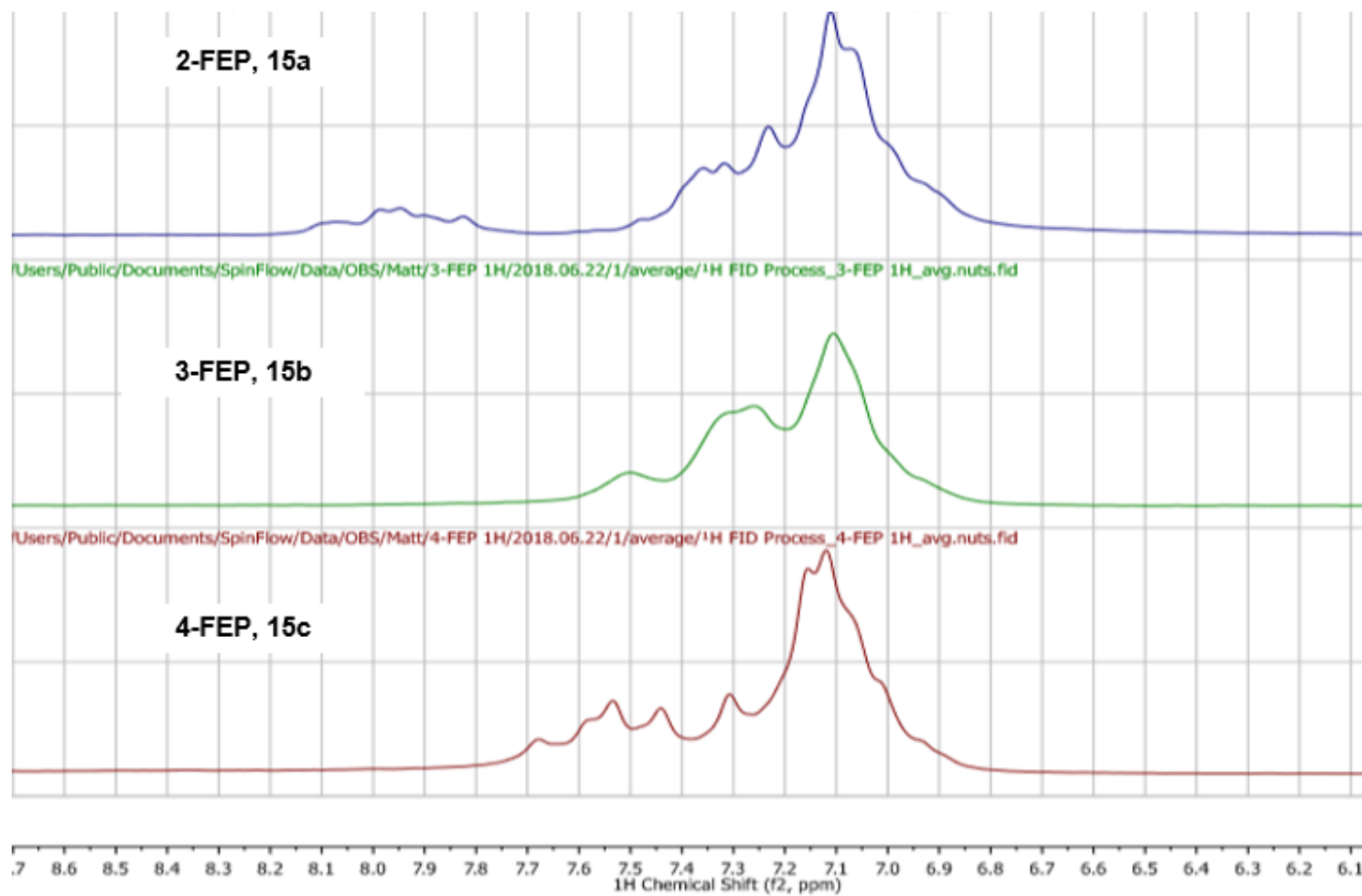


**Figure 144:** Stacked 60 MHz <sup>1</sup>H NMR spectra showcasing the aromatic region for the fluoroephedrine regioisomers (4-FEP, 15a–15c)

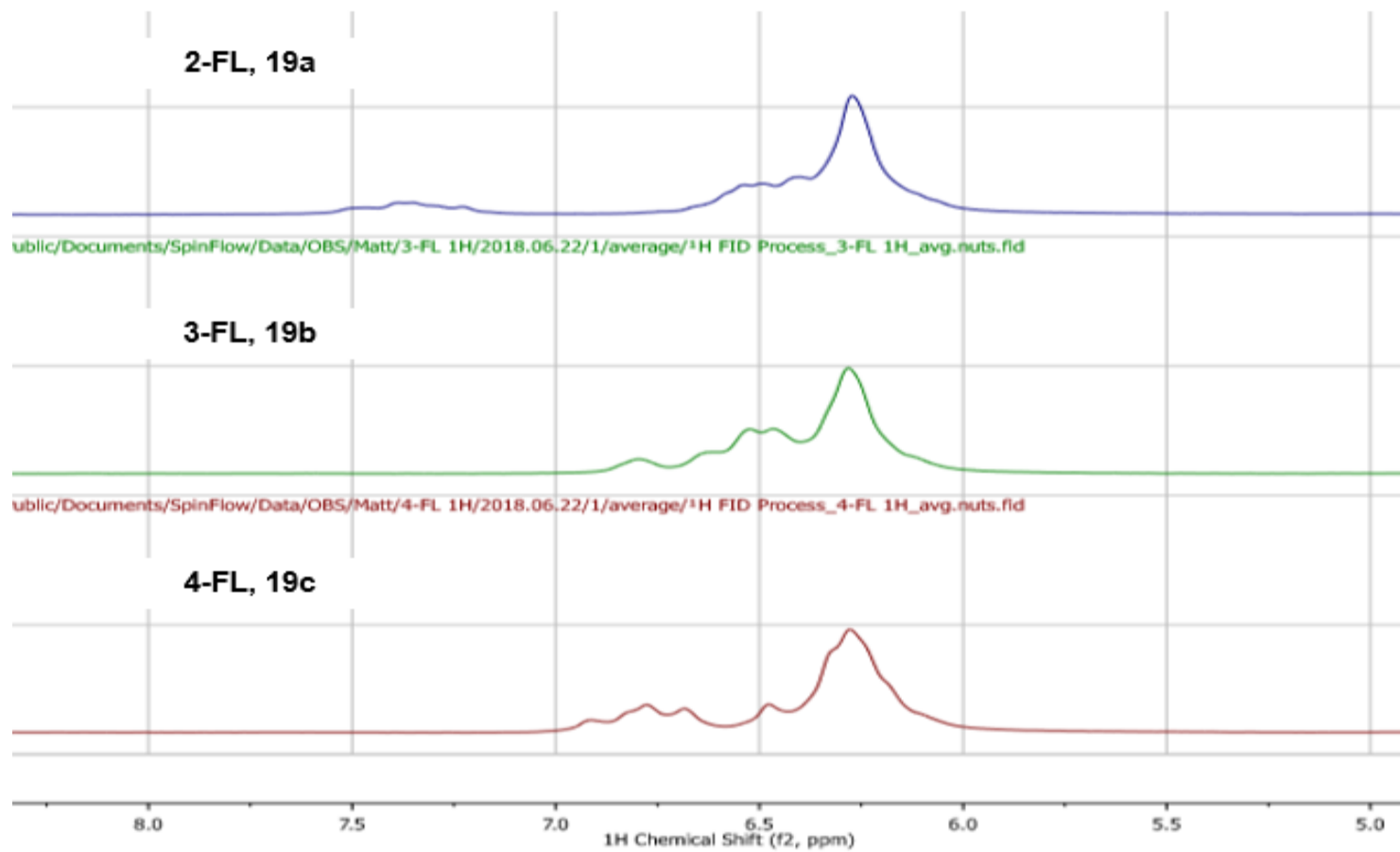


**Figure 145:** Stacked 60 MHz <sup>1</sup>H NMR spectra showcasing the aromatic region for the fluorolintane regioisomers (FL, **19a–19c**)



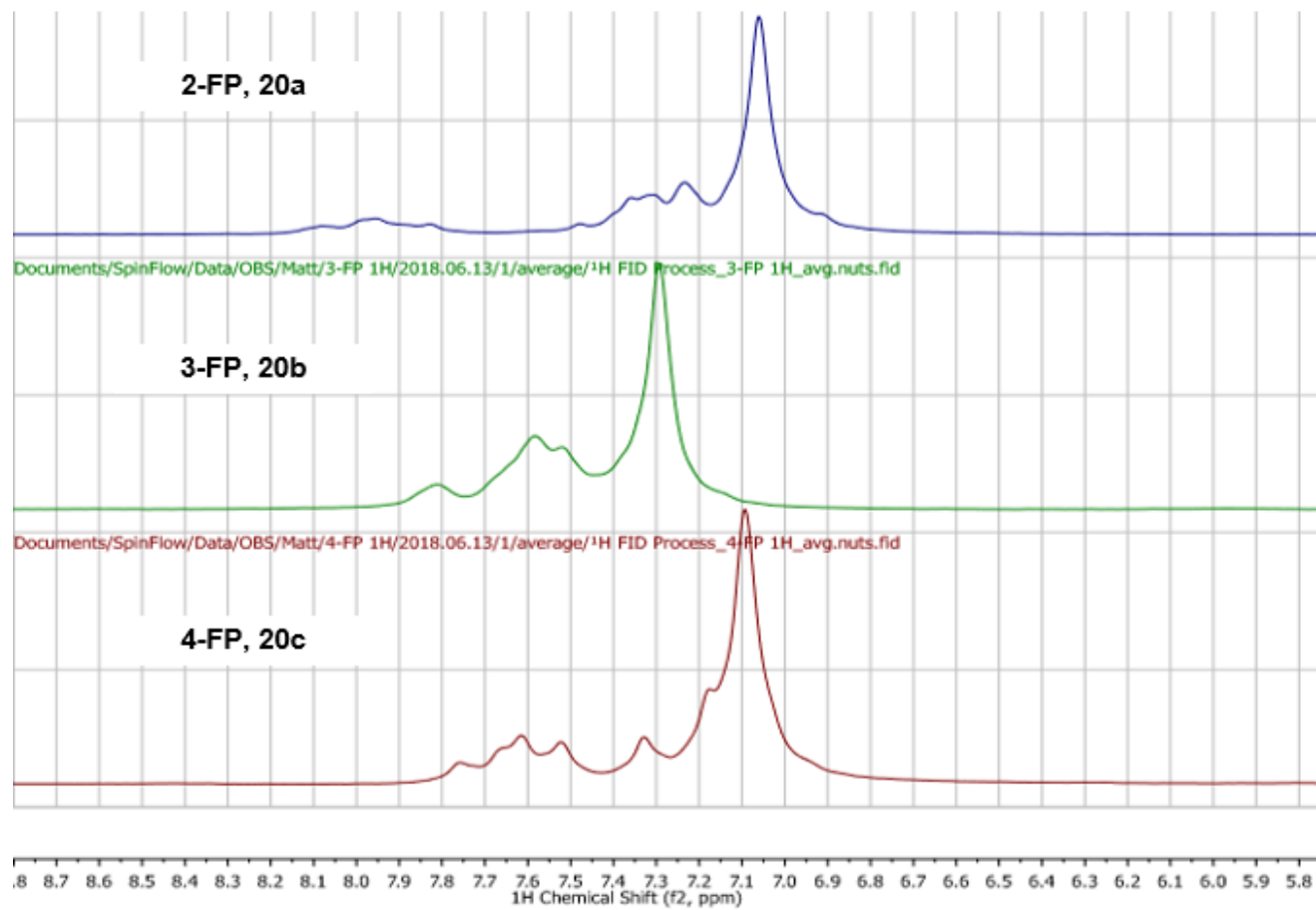


**Figure 146:** Stacked 60 MHz <sup>1</sup>H NMR spectra showcasing the aromatic region for the fluphenidone regioisomers (FP, 20a–20c)

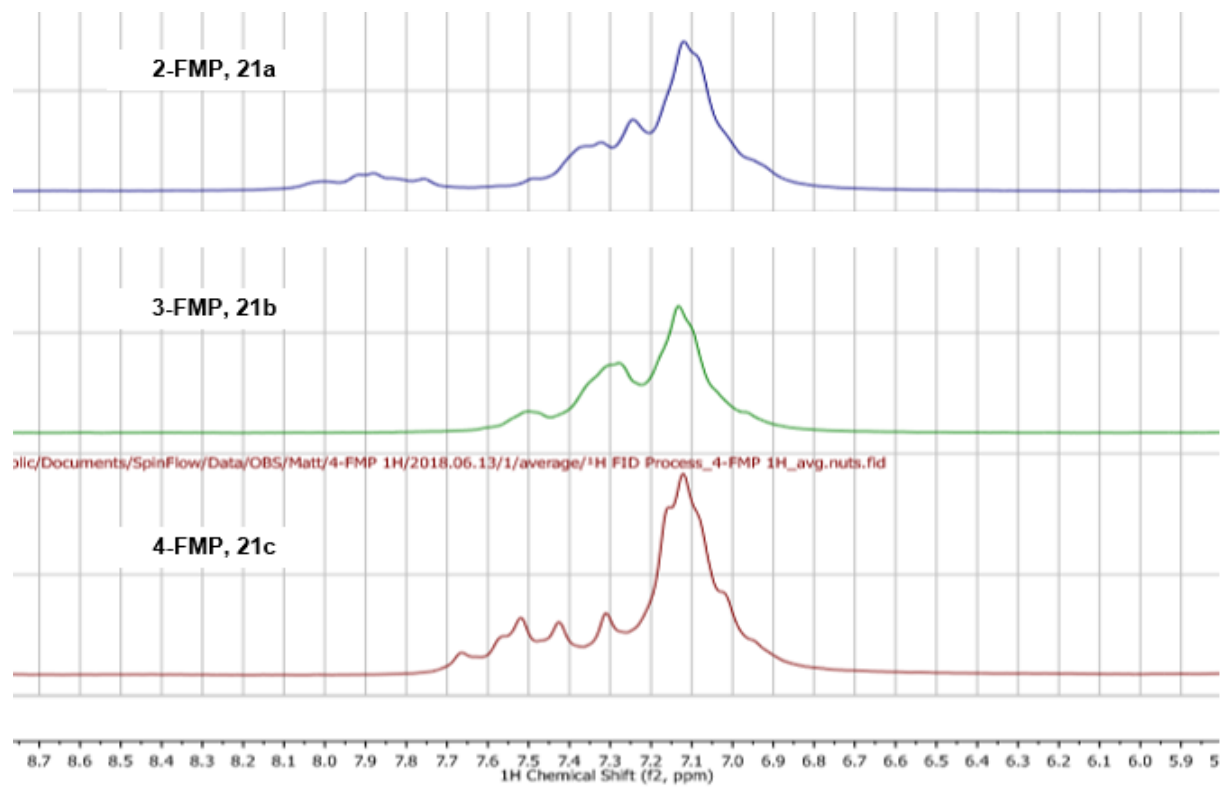


**Figure 147:** Stacked 60 MHz <sup>1</sup>H NMR spectra showcasing the aromatic region for the fluoromephedrine regioisomers (FMP, 21a–21c)

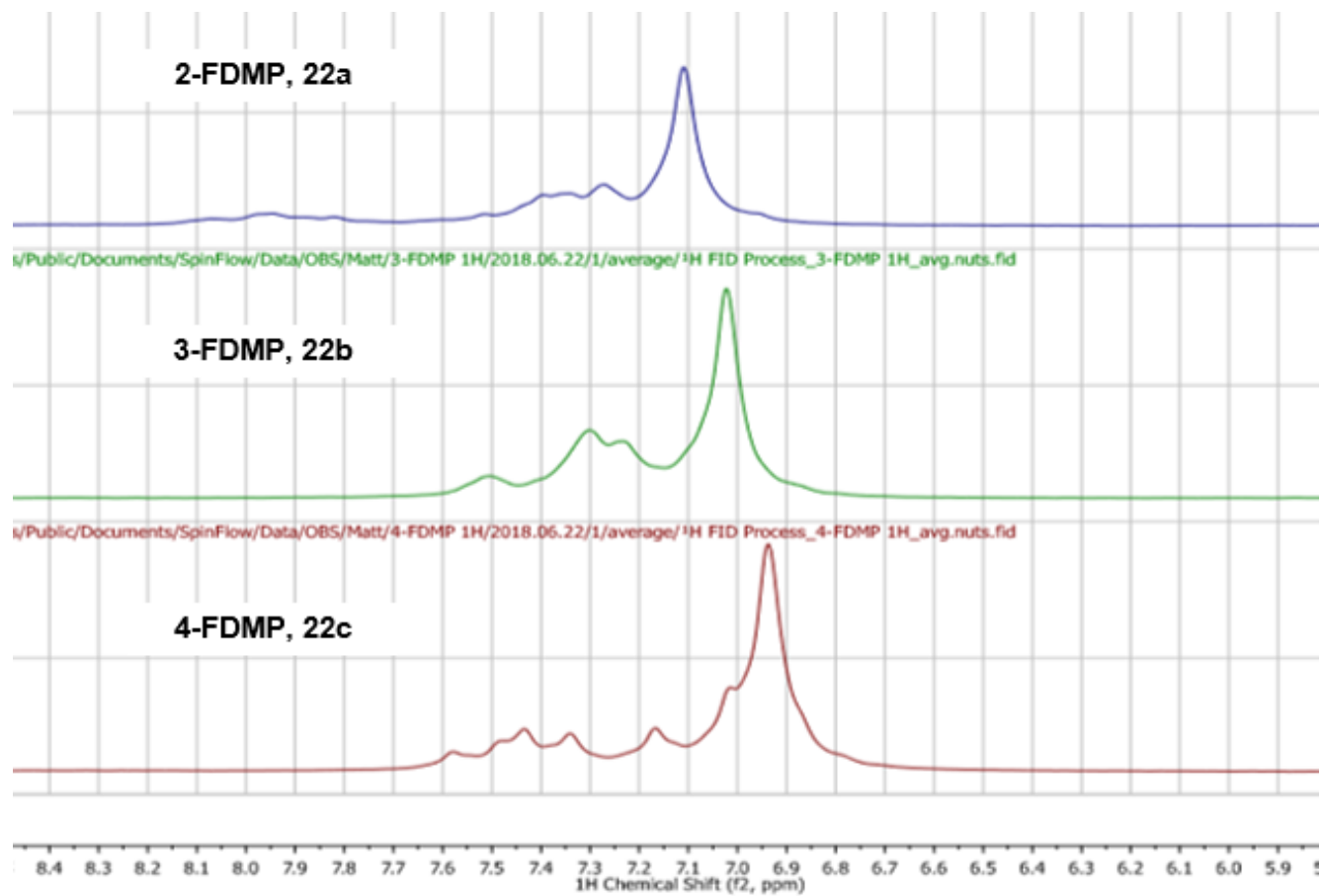


**Figure 148:** Stacked 60 MHz <sup>1</sup>H NMR spectra showcasing the aromatic region for the fluorodimephenidine regioisomers (FDMP, 22a–22c)

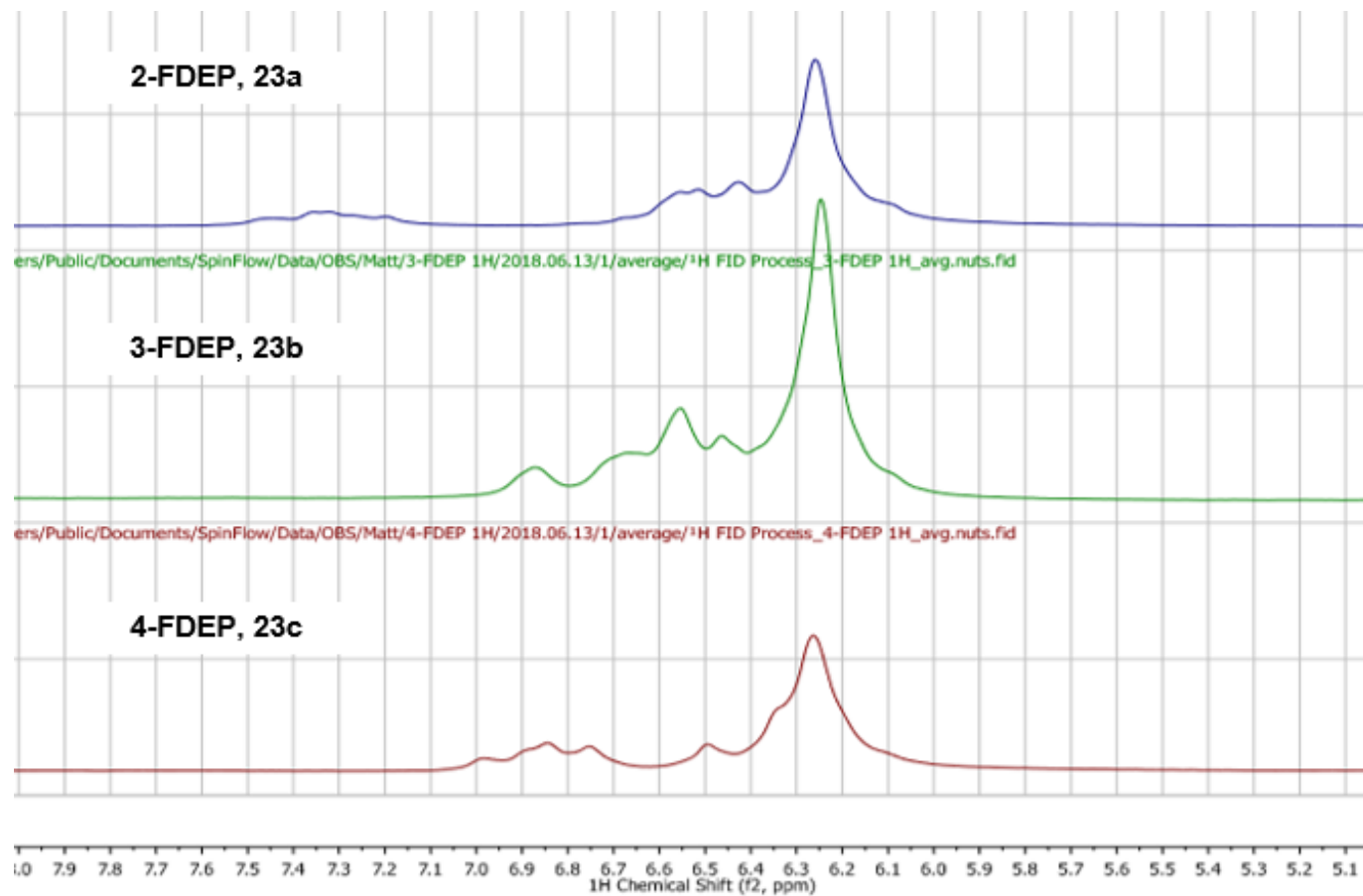


**Figure 149:** Stacked 60 MHz <sup>1</sup>H NMR spectra showcasing the aromatic region for the fluorodiephenidine regioisomers (FDEP, 23a–23c)

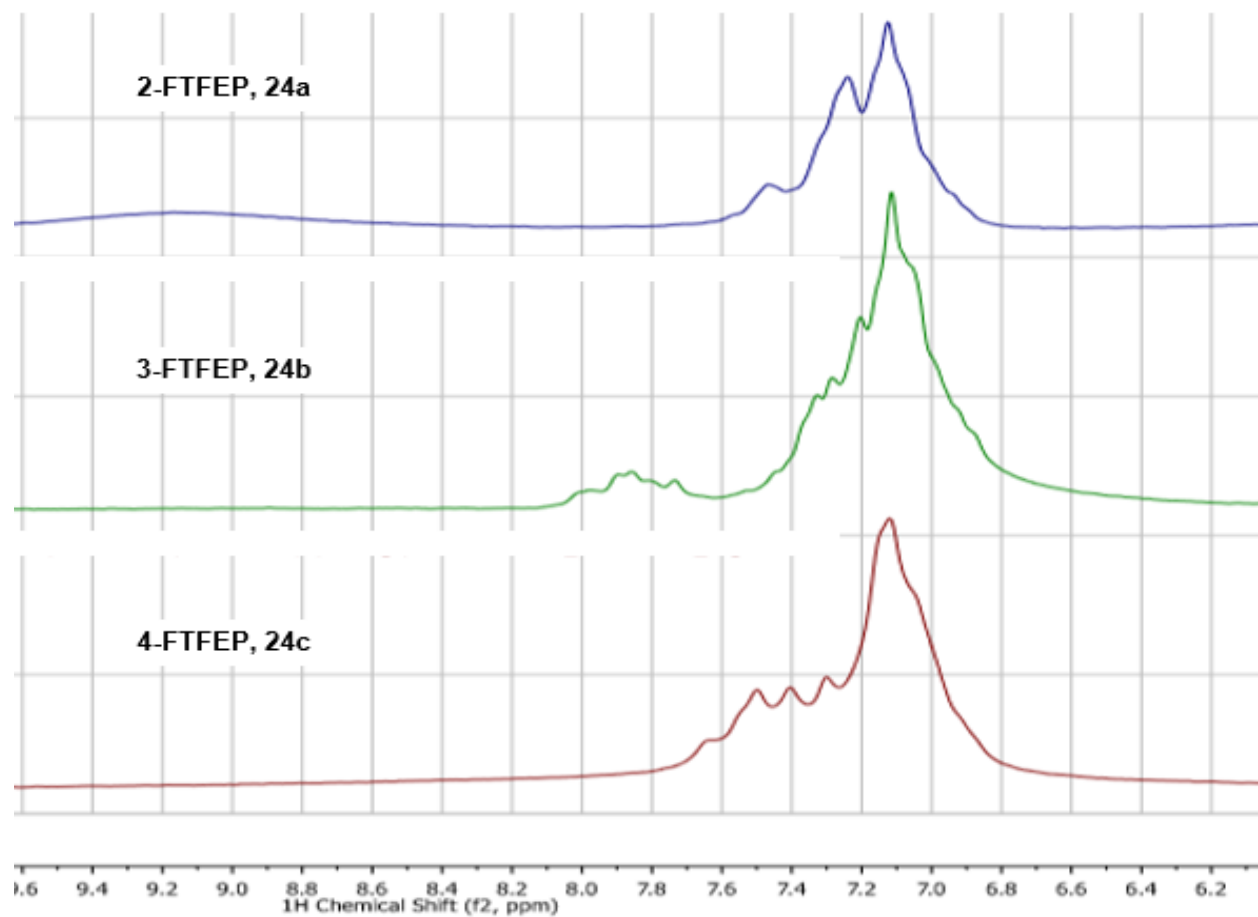


**Figure 150:** Stacked 60 MHz <sup>1</sup>H NMR spectra showcasing the aromatic region for the fluorotrifluoroephenidine regioisomers (FTFEP, **24a–24c**)

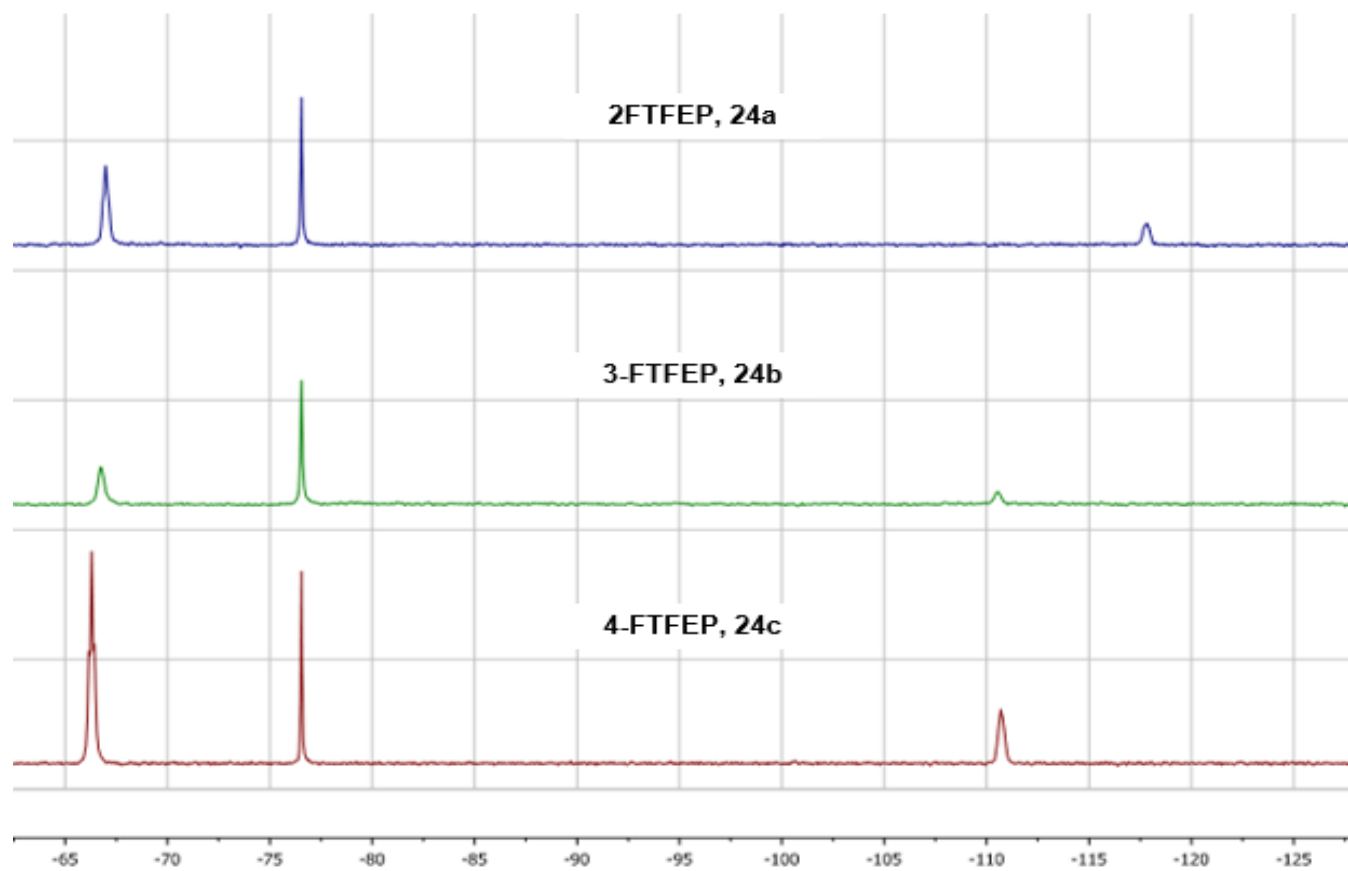


**Figure 151:** Stacked 60 MHz  $^{19}\text{F}$  NMR spectra for the fluorotrifluoroephenidine regioisomers (FTFEP, **24a–24c**)

**Table 43:** Table containing  $^{19}\text{F}$  NMR chemical shift data for all monofluorinated diphenidine analogues

<b>Compound no.</b>	<b>Compound name</b>	<b><math>^{19}\text{F}</math> chemical shift (<math>\delta</math> ppm)</b>
<b>15a</b>	2-fluoroephenidine	-118.64
<b>15b</b>	3-fluoroephenidine	-111.36
<b>15c</b>	4-fluoroephenidine	-112.16
<b>19a</b>	2-fluorolintane	-118.86
<b>19b</b>	3-fluorolintane	-111.96
<b>19c</b>	4-fluorolintane	-112.43
<b>20a</b>	2-fluphenidine	-115.20
<b>20b</b>	3-fluphenidine	-110.96
<b>20c</b>	4-fluphenidine	-110.89
<b>21a</b>	2-fluoromephenidine	-118.24
<b>21b</b>	3-fluoromephenidine	-111.26
<b>21c</b>	4-fluoromephenidine	-111.94
<b>22a</b>	2-fluorodimephenidine	-115.80
<b>22b</b>	3-fluorodimephenidine	-110.71
<b>22c</b>	4-fluorodimephenidine	-110.64
<b>23a</b>	2-fluorodiephenidine	-117.89
<b>23b</b>	3-fluorodiephenidine	-111.03
<b>23c</b>	4-fluorodiephenidine	-111.29
<b>24a</b>	2-fluorotrifluoroephenidine	-66.20 ( $\text{CF}_3$ ), -117.81
<b>24b</b>	3-fluorotrifluoroephenidine	-66.20 ( $\text{CF}_3$ ), -110.54
<b>24c</b>	4-fluorotrifluoroephenidine	-66.20 ( $\text{CF}_3$ ), -110.79

## 6.7. Quantitative 60 MHz analysis

Quantitative analysis was attempted on the 60 MHz Pulsar instrument in order to show the possibility of being able to determine how much active component is present in a street sample. The 4-FEP sample was chosen for the quantitative analysis with trifluoroacetic acid (TFA, 0.1 % v/v) used as an internal standard to calculate peak area ratios. 5 samples were prepared in a concentration range of 5 mg mL<sup>-1</sup> to 15 mg mL<sup>-1</sup>. A <sup>19</sup>F NMR spectrum was acquired for each of these samples, with each spectrum being acquired in triplicate. The sample <sup>19</sup>F signals and that of the TFA were integrated and a ratio was calculated (Table 44).

**Table 44:** Integrated area values for the calibration solutions from <sup>19</sup>F NMR experiments on a 60 MHz instrument

Concentration (mg mL <sup>-1</sup> )	Integrated area ratios		
	Run 1	Run 2	Run 3
5	5.73	5.8	5.68
7.5	7.07	7.16	6.89
10	8.34	8.28	8.22
12.5	9.59	9.62	9.58
15	10.8	10.76	10.91

The graph (figure 152) shows that there is a good potential to perform quantitative analysis on a low field NMR system. The correlation coefficient for the calibration graph is acceptable (0.9985) and results show good repeatability with RSD values for each concentration samples < 2%. The LOD and LOQ of the system are 1.68 and 3.20 mg mL<sup>-1</sup> respectively and these are below the usual amounts of sample that are obtained from seized samples.

In a similar manner to the fluoroamphetamine (FA, chapter 3) quantitative analysis using <sup>19</sup>F NMR, on the Pulsar instrument, the calibration graph does not go through the origin ( $x = 0, y = 0$ ). This is due to noise of the baseline associated with the collection of the spectrum. In order to avoid this an average integration of the noise around each signal would be needed and subtracted from the integration value of this peak. This is not performed due to time



restraints associated with the processing of each spectrum and multiple repeats. Also the main aim is for this to be performed by people with less scientific background who would not be familiar with processing techniques and the calibration graph has shown it is not necessary. A 5 second relaxation delay ensures that there is enough of a gap in between pulses to allow a full  $90^\circ$  relaxation. A  $2.5 \text{ mg mL}^{-1}$  was ran and fell within the linear response, however adding another standard below this would fall below the limit of detection (LOD).

Further testing would be needed to confirm optimisation related to the number of scans and spectral window in order to show that the LOD and LOQ of the system have been fully optimised. Testing on further classes would be needed in order to show that qualitative analysis can be performed on multiple classes and not just diphenidine analogues.

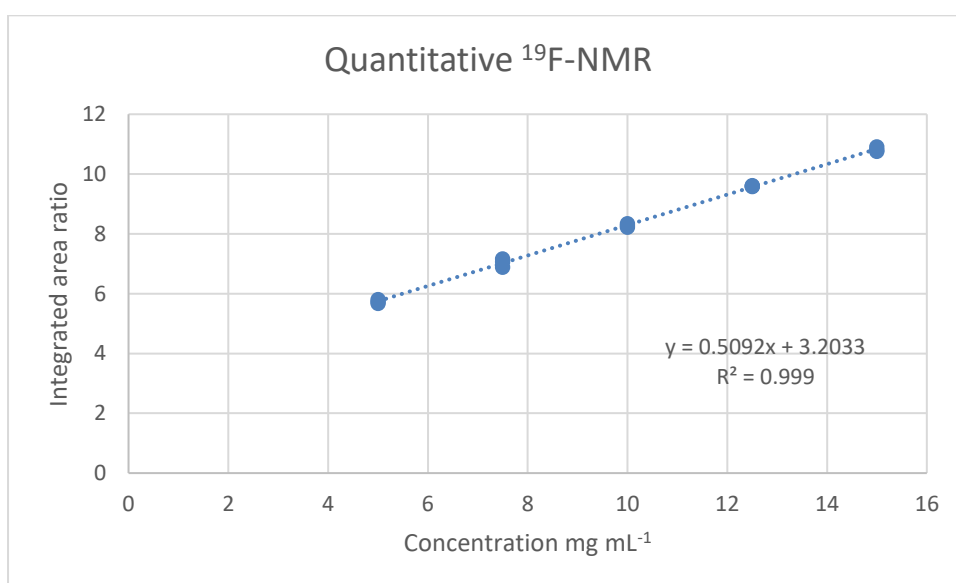


**Figure 152:** Calibration graph for the 4-FEP isomer using  $^{19}\text{F}$  NMR spectroscopy on a 60 MHz instrument

## 6.8. Conclusions

Twenty-one monofluorinated diphenidine analogues were synthesised in order to show the ease of production within clandestine labs. All reference materials were shown to be >95% pure with yields ranging from 33-68%. All compounds were fully characterised using a range of analytical techniques.

Presumptive testing using a range of test reagents showed initial presence of possible classes within a solution. This was especially true when distinguishing between secondary and tertiary amines. The Marquis, Mandelin, Scott's and Simon's reagents should be used in combination with one another to help show the class present. In a similar manner to the halogenated diphenidines, it is not possible to distinguish regioisomers within a class using colour test reagents.

A GC-MS method was developed which helped to separate different classes with mixtures used where the fluorine substituent were in matching positions on the benzene ring. This when combined with the mass spectrometry data provides identification of the class within 35 minutes. Changing the amine does show some difficulties in separation of the regioisomers within a class, especially those where the amine is a group rather than a chain, as with the FP and FL compounds. However, it is unlikely that samples would appear as a mixture, on the illicit drugs market, containing more than one of the same class of fluorinated diphenidine analogue. No street samples were tested as no street samples have been encountered containing compounds synthesised in this instance.

Finally, 60 MHz NMR can help to identify the class of compound present as well as the specific isomer within a class. This was achieved using a combination of both  $^1\text{H}$  and  $^{19}\text{F}$  experiments. It was observed that using the aliphatic region of the  $^1\text{H}$  spectrum would help to identify the class, while the aromatic region helps to identify the isomer within the class. It was also shown from initial testing that the 60 MHz instrument can also be used to perform quantitative analysis, with more testing needed to clearly show its ability to

determine amounts of active ingredients within street samples. This demonstrates that 60 MHz NMR spectroscopy can be employed in a presumptive testing technique due to the speed and ease of testing, as experiments are performed in under 5 minutes with little sample preparation needed.

## 7. Chapter 7 - Separation and identification of polyfluorinated ephenidine regioisomers

### 7.1. Overview

Ephenidine has been reported in the literature previously-<sup>111, 112</sup>, however there has been no previous reports of any fluorinated derivatives emerging onto the drugs market. One major problem encountered by forensic laboratories and law enforcement agencies is the ability to detect new compounds as soon as they emerge, with little reference data available to help in the identification. Difficulties also emerge when more than one fluorine atom appears within a compound as a spectrum can become more confusing and difficult to interpret.

This chapter will aim to synthesise the difluorinated derivatives of ephenidine along with the tri, tetra and pentafluorinated derivatives. Full characterisation will be performed using a range of analytical techniques including GC-MS and NMR. <sup>19</sup>F NMR will be utilised in order to provide spectra that are easier to interpret compared to the <sup>1</sup>H NMR spectra.

A GC-MS method will be developed in order to try and separate the nine polyfluorinated ephenidine derivatives. 60 MHz NMR will also be used to acquire <sup>1</sup>H and <sup>19</sup>F spectra in order to show the possibility of using “low field” NMR as a new presumptive testing device. Comparisons will be made in order to show the possibility of distinguishing between the different regioisomers. Two dimensional experiments will be developed on the 60 MHz NMR in order to further help with the identification of the different regioisomers.

## 7.2. Synthesis

The six difluoroephenedine derivatives (**DFEP**, **15d–15i**) along with the trifluoro (**TriFEP**, **15j**), tetrafluoro (**TeFEP**, **15k**) and pentafluoroephenedine (**PFEP**, **15l**) samples were prepared as their corresponding hydrochloride salts. These were prepared to show possible compounds that could be made in future, as popularity in the production of fluorinated derivatives has been reported to be increasing.<sup>2</sup>

All target compounds were synthesised, as racemic mixtures, using the same methodology as the diphenidine derivatives using the requisite aldehyde. Reference materials were produced as stable, colourless to off-white powders with overall yields ranging from 48–64%. Solubility tests showed the hydrochloride salts to be soluble in water, methanol, dichloromethane and dimethylsulfoxide at a concentration of 10 mg mL<sup>-1</sup>. In order to show compounds had been correctly synthesised, ready for analysis, full structural characterisation was carried out using <sup>1</sup>H NMR, <sup>13</sup>C NMR and <sup>19</sup>F NMR. The purity of all samples was ascertained by NMR and GC-MS analysis and shown to be >95% in all cases.

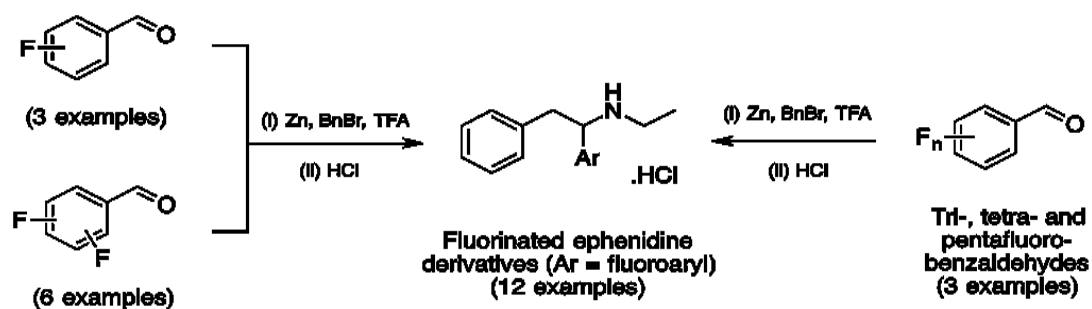


**Figure 153:** Reaction scheme for the synthesis of the polyfluorinated ephenidine compounds (**15d – 15l**)

The backbone of the polyfluorinated ephenidine isomers provides a very similar aliphatic region when using <sup>1</sup>H NMR. The only main difference between these compounds comes in the aromatic region of the proton spectra, with <sup>19</sup>F NMR being utilised in order to better show the possibility of distinguishing between isomers. All spectra were run in DMSO-d<sub>6</sub> with a solvent peak at 2.50

ppm. Some spectra contain acetone and water residual peaks at 2.09 ppm and 3.33 ppm respectively. Acetone is used in the recrystallization process and so trace amounts may be present in the NMR spectra, which may account for slight losses in purities reported. Trace amounts of water may also be present in DMSO- $d_6$ . In addition, as hydrochloride salts were produced, some compounds may present as a hydrated salt.

All polyfluorinated ephenidine isomers show a triplet peak at 1.23 ppm representing the three  $CH_3$  protons of the ethyl chain. There are also two multiplet peaks, representing the  $CH_2$  of the ethyl chain, at 2.80–2.90 ppm that show both protons exist in different chemical environments. This could be due to potential coupling with fluorines in the phenyl ring, as the 2,6-DFEP isomer does show a difference with only one quartet peak representing two protons, seen at 2.94 ppm. The fluorines in 2,6-DFEP may not interact with the ethyl chain, which would then result in both protons in the  $CH_2$  existing in the same chemical environment. In a similar way to the diphenidine regioisomers, there is a multiplet at 4.80 ppm that represents the chiral centre proton. Two peaks at 3.15 ppm and 3.80 ppm with a splitting pattern of a triplet and a doublet of doublets respectively represent the  $CH_2$  of the benzyl group and exist in different chemical environments based on the rotation of the compounds. All aliphatic regions show the same pattern for all polyfluorinated ephenidine regioisomers, meaning they cannot be distinguished based on this region.

Two amine protons are present for all compounds (that were isolated as the hydrochloride salts) and the chemical shifts of these vary between 9.20 and 10.50 ppm for each sample. The main difference between each  $^1H$  NMR spectrum comes in the aromatic regions. For the tri-, tetra- and pentafluoroephenidine samples the number of protons stated through the integration helps to identify, which sample is present, as the number of protons in the aromatic region decreases from seven to five as the number of fluorine atoms added to the benzene ring increases. However, these differences in the aromatic regions only help when identifying compounds found as individual components. When multiple difluoroephenidine regioisomers are seen as a mixture, there is overlap in these aromatic peaks making it difficult to

determine which compound is present or how many samples are present. Stacked  $^1\text{H}$  NMR spectra, acquired using a 400 MHz instrument, for the aromatic region of DFEP is shown in figure 155 whilst the full range (0-12 ppm)  $^1\text{H}$  NMR spectra of the 2,3-difluoroephedrine isomer (2,3-DFEP, **15d**) is shown in Figure 154.

$^{19}\text{F}$  NMR spectroscopy is required in order to help distinguish which isomer may be present in street samples and also to aid with mixture analysis. The  $^{19}\text{F}$  NMR chemical shift data (Table 45), obtained from a 60 MHz “benchtop” Pulsar<sup>®</sup> NMR spectrometer, shows that identification can be aided using this experiment in conjunction with the  $^1\text{H}$  NMR experiment.

**Table 45:** Chemical shift values for a number of polyfluorinated ephedrine regioisomers.  
TFA used as an internal standard ( $\delta$  ppm = -76.55)

Compound no.	Compound abbreviation	Chemical shift ( $\delta$ ppm)
<b>15d</b>	2,3 – DFEP	-140.18, -144.23
<b>15e</b>	2,4 – DFEP	-110.70, -114.48
<b>15f</b>	2,5 – DFEP	-118.58, -124.18
<b>15g</b>	2,6 – DFEP	-113.68
<b>15h</b>	3,4 – DFEP	-139.56, -139.70
<b>15i</b>	3,5 – DFEP	-110.62
<b>15j</b>	TriFEP	-163.00, -138.89, -135.30
<b>15k</b>	TeFEP	-157.68, -156.32, -142.77, -139.52
<b>15l</b>	PFEP	-163.30, -153.79, -140.90

The 2,6-DFEP and 3,5-DFEP isomers are both easily identifiable based on the  $^{19}\text{F}$  NMR screening experiment due to only having one peak, through the symmetry of the benzene ring. The chemical shifts are also far enough apart that the two compounds are easily distinguishable from one another. The 2,3-DFEP; 2,4-DFEP; 2,5-DFEP and 3,4-DFEP samples all give two peaks when using  $^{19}\text{F}$  NMR and can be identified as single components. The TriFEP and PFEP samples both give three  $^{19}\text{F}$  NMR signals, based on symmetry of the fluorine atoms, while the TeFEP is the only derivative that gives rise to four peaks in the  $^{19}\text{F}$  NMR spectra. When using a 60 MHz benchtop NMR the speed of the analysis is quicker than most presumptive testing methods with the experiment only taking 3 minutes to perform. However, when some of the

compounds are run as mixtures there is some overlap due to the broadness of the peaks (e.g. 2,4-DFEP and 3,5-DFEP) meaning further experiments are needed in order to fully distinguish between the regioisomers.  $^{19}\text{F}$  NMR in this case provides a useful experiment due to the simplicity of the spectra produced.



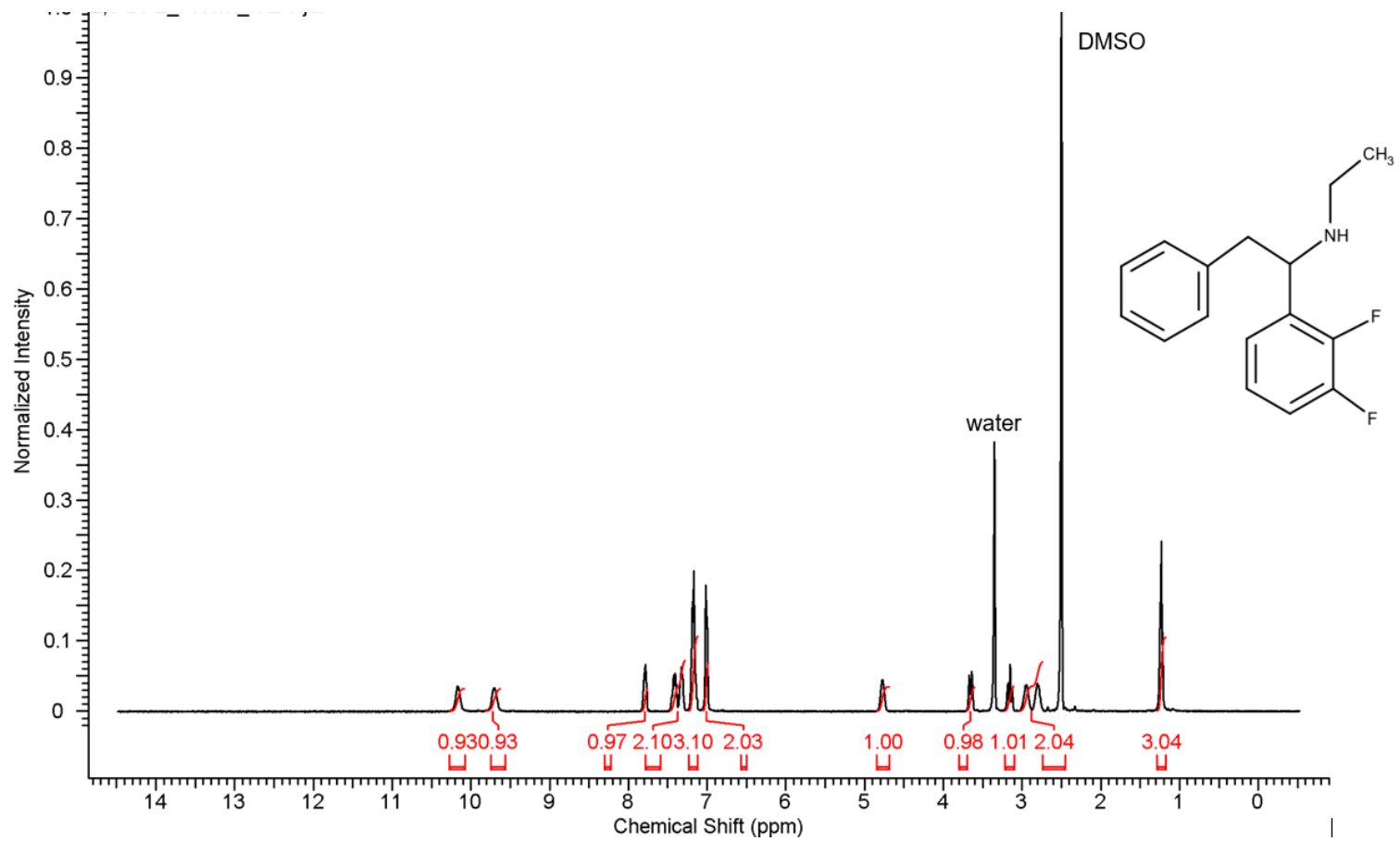


**Figure 154:** <sup>1</sup>H NMR spectrum (400 MHz) of the 2,3-difluoroephedrine (2,3-DFEP, **15d**) isomer run in DMSO-d<sub>6</sub> (δ ppm = 2.50)

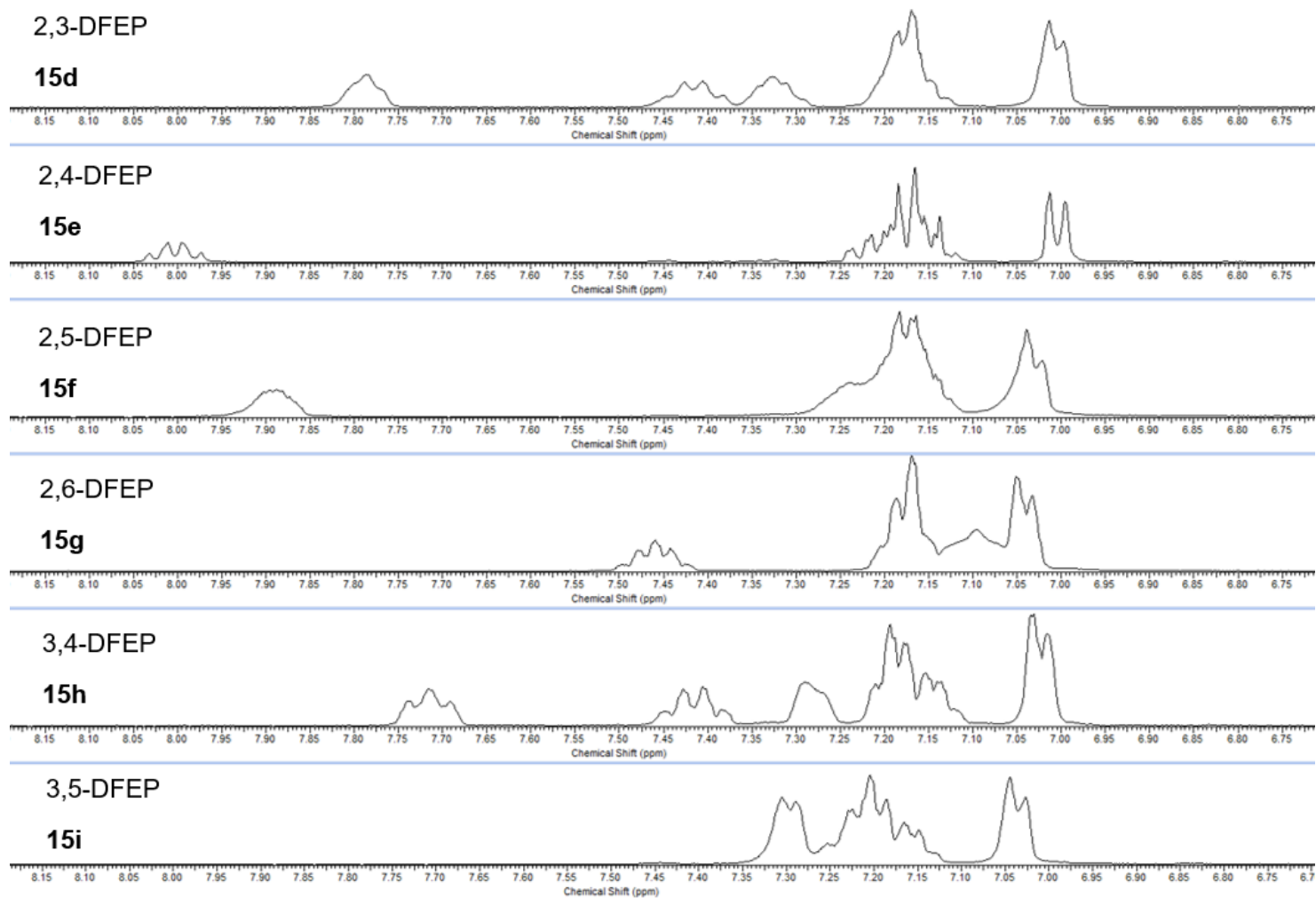


**Figure 155:** Stacked <sup>1</sup>H NMR spectra for the DFEP regioisomer aromatic regions run in DMSO-d<sub>6</sub> (δ ppm = 2.50) acquired using a 400 MHz instrument

### 7.3. Presumptive testing

The presumptive testing for difluorinated and polyfluorinated ephenidine regioisomers have not previously been reported and were performed using the United Nations recommended guidelines, in a similar way to the diphenidine regioisomers.<sup>118</sup> A range of test reagents were used in this study including (i) Marquis test; (ii) Mandelin test; (iii) Simon's test; (iv) Robadope's test; (v) Scott's test and (vi) Zimmerman test. The preparation of the reagents and test procedure is detailed in the experimental section (section 2.2). A solution of each reference standard ( $10 \text{ mg mL}^{-1}$ ) was prepared in deionised water and a couple of drops placed into a dimple well of a spotting tile. The required presumptive test reagent (1-2 drops) was then added and any colour change upon initial addition of the reagents were noted and observations were made again after a five minute time period (Table 46).

Marquis, Simon's and Zimmerman's reagents were the only tests to produce a noticeable colour change from the blank water solution. All solutions gave a positive reaction with the Marquis reagent, creating a yellow colour, which fades to a colourless solution after being left for five minutes. All solutions reacted in a similar way which makes identification of a specific isomer difficult. All samples also reacted in a similar way with the Zimmerman reagent and created a pale yellow precipitate, in a similar manner to the diphenidine reagents, which is believed to be the free base form of the drug, which is insoluble in water. Similar to the Marquis reagent all regioisomers reacted the same with the Zimmerman reagent making it difficult to distinguish between compounds.

The final reagent to give a positive colour change was Simon's reagent. Simon's test works through the reaction of the secondary amine with aldehyde, followed by a reaction with sodium nitroprusside to produce the imine. This iminium salt is hydrolysed to produce the Simon-Awe complex. The difluorinated ephenidine samples produce a red/brown colour when reacted with Simon's reagent, which could result from the reaction of sample with the nitroprusside coordination centre to produce a complex, while producing a

sodium salt that would have a natural red colour when dissolved as an aqueous solution. Each compound produces a slightly different colour when reacted with Simon's reagent; however, it is not a reliable difference as it relies on the user's discretion to determine the difference in colour change and intensities of colour may vary with concentrations used. As a presumptive test, Simon's reagent should be used in combination with the Marquis reagent in order to determine the possible presence of a polyfluorinated ephedrine isomer.

**Table 46:** Colour changes observed with presumptive test reagents for the DFEP (**15d-15i**) regioisomers, TriFEP (**15j**), TeFEP (**15k**) and PFEP (**15l**) compounds immediately after addition and after 5 minutes of addition

	Marquis		Mandelin		Simon's		Robadope		Scotts		Zimmerman	
	Colour change	Colour after 5 minutes	Colour change	Colour after 5 minutes	Colour change	Colour after 5 minutes	Colour change	Colour after 5 minutes	Colour change	Colour change after 5 minutes	Colour change	Colour change after 5 minutes
<b>15d</b>	yellow	colourless	-	-	light brown	light brown	-	-	-	-	- pale yellow ppt	- pale yellow ppt
<b>15e</b>	light yellow	colourless	-	-	dark brown	dark brown	-	-	-	-	- pale yellow ppt	- pale yellow ppt
<b>15f</b>	light yellow	colourless	-	-	brown	brown	-	-	-	-	- pale yellow ppt	- pale yellow ppt
<b>15g</b>	yellow	colourless	-	-	red	red	-	-	-	-	- pale yellow ppt	- pale yellow ppt
<b>15h</b>	light yellow	colourless	-	-	brown	brown	-	-	-	-	- pale yellow ppt	- pale yellow ppt
<b>15i</b>	yellow	colourless	-	-	brown	brown	-	-	-	-	- pale yellow ppt	- pale yellow ppt
<b>15j</b>	yellow	colourless	-	-	dark red	dark red	-	-	-	-	- pale yellow ppt	- pale yellow ppt
<b>15k</b>	yellow	colourless	-	-	brown	brown	-	-	-	-	- pale yellow ppt	- pale yellow ppt
<b>15l</b>	yellow	colourless	-	-	brown	brown	-	-	-	-	- pale yellow ppt	- pale yellow ppt

## 7.4. Thin layer chromatography

Thin layer chromatography has been performed on the six difluoroephenidine regioisomers and the three polyfluorinated compounds using the same method as used for the thirteen diphenidine derivatives (see section 4.4). Average  $R_f$  values have been reported (Table 47) based on the averages from six repeats. The examination of these  $R_f$  values show that there is limited separation based on this measurement. The TriFEP (**15j**), TeFEP (**15k**) and PFEP (**15l**) compounds all show a much lower  $R_f$  value when compared to the difluoroephenidine isomers, apart from the 2,4-DFEP isomer (**15e**). The remaining DFEP compounds (**15d**, **15f–15i**) all have very similar  $R_f$  values and so cannot be separated based on TLC experiments.

**Table 47:** Thin Layer Chromatography data for the nine polyfluorinated ephenidine regioisomers (**15d–15l**)

	Compound name	Spot colour under UV light (254 nm)	Spot colour after staining with modified Dragendorff-Ludy-Tenger Reagent	$R_f$ value
<b>15d</b>	2,3-difluoroephenidine	Black spot	Blood-red spot	0.87
<b>15e</b>	2,4-difluoroephenidine	Black spot	Blood-red spot	0.75
<b>15f</b>	2,5-difluoroephenidine	Black spot	Blood-red spot	0.80
<b>15g</b>	2,6-difluoroephenidine	Black spot	Blood-red spot	0.83
<b>15h</b>	3,4-difluoroephenidine	Black spot	Blood-red spot	0.84
<b>15i</b>	3,5-difluoroephenidine	Black spot	Blood-red spot	0.80
<b>15j</b>	2,3,4-trifluoroephenidine	Black spot	Blood-red spot	0.72
<b>15k</b>	2,3,4,5-tetrafluoroephenidine	Black spot	Blood-red spot	0.74
<b>15l</b>	2,3,4,5,6-pentafluoroephenidine	Black spot	Blood-red spot	0.70

## 7.5. Gas chromatography – mass spectroscopy

The employed qualitative GC-MS method required an extremely straightforward solvation of the samples in methanol (1 mg mL<sup>-1</sup>) followed by direct injection into the instrument. No derivatisation step was required. All polyfluorinated regioisomers (**15d–15l**) were run individually initially, using the general screening method (section 2.4.3), before being run as a mixture in order to determine retention times. Retention times ( $R_t$ ) and relative retention times ( $RR_t$ ), in relation to the internal standard eicosane, can be seen in Table 48, while the overlapped spectra of the chromatograms along with the polyfluorinated ephenidine mixture can be seen in figure 165.

**Table 48:** GC-MS retention times for the polyfluorinated ephenidine regioisomers along with relative retention times compared to eicosane

Compound no.	Compound abbreviation	Compound Retention time ( $R_t$ / mins)	Eicosane Retention time (mins)	Relative Retention time ( $RR_t$ )
15d	2,3-DFEP	9.96	12.67	0.77
15e	2,4-DFEP	9.51	12.67	0.75
15f	2,5-DFEP	9.67	12.67	0.76
15g	2,6-DFEP	9.53	12.67	0.75
15h	3,4-DFEP	10.09	12.67	0.80
15i	3,5-DFEP	9.58	12.67	0.77
15j	TriFEP	9.77	12.67	0.77
15k	TeFEP	9.33	12.67	0.74
15l	PFEP	8.59	12.67	0.68

The relative retention times show that all polyfluorinated ephenidine isomers can be separated using GC-MS, apart from the 2,4-DFEP and 2,6-DFEP compounds. The two compounds cannot be distinguished from one another when run as a mixture (figure 165) as the two peaks co-elute making it impossible to identify one from the other. Even when the oven temperature programme was slowed to a ramp of 1°C/min or held on an isothermal ramp, the two compounds do not separate from one another. The GC-MS method was not validated in this case due to both peaks co-eluting and a new separation technique is needed to be able to identify these compounds from one another.

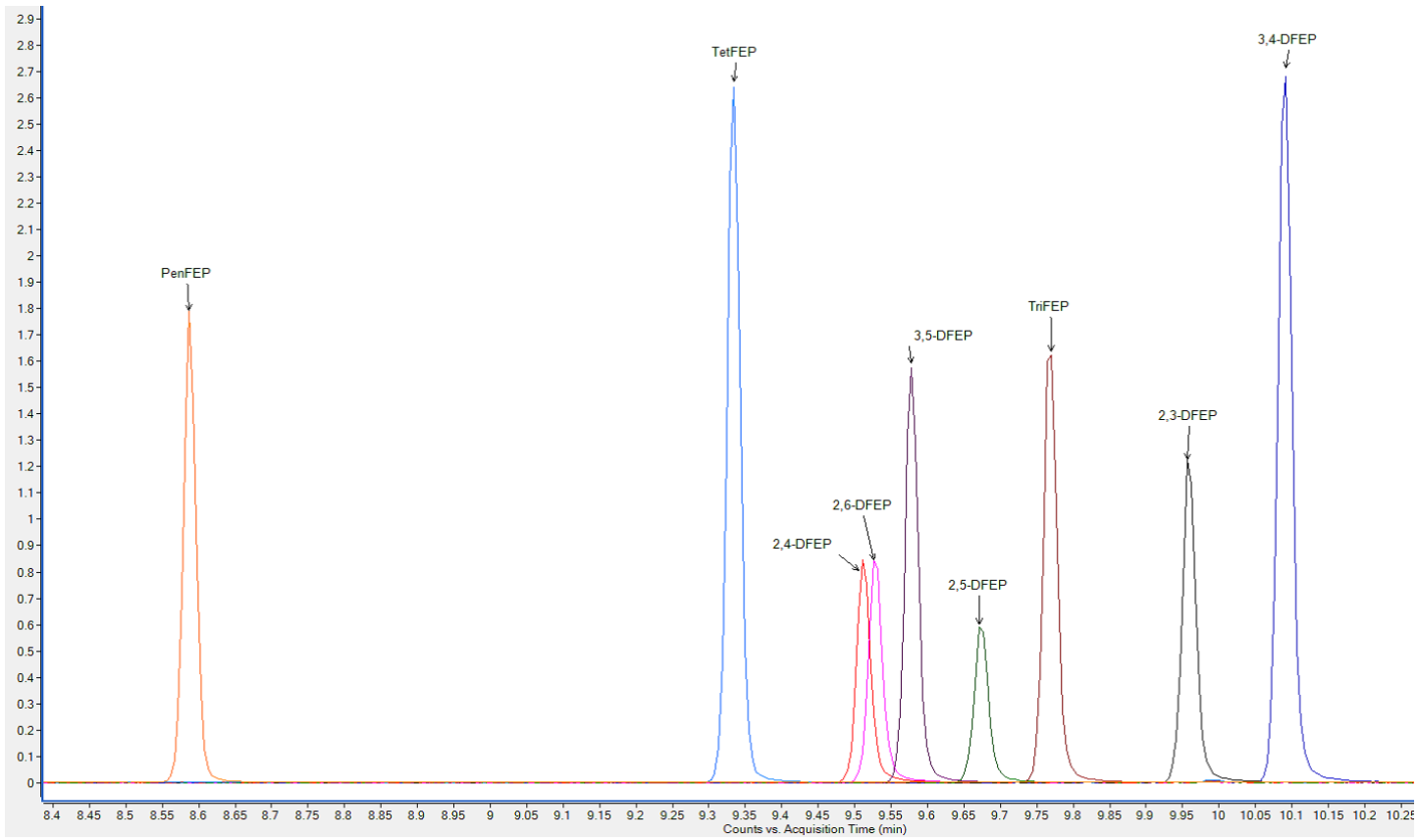


**Figure 156:** GC-MS chromatographs for all nine polyfluorinated ephenidines (**15d–15l**)



There is also no way to distinguish these two DFEP compounds based on the mass spectroscopy data as the spectra is the same for all of the regioisomers and can be seen in figure 157. The base peak, with a mass to charge ( $m/z$ ) value of 170.1, is derived in a similar way to the diphenidine regioisomers explained previously with the benzyl group removed to leave just the ethyl chain and phenyl ring with the di-substituted fluorine. The ethyl chain is then removed to produce a secondary peak of  $m/z$  142.0, with a peak also present at  $m/z$  91.0 representing the benzyl cation. This fragmentation pattern can be seen in figure 158. The  $m/z$  ratio for the base and secondary peaks, for the tri, tetra and pentafluorinated derivatives, then increases by a mass of one fluorine atom per compound and has distinguishable mass spectra (figure 159), creating unique values and distinguishable mass spectra.

The mass spectrometry in combination with GC allows identification of these three compounds in under 15 minutes, however the co-elution of the 2,4 and 2,6-DFEP isomers and matching mass spectra means a new instrument and technique is needed for identification purposes.

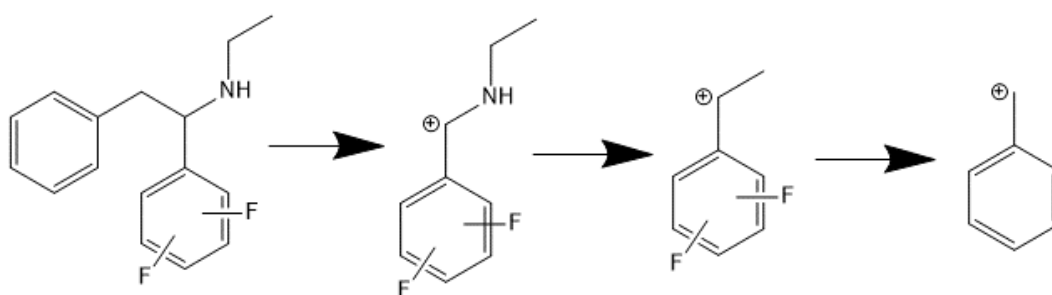


**Figure 157:** Mass spectrometry fragmentation pattern for polyfluorinated ephenidine regioisomers

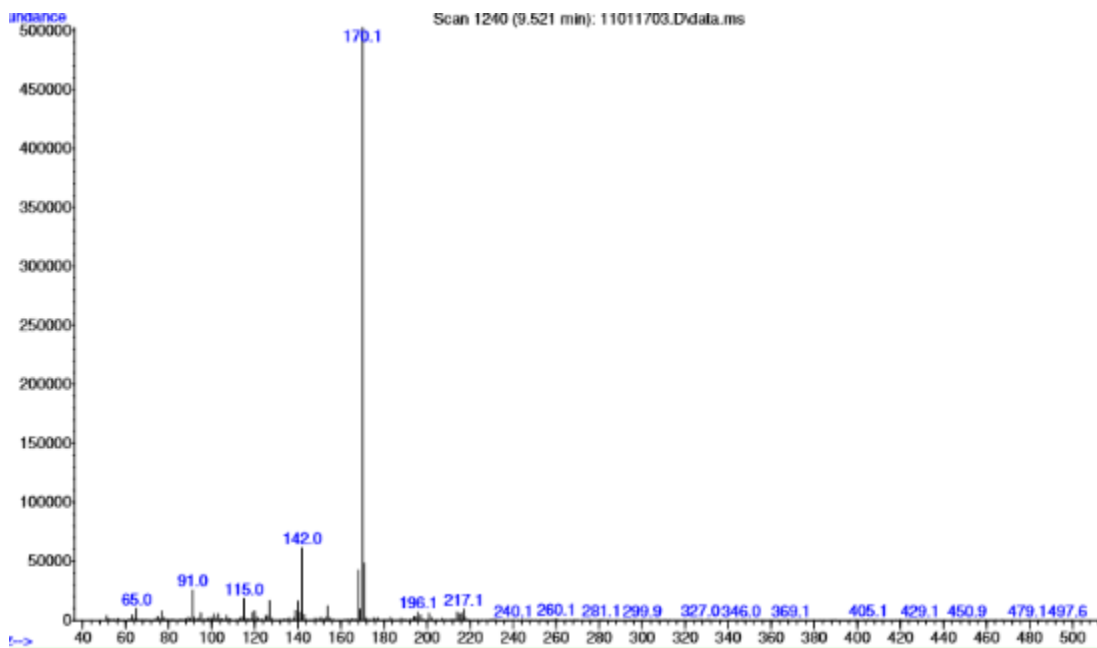


**Figure 158:** EI-MS spectra for all the DFEP regioisomers (**15d–15i**)

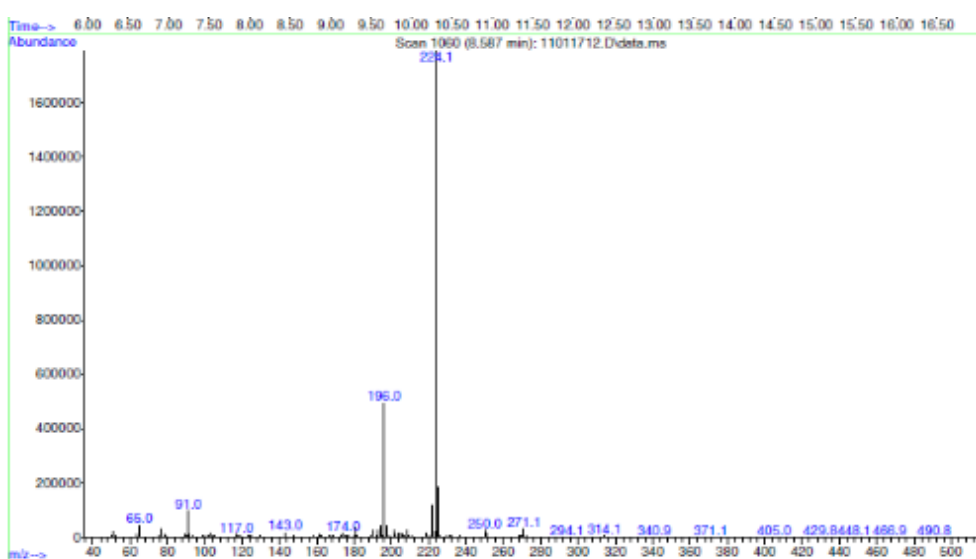
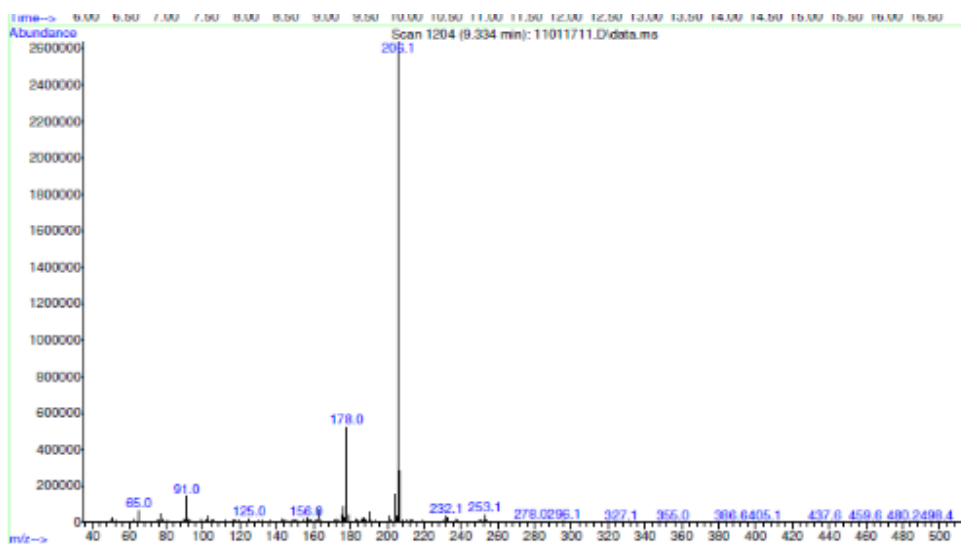
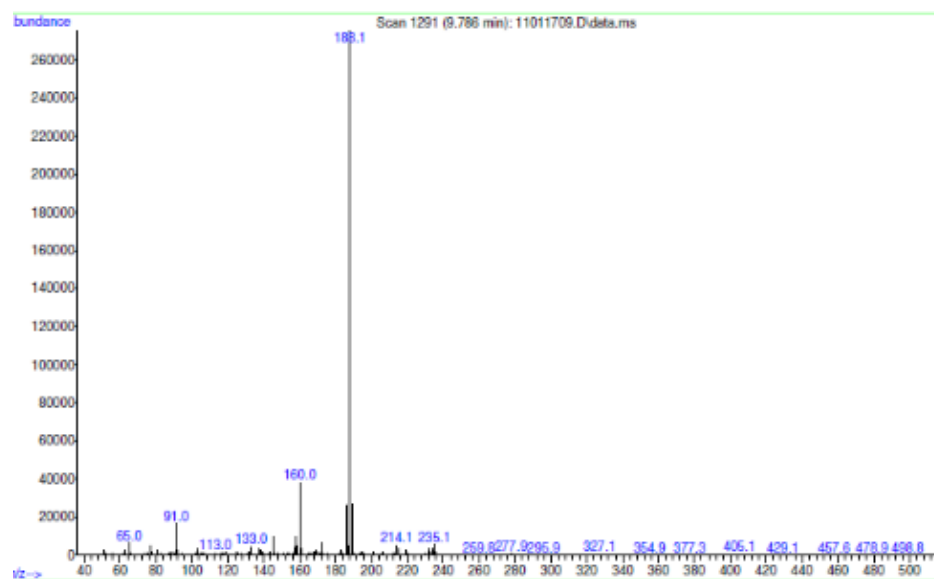
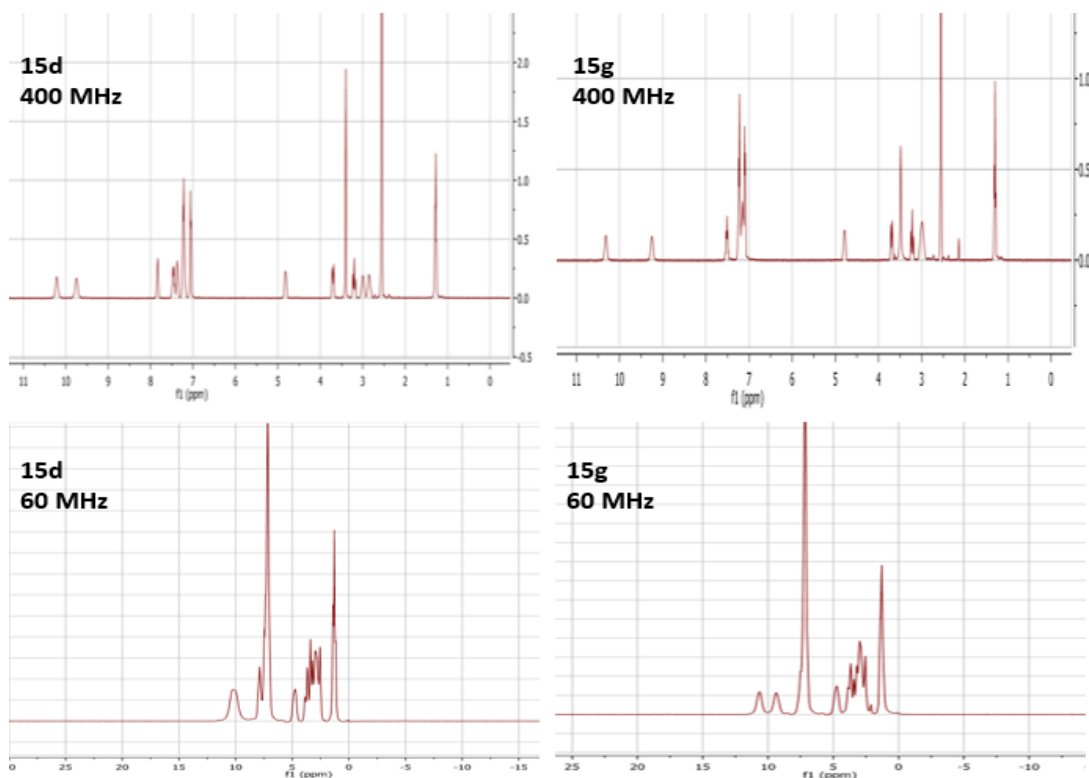


Figure 159: EI-MS spectra for the TriFEP, TeFEP and PFEP compounds

## 7.6. 60 MHz NMR screening

Due to the poor ability of current presumptive test reagents to distinguish between the polyfluorinated regioisomers, and the coelution of the 2,4 and 2,6 isomers using GC-MS, a new technique is needed that will be able to identify specific isomers in a quick, reliable manner. A 60 MHz Pulsar NMR instrument (Oxford Instruments, Abingdon, Oxfordshire) was used to obtain both  $^1\text{H}$  and  $^{19}\text{F}$  NMR spectra to help distinguish between the nine compounds. This instrument allows complex structural analysis to be performed similar to the 400 MHz NMR spectrometer, with less expense and less expert knowledge required to perform experimentation. The  $^1\text{H}$  NMR spectra were obtained for each individual compound at a concentration of  $10\text{ mg mL}^{-1}$ . Samples were prepared in the same manner as those used to obtain spectra on the 400 MHz instrument and each spectrum was acquired using 8 scans. It was observed from the 400 MHz that the aliphatic region of the spectrum matches for all ephenidine isomers and that the main differences can be seen in the aromatic region. The 60 MHz instrument still shows similarities in this aliphatic region for all regioisomers and the main pattern of the whole spectra carries over, even though slight resolution is lost and peaks broaden with the loss of splitting patterns, as the magnetic field is weaker for the 60 MHz measurements compared to those conducted on the 400 MHz instrument (figure 160).



**Figure 160:** <sup>1</sup>H NMR comparison using 400 MHz and 60 MHz instruments for the 2,3-DFEP (**15d**) and 2,6-DFEP (**15g**) isomers

The main differences between each isomer still appears in the aromatic region, even with the broadening of peaks and loss of splitting patterns, meaning this can be used to help with identification of samples. Although the aliphatic regions of each regioisomer are very similar there are clear differences in the patterns of spectra, for all the DFEP isomers (**15d-15i**) samples in the aromatic regions between 6 ppm and 8.5 ppm (figure 161).

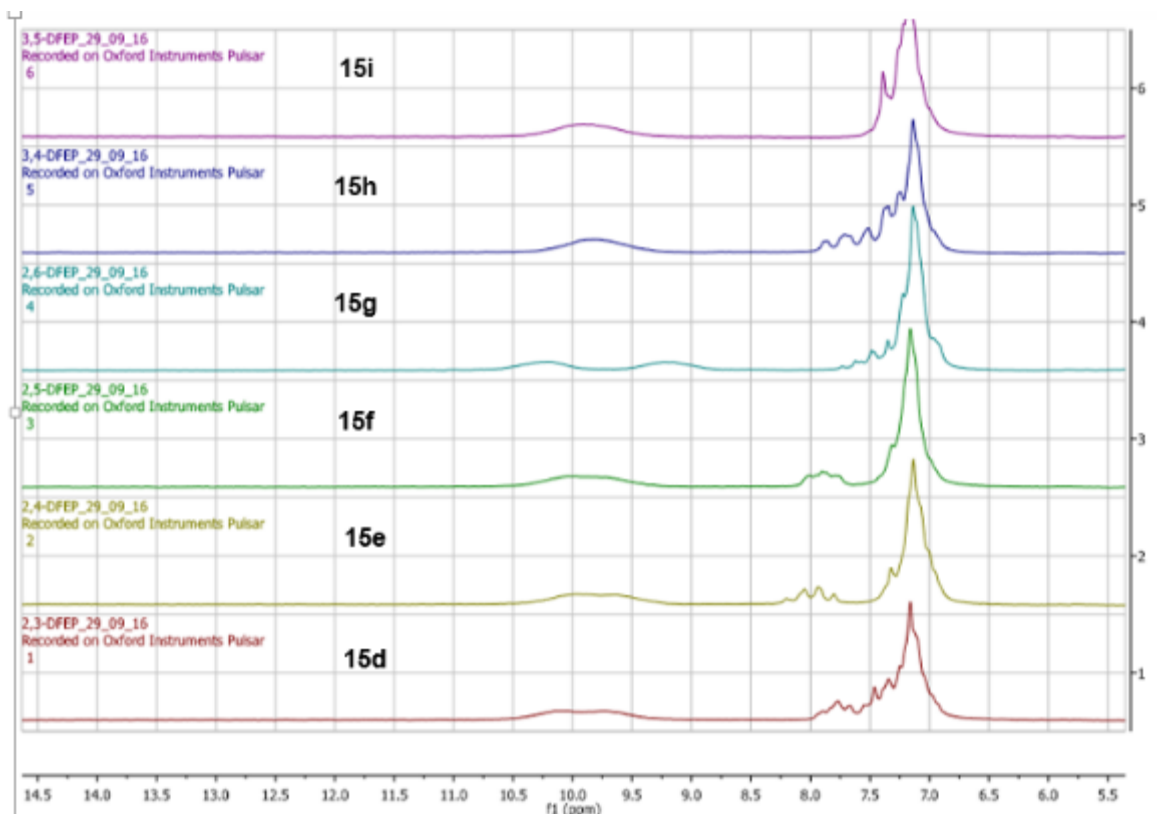


**Figure 161:** Stacked  $^1\text{H}$  NMR spectra for all DFEF regioisomers (**15d–15i**) focusing on the aromatic region

The ability of this  $^1\text{H}$  NMR experiment to distinguish between the 2,4-DFEP (**15e**) and 2,6-DFEP (**15g**) is important, as it is difficult to distinguish these two compounds using both GC-MS and presumptive colour tests, as individual components. This shows the potential of the 60 MHz Pulsar instrument to become a new presumptive test with the ability to provide an initial idea as to the sample present in under five minutes. This  $^1\text{H}$  NMR experiment works well with one component samples, however identifying samples becomes more difficult if multiple polyfluorinated ephenidines are present, as the spectra becomes more complex and peaks begin to coalesce. Hence, further experiments were performed using the 60 MHz Pulsar NMR in order to help identify samples present in mixtures.

A  $^{19}\text{F}$  NMR experiment was performed using the 60 MHz instrument. Again, all samples were run individually using matching number of scans and relaxation delay to create another run that would be performed in 3.5 minutes. All samples were run with the inclusion of TFA as an internal standard ( $\delta = -$

75.66 ppm) in order to gain an accurate  $^{19}\text{F}$  shift for the samples. All sample chemical shifts can be seen in Table 49.

**Table 49:**  $^{19}\text{F}$  chemical shift data for the polyfluorinated ephenidine regioisomers (**15d** – **15l**) using 60 MHz NMR instrument

Compound no.	Compound abbreviation	Chemical shift ( $\delta$ ppm)
<b>15d</b>	2,3 – DFEP	-140.22, -144.25
<b>15e</b>	2,4 – DFEP	-110.32, -114.25
<b>15f</b>	2,5 – DFEP	-118.41, -124.27
<b>15g</b>	2,6 – DFEP	-113.67
<b>15h</b>	3,4 – DFEP	-139.61
<b>15i</b>	3,5 – DFEP	-110.48
<b>15j</b>	TriFEP	-163.00, -138.89, -135.30
<b>15k</b>	TeFEP	-137.68, -142.50, -156.31, -157.48
<b>15l</b>	PFEP	-140.80, -153.79, -163.20

All samples show very similar chemical shifts to the 400 MHz NMR data gained from characterisation of the samples. The main significant difference between the 400 MHz and 60 MHz measurements is the broadening of peaks due to a loss of resolution. This creates a merging of fluorine peaks for the 3,4-DFEP sample, which shows 2 peaks using 400 MHz NMR but combines to one using 60 MHz NMR, although the splitting of the peaks still suggests two chemical environments are present. All DFEP isomers show distinctive chemical shifts and due to the simplicity of the spectra can be separated on both chemical shifts and the number of peaks (**Error! Reference source not found.**71). When combined with  $^1\text{H}$  NMR, this data can be used in the identification of a poly-fluorinated ephenidine isomer that prior to the measurement had not been detected before. Again some peaks may overlap when certain combinations of isomers are observed in the same sample and so a  $^{19}\text{F}$  *J*-resolved and  $^{19}\text{F}$  TOCSY experiment were developed on the 60 MHz instrument to help identify samples in mixtures.

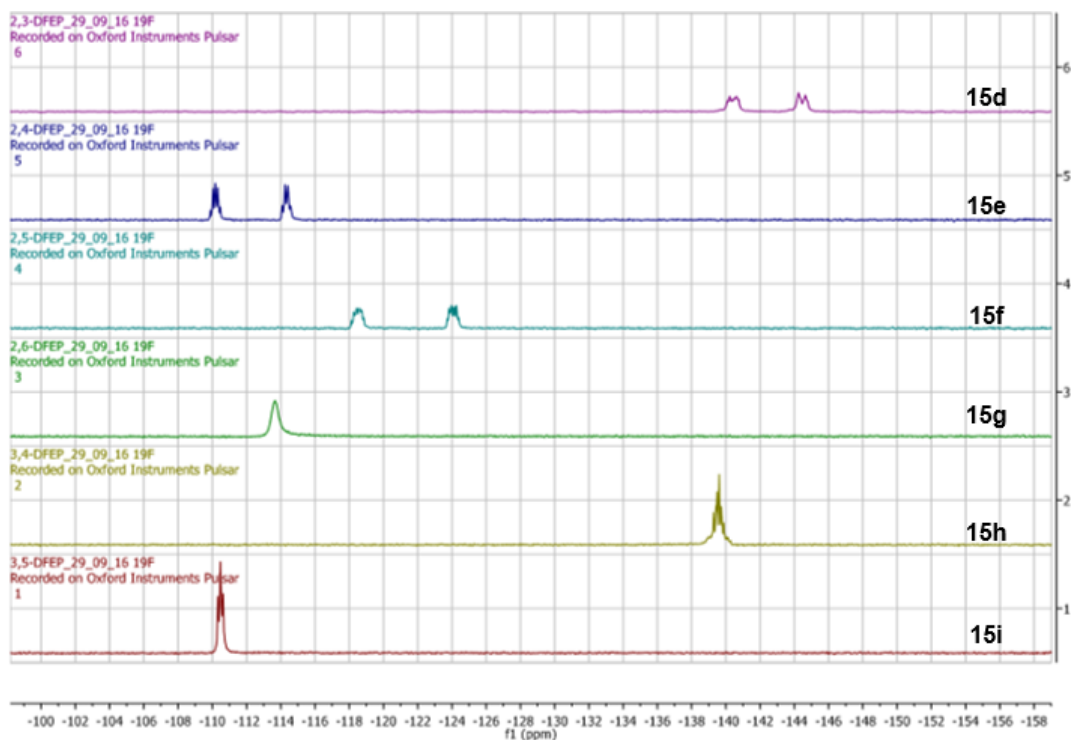


**Figure 162:** Stacked  $^{19}\text{F}$  NMR spectra for all DFEP isomers (**15d–15i**)

The tri, tetra and pentafluoroephenidine regioisomers can also be identified based on the number of peaks and shifts. The trifluoroephenidine (**15j**) and pentafluoroephenidine samples (**15i**) both produce three peaks in the  $^{19}\text{F}$ -NMR spectra, due to matching chemical environments in the pentafluoro derivative, through symmetry in the phenyl ring. However, the peaks are easily distinguishable from one another and from the four peaks produced by the tetrafluoroephenidine isomer (**15k**) as seen in figure 162.



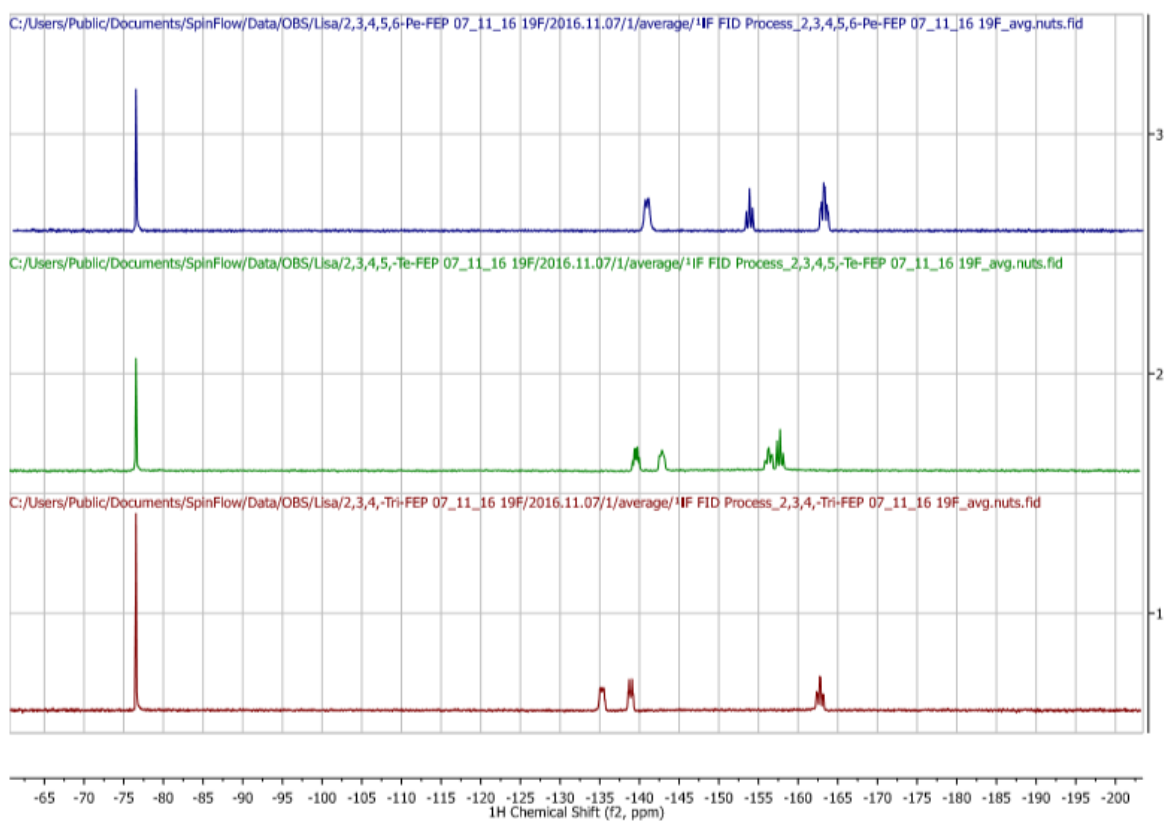


**Figure 163:** Stacked  $^{19}\text{F}$  NMR spectra for the tri (bottom), tetra (middle) and pentafluoroephenidine (top) regioisomers (**15j–15k**) using 60 MHz NMR

The simplicity of the  $^{19}\text{F}$  NMR spectra makes it an ideal experiment to use as a replacement presumptive test to show the possibility of a DFEP isomer being present in a sample. This can then be used in combination with  $^1\text{H}$  NMR data to further solidify the identification of the regioisomer present.

## 7.7. 60 MHz NMR *J*-resolved experiments

*J*-resolved NMR experiments were performed, for all six DFEP regioisomers, using the 60 MHz Pulsar instrument. Development of the experimental protocol with respect to the number of scans and points to acquire along both dimensions was optimised in order to produce sufficiently resolved signals in the *J*-resolved spectra. Spectra produced shows the relevant chemical shift of peaks along the *f*<sub>2</sub> axis, with the multiplicity from the splitting displayed along the *f*<sub>1</sub> axis. This helps to further identify the compound present, using the 60 MHz instrument, as <sup>19</sup>F NMR experiments show little of the coupling and splitting details produced using 400 MHz instruments. The <sup>19</sup>F *J*-resolved experiment can also further distinguish between the six DFEP isomers based on the coupling and splitting information produced. The spectra produced for the DFEP regioisomers (**15d–15i**) can be seen in figure 164–figure 169 and shows the difference in appearance between each of the spectra.

The 2,3-DFEP (**15d**) and 3,4-DFEP (**15h**) regioisomers both show the highest coupling constants with a distance of 0.2 and 0.22 ppm respectively from the centre alignment to each signal on the spectra. This equates to a coupling constant value between 12–13.2 Hz, and is consistent with <sup>3</sup>J<sub>FF</sub> coupling being manifest. There is a major difference between the two spectra as more coupling is observed in the 3,4-DFEP spectra. This could be explained through the presence of proton nuclei on the 2'- and 5'-positions of the benzene ring coupling to the fluorine, which would not occur when fluorine is present on the 2'-position of the benzene ring. The extra coupling is observed in the 3,5-DFEP (**15i**) isomer as well which shows a <sup>4</sup>J<sub>FF</sub> coupling of 4.8 Hz. This <sup>4</sup>J<sub>FF</sub> coupling constant value is also seen with the 2,4-DFEP isomer (**15e**), however no extra coupling is observed. 2,5-DFEP (**15f**) displays <sup>5</sup>J<sub>FF</sub> coupling with a coupling constant value of 10.2 Hz. The main DFEP isomer which can be easily identified using a <sup>19</sup>F *J*-resolved experiment is the 2,6-DFEP (**15g**) compound based on the inability of the experiment to show any coupling.

This 2D experiment helps to clearly distinguish between the regioisomers and with a longer experimental run time should be used after the  $^1\text{H}$  and  $^{19}\text{F}$  NMR presumptive testing has been performed to provide a more confirmatory response. A 2D TOCSY NMR was also performed in order to show the ability of 60 MHz NMR to distinguish between the DFEP regioisomers.

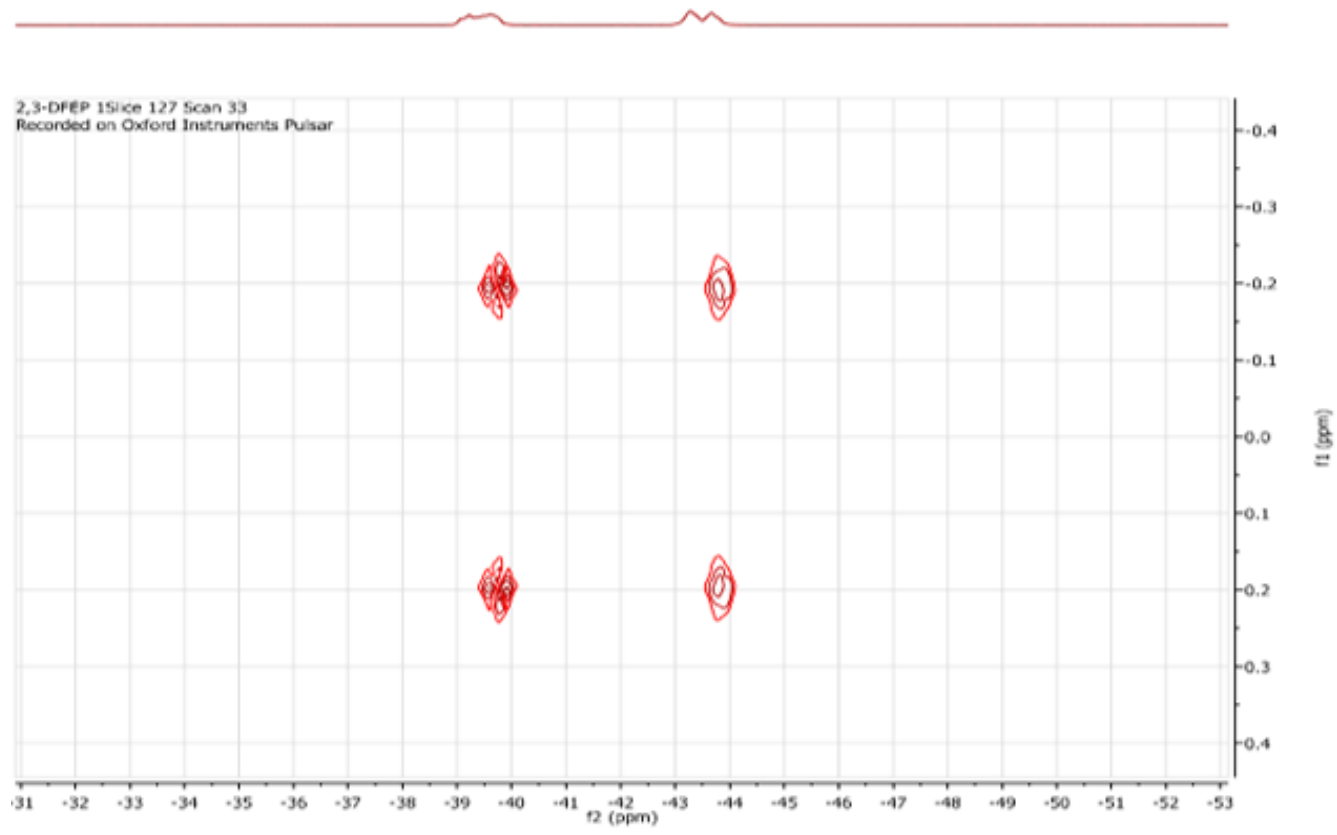


**Figure 164:**  $^{19}\text{F}$  NMR *J*-resolved spectrum for the 2,3-difluorophenidine (**15d**) sample

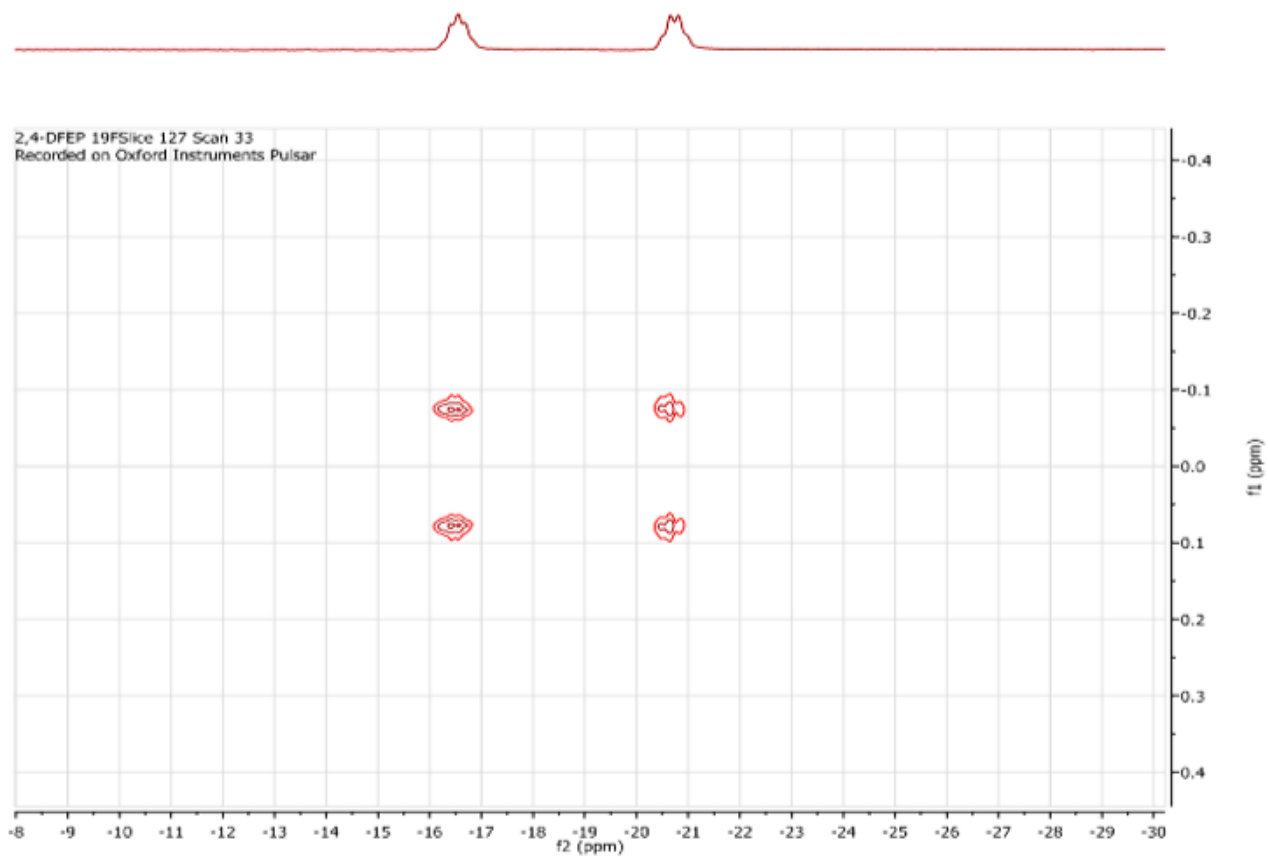


**Figure 165:**  $^{19}\text{F}$  NMR  $J$ -resolved spectrum for the 2,4-difluorophenidine (**15e**) sample

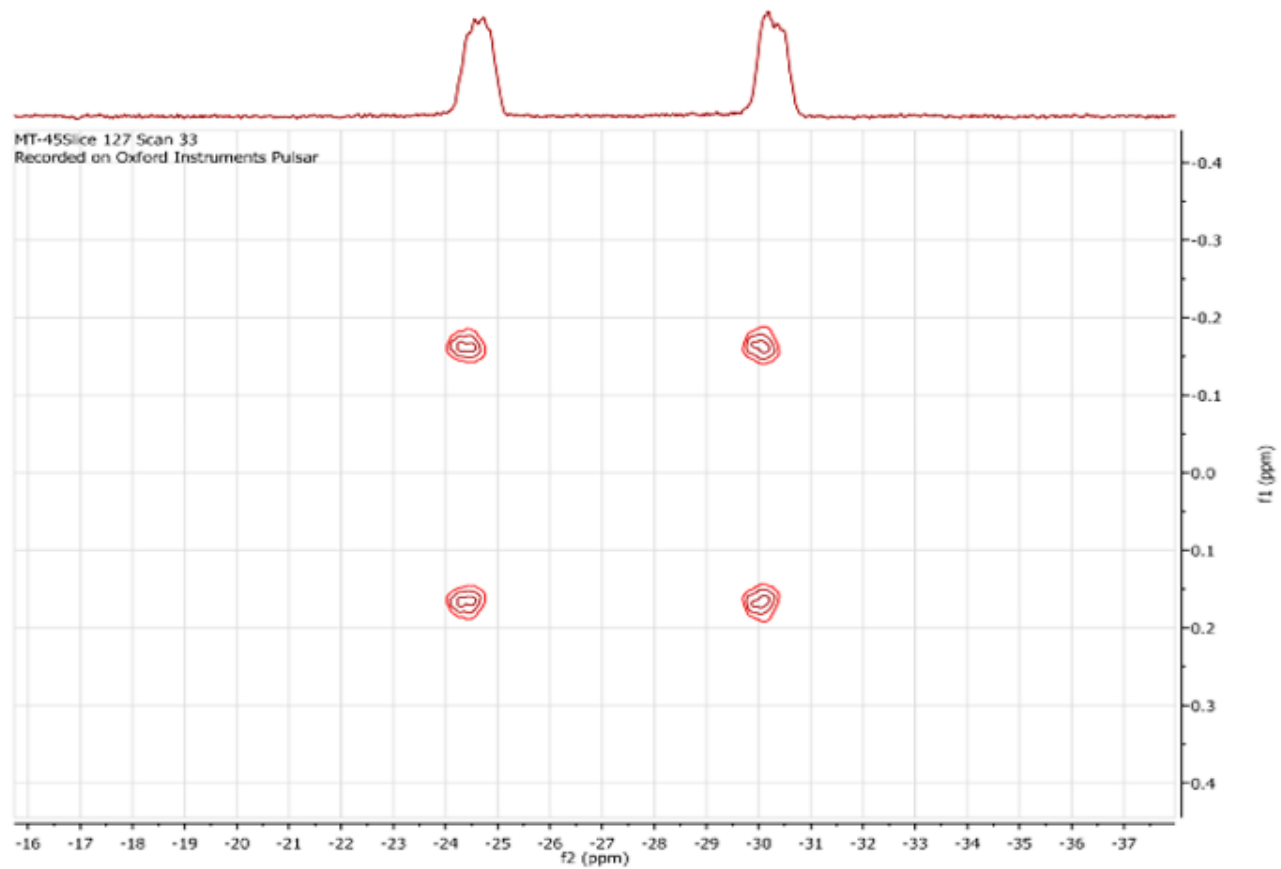


**Figure 166:**  $^{19}\text{F}$  NMR  $J$ -resolved spectrum for the 2,5-difluorophenidine (**15f**) sample

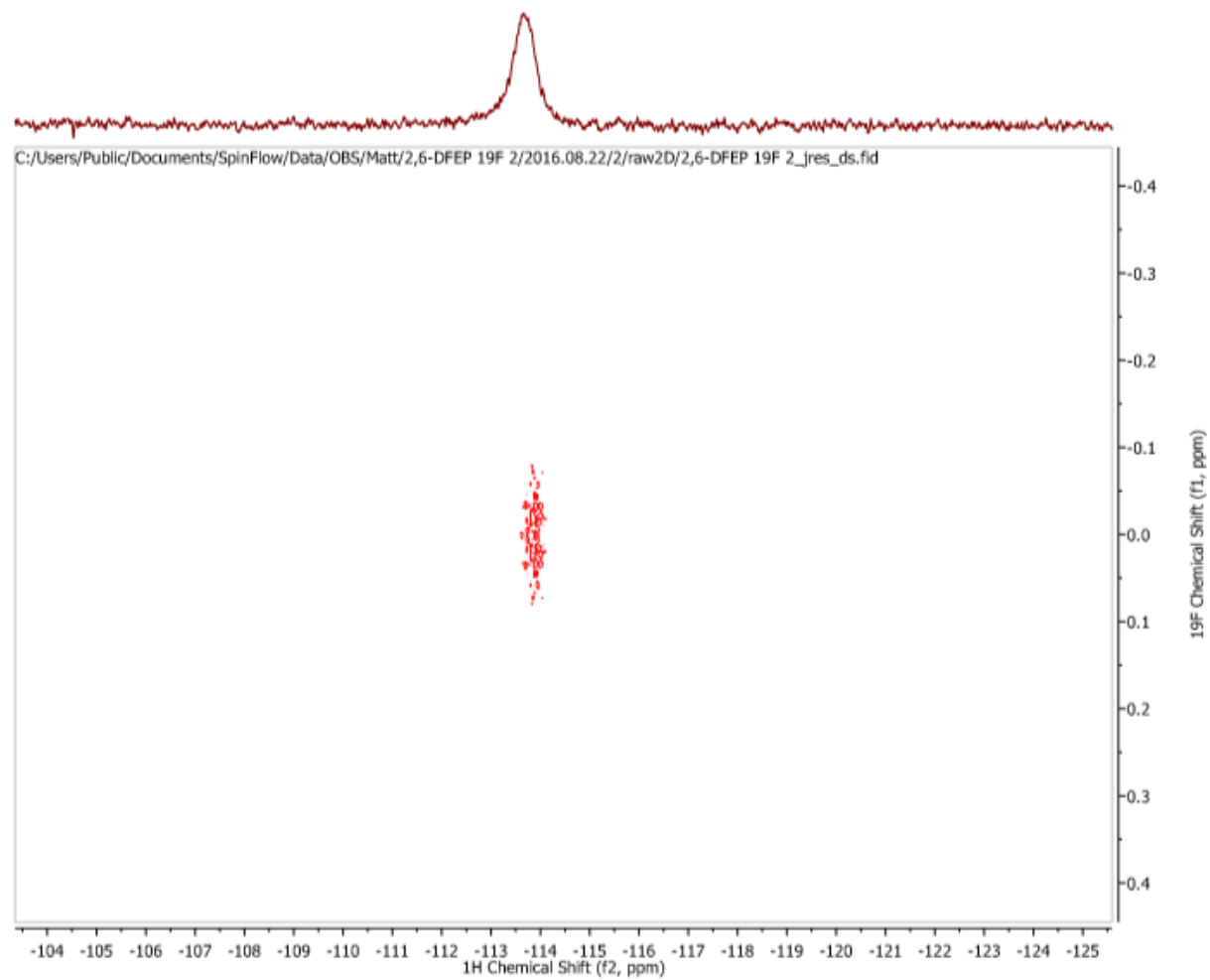


**Figure 167:**  $^{19}\text{F}$  NMR *J*-resolved spectrum for the 2,6-difluorophenidine (**15g**) sample

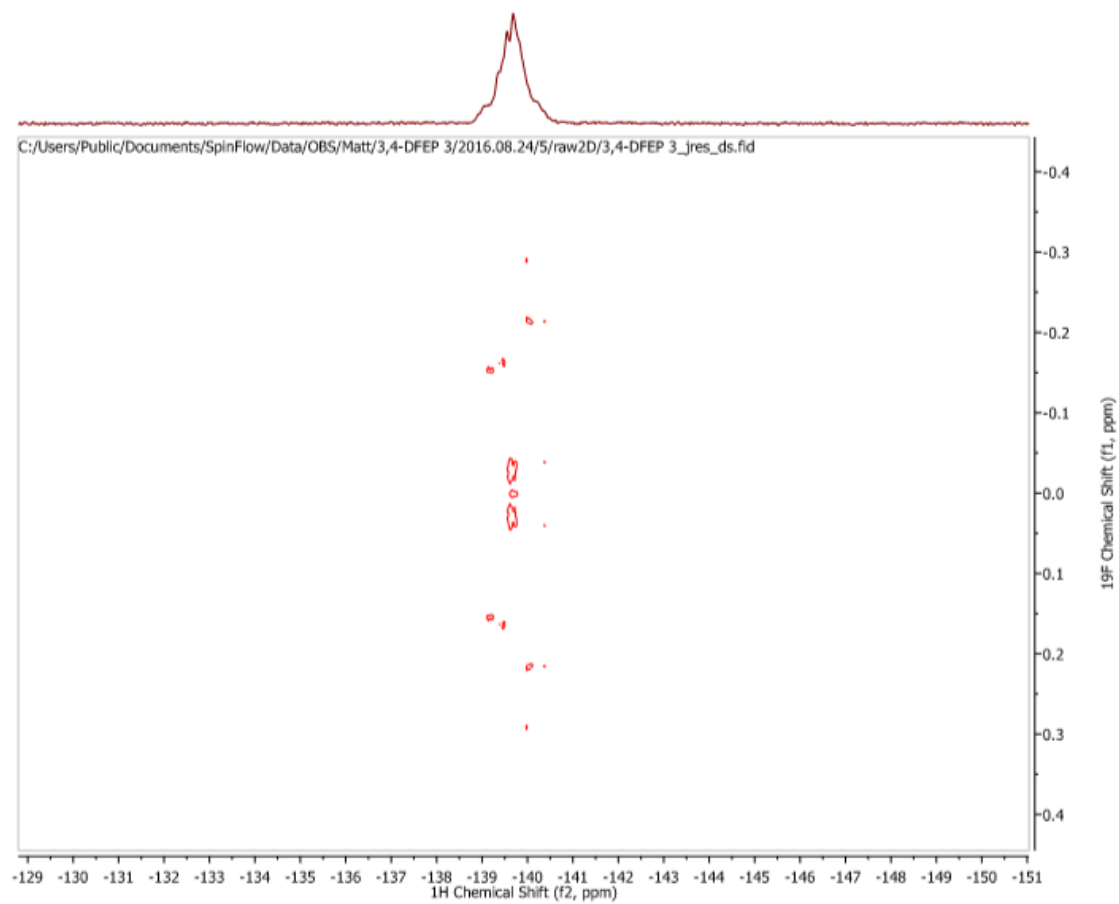


**Figure 168:**  $^{19}\text{F}$  NMR *J*-resolved spectrum for the 3,4-difluorophenidine (**15h**) sample



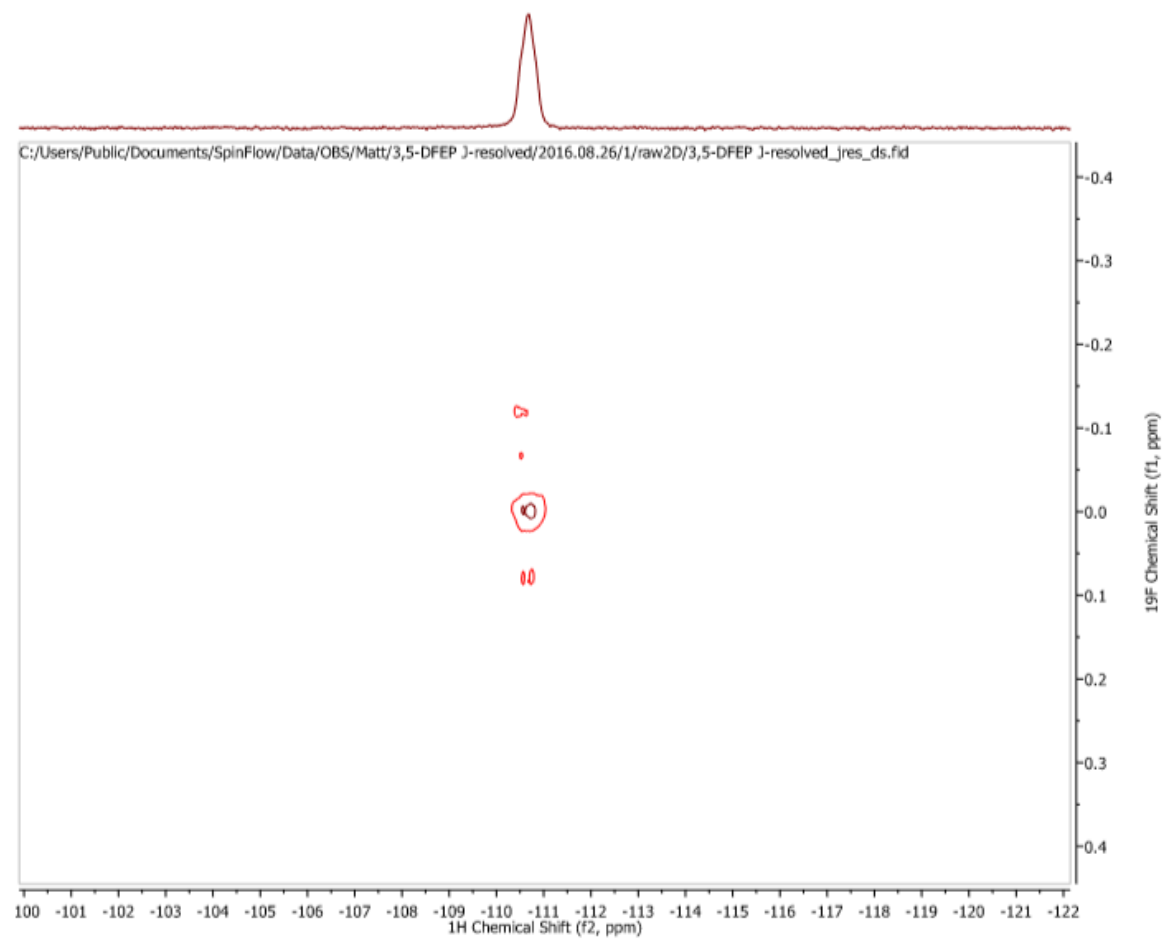


**Figure 169:**  $^{19}\text{F}$  NMR  $J$ -resolved spectrum for the 3,5-difluorophenidine (**15i**) sample

## 7.8. <sup>19</sup>F-TOCSY NMR

<sup>19</sup>F Total Correlation Spectroscopy (TOCSY) NMR experiments were run on the 60 MHz Pulsar instrument in order to try to resolve the six DFEP regioisomers. In a similar manner to the <sup>19</sup>F *J*-resolved experiments the number of scans and collection points was optimised in order to gain sufficient signal-to-noise. The spectrum produced is a product of the spin-spin coupling observed from the fluorine atoms in the molecule. The offset value was set in the middle of all chemical shifts, and was uncorrected, hence the reason the chemical shifts in both the f1 and f2 dimension does not match the <sup>19</sup>F NMR chemical shifts reported previously. The TFA peak is observed as an individual signal as no coupling is seen with the internal standard, however it can be used to track back to the chemical shift values. Cross-peaks are generated in the spectrum when coupling between fluorine nuclei occurs. The easiest cross-peak to observe is for 2,5-DFEP which has chemical shifts of -118.41 ppm and -124.27 ppm, which is seen around -2 ppm and -10 ppm on the TOCSY spectrum (**Error! Reference source not found.**). The 3,4-DFEP contains two peaks, that overlap at a chemical shift of -139.61 ppm, and this signal can be seen in the TOCSY spectrum when it is enlarged (**Error! Reference source not found.**<sup>80</sup>). This signal appears close to one of the signals responsible for generating a cross peak for the coupling of 2,3-DFEP at 0–5 ppm in the TOCSY spectrum. The 2,6-DFEP and 2,5-DFEP isomers both only contain one peak for <sup>19</sup>F-NMR, due to symmetry, and these appear as individual signals in the TOCSY spectrum. The remaining cross-peak is created by the coupling of the fluorine nuclei in 2,4-DFEP. This observed between -23 ppm and -30 ppm in the TOCSY spectrum, representing peaks at -110.32 ppm and -114.25 ppm from the <sup>19</sup>F NMR experiments.

This TOCSY experiment can distinguish between mixtures of DFEP regioisomers and can be used in combination with the *J*-resolved experiment to further identify compounds present. These experiments take longer to run than the <sup>1</sup>H and <sup>19</sup>F NMR experiments, and so would be used afterwards to

confirm the chemical identity ascertained from running the two presumptive NMR experiments on the 60 MHz instrument.

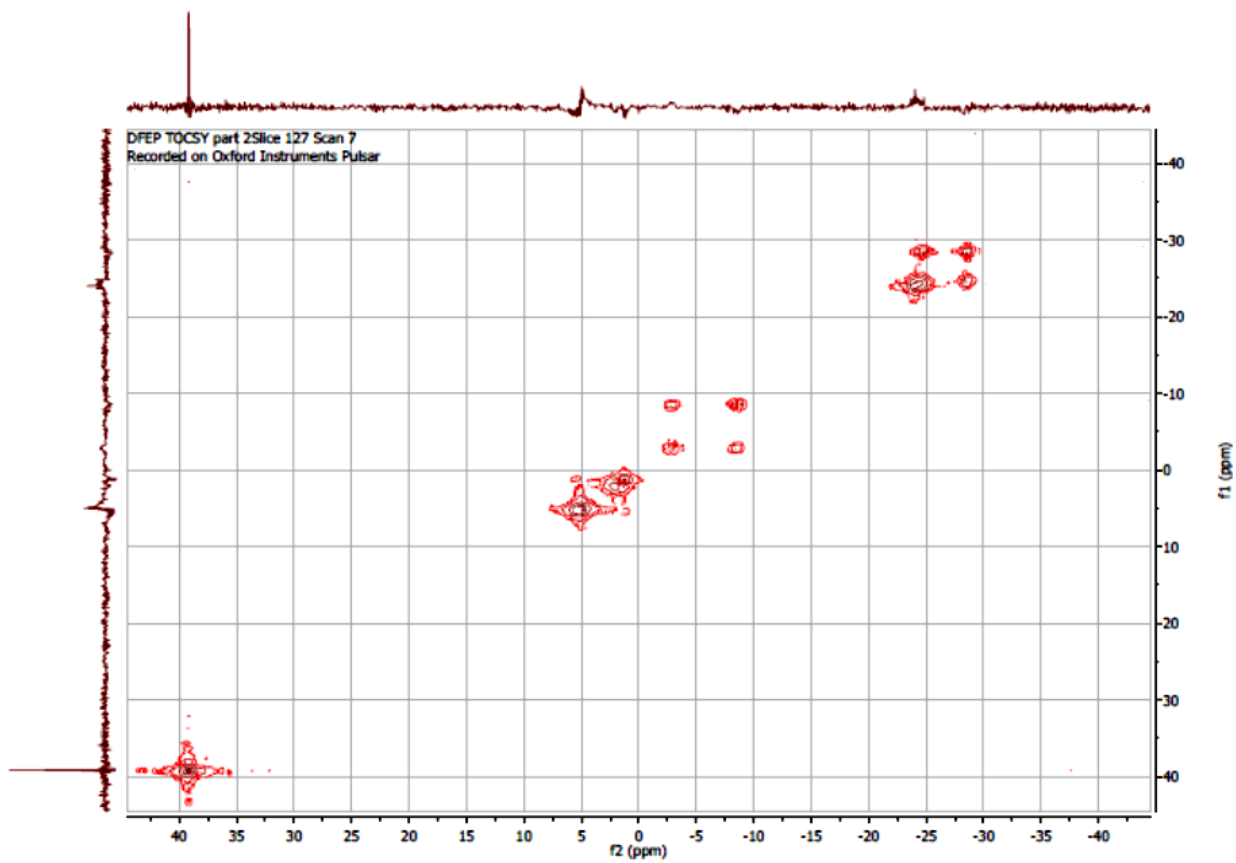


**Figure 170:**  $^{19}\text{F}$  NMR TOCSY spectrum of a mixture of six DFEP (**15d-15i**) regioisomers

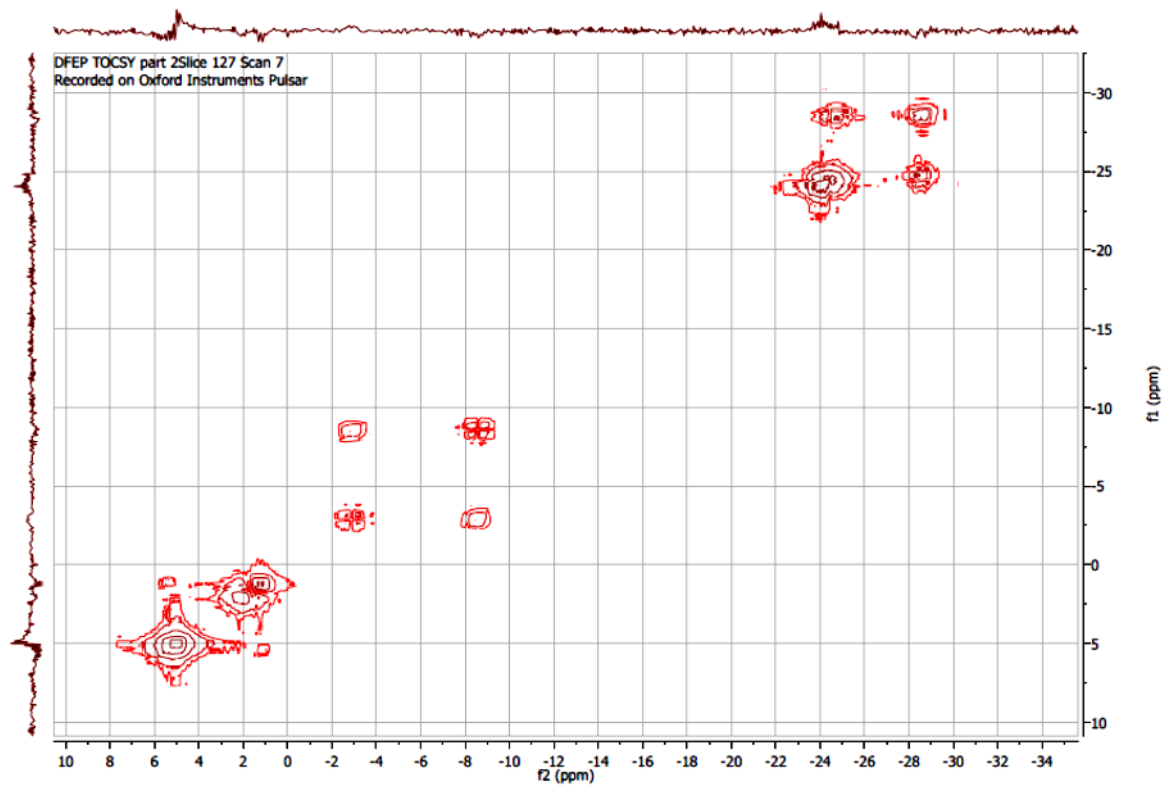


**Figure 171:** Truncated  $^{19}\text{F}$  NMR TOCSY spectrum shown in figure 190 to highlight the coupling interactions

## 7.9. Conclusions

The six difluoroephenidine regioisomers (**15d-15i**) were fully synthesised along with the tri (**15j**), tetra (**15k**) and pentafluoroephenidine (**15l**) compounds. All samples were shown to be pure (>95%) in order for full characterisation to be performed and reference spectra to be produced.

Presumptive testing was performed and showed that a combination of the Marquis and Simon's reagents can help to show the possibility of the presence of a polyfluorinated ephenidine isomer. However, the use of both reagents does not allow the nine compounds to be distinguished from one another.

A GC-MS method was also developed and showed difficulties separating the 2,4-DFEP and 2,6-DFEP isomers, even with further methods attempted. The remaining polyfluorinated ephenidines were fully baseline separated using the method developed in under 11 minutes.

60 MHz NMR was used as a possible presumptive test replacement with  $^1\text{H}$  and  $^{19}\text{F}$  experiments performed. Spectra for all compounds showed that distinguishing features are found in all compounds to allow possible identification between isomers.  $^{19}\text{F}$  chemical shifts began to show that the isomers could also be distinguished from one another. Two dimensional  $^{19}\text{F}$  experiments (COSY and TOCSY) were then developed which further distinguished the six difluoroephenidine regioisomers from one another, with less sample preparation required. The ability of the 60 MHz Pulsar spectrometer to perform the 2-dimensional experiments to help confirm the isomer present as well as a unique aromatic region to each of the other difluoro derivatives mean that the technique can start to be considered as a confirmatory test as well as a presumptive test.

## 8. Final conclusions and future work

A range of diphenidine derivatives and analogues including both mono and poly fluorinated and non-fluorinated compounds have been synthesised with yields all greater than 20%. Diphenidine analogues were also produced by altering the amine in the synthesis method. This shows the ability to alter structures and the ease of clandestine labs to produce these samples with synthesis only taking 2 hours. It also shows the difficulties facing analytical and forensic scientists for detection with new substances produced so easily and reference spectra constantly changing.

All diphenidine and ephenidine derivatives along with the fluorinated cathinones and amphetamines were all analysed using a full range of presumptive colour test reagents. In the case of the fluoromethcathinone and trifluoromethylmethcathinone regioisomers the Zimmerman reagent is able to provide a characteristic test. The Simon's reagent provides the ability to distinguish between the fluoromethcathinone regioisomers, however the difference in colour between the trifluoromethylmethcathinone regioisomers is less clear. The Robadope reagent can provide a characteristic test for the detection of amphetamines, however no difference is seen between the three fluorinated isomers. The Scott's reagent is characteristic for the diphenidine derivatives as well as providing more false positives for the detection of cocaine. This false positive provides difficulties for law enforcement as it produces confusion as to whether charging occurs under the Misuse of Drugs Act (1971) or the Psychoactive Substances Act (2016). All fluorinated ephenidine and diphenidine analogues can be identified using a combination of the Marquis, Mandelin's, Scott's and Simon's reagents, however different regioisomers cannot be distinguished from another. In the case of regioisomers they will produce the same  $\lambda_{\max}$  values which means UV attachments would not further separation and detection. In the case of presumptive colour tests a reagent testing kit could cost between £10-£20 with no way of determining an exact class with confidence.

A validated GC-MS method was developed for the separation and detection of the fluorinated cathinone and amphetamine regioisomers, diphenidine derivatives, halogenated derivatives and fluorinated diphenidine analogues. All FMC, TFMMC and FA isomers could be distinguished from one another within 11 minutes, however baseline separation could not be achieved for the 3'- and 4'-fluoroamphetamine regioisomers. LOD for all compounds ranged from 7.9 – 13.2  $\mu\text{g mL}^{-1}$ . All diphenidine derivatives were baseline separated in 45 minutes with LOD ranging from 4.5 – 12  $\mu\text{g mL}^{-1}$ . The halogenated diphenidines and fluorinated diphenidine analogues were split into positional isomer mixes for validation with all compounds distinguished from one another with the aid of SIM mode. LOD ranged from 6.5 – 16  $\mu\text{g mL}^{-1}$ . For all mixtures the run times for separation exceed 25 minutes which limits the number of samples that could be performed on these methods. The limits of detection and quantification are the lowest out of all analytical methods used in these studies.

60 MHz NMR was used for all compounds to show the similarities compared to 400 MHz NMR analysis. Spectra patterns and splitting patterns were consistent between both instruments with the 60 MHz instrument able to distinguish between regioisomers. A combination of  $^{19}\text{F}$  and  $^1\text{H}$  NMR experiments could be performed in 10 minutes. The spectra produced for both allowed regioisomers to be distinguished from one another based on both aliphatic regions, for class of compound, and aromatic regions for the position of the substituent groups on the benzene ring. Compounds containing fluorine also showed characteristic chemical shifts that aid with identification. 2D  $^{19}\text{F}$  NMR experiments were also developed for the differentiation of difluorinated ephenidine derivatives. Quantitative analysis was performed on both fluoroephenidine (FEP) and fluoroamphetamine (FA) isomers in order to show the potential of using 60 MHz NMR as a new presumptive test for quantitative analysis as well as qualitative.

Finally two tablets, presumed to be MDMA, were analysed both qualitatively and quantitatively. Analysis was performed using colour tests, GC-MS analysis and 60 MHz NMR. The Robadope reagent produced a positive



reaction, resembling the response of the fluoroamphetamine regioisomers, however it was not possible to identify which isomer was present. Both the GC-MS and 60 MHz NMR confirmed that both tablets contained 4-fluoroamphetamine. The GC-MS showed that the tablets contained 40% and 49% of 4-FA respectively, with the  $^{19}\text{F}$  NMR calibration of 4-FA agreeing with the %composition within  $\pm 2\%$ . This again shows the ability of 60 MHz instruments to become a presumptive test for the initial identification of NPS.

When comparing the presumptive testing side of analysis between the 60 MHz NMR and presumptive colour tests there are some similarities. Both techniques allow classes to be originally identified when a combination of colour tests are used and the aliphatic region of NMR spectrum is studied. Both techniques could be used by personal in law enforcement due to ease of use and at public environments such as festivals and airports due to being “field deployable”. However, the presumptive colour tests cannot distinguish between regioisomers which makes it less favourable to the 60 MHz NMR, which when using the aromatic and aliphatic regions of the  $^1\text{H}$  NMR experiment and  $^{19}\text{F}$  NMR experiment, where necessary, can distinguish between regioisomers.

When comparing the 60 MHz NMR approach and the various methods employed in terms of which technique is more advantageous, there are multiple points to consider. Table 50 shows the comparison between the 60 MHz NMR approach and GC-MS methods with points made throughout the study and taking into account operational costs, instrumental cost and ease of operation.

**Table 50:** Instrumental comparison between the 60 MHz NMR and the GC-MS

60 MHz NMR	GC-MS
<ul style="list-style-type: none"> <li>• Instrument costs around £50k</li> <li>• Not currently utilised in forensic labs</li> <li>• Low operational costs but high maintenance costs</li> <li>• Can be used and processed by non-scientists</li> <li>• Easier sample preparation compared to GC-MS</li> <li>• Easy sample processing especially for <math>^{19}\text{F}</math> NMR where only a couple of signals will be observed.</li> <li>• Both <math>^1\text{H}</math> and <math>^{19}\text{F}</math> NMR experiments can be performed within 5 minutes.</li> <li>• Regioisomers can be easily distinguished from another when run as individual components. Difficulties may be seen when mixtures are run, however longer 2-D experiments can help to distinguish compounds.</li> <li>• Field deployable</li> </ul>	<ul style="list-style-type: none"> <li>• Instrument can cost upwards of £200k</li> <li>• Can cost £200 per sample when sent off for testing</li> <li>• Low operational cost but high maintenance costs</li> <li>• Expertise needed for running and processing samples</li> <li>• Sample runs last 20 minutes and longer</li> <li>• Easily separates mixtures with only a couple of examples showing co-elution.</li> <li>• Currently used by forensic laboratories and can be used for evidence collection</li> <li>• No portability available</li> </ul>

This shows that the 60 MHz NMR has an ability to identify compounds easily when individual components are analysed. 60 MHz NMR instrumentation would be more favourable in the instance of finance, due to a cheaper operating system and matching operational costs. For law enforcement and organisations such as Greater Manchester Police the 60 MHz NMR would be ideal to initially test street samples to show what samples could potentially contain. This would then cut down on costs currently spent to send samples for forensic testing, that may not be needed if samples contain only non-controlled substances such as caffeine or paracetamol. Use of the 60 MHz NMR in environments such as police custody and festivals is possible due to the system being field deployable, which is not possible with the GC-MS instrument. Difficulties with mixtures does occur with the 60 MHz instrument and requires more complex and longer 2-D experiments such as TOCSY to begin to distinguish compounds in a complete mixture.

As a final conclusion the 60 MHz NMR would provide a better initial presumptive test to instruments and techniques already available due to costs, ease of sample preparation, ease of data processing and the sample throughput speed already mentioned. Techniques such as UV analysis and reagent colour testing provide a possible identification of class, however they do not distinguish between regioisomers and cannot pick out an individual component. The GC-MS would then be used as the confirmatory test to clarify what has been stated by the 60 MHz NMR.

Future work will include further quantification analysis using 60 MHz on a greater range of NPS classes. This can also include the possibility of using  $^1\text{H}$  NMR experiments to produce calibration graphs with maleic acid as a possible alternative as an internal standard. Maleic acid would act in a similar manner to trifluoroacetic acid in the fact that it would only produce a single peak in the  $^1\text{H}$  NMR spectra. A greater range of compounds must also be run on 60 MHz NMR instruments in order to produce a bigger database. This will then help further with the identification of NPS and can also aid with identification when new emerging compounds are first encountered. Further work on 2-D experiments such as TOCSY can be performed to help show the ability of the 60 MHz to further analyse mixtures. A final process would be to test the 60 MHz instrument in locations such as police custodies and festival locations to show whether the instrument can analyse samples as and when they are seized in a repetitive and accurate manner.

## 9. References

1. Legislation.gov, 2016.
2. S. Purser, P. R. Moore, S. Swallow and V. Gouverneur, *Chem. Soc. Rev.*, 2008, 37, 320-330.
3. M. Philp and S. Fu, *Drug Testing and Analysis*, 2018, 10, 95-108.
4. N. V. Cozzi, S. D. Brandt, P. F. Daley, J. S. Partilla, R. Rothman, B., A. Tulzer, H. H. Sitte and M. H. Baumann, *European Journal of Pharmacology*, 2013, 699, 180-187.
5. Legislation.gov, Misuse of Drugs Act 1971, <https://www.legislation.gov.uk/ukpga/1971/38/>, (accessed 4 March 2017, 2017).
6. ISB, 1908.
7. Legislation.gov, Medicines Act 1968, [www.legislation.gov.uk/ukpga/1968/67/](http://www.legislation.gov.uk/ukpga/1968/67/), (accessed 20 June 2018, 2018).
8. Legislation.gov, 2001.
9. Legislation.gov, 2005.
10. DrugScope, What are the UK Drug Laws?, <http://www.drugwise.org.uk/what-are-the-uk-drug-laws/>, (accessed 18 January 2017, 2017).
11. D. Nutt, W. King La Fau - Saulsbury, C. Saulsbury W Fau - Blakemore and C. Blakemore, *The Lancet*, 2007, 369, 1047-1053.
12. Gov.UK, 2017.
13. NICE, Controlled drugs and drug dependence, <https://bnf.nice.org.uk/guidance/controlled-drugs-and-drug-dependence.html>, (accessed 06/04/2019).
14. DrugScope, Business as usual? A status report on new psychoactive substances (NPS) and "club drugs" in the UK, <https://www.drugwise.org.uk/wp-content/uploads/businessasusual>, (accessed 15 February 2017, 2017).
15. A. T. King La Fau - Kicman and A. T. Kicman, *Drug Testing and Analysis*, 2011, 3, 401-403.
16. H. R. Sumnall, J. Evans-Brown M Fau - McVeigh and J. McVeigh, *Drug Testing and Analysis*, 2011, 3, 515-523.
17. F. I. Carroll, S. W. Lewin Ah Fau - Mascarella, H. H. Mascarella Sw Fau - Seltzman, P. A. Seltzman Hh Fau - Reddy and P. A. Reddy, *Annals of the New York Academy of Sciences*, 2012, 1248, 18-38.
18. S. Elliott and J. Evans, *Forensic Science International*, 2014, 243, 55-60.
19. P. R. Smith and S. R. Morley, *Essentials of Autopsy Practice*, 2017, 59-85.

20. D. Favretto, F. Pascali Jp Fau - Tagliaro and F. Tagliaro, *Journal of Chromatography A*, 2013, 1287, 84-95.
21. C. V. Gine, M. V. Espinosa If Fau - Vilamala and M. V. Vilamala, *Drug Testing and Analysis*, 2014, 6, 819-824.
22. Gov.UK, New Psychoactive Substances Review – Report of the expert panel, <https://www.gov.uk/government/publications/new-psychoactive-substances-review-report-of-the-expert-panel>, (accessed 22 November 2017, 2017).
23. UNODC, UNODC Early Warning Advisory on New Psychoactive Substances, <https://www.unodc.org/LSS/Home/NPS>, (accessed 21 January 2018, 2018).
24. K. Y. Rust, A. M. Baumgartner Mr Fau - Dally, T. Dally Am Fau - Kraemer and T. Kraemer, *Drug Testing and Analysis*, 2012, 4, 402-408.
25. J. Tetley and C. Crean, *Philosophical transactions of the royal society of London Series B Biological Sciences*, 2015, 5.
26. R. P. Archer, R. Treble and K. Williams, *Drug Testing and Analysis*, 2011, 3, 505-514.
27. EMCDDA, New psychoactive substances in Europe - An update from the EU Early Warning System., [http://www.emcdda.europa.eu/publications/rapid-communications/2015/new-psychoactive-substances\\_en](http://www.emcdda.europa.eu/publications/rapid-communications/2015/new-psychoactive-substances_en), (accessed 5 April 2018, 2018).
28. C. D. Rosenbaum, K. M. Carreiro Sp Fau - Babu and K. M. Babu, *Journal of medical toxicology*, 2012, 8, 15-32.
29. J. M. Prosser and L. S. Nelson, *Journal of medical toxicology*, 2012, 8, 33-42.
30. M. A. Ghorbani, S. Zabiulla, B. A. Bushra and S. V. Mamatha, *Research Journal of Pharmacy and Technology*, 2015, 8, 611-628.
31. B. Moosmann, L. A. King and V. Auwarter, *World Psychiatry*, 2015, 14, 248.
32. G. Hoiseth, S. S. Tuv and R. Karinen, *Forensic Science International*, 2016, 268, 35-38.
33. J. Wallach and S. D. Brandt, *Handbook of experimental Pharmacology*, 2018, 1-43.
34. J. Wallach and S. D. Brandt, *Handbook of experimental pharmacology*, 2018, 1-48.
35. R. Karinen and G. Hoiseth, *Forensic Science International*, 2017, 276, 120-125.
36. J. P. Smith, C. E. Sutcliffe Ob Fau - Banks and C. E. Banks, *Analyst*, 2015, 140, 4932-4948.
37. M. Liechti, *Swiss Medical Weekly*, 2015, 145.

38. T. F. Borders, X. Booth Bm Fau - Han, P. Han X Fau - Wright, C. Wright P Fau - Leukefeld, R. S. Leukefeld C Fau - Falck, R. G. Falck Rs Fau - Carlson and R. G. Carlson, *Addiction*, 2008, 103, 800-808.
39. K. C. Lan, F. C. Lin Yf Fau - Yu, C. S. Yu Fc Fau - Lin, P. Lin Cs Fau - Chu and P. Chu, *Journal of the Formosan Medical Association*, 1998, 97, 528-533.
40. E. Gouzoulis-Mayfrank, K. A. Hermle L Fau - Kovar, H. Kovar Ka Fau - Sass and H. Sass, *Nervenarzt*, 1996, 67, 369-380.
41. B. K. Logan, *Forensic Science Review*, 2002, 14, 133-151.
42. D. Sulzer, N. W. Sonders Ms Fau - Poulsen, A. Poulsen Nw Fau - Galli and A. Galli, *Progress in Neurobiology*, 2005, 75, 406-433.
43. K. J. Broadley, *Pharmacology and Therapeutics*, 2010, 125, 363-375.
44. J. R. Shoblock, S. D. Maisonneuve Im Fau - Glick and S. D. Glick, *Psychopharmacology*, 2003, 170, 150-156.
45. L. G. Kiloh and S. Brandon, *British Medical Journal*, 1962, 2, 40-43.
46. M. Laloup, V. Tilman G Fau - Maes, G. Maes V Fau - De Boeck, P. De Boeck G Fau - Wallemacq, J. Wallemacq P Fau - Ramaekers, N. Ramaekers J Fau - Samyn and N. Samyn, *Forensic Science International*, 2005, 153, 29-37.
47. E. Han, J. Miller E Fau - Lee, Y. Lee J Fau - Park, M. Park Y Fau - Lim, H. Lim M Fau - Chung, F. M. Chung H Fau - Wylie, J. S. Wylie Fm Fau - Oliver and J. S. Oliver, *Journal of Analytical Toxicology*, 2006, 30, 380-385.
48. M. Nieddu, L. Burrari, E. Baralla, V. Pasciu, M. V. Varoni, I. Briguglio, M. P. Demontis and G. Boatto, *Analytical Toxicology*, 2016, 40, 492-497.
49. K. A. Mortier, W. E. Maudens Ke Fau - Lambert, K. M. Lambert We Fau - Clauwaert, J. F. Clauwaert Km Fau - Van Bocxlaer, D. L. Van Bocxlaer Jf Fau - Deforce, C. H. Deforce Dl Fau - Van Peteghem, A. P. Van Peteghem Ch Fau - De Leenheer and A. P. De Leenheer, *Journal of Chromatography B*, 2002, 779, 321-330.
50. L. Biljsma, J. V. Sancho, E. Pitarch, M. Ibanez and F. Hernandez, *Journal of Chromatography A*, 2009, 1216, 3078-3089.
51. S. S. Johansen and T. M. Hansen, *International Journal of Legal Medicine*, 2012, 126, 541-547.
52. F. Linsen, R. P. Koning, M. van Laar, R. J. Niesink, M. W. Koeter and T. M. Brunt, *Addiction*, 2015, 110, 1138-1143.
53. J. Rohrich, T. Becker J Fau - Kaufmann, S. Kaufmann T Fau - Zornlein, R. Zornlein S Fau - Urban and R. Urban, *Forensic Science International*, 2012, 215, 3-7.
54. S. Al-Abri, J. M. Meier Kh Fau - Colby, C. G. Colby Jm Fau - Smollin, N. L. Smollin Cg Fau - Benowitz and N. L. Benowitz, *Clinical Toxicology*, 2014, 52, 1292-1295.
55. P. Kalix, *Pharmacology and Toxicology*, 1992, 70, 77-86.

56. J. M. Hagel, R. Krizevski, K. Kilpatrick, Y. Sitrit, F. Marsolais, E. Lewinsohn and P. J. Facchini, *Genetics and Molecular Biology*, 2011, 34, 640-646.
57. K. B. Hugins, Cathinone: History, Synthesis and Human Applications, <http://www.slideshare.net/KevinHugins/cathinone-history-synthesis-and-human-applications>, (accessed September 2 2017, 2017).
58. H. Halbach, *Bulletin of the World Health Organisation*, 1972, 47, 21-29.
59. N. Hohmann, G. Mikus and D. Czock, *Deutsches Arzteblatt International*, 2014, 111, 116-139.
60. S. W. K. Toennes, G F, *Clinical Chemistry*, 2002, 48, 1715-1719.
61. A. M. Moradi, A. Al-Meshal, F. M. Nasir and S. El-Feraly, *Chromatographia*, 1989, 27, 201-204.
62. R. F. Calkins, G. B. Aktan and K. L. Hussain, *Journal of Psychoactive Drugs*, 1995, 27, 277-285.
63. H. Belhadj-Tahar and N. Sadeg, *Forensic Science International*, 2005, 153, 99-101.
64. J. DeRuiter, L. Hayes, A. Valaer and C. R. C lark, *Journal of Chromatographic Science*, 1994, 32, 552-564.
65. B. D. C. Paul, K A, *Journal of Analytical Toxicology*, 2001, 25, 525-530.
66. J. Beyer, F. T. Peters, T. Kraemer and H. H. Maurer, *Journal of Mass Spectrometry*, 2007, 42, 150-160.
67. J. D. Power, P. McGlynn, K. Clarke, S. McDermott, P. Kavanagh and J. O'Brien, *Forensic Science International* 2011, 212, 6-12.
68. R. P. Archer, *Forensic Science International*, 2009, 185, 10-20.
69. A. Rickli, M. C. Hoener and M. E. Liechti, *European Neuropsychopharmacology*, 2015, 25.
70. N. Nic Daeid, K. A. Savage, D. Ramsay, C. Holland and O. B. Sutcliffe, *Science and Justice*, 2014, 54, 22-31.
71. S. A. Shah, N. I. Deshmukh, J. Barker, A. Petróczi, P. Cross, R. Archer and D. P. Naughton, *Journal of Pharmaceutical and Biomedical Analysis*, 2012, 61, 64-69.
72. P. D. Maskell, G. De Paoli, C. Seneviratne and D. J. Pounder, *Journal of Analytical Toxicology*, 2011, 35, 188-191.
73. S. Gibbons and M. Zloh, *Bioorganic and Medicinal Chemistry Letters*, 2010, 20, 4135-4139.
74. W. Kolodziejczyk, J. Jodkowski, T. M. Holmes and G. A. Hill, *Journal of Molecular Modelling*, 2013, 19, 1451-1458.
75. M. R. Meyer, C. Vollmar, A. E. Schwaninger, E. Wolf and H. H. Maurer, *Journal of Mass Spectrometry*, 2012, 47, 253-262.
76. S. P. Davies, M. Button, J. Dargan, P. I. Wood, D. M. Archer, R. Ramsey, J. Lee, T. Holt, D. W., Two cases of confirmed ingestion of

the novel designer compounds: 4-methylmethcathinone (Mephedrone) and 3-fluoromethcathinone., <http://www.the-ltg.org/data/uploads/posters/methcase>., (accessed 13 September 2016, 2016).

77. D. Ammann, D. McLaren Jm Fau - Gerostamoulos, J. Gerostamoulos D Fau - Beyer and J. Beyer, *Journal of Analytical Toxicology*, 2012, 36, 381-389.
78. K. Tsujikawa, K. Mikuma T Fau - Kuwayama, H. Kuwayama K Fau - Miyaguchi, T. Miyaguchi H Fau - Kanamori, Y. T. Kanamori T Fau - Iwata, H. Iwata Yt Fau - Inoue and H. Inoue, *Drug Testing and Analysis*, 2013, 5, 670-677.
79. J. Swinson, *Pharmachem*, 2005, 26-27.
80. R. Filler and R. Saha, *Future medicinal chemistry*, 2009, 1, 777-791.
81. J. P. Begue and D. Bonnet-Delpon, *John Wiley and Sons*, 2008, 335-336.
82. S. D. Brandt, N. V. Daley Pf Fau - Cozzi and N. V. Cozzi, *Drug Testing and Analysis*, 2012, 4, 525-529.
83. O. I. Khreit, M. H. Grant, T. Zhang, C. Henderson, D. G. Watson and O. B. Sutcliffe, *Journal of Pharmaceutical and Biomedical Sciences*, 2013, 72, 177-185.
84. H. W. Morris, J., *Drug Testing and Analysis*, 2014, 6, 614-632.
85. D. C. Javitt and S. R. Zukin, *The American Journal of Psychiatry*, 1991, 148, 1301-1308.
86. A. M. J. Baumgartner, P. F. Black, C. T., *Journal of Forensic Science*, 1981, 26, 578-581.
87. P. F. W. White, W. L. Trevor, A.J. . *Anaesthesiology*, 1982, 56, 119-136.
88. N. A. Anis, S. C. Berry, N. R. Burton and D. Lodge, *British Journal of Pharmacology*, 1983, 79, 565-575.
89. J. H. Li, B. Vicknasingam, Y. W. Cheung, W. Zhou, A. W. Nurhidayat, D. C. Jarlais and R. Schottenfeld, *Substance abuse and rehabilitation*, 2011, 2, 11-20.
90. M. K. Huang, Liu, C. Li ,J. H. Huang, S.D., *Journal of Chromatography B*, 2005, 820, 165-173.
91. M. Licata, G. Pierini and G. Popoli, *Journal of Forensic Science*, 1994, 39, 1314-1320.
92. B. L. G. Roth, S. Arunotayanun, W. Huang, X. P. Setola, V. Treble, R. Iversen, L., *PLoS One*, 2013, 8.
93. O. Corazza, *Human Psychopharmacology*, 2012, 27, 145-149.
94. M. Wikström, G. Thelander, M. Dahlgren and R. Kronstrand, *Journal of Analytical Toxicology*, 2013, 37, 43-46.
95. H. Morris and J. Wallach, *Drug Testing and Analysis*, 2014, 6, 614-632.



96. A. Helander, *Clinical Toxicology*, 2014.
97. K. Hasegawa, A. Wurita, K. Minakata, K. Gonmori, H. Nozawa, I. Yamagishi, K. Watanabe and O. Suzuki, *Forensic Toxicology*, 2015, 33, 45-53.
98. K. Kudo, Y. Usumoto, R. Kikura-Hanajiri, N. Sameshima, A. Suji and N. Ikeda, *Legal Medicine*, 2016, 17, 421-426.
99. K. Hofer, C. Degrandi, D. Muller, U. Zurrer-Hardi, S. Wahl, C. Rauber-Luthy and A. Ceschi, *Clinical Toxicology*, 2014, 52, 1288-1291.
100. A. Wurita, K. Hasegawa, K. Minakata, K. Watanabe and O. Suzuki, *Forensic Toxicology*, 2014, 32, 331-337.
101. S. P. Elliot, S. D. Brandt, J. Wallach, H. Morris and P. V. Kavanagh, *Analytical Toxicology*, 2015, 39, 287-293
102. G. Mclaughlin, N. Morris, P. V. Kavanagh, J. D. Power, J. O'Brien, B. Talbot, S. P. Elliot, J. Wallach and S. D. Brandt, *Drug Testing and Analysis*, 2015, 8, 98-109.
103. B. O. Boateng, M. Fever, D. Edwards, P. Petersson, M. R. Euerby and O. B. Sutcliffe, *Journal of Pharmaceutical and Biomedical Sciences*, 2018, 153, 238-247.
104. J. W. Lowdon, R. E. Alkirkit Smo Fau - Mewis, D. Mewis Re Fau - Fulton, C. E. Fulton D Fau - Banks, O. B. Banks Ce Fau - Sutcliffe, M. Sutcliffe Ob Fau - Peeters and M. Peeters, *Analyst*, 2018, 143, 2002-2007.
105. M. De Montis, P. Devoto, A. Bucarelli and A. Tagliamonte, *Pharmacological Research Communications*, 1985, 17, 471-478.
106. P. Paroli E Fau - Nencini, M. Nencini P Fau - Moscucci and M. Moscucci, *Pharmacological Research Communications*, 1984, 16, 915-922.
107. S. Massa, A. Di Santo R Fau - Mai, M. Mai A Fau - Artico, G. C. Artico M Fau - Pantaleoni, R. Pantaleoni Gc Fau - Giorgi, M. F. Giorgi R Fau - Coppolino and M. F. Coppolino, *ArchPharm*, 1992, 325, 403-409.
108. S. Massa, M. Stefancich G Fau - Artico, F. Artico M Fau - Corelli, R. Corelli F Fau - Silvestri, G. C. Silvestri R Fau - Pantaleoni, D. Pantaleoni Gc Fau - Fanini, G. Fanini D Fau - Palumbo, R. Palumbo G Fau - Giorgi and R. Giorgi, *Farmaco*, 1989, 44, 763-777.
109. C. S. Wink, G. M. Meyer, D. K. Wissenbach, A. Jacobsen-Bauer, M. R. Meyer and H. H. Maurer, *Drug Testing and Analysis*, 2014, 6, 1038-1048.
110. C. S. Wink, G. M. Meyer, J. Zapp and H. H. Maurer, *Analytical & Bioanalytical Chemistry*, 2015, 407, 1545-1557.
111. H. Kang, P. Park, Z. A. Bortolotto, S. D. Brandt, T. Colestock, J. Wallach, G. L. Collingridge and D. Lodge, *Neuropharmacology*, 2017, 112, 144-149.

112. D. Vodovar and B. Megarbane, *Fundamental and clinical Pharmacology*, 2018, 32, 652-653.
113. G. H. Hollister LE , L. E. Holister and H. K. Gillespie, *The Journal of clinical pharmacology and the journal of new drugs*, 1970, 10, 103-109.
114. Y. S. Fau, H. Yoshimura and H. Yoshimura, *Xenobiotica*, 1974, 4, 529-535.
115. S. F. Yoshihara, H. Yoshimura and H. Yoshimura, *Chemical & Pharmaceutical Bulletin*, 1972, 20, 1906-1912.
116. H. F. Hucker, S. F. Stauffer and R. E. Rhodes, *Experientia*, 1972, 28, 430-431.
117. L. G. Xie and D. J. Dixon, *Chemical Science*, 2011, 11.
118. UNODC, Screening Colour Tests, [https://www.unodc.org/documents/scientific/Screening\\_Colour\\_Test\\_ATS](https://www.unodc.org/documents/scientific/Screening_Colour_Test_ATS), (accessed 16 February 2016, 2016).
119. L. Harper, J. Powell and E. M. Pijl, *Harm Reduction Journal*, 2017, 14.
120. SCITEC, Screening Colour Test and Specific Colour Tests for the Detection of Methylendioxyamphetamine and Amphetamine Type Stimulants, [https://www.unodc.org/documents/scientific/Screening\\_Colour\\_Test\\_ATS](https://www.unodc.org/documents/scientific/Screening_Colour_Test_ATS), (accessed 23 February 2018, 2018).
121. K. Toole, M. Philip, N. Krayem, S. Fu, R. Shimmon and S. Taflaga, *Methods in Molecular Biology*, 2018, 1810, 1-11.
122. M. Philip, R. Shimmon, N. Stojonovska, M. Tahtouh and S. Fu, *Analytical Methods*, 2013, 5, 5402-5410.
123. M. Philp, R. Shimmon, M. Tahtouh and S. Fu, *Journal of visualized experiments*, 2018, 132.
124. C. Darsigny, M. Leblanc-Couture and I. Desgagné-Penix, *Austin Journal of Forensic Science and Crimonology*, 2018, 5, 1-9.
125. K. E. Hafer and T. A. Brettell, *Forensic Science*, 2018.
126. G. Bonchev, S. Zlateva and P. Morinov, *Journal of IMAB*, 2017, 23, 1603-1606.
127. W. Nowatzke, J. Zeng, A. Saunders and J. Turk, *Journal of Pharmaceutical and Biomedical Analysis*, 1999, 20, 815-828.
128. Y. Boumrah, M. Rosset, Y. Lecompte, S. Bouanani and A. Dahmani, *Egyptian Journal of Forensic Science*, 2014, 4, 90-99.
129. Y. Nakazono, *Forensic Toxicology*, 2013, 31, 241-250.
130. U. Holzgrabe, *Journal of Pharmaceutical and Biomedical Analysis*, 2005, 38.
131. I. C. P. Smith and D. E. Blandford, *Analytical Chemistry*, 1995, 67, 509-518.

132. F. A. Bovey, P. A. Mirau and H. S. Gutowsky, *Nuclear Magnetic Resonance Spectroscopy*, Elsevier Publishing, Second edition edn.
133. J. W. Emsley, *High Resolution Nuclear Magnetic Resonance Spectroscopy*, Pergamon Press 2013.
134. H. E. Gottlieb, V. Kotlyar and A. Nudelman, *Journal of Organic Chemistry*, 1997, 62, 7512-7515.
135. T. C. Ayres, *British Medical Journal*, 2012.
136. S. D. Brandt, H. R. Sumnall, F. Measham and J. Cole, *Drug Testing and Analysis*, 2010, 2, 377-382.
137. F. Fowler, B. Voyer, M. Marino, J. Finzel and M. Veltri, *Analytical Methods*, 2015, 18, 7907-7916.
138. S. Winiwarter, M. Ridderstrom, A. L. Ungell, T. B. Andersson and L. Zamora, *Comprehensive Medicinal Chemistry II*, 2007, 5, 531-544.
139. P. Rosner, U. Quednow B Fau - Girreser, T. Girreser U Fau - Junge and T. Junge, *Forensic Science International*, 2005, 148, 143-156.
140. E. Le Gall, C. Haurena, S. Sengmany, T. Martens and M. Troupel, *Journal of organic Chemistry*, 2009, 74, 7970-7973.
141. J. E. Samuels, Color Test Reagents/Kits for Preliminary Identification of Drugs of Abuse, <https://www.ncjrs.gov/pdffiles1/nij/183258>, (accessed 14 June 2017, 2017).
142. SCITEC, Chemistry and Reaction Mechanisms of Rapid Tests for Drugs of Abuse and Precursors Chemicals, [www.unodc.org/pdf/scientific/SCITEC6](http://www.unodc.org/pdf/scientific/SCITEC6), (accessed 1 August 2017, 2017).
143. M. R. Crampton, *Advances in Physical Organic Chemistry*, 1969, 7, 211-257.
144. A. R. Winstock, Dosing for pleasure and why less is often more <https://www.globaldrugsurvey.com/dosing-for-pleasure-and-why-less-is-often-more/>, (accessed 07 June 2019).
145. A. C. Parrott, *Psychopharmacology*, 2004, 173, 234-241.
146. M. C. A. Marcelo, K. C. Mariotti, R. S. Ortiz, M. F. Ferrao and M. J. Anzanello, *Microchemical Journal*, 2016, 127, 87-93.
147. P. M. Geyer, M. C. Hulme, J. P. B. Irving, P. D. Thompson, R. N. Ashton, R. J. Lee, L. Johnson, J. Marron, C. E. Banks and O. B. Sutcliffe, *Analytical and Bioanalytical Chemistry*, 2016, 408, 8467-8481.